



## **Zeolite Catalysts for the Selective Conversion of Sugars into Polymer Monomers**

**Tosi, Irene**

*Publication date:*  
2019

*Document Version*  
Publisher's PDF, also known as Version of record

[Link back to DTU Orbit](#)

*Citation (APA):*  
Tosi, I. (2019). *Zeolite Catalysts for the Selective Conversion of Sugars into Polymer Monomers*. Technical University of Denmark.

---

### **General rights**

Copyright and moral rights for the publications made accessible in the public portal are retained by the authors and/or other copyright owners and it is a condition of accessing publications that users recognise and abide by the legal requirements associated with these rights.

- Users may download and print one copy of any publication from the public portal for the purpose of private study or research.
- You may not further distribute the material or use it for any profit-making activity or commercial gain
- You may freely distribute the URL identifying the publication in the public portal

If you believe that this document breaches copyright please contact us providing details, and we will remove access to the work immediately and investigate your claim.

# Zeolite Catalysts for the Selective Conversion of Sugars into Polymer Monomers

Ph.D. dissertation by Irene Tosi



Technical University of Denmark

Supervisors

Professor Anders Riisager

Dr. Esben Taarning

May 2019



# Preface

This Ph.D. dissertation describes the work performed in the period from May 2016 to May 2019 at the Centre for Catalysis and Sustainable Chemistry, Department of Chemistry of the Technical University of Denmark (DTU). The work was part of the project Cat2BioChem supported by the Innovation Fund Denmark and involving the collaboration of Haldor Topsøe A/S and Perstorp AB. The work was supervised by Prof. Anders Riisager (DTU) and Dr. Esben Taarning (HTAS). In addition, scientists from university and companies helped in the project and their contributes are highlighted in the Acknowledgements and in the different chapters.

The thesis is divided into 7 chapters. Chapter 1 gives an overview of the state of the art of the research for the conversion of carbohydrates into chemical products using zeolites as the catalysts. Zeolitic materials and their use as Lewis acidic catalysts for the production of different bio-based compounds are introduced and the aim of the project of the thesis is explained. In Chapter 2, the experimental methods used for obtaining the results are explained in detail. The discussion of the results is presented in Chapters 3 to 6, each chapter includes a short introduction and conclusions relative to the different topics in order to facilitate the reading and the understanding of results of the different subjects. The project included the study of different processes for the conversion of carbohydrates into chemical products and the study of the preparation and characterization of the catalysts. First, the results describing the conversion of carbohydrates are explained. Chapter 3 describes the conversion of hexoses and Chapter 4 the conversion of glycolaldehyde. The last two chapters include the description of the results relative to the synthesis and characterization of the catalysts and the effect of modifications in the catalytic system is presented. Chapter 5 describes the synthesis of the stannosilicate catalysts and Chapter 6 the characterization of their structures, including modifications. Finally, Chapter 7 provides overall conclusions of the work.

Irene Tosi  
Kgs. Lyngby, Denmark,  
May 2019





# Acknowledgements

I thank my supervisors, Prof. Anders Riisager and Dr. Esben Taarning, for the opportunity to work in the project and be part of their research groups, both in DTU and HTAS, during the last three years.

As research and ideas always thrive on the collaboration with different people, I need to acknowledge many for the help given during these years. First, I want to thank Senior Researcher Sebastian Meier (DTU), who helped me and supported me in work, as well as in all the different situations concerning the Ph.D. life. The NMR experiments presented for the analysis of the reaction mixtures were optimized together and the results of the research were interpreted after detailed discussions. Thank you for sharing knowledge and experience, for always being available to listen and actively help, thank you for the patience and care showed from the beginning until the end of my Ph.D. Second, I want to thank Research Scientist Juan S. Martinez-Espin (HTAS), who flanked me during the last year and half of my work in studying the catalytic system and finalizing my project. I am glad for the confidence, the positive attitude and the stimulating environment that I found in working together.

It was a pleasure to be part of the Cat2BioChem project and I want to express my gratitude to all collaborators. Ph.D. Samuel G. Elliot and Bo Jessen (DTU), who experienced my same path, for their constant presence that made every deadline a bit easier. In particular, I thank Samuel for working patiently beside me and for the professional and personal growth that we achieved in these three years. I am grateful for the great job that Prof. Robert Madsen carried out for us in administrating and coordinating the entire project. Finally, I want to acknowledge all the collaborators from Perstorp AB and, in particular, Stefan Lundmark, Oleg Pajalic, Pia Wennerberg and David Löf, who followed the work continuously. Moreover, they welcomed me in Perstorp AB for my “external stay” in February 2019, making my experience great.

I am glad for being part of the Sustainable Chemicals group (HTAS) and the Catalysis and Sustainable Chemistry group (CSC DTU) and I want to thank all members. In particular, I want to thank Dr. Søren Tolborg (HTAS) and Dr. Irantzu Sádaba (HTAS) for assisting me and teaching me the research background at the beginning of my Ph.D. I am grateful for the help of Dr. Søren Birk Rasmussen (HTAS) in understanding and optimizing the characterization FT-IR of the catalytic materials. Moreover, I am thankful to the DTU NMR Center that gave me the opportunity to use advanced instruments and improve considerably the quality of my work. I also want to mention MSc. Annalisa Sacchetti and MSc. Luca Piccirilli, who have worked for six months with me in the laboratory, creating a cheerful environment and different working perspectives.

I extend my acknowledgements to all the technicians, who always find solutions to the daily problems, with specific attention to Andreas Graff Pedersen and the workshop at DTU for the helpfulness. I thank colleagues working on different projects at HTAS, Samin, Rik, Christian, and at DTU, Vanessa, Fabricius, Alex, Fabrizio, Rouzana, Mathias and all the friends who supported me here in Denmark, Lubo, Nedo, Yara, Massimo, Elena, Alessia, Elisa, Martina, all the girls who enjoyed playing volleyball together and many others. Thanks to Nicola. Finally, I want to thank the support received from Italy, the group of Catalysis at the Department of Industrial Chemistry of the University of Bologna, my best friends Mari, Niki, Cassi and Marti, my dear family, Ines, Renzo, Monica, Marco, Leonardo and Silvia. Thank all of you for being part of my life and for giving me the courage to overcome any obstacle.



# Abstract

The current society is highly dependent on materials derived from fossil feedstock, but the emergent environmental issues impose urgent changes in the production of chemicals. However, the transition to the use of sustainable sources requires the development of new technologies capable of processing the chemical functionality of the new starting materials. The Cat2BioChem project aimed to develop methodologies for the production of bio-based monomer polymers. In particular, the work performed in this thesis focused on the conversion of carbohydrates into different hydroxy esters using stannosilicate catalysts. The study started with understanding the already known process for the production of methyl lactate from hexoses using Sn-Beta zeolite as the catalyst. Methyl lactate is the monomer of polylactic acid, the most common bio-based biodegradable plastic, and the optimization of the parameters of the chemocatalytic production process can widen the applicability of the material.

The use of 1D and 2D NMR techniques allowed following the formation of intermediates and products over time. In the thesis, the role of methyl glycosides during the conversion of carbohydrates in methanol using zeolite catalysts is discussed in detail and a kinetic model for the formation of methyl lactate from hexoses is proposed. Fructose was identified as central reactive specie during the reaction starting from both sucrose and glucose. Thus, a method for the production of fructose from the cheaper and more available sucrose using commercial zeolite catalysts is also presented. The work continued with the study of the conversion of glycolaldehyde under similar conditions to the process for methyl lactate considered previously. In this case, the ability of the Lewis acidic catalyst to promote aldolic pathways led to the formation of a four-carbon hydroxy ester, methyl vinyl glycolate (MVG), as the main product. The molecule of MVG includes functionalities interesting for polymer applications and represents a new building block for the creation of bio-based materials. Different parameters involved in the process were studied and a kinetic model for the formation of MVG from glycolaldehyde is currently under investigation.

The last part of the thesis focuses on the optimization of the catalytic system used for the conversion of carbohydrates into hydroxy esters. Modifications in the procedure for the synthesis of Sn-Beta zeolite can improve the performances of the catalyst and facilitate the application in industrial processes. Thus, the effect of different parameters involved during the preparation of the catalysts was explored. Mesoporous stannosilicates showed improved activity during the conversion of large substrates at short times. Moreover, the catalytic materials were characterized using different techniques in order to investigate the structure-activity relation. The study analyzed the interaction between the catalyst and additives, such as alkali salts, in order to achieve better understanding of the structures active in the formation of the desired products and help in the future design of new catalysts. In conclusion, this thesis contributes to enlarge the current knowledge about the processes for the production of bio-based monomers, explaining the parameters relevant for the conversion of carbohydrates and considering routes for the optimization of the catalytic system.



# Resumé

Samfundet er i dag meget afhængig af kemikalier og materialer produceret fra fossile og ikke-vedvarende ressourcer, men voksende miljøhensyn kræver hastige forandringer til mere bæredygtig produktion. Overgangen til brug af vedvarende ressourcer kræver udvikling af nye teknologier, der kan omdanne funktionaliteten af disse nye udgangsmaterialer. Cat2BioChem projektets mål var, at udvikle metoder til produktion af bio-baserede monomere til polymere. Forskningsarbejdet der er udført i denne afhandling fokuserede i særdeleshed på at omdanne kulhydrater til forskellige hydroxyestere ved brug af stannosilikat katalysatorer. Studiet blev indledt med opbygning af forståelse af den allerede kendte proces for produktion af methyllaktat fra hexoser ved brug af en Sn-Beta zeolit som katalysator. Methyllaktat er et monomerisk derivat af polymeren polylaktat syre, som er den mest anvendte bio-baserede bionedbrydelige plastic. Optimering af proces parametre for den kemokatalytisk fremstilling af methyllaktat kan potentielt udbrede anvendelsen af det polymeriske materiale.

Anvendelse af 1D og 2D NMR spektroskopi gjorde det muligt at følge dannelsen af intermediater og produkter over tid under methyllaktat processen. Afhandlingen indeholder en detaljeret diskussion af methylglykosiders rolle i zeolitkatalyseret omdannelse af kulhydrater i methanol, og der blev opstillet en kinetisk model for dannelsen af methyllaktat fra hexoser. Fruktose blev identificeret som et centralt reaktivt specie både ved omdannelse af sukrose og glukose. Ud fra dette blev en metode udviklet til fremstilling af fruktose fra den billigere og lettere tilgængelige sukrose ved brug af kommercielle zeolitkatalysatorer. Omdannelse af glykolaldehyd blev endvidere studeret med udgangspunkt i de diskuteret reaktionsbetingelser anvendt for dannelsen af methyllaktat fra hexoser. I dette tilfælde fremmede katalysatorens Lewis sure egenskaber aldol kondensations reaktionsveje og dannelse af hydroxyesteren methylvinylglykolat (MVG) med fire kulstofatomer som hovedprodukt. MVG molekylet indeholder funktionelle grupper, som er interessante for molekylets anvendelse til polymere, hvilket gør MVG til en byggesten for nye bio-baserede materialer. Adskillige parametre blev studeret for reaktionen, og en kinetisk model for dannelsen af MVG fra glykolaldehyd er under udvikling.

I den sidste del af afhandlingen blev fokuseret på optimering af det katalytiske system anvendt til omdannelse af kulhydrater til hydroxyestere. Ved at modificere syntesen af Sn-Beta zeolitten kan katalysatorens præstation forbedres, hvorved anvendelsen i industrielle processer forenkles. Derfor blev effekten af forskellige parametre i katalysatorsyntesen undersøgt. Mesoporøse stannosilikater udviste øget katalytisk aktivitet ved omdannelse af store substrater over kort tid. Det katalytiske materiale blev karakteriseret ved brug af forskellige teknikker for at undersøge sammenhængen mellem struktur og aktivitet. Undersøgelserne analyserede interaktionen mellem katalysatoren og additiver såsom alkaliske salte for at opnå bedre strukturel forståelse af de aktive centre involveret i dannelsen af ønskede produkter, og for at bidrage til fremtidig design af katalysatorer.

Samlet set bidrager denne afhandling med ny viden og indsigt omkring processer til at producere bio-baserede monomere fra kulhydrater ved at give resultater, der forklarer relevante parametre for omdannelsen af kulhydrater og betragter veje til at optimere det katalytiske system.



# List of Abbreviations

[deSi] Sn-Beta : Tin zeotype with the desilicated *BEA framework	PDADMA : Polydiallyldimethylammonium chloride
[DR] Sn-USY : Tin zeotype with the USY framework modified by "dissolution-reassembly" procedure	PLA : Polylactic Acid
[ST] Sn-USY : Tin zeotype with the USY framework modified by "surfactant template" procedure	SEM : Scanning Electron Microscopy
1D : 1-Dimensional	Sn-Beta : Tin zeotype with the *BEA framework
2D : 2-Dimensional	Sn-MFI : Tin zeotype with MFI framework
3DE : 3-Deoxy esters	Sn-USY : Tin zeotype with the USY framework
3DG : 3-Deoxyglucosone	SSIE : Solid-State Ion-Exchange
3DL : 3-Deoxy lactones	TCD : Thermal Conductivity Detector
AGF : 1,6-Anhydroglucofuranose	TEAOH : Tetraethylammonium hydroxide
AGP : 1,6-Anhydroglucopyranose	TEOS : Tetraethyl orthosilicate
CTAB : Cetyltrimethylammonium bromide	THM : 2,5,6-Trihydroxy-3-hexanoate
DeAl-Beta : Dealuminated Beta zeolite	Ti-Beta : Titanium zeotype with the *BEA framework
DFT : Density-Function Theory	TOCSY : Total Correlation Spectroscopy
DHA : Dihydroxyacetone	TPD : Temperature-Programmed Desorption
DMSO : Dimethyl sulfoxide	TS-1 : Titanium Silicalite-1
DPM : Methyl 2,5-dihydroxy-3-pentenoate	VG : Vinylglyoxal
ERO : Erythrose	XRD : X-Ray Diffraction
ERU : Erythrulose	XRF : X-Ray Fluorescence
Fru : Fructose	Zr-Beta : Zirconium zeotype with the *BEA framework
FT-IR : Fourier-Transform Infrared Spectroscopy	
GA : Glycolaldehyde	
GA-DMA : Glycolaldehyde dimethyl acetal	
GA-HA : Glycolaldehyde hemiacetal	
GLA : Glyceraldehyde	
Glu : Glucose	
HLB : Hydroxy-butylolactone	
HFCS : High-Fructose Corn Syrup	
HMF : 5-Hydroxymethylfurfural	
HSQC : Heteronuclear Single-Quantum Coherence	
MAS : Magic-Angle Spinning	
Me-fru : Methyl fructosides	
Me-glu : Methyl glucosides	
MGA-DMA : Methyl glycolaldehyde dimethyl acetal	
ML : Methyl lactate	
MMHB : Methyl-4-methoxy-2-hydroxybutanoate	
MVG : Methyl vinyl glycolate	
MVP : Meerwein-Ponndorf-Valery	
NMR : Nuclear Magnetic Resonance	
NPA : n-Propylamine	
PAL : Pyruvaldehyde	





# Table of Contents

## Chapter 1 Introduction

<b>1.1 Zeolites and Zeotypes.....</b>	<b>1</b>
1.1.1 Zeolites as solid acid catalyst .....	1
1.1.2 Preparations and modifications of zeolites .....	2
1.1.3 Mesoporous zeolites.....	3
1.1.4 Zeotypes and Lewis acidic zeolites .....	3
1.1.5 Preparation of Sn-Beta zeolites .....	5
1.1.6 Active sites in Sn-Beta zeolites .....	6
1.1.7 Characterization of the acidity in Lewis acidic zeolites .....	8
1.1.8 Mechanisms of deactivation of stannosilicates during conversion of biomasses .....	9
<b>1.2 Carbohydrates as an Alternative Source of Chemicals.....</b>	<b>11</b>
1.2.1 Research for alternatives to the use of fossil feedstock .....	11
1.2.2 Sugars as bio-based feedstock for the production of chemicals .....	11
1.2.3 Isomerization of glucose to fructose .....	13
1.2.4 Processes for the isomerization of carbohydrates catalyzed by zeolites.....	16
1.2.5 The conversion of carbohydrates into alkyl lactates .....	17
1.2.6 Insight into the processes for the conversion of carbohydrates catalyzed by Sn-Beta zeolites .....	19
1.2.7 Conversion of glycolaldehyde into methyl vinyl glycolate.....	21
<b>1.3 Aim of the thesis .....</b>	<b>24</b>

## Chapter 2 Experimental Methods

<b>2.1 Experimental Methods for the Preparation and the Characterization of the Catalytic Materials.....</b>	<b>25</b>
2.1.1 Procedures for the synthesis of stannosilicates .....	25
2.1.2 Procedures for the preparation of mesoporous stannosilicates.....	26
2.1.3 Characterization of the catalytic materials.....	27
<b>2.2 Experimental Methods for the Study of the Conversion of Carbohydrates .....</b>	<b>30</b>
2.2.1 Catalytic conversion of carbohydrates .....	30
2.2.2 Analysis of processes for the conversion of carbohydrates.....	31

**Chapter 3 Conversion of Hexoses Using Zeolite Catalysts**

<b>3.1 Zeolites with Balanced Brønsted and Lewis Acidity for the Conversion of Sucrose into Fructose</b> .....	33
3.1.1 Experimental details: NMR spectroscopy for the study of complex mixtures.....	34
3.1.2 Design of a two-step process for the conversion of sucrose into fructose .....	35
3.1.3 Zeolites with balanced Brønsted and Lewis acidity .....	37
3.1.4 Investigations on the formation and the hydrolysis of methyl fructosides.....	39
3.1.5 Conclusions on the study for the conversion of sucrose into fructose catalyzed by zeolites .....	42
<b>3.2 The Role of Methyl Glycosides during the Conversion of Hexoses in Methanol</b> .....	43
3.2.1 The role of the formation of methyl fructosides in the conversion of hexoses in methanol catalyzed by solid acids .....	43
3.2.2 Formation of methyl fructosides from glucose at 160 °C using post-treated Sn-Beta zeolite catalysts .....	45
3.2.3 The reactivity of methyl fructosides in the presence of different zeolites .....	46
3.2.4 Conclusions on the study of the role of methyl glycosides during the conversion of carbohydrates in methanol .....	49
<b>3.3 Kinetic Analysis of the Production of Methyl Lactate from Hexoses Catalyzed by Sn-Beta Zeolites</b> .....	50
3.3.1 Conversion of hexoses into methyl lactate using hydrothermal Sn-Beta catalyst.....	50
3.3.2 Kinetic analysis of the process for the conversion of hexoses into methyl lactate.....	52
3.3.3 Improving the productivity in methyl lactate by the addition of small amounts of water .....	53
3.3.4 Comparison in the production of methyl lactate using different starting substrates.....	54
3.3.5 Comparison between hydrothermal and post-synthetic Sn-Beta zeolites .....	55
3.3.6 The role of methyl glycosides in the conversion of different substrates catalyzed by post-treated Sn-Beta zeolite .....	56
3.3.7 Conversion of different keto-hexoses: comparison between fructose and sorbose.....	58
3.3.8 Conclusions on the kinetic analysis of the production of methyl lactate from carbohydrates catalyzed by Sn-Beta zeolites .....	59

**Chapter 4 Conversion of Glycolaldehyde into Bio-Based Chemicals**

<b>4.1 Conversion of Glycolaldehyde Using Sn-Beta Catalysts</b> .....	60
4.1.1 The process for the formation of MVG from glycolaldehyde.....	61
4.1.2 The study of the reaction conditions for the conversion of glycolaldehyde.....	64
4.1.3 Effect of water on rate and MVG formation .....	65
4.1.4 The role of MGA-DMA.....	67
4.1.5 The presence of alkali salts in the reaction mixtures .....	68

---

4.1.6	Formation of MVG using erythulose as starting reagent .....	72
4.1.7	Conclusions on the study for the conversion of glycolaldehyde catalyzed by Sn-Beta zeolites .....	75
 <b>Chapter 5 Development of Synthetic Procedures for the Preparation of Tin-Containing Zeolite Catalysts</b>		
5.1	Exploring the Parameters for the Synthesis of Sn-Beta Zeolites .....	77
5.1.1	Comparison between hydrothermal and post-treated Sn-Beta catalysts .....	78
5.1.2	Sn-Beta catalysts containing residual aluminum.....	80
5.1.3	Synthesis of Sn-Beta zeolites containing different amounts of tin.....	82
5.1.4	The addition of a washing step in the procedure for the removal of extra-framework species .....	84
5.1.5	Conclusions on the study of the parameters for the synthesis of Sn-Beta zeolites .....	85
5.2	Synthesis and Use of Mesoporous Stannosilicates for the Production of Methyl Lactate .....	86
5.2.1	Synthesis and characterization of stannosilicates with different porous systems .....	86
5.2.2	The activity of mesoporous stannosilicates in the conversion of carbohydrates into methyl lactate.....	88
5.2.3	Conclusions on the study of mesoporous stannosilicates as catalysts for the production of methyl lactate .....	92
 <b>Chapter 6 Characterization of the Structure-Activity Relation of Sn-Beta Zeolites</b>		
6.1	Characterization of Sn-Beta Zeolites Using FT-IR Spectroscopy of <i>In Situ</i> Adsorbed Deuterated Acetonitrile as Probe Molecule.....	93
6.1.1	FT-IR characterization of zeolites and the use of deuterated acetonitrile as a probe molecule for active sites Lewis acidity.....	94
6.1.2	Sn-Beta catalysts with different tin content.....	95
6.1.3	Calcination of the dealuminated Beta zeolite precursor.....	97
6.1.4	Characterization of regenerated catalysts.....	100
6.1.5	Conclusions on the study for the characterization of Sn-Beta zeolites by FT-IR spectroscopy and <i>in situ</i> adsorbed deuterated acetonitrile probe molecule.....	103
6.2	Characterization of the Interaction between Sn-Beta Catalysts and Alkali Salts.....	104
6.2.1	Ammonia as probe molecule for the characterization of solid acids.....	104
6.2.2	Ammonia as probe molecule for studying the acidity of Sn-Beta modified by alkali ions .....	105
6.2.3	Deuterated acetonitrile as probe molecule for studying the acidity of Sn-Beta zeolites modified by alkali ions .....	109
6.2.4	Titration of Sn-Beta active sites by potassium carbonate .....	111
6.2.5	Conclusions on the study for the characterization of the interaction between Sn-Beta zeolites and alkali salts .....	113

---

## 6.3 Conversion of Carbohydrates Using Sn-Beta Catalysts in the Presence of Additional Metals 114

6.3.1	Modification of Sn-Beta catalysts with metals .....	114
6.3.2	Homogeneous additives during the conversion of glucose to methyl lactate .....	114
6.3.3	Sn-M-Beta catalysts for the conversion of sugars .....	117
6.3.4	The time-resolved formation of methyl lactate over Sn-M-Beta catalysts compared to the kinetic model proposed for Sn-Beta zeolites .....	119
6.3.5	The use of Sn-Mn-Beta zeolite for replacing the addition of homogeneous potassium carbonate in the production of methyl lactate.....	120
6.3.6	Conclusions on the study of the conversions of sugars by Sn-Beta in the presence of additional metals	121

## Chapter 7 Conclusions

Conclusions.....	122
------------------	-----

## Appendix A Case Study on Homogeneous Catalysis

### Conversion of Glucose in Aqueous Solutions Catalyzed by $\text{CrCl}_3$ ..... 124

A.1	Identification of formed acetals in the conversion of glucose catalyzed by $\text{CrCl}_3$ .....	125
A.2	Formation of branched hexose during the conversion of glucose catalyzed by $\text{CrCl}_3$ .....	126
A.3	Identification of different hexoses.....	127
A.4	Reactions catalyzed by $\text{CrCl}_3$ starting from glucose.....	127
A.5	Conclusion on the study for the identification of products and intermediates during the conversion of glucose in water catalyzed by $\text{CrCl}_3$ .....	128

## Appendix B Applications

B.1	MVG as reactive diluent in alkyd paints .....	129
B.2	MVG as monomer in UV-cured coatings .....	129
B.3	The epoxide of MVG in cationic UV-cured coatings .....	130
B.4	Conclusions on the study of the applicability of MVG in coatings .....	130

## References ..... 131

## Supplementary Information

SI.1	Catalysts characterization .....	144
SI.2	Structures .....	149

# Chapter 1

## Introduction

This chapter aims to give a general overview on the subjects studied in this work. Previous work has been carried out on the conversion of carbohydrates catalyzed by zeolites and this introduction can include only a short summary of few examples. The chapter is divided into three sections, representing the two main research fields of this thesis and a brief overview of the project. The first section includes a discussion on zeolite and zeotype catalysts, with particular attention to stannosilicates and Sn-Beta zeolites. The second section analyzes reactions and processes for the conversion of carbohydrates into bio-based chemical products. Finally, the third section explains the aim of the thesis and the guidelines used during the project.

### 1.1 Zeolites and Zeotypes

Zeolites and zeotypes are commonly used in heterogeneous catalysis. They are known as mineral enzymes,<sup>1</sup> as they are inorganic crystalline materials, formed by the regular arrangement of channels and cages, leading to a porous structure with highly defined dimensions. The regular porosity allows high selectivity when zeolites are used as catalysts and, thus, they find applications in a wide range of industrial processes.<sup>2</sup> In this section, a short introduction on materials, synthesis and modifications of zeolites is presented. In particular, the use of Lewis acidic zeolites in catalysis is considered. In fact, the research of processes for the conversion of polar and extensively functionalized molecules present in biomass needs catalysts with activity different from materials used for the conversion of hydrocarbons. Lewis acidity is usually a desired feature, because it allows the coordination and the activation of compounds rich in polar functional groups, such as carbohydrates.<sup>3,4</sup> During the last decade, the study for the preparation of stannosilicates and the activity of Sn-Beta zeolites has represented a central topic in heterogeneous catalysis.<sup>5</sup> Finally, the section includes an overview on the methods of catalyst deactivation.

#### 1.1.1 Zeolites as solid acid catalyst

Zeolites are microporous crystalline silicoaluminates. Their structure is made of  $\text{TO}_4$  tetrahedra ( $\text{T} = \text{Si}, \text{Al}$ ) interconnected by shared-corner oxygens.<sup>6</sup> Different connections lead to different spatial arrangements of channels and cages, giving different porous structures called zeolite frameworks. The International Zeolite Association (*IZA*) is responsible for identifying and classifying each framework with a three-letter code. In 2017, 236 structures were available, 40 of which were natural.<sup>7</sup> Due to their unique regular porosity and their ability to exchange ions, zeolites find many applications as adsorbents, ion-exchangers and catalysts.<sup>2</sup> The presence of well-defined channels introduced the concept of shape-selectivity in heterogeneous catalysis. Different types of selectivity in molecular sieves were illustrated in 1984 by M. Csicsery.<sup>8</sup> Shape selectivity occurs when only part of the reactants can diffuse in, and part of the products can diffuse out of the pores

because of their dimensions. Besides the selectivity for products and reactants, the pathway of the reaction is also determined by transition-state selectivity. In this case, products derived from bulky transition states are not formed. Thus, reactions catalyzed by zeolites are highly selective for the compounds with shapes and dimensions matching the catalyst porous structure.

Traditionally, the most important application of zeolites as catalyst in industry is the use of zeolite Y for fluid catalytic cracking of petroleum hydrocarbons.<sup>9</sup> Zeolites are known as solid acids. The presence of  $\text{Al}^{3+}$  in the framework introduces a negative charge, which is balanced by the presence of a counter-ion (Figure 1.1). Commercial products are available in the  $\text{NH}_4^+$ ,  $\text{Na}^+$  and  $\text{H}^+$  forms. These ions are mobile and can be easily exchanged, allowing applications as ion-exchange materials.<sup>2</sup> When the H-form of a zeolite is in solution, it can leach the proton and behave as *proton donor*, according to the Brønsted-Lowry definition of acid. The acid sites of a zeolite are, thus, proportional to the content of aluminum.<sup>1</sup> Moreover, aluminum can form a Lewis acidic center and confer both types of acidity (Brønsted and Lewis acidity) to the material. Typically, Lewis acidic properties are induced by thermal treatments, which dislocate the aluminum from the framework, creating extra-framework Lewis acidic sites. These properties are fundamental to the catalytic activities.<sup>10</sup>

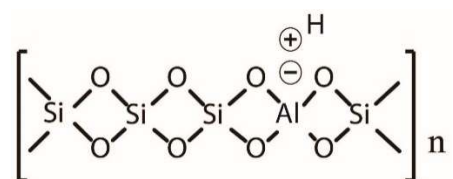


Figure 1.1. Simplification of the zeolitic framework.

### 1.1.2 Preparations and modifications of zeolites

In the last 50 years, plenty of synthetic procedures have been proposed for the preparation of zeolites.<sup>11</sup> Union Carbide commercialized the highly aluminum-rich zeolites A and X in 1959.<sup>12</sup> After the first studies by Barrer and Milton,<sup>12</sup> the hydrothermal process became the most popular process for the general synthesis of porous inorganic materials. Hydrothermal synthesis consists in the treatment of the aqueous mixtures of the precursors under conditions of high temperature and pressures in a closed environment. Preparations are performed in alkaline media in order to increase the solubility of silicon and aluminum sources and they involve the use of an organic template able to direct the order of the structure. Other proposed routes are the solvothermal and ionothermal synthesis,<sup>13</sup> in which different solvents, such as ethers or ionic liquid, are used.

After the commercialization of zeolitic materials, post-synthetic modifications became also important routes for the preparation of catalysts from zeolites. Hydrothermal procedures often involve harsh reaction conditions, such as high temperatures and pressures or extremely alkaline solutions. Thus, *top-down* modifications allow the preparation of materials with different properties starting from commercially available products.<sup>14</sup> The most common treatments consist in the alkaline desilication and the acidic dealumination. Both demetallation approaches remove framework elements and modify the Si/Al ratio. Since the acidic properties depend strictly on the content of aluminum, the procedures change the acidity of the starting zeolite. The procedures thus introduce vacancies and enlarge the zeolite cavities by the formation of “holes” in the framework. However, such treatments are often difficult to control and lead to the formation of extra-framework species.<sup>15</sup>

### 1.1.3 Mesoporous zeolites

Microporous (pore width  $< 20$  Å) catalysts can suffer from diffusional limitations for substrates and products, and can be limited in the conversion of bulky substrates. Biomass is mainly formed by natural homo- and heteropolymers. Thus, large-pores zeolites find more applications than small-pores zeolites as catalysts for biorefinery processes.<sup>16</sup> For this reason, research on mesoporous and hierarchical catalysts has lately become a central topic in heterogeneous catalysis. Moreover, large-pore catalysts have longer time-lives compared to their microporous counterparts, because the effect of deactivation by accumulation of carbon residues (coke) and obstruction of the porosity has a reduced impact in larger cavities.<sup>17</sup> In general, the term mesopores refers to cavities with dimensions of 20-500 Å. On the other hand, the term “hierarchical” means the regular interconnection of channels with different dimensions. In hierarchical zeolites, the two levels of porosity act synergistically in catalysis, mesopores avoid diffusional limitations and micropores limit the reaction space.<sup>18</sup> Many research groups have focused on finding effective methodologies for the preparation of hierarchical zeolites.<sup>19</sup> In general, it is possible to distinguish *bottom-up* and *top-down* procedures (Table 1.1). *Bottom-up* procedures consist in the modifications of the hydrothermal synthesis of zeolites and usually include the use of templates that direct the synthesis (hard templating, soft templating or non-templating methods). After crystallization, the templates are removed by calcination or dissolution.<sup>18</sup>

On the other hand, *top-down* procedures start from microporous materials and involve post-synthetic treatments in order to introduce a secondary porosity. They include demetallation, delamination or recrystallization of the starting materials.<sup>18</sup> Post-synthetic modifications include treatments with steam,<sup>20</sup> acids or bases and also more sophisticated approaches. The most common method involves a basic treatment,<sup>21</sup> which leads to the leaching of structural Si and creates “holes” in the framework. The simple desilication by alkaline treatment is not easily controllable and often requires the use of external pore-directing agents.<sup>21</sup> Notably, the demetallation (desilication and dealumination) changes other properties of the zeolite, such as the acidity. Moreover, the demetallation approach introduces defects in the zeolite framework, which still have an unclear role in catalysis.<sup>21</sup> Recently, crystal rearrangement by surfactant templating has received much attention as effective post-synthetic protocols for tuning the porosity of solids in a controlled way.<sup>22</sup> The term defines approaches in which an amphiphilic molecule (surfactant) acts as template in the reorganization of the zeolite structural units. The method can follow either two-step protocols or direct mesostructuring. In the first case, the zeolite is first dissolved in a base, and then reassembled in a hydrothermal process in the presence of the template.<sup>23</sup> In the second case, the direct mesostructuring involves the treatment of the zeolite with the surfactant in alkaline media. This latter process allows obtaining highly organized hierarchical structures.<sup>24</sup>

Table 1.1. Most common *bottom-up* and *top-down* procedures for the preparation of mesoporous zeolites.<sup>19</sup>

<b><i>Bottom-up</i> procedures</b>	<b><i>Top-down</i> procedures</b>
Hard-templating	Desilication
Soft-templating	Dealumination
Non-templating	Recrystallization

### 1.1.4 Zeotypes and Lewis acidic zeolites

Zeolites are able to exchange ions in solution and they can leach protons or gain other counter-ions, such as  $\text{Na}^+$  or  $\text{NH}_4^+$ . In zeolites, aluminum in different coordination sites is the most commonly responsible element for Lewis acidic behaviors.<sup>10</sup> Extra-framework aluminum is usually present in small amounts as a synthetic defect or it can be introduced by post-synthetic treatments, which partially break the structure.<sup>15</sup> Zeotypes are



## 1.1 Zeolites and Zeotypes

defined as the zeolitic materials that lack in aluminum. They can be constituted only by silica or contain metals able to replace the aluminum in the framework.<sup>25</sup>

Silica-based zeotypes are called Silicalites. In theory, these materials do not possess any Brønsted acidity, since the framework is neutral. Silicates have mostly been used in catalysis as supports of active species such as encapsulated metal nanoparticles.<sup>26,27</sup> On the other hand, metals with Lewis acidic properties can replace the aluminum in a zeolite matrix leading to Lewis acidic zeolites. The most common metals used in such replacements are Ti, Ga, Zr, Zn and Sn. In this case, the *proton donor* behavior of the material is suppressed, but the structure acquires high *coordinative* ability. In general, the introduction of a Lewis acidic metal allows the coordination and activation of electron-rich groups, such as hydroxy groups. For this reason, Lewis acidic sites have been widely explored for the conversion of biomass-derived compounds such as sugars, which contain many polar functional groups.<sup>25</sup>

In Titanium Silicalite-1 (TS-1), the titanium is incorporated into an aluminum-free MFI zeolite framework and TS-1 has found great success in industry as a catalyst for processes of partial oxidation.<sup>28</sup> TS-1 was first discovered in 1983 by Taramasso et al.<sup>29</sup> It showed excellent properties as catalyst for the oxidation of alcohols and epoxidation of olefins, becoming rapidly a commercial system for the production of catechol and hydroquinone from phenol.<sup>30</sup> Thereafter, the synthesis of a titanium zeolite with a Beta framework was proposed.<sup>31</sup> Ti-Beta presented lower catalytic activity compared TS-1, but the larger porosity allowed a more efficient oxidation of bulky molecules.<sup>32</sup> Zinc zeolites have also been investigated, since zinc is the active site of several homogeneous complexes and natural enzymes and they have shown good catalytic activity as Lewis acidic catalysts.<sup>33</sup> Zirconium has also been studied as Lewis acidic center in zeolites, resulting in high catalytic activity for the MPVO reaction using Zr-Beta.<sup>34</sup>

Examples of introduction of tin into zeolite frameworks were reported since the early 90s,<sup>35</sup> but the discovery of the first synthesis of Sn-Beta zeolites is ascribed to Corma et al. in 2001.<sup>36</sup> Since then, the acidic properties and catalytic activity of the material have been investigated extensively.<sup>37</sup> First, Sn-Beta received has much attention for the excellent catalytic properties in oxidations and reductions. Sn-Beta has shown high chemoselectivity in Baeyer-Villiger oxidations of ketones with hydrogen peroxide oxidant.<sup>36,38</sup> Afterwards, it has been used for the catalysis of different types of reactions, such as Meerwein-Ponndorf-Verlery<sup>39</sup> and Oppenauer oxidation (Figure 1.2).<sup>40,41</sup> More recently, Sn-Beta zeolites have been studied for their ability to promote the conversion of carbohydrates, creating new opportunities for the replacement of enzymatic processes with heterogeneous catalysis in the production of chemicals from renewable sources.<sup>42</sup> Sn-Beta zeolites have shown high catalytic activity in the isomerization of glucose to fructose<sup>43</sup> and in the production of lactates from carbohydrates.<sup>44</sup>

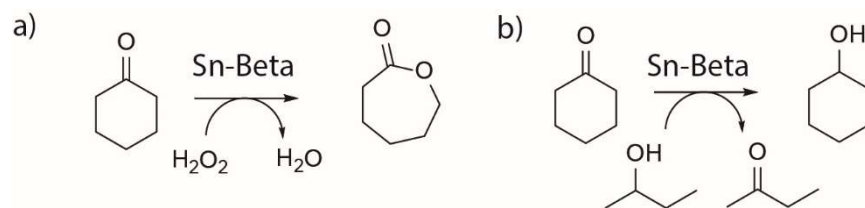


Figure 1.2. Redox reactions catalyzed by Sn-Beta zeolites a) Baeyer-Villiger Oxidation of cyclohexanone to ε-caprolactone<sup>36</sup> and b) Meerwein-Ponndorf-Valery Reduction of cyclohexanone with 2-butanol.<sup>38</sup>

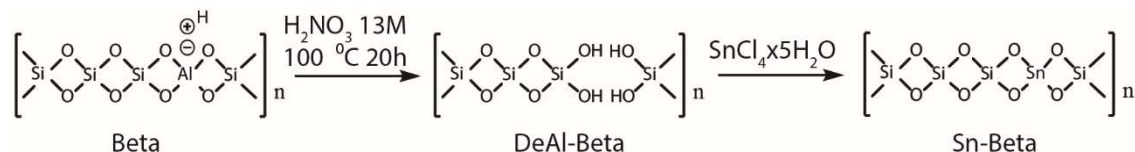
Thus, tin-containing zeolites are considered the most active and promising materials for the transformations of biomasses. Stannosilicates have been largely studied in their preparation methodologies and catalytic properties.<sup>5</sup> Although studies for the incorporation of tin into different types of frameworks are available in

literature,<sup>45,46</sup> Sn-Beta zeolites are commonly considered the most active catalysts. Recently, modifications of Sn-Beta zeolites, in which alkali metals are incorporated into the Beta zeolite framework during the synthesis, have shown to influence the selectivity during processes for the conversion of biomasses.<sup>47</sup> The effect of alkali ions on zeotypes was already reported for TS-1.<sup>48</sup> The presence of alkali metal ions during the synthesis of TS-1 catalysts leads to inactive materials. However, if added in small amounts in the epoxidation reaction media, they influence the selectivity. Alkali ions change the catalytic activity of zeotypes by modifying the active sites by ion-exchange with protons in the framework.<sup>49</sup>

### 1.1.5 Preparation of Sn-Beta zeolites

Sn-Beta zeolites can be prepared following different approaches. In *bottom-up* (hydrothermal synthesis) procedures, a gel formed by a mixture of the silica source, the tin precursor, water and the organic template is prepared. The crystallization of the mixture requires the use of a mineralizing agent (HF). Fluoride mineralizers are often used for the preparation of zeotypes containing metals different from  $\text{Al}^{3+}$ .<sup>50</sup> In fact, the fluoride creates stable dissolvable complexes with most metals and avoids their precipitation as hydroxides or oxides in the aqueous media of the synthesis.<sup>11</sup> The use of HF, the long times required for the crystallization and the formation of large crystals ( $>1\ \mu\text{m}$ ) are the main drawbacks of the hydrothermal procedure. The crystallization time can be slightly tuned by adjusting the parameters of the synthesis. It has been demonstrated<sup>51</sup> that the water content of the initial gel affects the duration of the crystallization and reduced times are achieved by the use of low amounts of water. The final materials show the same coordination of tin and catalytic activity for different water contents in the gel.<sup>51</sup> On the other hand, the amount of tin influences the duration of the preparation and the shape of the crystals.<sup>52</sup> Short times can be used for samples containing low amounts of tin, but the resulting materials have less active sites per gram of catalyst. Other methods proposed for the reduction of the duration of the crystallization are the use of zeolite seeds<sup>53</sup> or steam-assisted crystallizations.<sup>54</sup>

In order to overcome the disadvantages of the hydrothermal synthesis, other procedures towards Sn-Beta zeolites have been investigated. In 2012, Hammond et al.<sup>55</sup> proposed a *top-down* (post-synthetic) procedure for the synthesis of Sn-Beta zeolites. The commercial aluminum-containing Beta zeolite can be dealuminated by acidic treatment with  $\text{HNO}_3$  at  $100\ ^\circ\text{C}$ . After the treatment, the zeolite contains vacancies in the framework, which can host a new coordinated metal, such as tin (Scheme 1.1). The content of aluminum in the final material can be tuned by changing the time of the treatment, which can result in the preparation of multifunctional zeolites, containing both Lewis and Brønsted acid sites.<sup>56</sup> The procedure has been applied for the preparation of Lewis acidic zeolites containing different metal centers.<sup>57</sup>



Scheme 1.1. Post-synthetic procedure for Sn-Beta synthesis in agreement with Hammond et al.<sup>55</sup>

Several methodologies have been studied for the incorporation of tin inside the dealuminated zeolite. Grafting with solvents<sup>58</sup> or vapors,<sup>59,60</sup> wet impregnation<sup>61</sup> and Solid-State Ion-Exchange (SSIE)<sup>55</sup> are the procedures proposed (Table 1.2). Different procedures lead to different incorporation of tin and different activity.<sup>61,62</sup> The hydrothermal synthesis usually present a more efficient incorporation of the tin compared to post-synthetic procedures, resulting in higher catalytic activity of the final materials.<sup>63</sup> Post-synthetic procedures can lead to materials with small crystals and allow the incorporation of high amounts of tin. However, the resulting

## 1.1 Zeolites and Zeotypes

materials are more hydrophilic than hydrothermal catalysts due to the presence of many defects in the framework.<sup>64</sup> On the other hand, the procedure is simple and scalable.<sup>55</sup> Thus, the procedure allows a wide range of applications for industrial-level productions and most of the catalysts studied in this work were prepared using this method.

Table 1.2. Methods for the post-synthetic incorporation of tin in dealuminated zeolites

Method	Description
Grafting with solvents	The dealuminated zeolite was dehydrated and suspended in isopropanol and $\text{SnCl}_4 \cdot 5\text{H}_2\text{O}$ . The suspension was refluxed under $\text{N}_2$ for 7 hours. <sup>58</sup>
Grafting with $\text{SnCl}_4$ vapors	The dealuminated zeolite was reacted with anhydrous $\text{SnCl}_4$ at 100 °C under inert atmosphere overnight. <sup>59,60</sup>
Solid-State Ion-Exchange	The dealuminated zeolite was grinded with tin(II) acetate for 15 minutes. <sup>55</sup>

### 1.1.6 Active sites in Sn-Beta zeolites

Many spectroscopic studies and theoretical calculations have been performed in order to characterize the active sites in Sn-Beta zeolites and to correlate them to the catalytic performance.<sup>65–67</sup> Tin can be incorporated in the framework of Beta zeolites in different ways and the identification of the structures of the active sites is essential for the understanding of the structure-activity relation.<sup>68</sup> Different synthetic procedures lead to the formation of different materials with different activity.<sup>62</sup> Generally, hydrothermal Sn-Beta zeolites have hydrophobic and defect-free frameworks, while post-synthetic Sn-Beta zeolites have hydrophilic defective frameworks, resulting in different catalytic activity. Thus, the tin can be incorporated at different crystallographic sites in the zeolites and different environments,<sup>69</sup> leading to different catalytic proprieties.

First, Boronat et al.<sup>70</sup> introduced the distinction between two different types of coordination that were identified as representative for different catalytic activity. In the first case, the tin finds oxygen-tetracoordination in a fully saturated environment, which is referred as “closed active site”. In the second case, the tin finds oxygen-tetracoordination in a partially hydrolyzed environment and is called “open active site”. It has been shown that the two sites have different acidic strength and catalytic activity. In particular, open sites have shown stronger interaction with probes for the Lewis acidity in FT-IR analysis<sup>70</sup> and they have been identified as the mainly responsible catalyst active sites for the isomerization of glucose.<sup>71, 72</sup> Similar sites with different reactivity have been previously described for TS-1 catalysts.<sup>73</sup> However, this description is only a simplified overview. “Closed” and “open” sites have been identified in dehydrated samples,<sup>74</sup> but they have also shown flexible coordination during catalysis in solution.<sup>75</sup> The “closed sites” in solution can partially hydrolyze, resulting in a “hydrolyzed-open site” (Figure 1.3).<sup>76</sup> Moreover, the tin can be incorporated into a Beta zeolitic framework in nine different crystallographic positions, called “T sites”.<sup>69</sup> Recently, the incorporation of the tin in at least six “T sites” was identified by  $^{119}\text{Sn}$  Magic-Angle Spinning (MAS) NMR spectroscopy by Kolyagin et al.<sup>63</sup> “Open” sites in different T geometries have shown different stability and acidic behavior.<sup>77</sup> Thus, for identifying the nature of an active site, presence of defects, hydrolysis and position in the framework need to be considered in order to rationalize the activity of different sites.<sup>69</sup>

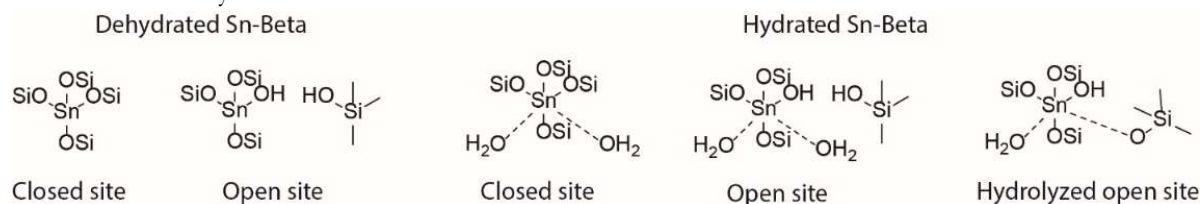


Figure 1.3. Open and close tin active sites in Sn-Beta zeolites, in agreement with Yakimov A. V. et al.<sup>76</sup>

The hydroxy groups next to the tin active site have a central role in the catalytic activity of Sn-Beta zeolites. The isomerization of glucose catalyzed by Sn-Beta zeolite has been used as reference process for the analysis of the structure-activity relation of the catalyst in many studies.<sup>78–80</sup> Results have been in agreement with the identification of the essential role of the hydroxy groups during the activation of the substrate *via* multidentate coordination and the promotion of the hydride shift.<sup>78</sup> The hydroxy groups can derive from the presence of internal silanols due to structural defects or from the adsorption of water molecules.<sup>79</sup> Thus, the different methods of preparation leading to different level of structural defects can be central for the activity. Moreover, the use of different solvents can determine the formation of hydroxy groups *in situ* during the reaction.<sup>80</sup>

The synergic activity of the hydroxy groups in the vicinity of the tin has also been identified as a responsible factor for preferential activity for the isomerization or the epimerization of glucose catalyzed by Sn-Beta zeolites.<sup>81</sup> In fact, the transition states for the two processes are different and it has been calculated that, differently from the case of the isomerization reaction, the Bilik-type transition state has lower activation energy in the absence of a hydroxy group.<sup>81</sup> The model can also explain the shift in selectivity from the isomerization of glucose to the epimerization upon post-synthetic exchange with alkali ions.<sup>82,83</sup> The alkali ion acts by exchange with the proton of a hydroxy group and eliminates the coordinative ability. The process has been studied by the use of tin silsesquioxanes as references for open active sites in Sn-Beta zeolites and results have suggested that the hydroxy groups crucial for the catalysis of isomerization and epimerization are associated with silanols adjacent to the tin.<sup>84,85</sup> Analogously, the same group has studied the catalytic activity of methyl-ligated silsesquioxanes as models for “closed” tin sites in Sn-Beta reporting significant low rates for the isomerization of glucose using this catalytic system.<sup>86</sup> The computational model proposes a reaction pathway that involves the cleavage of the Si-O-Sn bond, resulting in slower reaction rates compared to the use of Sn-Beta catalysts containing “open” sites.<sup>86</sup>

The interaction between Sn-Beta catalysts and the alkali salts has been investigated by FT-IR experiments. Otomo et al.<sup>87</sup> have explored the adsorption of deuterated acetonitrile on hydrothermal Sn-Beta modified by different alkali metals. The presence of alkali ions weakens the tin sites and the interaction of different ions is correlated to the size of the ion. Moreover, FT-IR characterizations have shown that the alkali metals interact with the silanols by ion-exchange. Density-Function Theory (DFT) calculations have demonstrated that water assumes an important role during the catalysis by the coordination around the cation, which affects the interaction between catalyst and substrate.<sup>88</sup>

Understanding how different distributions of the active sites influence the catalytic activity of the material is essential for the development of highly productive catalytic systems. In fact, the presence of spectator sites can decrease the turnover frequency of the catalyst<sup>89</sup> and sites involved in competitive reactions can decrease productivity and selectivity.<sup>90</sup> However, the development of spectroscopic techniques capable of studying the tin sites in the different configurations is still challenging. Extended X-Ray Absorption Fine Structure (EXAFS) has shown the ability to determine active sites distribution.<sup>91</sup> The use of <sup>119</sup>Sn Magic-Angle Spinning (MAS) NMR spectroscopy has allowed the characterization of the active sites in Sn-Beta zeolites<sup>75</sup> and, with the enhancement by Dynamic Nuclear Polarization, has enabled in-depth studies of the material.<sup>65,74</sup> However, the correlation between characterization studies and catalytic activity is still incomplete due to the difficult study of the catalyst in conditions similar to the reaction environments, i.e. in liquid solvents.<sup>10</sup>

## 1.1.7 Characterization of the acidity in Lewis acidic zeolites

Characterization of the acidity in solid acid is usually performed by the study and quantification of probe molecules that interact with the acid sites in the solid. The total acidity of solid acids can be determined by adsorption of pyridine or other bases in FT-IR experiments and by  $\text{NH}_3$ -TPD analysis (Temperature-Programmed Desorption).<sup>92</sup> However, the distinction of Brønsted and Lewis acid sites is usually complex because it requires the use of selective probe molecules. Ammonia is not a sensitive probe for distinguishing Lewis and Brønsted acidic sites. The use of reactive alkylamines (NPA n-propylamine) as adsorbants in TPD measurements can reveal the presence of Lewis or Brønsted sites.<sup>93</sup> In fact, these amines desorb in unchanged forms after the interaction with a Lewis acidic center, but they decompose by Hoffman elimination if protonated by the interaction with a Brønsted acid site.<sup>92,94</sup> The combined use of both ammonia and NPA allows a reliable quantification of the different types of acidity in Sn-Beta zeolites. However, NPA can overestimate the sites due to the interaction between adsorbants and terminal silanols,<sup>93</sup> especially in samples containing little amount of tin ( $\text{Si}/\text{Sn} > 150$ ) or in high presence of defects (post-synthetic preparations).

The adsorption of probe molecules and analysis by FT-IR spectroscopy have been largely applied for the study of the acidity in solid acids. Pyridine represents a common probe for quantitative analysis.<sup>93</sup> However, the reliability of the techniques can be limited by difficult accessibility of the sites using a bulky molecule. Moreover, pyridine is not able to distinguish between “open” and “closed” sites. Deuterated acetonitrile has been frequently applied as a probe molecule due to its small size and the possibility to study both Lewis and Brønsted acid sites. The interaction with the different active sites is visible with the shift of both CN and OH frequencies.<sup>95</sup> The adsorption of deuterated acetonitrile on Sn-Beta zeolites has shown the presence of two different interactions of the probe with the tin inside the zeolitic framework giving two different signals at  $2308\text{ cm}^{-1}$  and  $2316\text{ cm}^{-1}$  (Figure 1.4). These experimental results are in agreement with the catalytic activity and the theoretical simulations of open and closed active sites.<sup>70</sup> Among different probe molecules, the adsorption of deuterated acetonitrile has been identified as an optimal method for the characterization of framework tin.<sup>96</sup> The molar extinction coefficients for the interaction of deuterated acetonitrile with open and closed sites have been reported<sup>93</sup> and allow the use of the techniques for quantitative analysis.

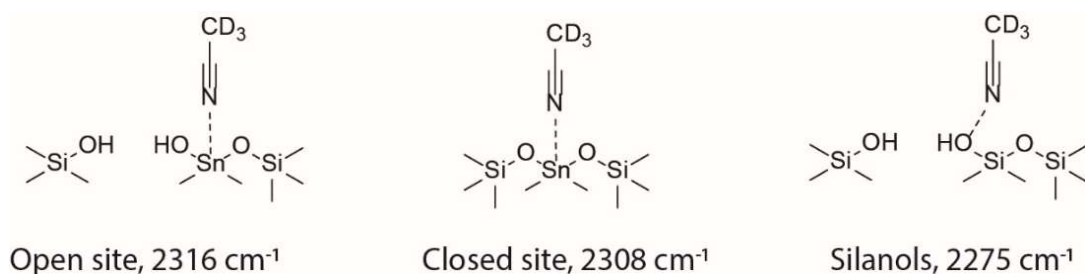


Figure 1.4. Adsorption of deuterated acetonitrile as probe for different tin sites in the framework of Sn-Beta zeolite, in agreement with Harris J. W. et al.<sup>93</sup>

More recently, Sushkevich et al.<sup>97</sup> have studied tin sites in Sn-Beta zeolites by the use of different probe molecules in FT-IR experiments. Deuterated acetonitrile, pyridine and 2,6-ditertbutylpyridine have been combined for the unambiguous identification of the sites. The bulky 2,6-ditertbutylpyridine is selective for the interaction with Brønsted acid sites and it has been applied to confirm the nature of the acid sites. In this study,<sup>97</sup> the authors have identified three types of tin sites on the surface of Sn-Beta materials: (i) Lewis acidic sites connected with the tin inside the framework, (ii) weak Brønsted acidic sites always connected with the tin inside the framework and (iii) weak Lewis acidic sites related to extra-framework tin oxide. Differently to the

previous studies,<sup>70</sup> the authors have attributed the peak of deuterated acetonitrile at 2308 cm<sup>-1</sup> to a weak Brønsted acidic site associated to tin inside the framework and not to a closed Lewis acidic site.

Probe molecules for solid state NMR characterization of the Lewis acidity in zeolites have also been described.<sup>98</sup> The adsorption of different probe molecules on Sn-Beta zeolites enriched with <sup>119</sup>Sn has been studied by <sup>119</sup>Sn Magic-Angle Spinning (MAS) NMR spectroscopy, adapted with the Carr-Purcell-Meiboom-Gill (CPMG) echo-train acquisition, in order to describe the interaction of the active sites with reactants and solvents.<sup>76</sup> The study has shown the different coordination for the interaction of water and other molecules. The adsorption of methanol and acetonitrile on tin resulted in pentacoordinated species, while hexacoordinated species were formed over time in the case of water, probably due to hydrolysis of the Si-O-Sn bonds. Finally, the hexacoordination on the strong tin sites, using isopropyl alcohol and isobutyl alcohol as probes, has suggested the possibility of dissociative interactions during the reactions with secondary alcohols.<sup>76</sup> Recently, <sup>31</sup>P NMR has been applied to characterize the active sites in Sn-Beta zeolites by the adsorption of trimethylphosphine oxide (TMPO).<sup>99</sup> The authors have optimized the correlation between different tin sites titrated with the probe and catalytic activity for the isomerization of glucose and aldol condensation reactions. The method has been proposed as a general technique for the quantitative characterization of active sites in microporous materials.<sup>99</sup>

### 1.1.8 Mechanisms of deactivation of stannosilicates during conversion of biomasses

The processes for the conversion of biomasses involve the presence of highly oxygenated compounds, which can be unstable under the reaction conditions and lead to complex polar mixtures. Thus, the catalysts encounter different conditions compared to the reactions occurring during the conversion of hydrocarbons in gas phase and the types of deactivation are different. The deactivation of heterogeneous catalysts in liquid media can be due to chemical, physical or mechanical degradation and follows mainly six types of mechanism.

1. The fouling is the process corresponding to the formation of coke in the conversion of hydrocarbons. It consists in the accumulation of insoluble products (byproducts, products or intermediates) on the catalyst, occluding the pores and the access to the active sites.
2. Mechanical degradation of the catalytic material can occur, resulting in too small particles.
3. The sintering is the process leading to the thermodynamically driven growth of crystals, a critical process under hydrothermal conditions. The process of sintering leads to the loss of surface area, reduction in the density of active sites and, in some cases, the collapse of the crystalline structures.
4. The poisoning refers to the chemisorption of species, which avoid the correct functioning of the catalyst.
5. The alteration of the active sites by the formation of new species can also occur.
6. Finally, one of the most common mechanism of deactivation for heterogeneous catalysts is the leaching of the active species in the reaction solution.<sup>100</sup>

The application of a catalytic system for industrial production requires high stability. The methods of deactivation can be irreversible or reversible, depending on the possibility of restoring the original activity by further treatments, typically by thermal methods.<sup>101</sup> Irreversible deactivation is highly undesired in process applications, but also reversible deactivation leads to additional costs and the need of regeneration steps.<sup>101</sup> Recently, studies on the intensification of the use of Sn-Beta in continuous operations have been reported.<sup>102</sup> Sn-Beta catalysts have shown high stability, productivity and selectivity for the production of bio-renewable lactone monomers by Baeyer-Villiger oxidations with H<sub>2</sub>O<sub>2</sub> as the oxidant.<sup>103</sup> Using hierarchical Sn-Beta

catalyst, the performances in the conversion of bulky ketones by the MVP reaction increase and high stability of the catalyst in continuous operation has been observed.<sup>104</sup>

The deactivation of different stannosilicates during the reactions of isomerization of xylose and dihydroxyacetone (DHA) at 100 °C has been studied considering the effect of different solvents, different zeolitic frameworks and procedures for the preparation of the catalysts.<sup>105</sup> The main mechanisms of deactivation are represented by the adsorption of carbon species on the active sites and the decrease in crystallinity. The latter process is more drastic for samples with small crystals sizes, indicating a higher tendency of losing crystallinity for materials prepared by post-synthetic procedures. Moreover, the use of water as solvent favors deactivation by coordinative changes to the metal inside the framework. In general, the higher stability of the catalyst is the main reason for the preferential choice of methanol or short chain alcohol compared to aqueous solvents. Leaching and fouling have also been addressed as mechanisms for deactivation of Lewis acidic catalysts,<sup>105</sup> however, they have not been identified as the main responsible processes.

The process of the deactivation of Sn-Beta zeolites during the isomerization of glucose in water at 100 °C has been extensively studied. Van der Graff and coworkers have compared the process with the deactivation of aluminum-containing Beta zeolites under the same conditions.<sup>106</sup> The FT-IR characterization of the spent catalysts has shown the high formation of insoluble deposits inside the micropores, leading to the obstruction of the access to the active sites. Structural deactivation has not been attributed to the leaching of tin, but to desilication resulting in increased mesoporosity. The deactivation process is accelerated by the use of water as the solvent and by the *in situ* formation of organic acids, such as the Lewis acid-catalyzed formation of lactic acid from glucose. The process for the isomerization of glucose catalyzed by Sn-Beta zeolite has been studied during continuous operation and the catalyst showed a generally high stability in organic solvents.<sup>107</sup> Thus, stability for over 700 hours was achieved for post-treated Sn-Beta zeolites at 100 °C in methanol.

The choice of the solvent has a central role in the process of deactivation of Sn-Beta zeolites during isomerization of glucose at 100 °C. The use of methanol as the solvent allows prolonged stability and only temporary deactivation, with the possible reactivation of the original properties by thermal treatment. In contrast, the use of water leads to permanent deactivation and destruction of the catalyst.<sup>107</sup> The mechanism of interaction of the water with the hydrothermal and post-treated Sn-Beta zeolites during isomerization of glucose in aqueous phase has been recently explored by Cordon et al.<sup>108</sup> The authors have shown that treatments with water gradually increased the hydrophilicity of the materials by hydrolysis of the framework. The catalytic activity of Sn-Beta zeolites requires the presence of hydroxy groups and the stability is strictly connected to the amount of silanols in the catalyst. While low density of silanols has a positive effect in the coordination and conversion of sugars molecules, a high density of silanols due to the hydrolysis of the framework destabilizes the relevant transition-states and leads to deactivation of the material.<sup>108–110</sup>

The optimum hydration of the catalyst is essential for optimal performances. The use of water as solvent leads to rapid deactivation. In contrast, the presence of small amounts of water in alcoholic reaction media improve activity, selectivity and life-time of the catalyst in continuous operation for both the isomerization of glucose at 100 °C and the conversion of fructose into methyl lactate at 160 °C.<sup>110</sup> Thus, the addition of small amounts of water prevents the deactivation of the catalysts mainly by influencing the modification of the active sites due to dehydration. The loss of Si-OH and Sn-OH species is minimized and the material is kept under the right level of hydration.<sup>109</sup>





## 1.2 Carbohydrates as an Alternative Source of Chemicals

Alternatives to the use of fossil feedstock are a central topic of interest in the current society. Technologies for the transformation of renewable sources are necessary in order to reduce the environmental impact of industrial productions. This thesis focused on the conversion of carbohydrates using zeolites as heterogeneous catalytic systems. In this section, a summary of the studied catalytic pathways is presented. Fructose is a central intermediate during the conversion of hexoses and the pathways for the production of fructose from cheaper sugars are explained. The work mainly considered the use of stannosilicates as catalysts for the conversion of carbohydrates. Sn-Beta zeolites have been successfully applied to the production of lactates,<sup>111</sup> the monomers for polylactic acids (PLA), the most common bio-based biodegradable plastics. Moreover, tin-containing zeolites have shown a generally high catalytic activity in promoting cleavages and rearrangements of carbohydrates into different  $\alpha$ -hydroxy esters.<sup>112</sup> Thus, new bio-based monomers for the production of polyesters were studied. Finally, the conversion of glycolaldehyde by cascade reactions leading to the formation of C4  $\alpha$ -hydroxy esters has been explored for the production of new bio-based chemical products.

### 1.2.1 Research for alternatives to the use of fossil feedstock

Current society is highly dependent on fossil feedstock. Most goods of the daily life are derived from petroleum. Indeed, the excessive use of fossil resources in the last centuries has caused many environmental problems. Extraction, refinery and use of oil are the main causes for the increased carbon emission into the atmosphere.<sup>113</sup> The consequences of this process include pollution and climate changes.<sup>114,115</sup> Environmental protection is then the first reason for the need to switch to different sources of energy and chemicals. All over the world, researchers from different sectors work on the optimization of the technologies required for the implementation of biorefineries.<sup>116,117</sup> Biorefineries use biomass as starting material for the production of chemicals and fuels, operating in similar ways as the petroleum-based refineries have functioned during the last centuries. Differently from hydrocarbons, biomass are highly functionalized species that cannot easily be used in gas phase. Thus, the conversion of biomass is carried out in liquid phase and aims to remove the excess of functionality. Consequently, also the platform of chemicals derived from the conversion of biomass is different from the chemicals obtained from oil.<sup>118</sup>

The word biomass indicates the organic matter derived from living plants.<sup>119</sup> Biomasses can be processed for the production of fuels and chemicals and they represent the most attractive rapidly renewable source of carbon. The use of biomass feedstock does not increase the carbon level in the air, since the gasses produced by its consumption are the same used in the photosynthetic process for the regeneration of new biomass. Therefore, finding new technologies for the transformation of plant-derived sources would be a natural method for reducing the emission of greenhouse gasses responsible for global warming.<sup>120</sup>

### 1.2.2 Sugars as bio-based feedstock for the production of chemicals

Carbohydrates are the most abundant compounds in biomass. Thus, the study of the conversion of carbohydrates into different products can bring important benefits in the development of biorefinery processes. The natural polymers cellulose and hemicellulose represent the most available resources of carbohydrates in biomasses. Cellulose is the most abundant natural polymer and represents a fundamental constituent of plant

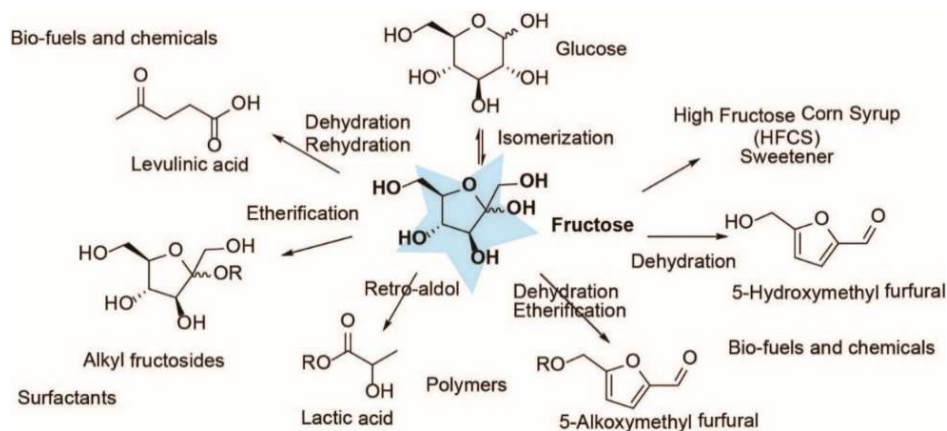


## 1.2 Carbohydrates as an Alternative Source of Chemicals

cell walls. Cellulose is formed by linear chains of glucose units connected *via* 1,4- $\beta$  glycosidic bonds. The many hydroxy groups of the monomer form a network of hydrogen bonds, which organize cellulosic chains into a crystalline structure. Thus, cellulose has high mechanical resistance.<sup>121</sup> Hemicellulose is also a part of the cellular wall in plants. It is constituted mainly by hexose and pentose sugars linked to each other irregularly. Opposite to cellulose, the presence of branches prevents a tight crystalline packaging of the chains and the polymer is amorphous. The absence of crystallinity in hemicellulose is reflected in the scarce physical and mechanical properties and in the propensity to undergo hydrolytic depolymerization in the presence of diluted acids or bases.<sup>121</sup>

Plant-derived products are commonly classified in first, second and third generation based on the origin of the converted biomass.<sup>122</sup> Simple carbohydrates belong to the first generation and their use for the production of chemicals is in competition with the dietary productions. The commercialization of bio-fuels derived from first generation biomasses has been harshly criticized, but the discussion on the most convenient source for chemicals and fuels is still open.<sup>123</sup> An optimal solution would use waste second generation biomasses derived from not edible materials. However, technologies for the efficient transformation of complex biomasses into chemical products are still not available. Second generation biomasses contain the sugar polymers cellulose and hemicellulose and the aromatic polymer lignin. The latter compound is widely studied for the potential application for the production of a novel platform of aromatic chemicals.<sup>124</sup> The use of cellulose as starting substrate is mainly limited by the difficult depolymerization of the crystalline structure. On the other hand, hemicellulose contains chemically different monomers, which complicate the selectivity control of monomer transformations. However, in both cases, the depolymerization of the natural biomass is followed by the conversion of the carbohydrate monomers into chemical products. Therefore, the study of the conversion of simple sugars remains a central topic for understanding and controlling the productivity of biorefinery processes.<sup>122</sup>

Fructose represents one of the most valuable hexoses, but is less abundant than glucose. Industrially, fructose is obtained by isomerization of glucose using glucose/xylose isomerase enzymes.<sup>125</sup> Currently, it is used in the food industry as a sweetener in the High-Fructose Corn Syrup (HFCS), which consists in a mixture of glucose and fructose derived from corn starch.<sup>126</sup> Furthermore, fructose is a key-intermediate in transformations of carbohydrates, it is reactive and can easily be converted into chemical products (Figure 1.1). Mechanistic studies have highlighted that the conversion of glucose proceeds via isomerization, forming the corresponding ketose as first reactive intermediate. Thus, fructose can be considered a platform molecule for the formation of bio-based products (Scheme 1.2).<sup>125</sup>

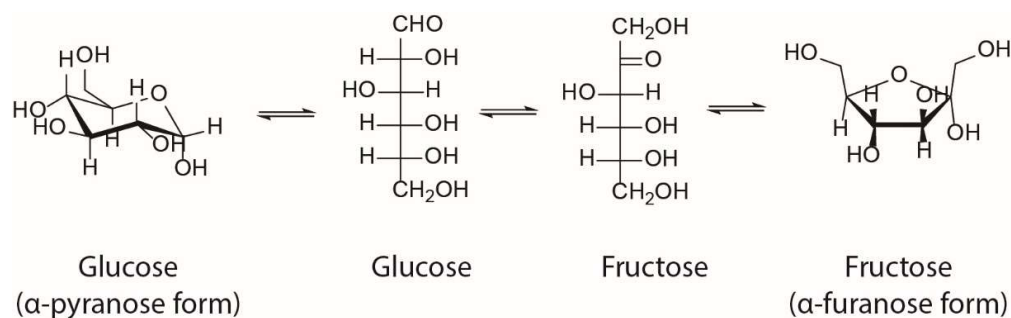


Scheme 1.2. Platform of chemicals derived from fructose.

Scheme 1.2 gives an overview of the possible products derived from fructose. Beyond the direct use as a sweetener, different chemical products can be obtained, which can be used in the production of fuels and materials. One of the most relevant processes is the dehydration of fructose to 5-hydroxymethylfurfural (HMF), which can be further converted into monomers for the production of novel polymers.<sup>127</sup> Thus, fructose represents an important substrate for the production of bio-based chemicals. However, processes for the production of fructose need to be optimized in order to apply these reactions at an industrial scale. The enzymatic procedure to obtain fructose has the general disadvantages of enzymatic reactions, such as needs of mild reaction conditions (temperature and pH), specific substrates and limited yields.<sup>125</sup> These drawbacks restrict the applicability of fructose to large-scale processes.

### 1.2.3 Isomerization of glucose to fructose

The mechanism of the isomerization of glucose to fructose catalyzed by enzymes follows three steps.<sup>128</sup> Firstly, glucose opens up to its acyclic form. Subsequently, the isomerization of the linear hexose occurs *via* a metal-assisted hydride shift between position 1 and 2. Finally, the ring closes to form fructose (Scheme 1.3).



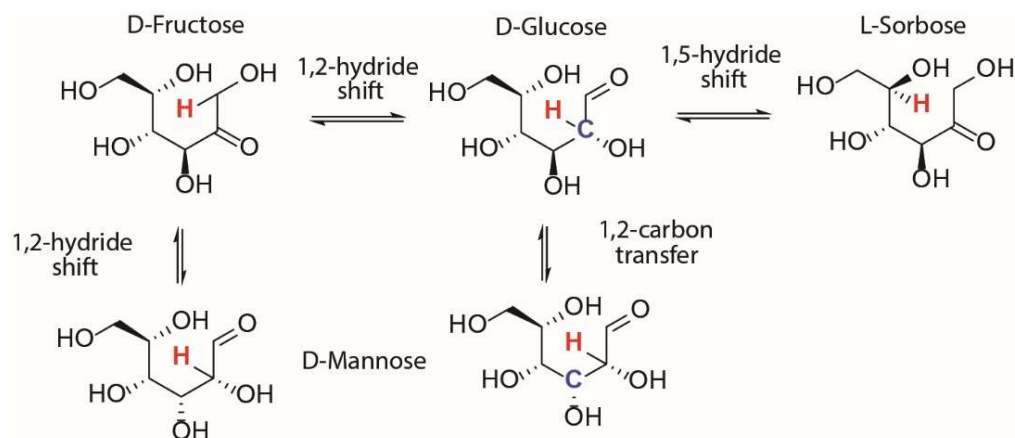
Scheme 1.3. Mechanism of the isomerization of glucose to fructose catalyzed by enzymes.

Optimal catalytic processes for the production of fructose have been investigated during the last years in order to replace enzymes and design systems resistant to a wide range of conditions and with long lifetimes. In particular, the isomerization of glucose into fructose has received much attention and many homogeneous and heterogeneous chemocatalytic systems have been proposed.<sup>125</sup> The first study of the interconversion between glucose and fructose was performed by Lobry de Bruyn and Van Ekenstein in 1895.<sup>129</sup> Afterwards, the chemocatalyzed isomerization of glucose has been extensively investigated as an alternative to the enzymatic process. In general, the reaction can be promoted by both acids and bases in homogeneous media. Considering the acidic process, high selectivity in fructose is barely obtained due to the further dehydration into 5-hydroxymethylfurfural (HMF).<sup>130</sup>

Lewis acid catalysts, such as homogeneous metal chlorides, have shown the highest activity in the chemocatalytic conversion of glucose to fructose. However, also in this case, the formation of the products derived from the dehydration of carbohydrates is favored.<sup>131</sup> The use of homogeneous Lewis acid salts as catalysts for the conversion of glucose can lead to three types of rearrangements resulting in isomeric carbohydrates. The hydride shift between positions 1 and 2 in glucose forms fructose. On the other hand, the shift between position 1 and 5 results in sorbose and the carbon transfer between position 1 and 2 gives mannose (Scheme 1.4).<sup>132</sup> Thus, optimal reaction conditions and catalyst design are needed in order to achieve high selectivity for the desired product. Although the base catalyzed process has been studied for many decades,<sup>133</sup> the use of basic catalysts is limited by the degradation of monosaccharides in alkaline media. More recently, researchers have focused on heterogeneous catalytic systems because their ease of use and recyclability

## 1.2 Carbohydrates as an Alternative Source of Chemicals

facilitate industrial applications. Several solid bases, such as metal oxides<sup>134</sup> or hydrotalcites,<sup>135</sup> and solids containing Lewis acidic metal sites<sup>136</sup> showed high catalytic activity.



Scheme 1.4. Different types of rearrangements catalyzed by Lewis acid metals starting from D-glucose.

Among the different heterogeneous catalysts, Sn-Beta zeolites have shown excellent catalytic properties for the isomerization of glucose into fructose.<sup>43</sup> The material was already known for its activity in promoting hydride shifts in MPV reductions of carbonyl compounds.<sup>38</sup> The mechanism for the isomerization of glucose catalyzed by Sn-Beta zeolites has been studied by the use of isotopic labelled glucose in <sup>13</sup>C and <sup>1</sup>H NMR experiments.<sup>137</sup> The isomerization occurs *via* intramolecular 1,2-hydride shift. Notably, Sn-Beta zeolites in solutions presented the same interaction with the substrate and the same mechanism as homogeneous Lewis acids and natural enzymes.<sup>71</sup> The same mechanism has been observed also in the case of the isomerization of xylose into xylulose.<sup>138</sup> The hydride shift between position 1 and 5 resulting in sorbose could also be promoted by Lewis acidic zeolites.<sup>139</sup> Sorbose finds application in the production of the Vitamin C.<sup>140</sup> The isomerization has been largely applied on different reactions and processes.<sup>58,141</sup>

The mechanism of interaction between carbohydrates and active sites is still under discussion. The bidentate binding of two oxygen of the sugar molecule has been initially proposed (Figure 1.5 a).<sup>137</sup> However, the presence of silanols adjacent to tin (in “open active sites”, Chapter 1.1.6) have been reported to favor the interaction between glucose and the catalyst.<sup>84</sup> Thus, the monodentate coordination of the C2-OH oxygen with the tin site and simultaneous stabilization by hydrogen-bond interaction between the carbonyl group and a silanol group adjacent to the tin has been suggested by DFT calculation (Figure 1.5 b).<sup>81</sup> On the other hand, when the silanol is not involved in the coordination of the substrate, the selectivity of the reaction changes.<sup>142</sup> In modified Sn-Beta zeolites, additional ions exchange with the protons of the silanol groups favors the epimerization of glucose *via* 1,2-carbon transfer.<sup>143</sup> The same shift in selectivity has been observed in the presence of borate salts<sup>83</sup> or using alcoholic solvents.<sup>142</sup> The presence of coordinated salts results in the catalysis of the epimerization reaction *via* Bilik mechanism, which converts glucose into mannose (Figure 1.5 c).<sup>144</sup> Thus, the catalytic system can be applied for the synthesis of rare sugars from different carbohydrates as a replacement of epimerase enzymes.<sup>145</sup>

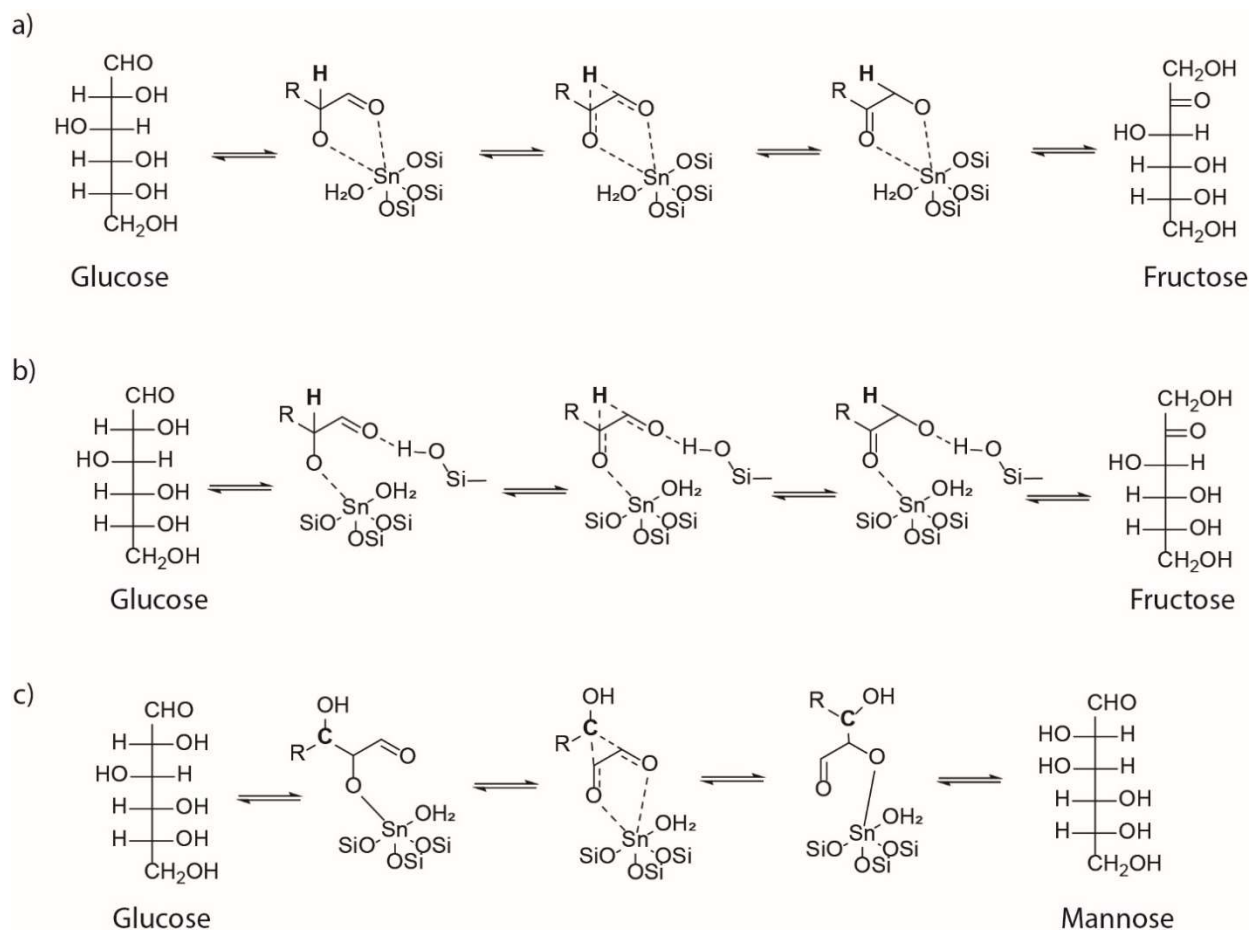


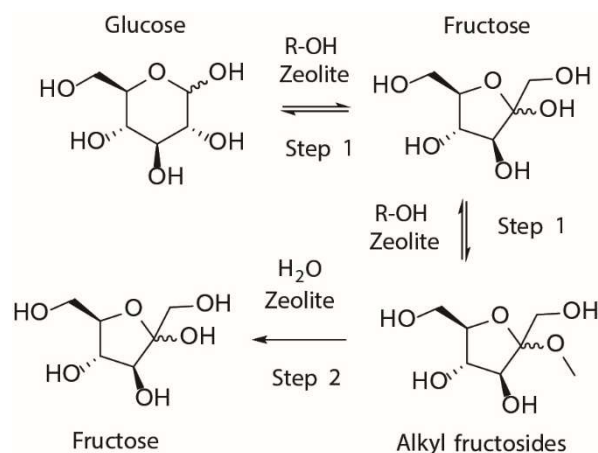
Figure 1.5. Proposed mechanisms for the isomerization and epimerization catalyzed by Sn-Beta zeolites a) 1,2-hydride shift by bidentate coordination to tin,<sup>137</sup> b) 1,2-hydride shift by monodentate coordination to tin and stabilization by interaction with a silanol group<sup>81</sup> and c) 1,2-carbon transfer during the epimerization via Bilik-type mechanism.<sup>83</sup>

The isomerization of glucose to fructose follows a first-order kinetics and the hydride-shift has been identified as rate-determining step.<sup>71</sup> The first-order kinetic constants calculated for different mono- and disaccharides show that stannosilicates are more active catalysts than titaniumsilicates and hydrophobic defect-free materials are more efficient than their hydrophilic counterparts.<sup>64</sup> Moreover, the reactions carried out in different solvents have different kinetics because the solvent molecules can compete with the substrate for the adsorption on the Lewis acidic sites.<sup>64</sup> The reactions catalyzed by heterogeneous and homogeneous Lewis acids follow the same mechanism and kinetics, as illustrated by the relevant Kinetic Isotopic Effect using either  $\text{AlCl}_3$ ,  $\text{CrCl}_3$  or Sn-Beta catalysts.<sup>146</sup> In addition, a kinetic model including parameters of deactivation of the catalyst and formation of byproducts has been studied, finding activation energy similar to the previously calculated value for tin framework sites<sup>71</sup> and confirming the loss in selectivity during the process due to the irreversible formation of byproducts.<sup>147</sup> The activation energy calculated by the group of Davis<sup>71</sup> corresponded to 21 kcal/mol and indicated the hydride shift as rate-determining step. Subsequently, Rai et al. have demonstrated that the reaction is facilitated when a silanol is adjacent to the tin active site.<sup>81</sup>

## 1.2.4 Processes for the isomerization of carbohydrates catalyzed by zeolites

Stannosilicates are the most active heterogeneous catalysts reported for the isomerization of glucose in aqueous media. First, Davis et al.<sup>43</sup> reported the increased activity of Sn-Beta zeolites for this reaction. Afterwards, many studies have been carried out in order to understand the mechanism and optimize the reaction conditions. Mesoporous frameworks have been tested, including Sn-MFI, Sn-MCM-41, Sn-SBA-15,<sup>68</sup> without resulting in high yields and the best catalytic system remained the Sn-Beta zeolite. In contrast, different studies have demonstrated that great yields of fructose are obtained tuning the properties of hierarchical zeolites.<sup>148</sup>

Saravanamurugan et al.<sup>149</sup> proposed the use of aluminum containing zeolites, such as USY, in short chain alcohols for a two-step, two-solvent system for the formation of fructose from glucose. In the first step, glucose isomerizes into fructose, which is rapidly trapped as alkyl fructosides in alcoholic solvents. Then, in the second step, the addition of water hydrolyzes the fructosides and high yields of fructose (55%) are achieved (Scheme 1.5).<sup>149</sup> The procedure allows the use of commercially available and reusable zeolite catalysts for the isomerization of glucose. The method has been applied to the isomerization of other monosaccharides, such as xylose into xylulose<sup>150</sup> and erythrose into erythrulose.<sup>151</sup>



Scheme 1.5. The two-step process for the isomerization of glucose using aluminum-containing zeolites.

The aluminum in silicoaluminates is responsible for the Lewis acidity that promotes the isomerization reactions. However, also the Brønsted acidity depends on the aluminum content (Chapter 1.1.1). High amounts of Brønsted acid sites promote the competitive formation of alkyl glucosides from glucose in the first step and make the production of fructose ineffective. <sup>1</sup>H-<sup>13</sup>C-HSQC experiments have been employed in order to distinguish the different forms of the sugars in alcoholic reaction mixtures and follow the formation of the different glycosides. Balanced Lewis and Brønsted acidity is fundamental in order to achieve high selectivity.<sup>152</sup> In all the cases presented, the zeolite H-USY (6) has shown the highest catalytic activity. Therefore, the mechanism of the isomerization of glucose catalyzed by H-USY (6) in methanol has been studied by advanced NMR techniques. The results indicate that the reaction catalyzed by aluminum-containing zeolites follows a 1,2-hydride shift mechanism, resembling the Sn-Beta and enzyme-catalyzed isomerization reactions.<sup>153</sup>

The same approach has been extended to the study of the formation of alkyl lavulins from glucose. In the proposed mechanism, glucose is converted via fructose after the formation of alkyl fructosides using alcoholic solvents. The reaction requires balanced Brønsted and Lewis acidity in order to promote both the isomerization of glucose to fructose and the following dehydration-rehydration step.<sup>154,155</sup> More recently, the possibility to produce 5-ethoxymethylfurfural (EMF) from glucose using commercial zeolites has been exploited.<sup>156</sup> These



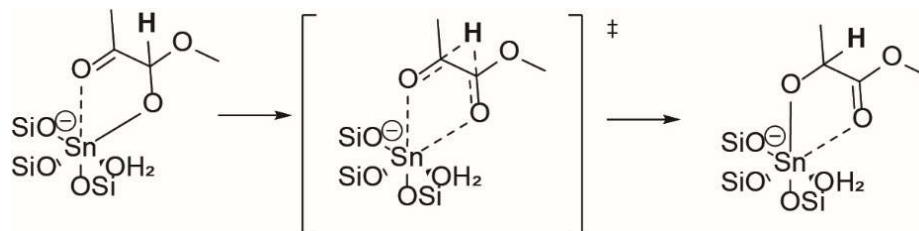
processes represent important routes for the conversion of renewable resources into bio-based chemicals and fuels since both EMF and alkyl levulinates are key intermediates in the production of different chemical products.<sup>156</sup>

### 1.2.5 The conversion of carbohydrates into alkyl lactates

During the last decade, the research into the catalytic production of 2-hydroxypropionic acid, also known as lactic acid (LA), from carbohydrates has received great attention. Lactic acid can be used as a platform-molecule for the production of different types of chemical products, such as alkyl lactates, pyruvic acid, acrylic acid and propylene glycol.<sup>157</sup> Moreover, it represents the monomer of polylactic acids (PLA), the most common bio-based and biodegradable plastics. Nowadays, LA is produced by fermentation of carbohydrates and then it is converted into the dimer L-lactide. PLA are synthesized by ring-opening polymerization of the dimer.<sup>158</sup> However, fermentation productions have some drawbacks for industrial applications, such as low productivity and complex downstream processes. Thus, many investigations have focused on finding chemocatalytic alternatives.

The first study on the conversion of trioses into lactates was reported in 2005 by Hayashi and Sasaki.<sup>159</sup> Since then, many studies have been performed on the application of homogeneous catalyst on the conversion of carbohydrates into lactates<sup>160</sup> and the best catalytic performances have been found with the use of tin halides as homogeneous catalysts.<sup>161</sup> Afterwards, heterogeneous catalysts have also been investigated. In particular, the aluminum-containing Y zeolites have shown high catalytic activity, resembling the mechanism of the biological synthesis of lactic acid catalyzed by the enzymes glyoxylases.<sup>162–164</sup> In 2009, the use of Sn-Beta zeolites as the catalysts for the isomerization of trioses in alcoholic solvents was reported. The proposed mechanism for the conversion of dihydroxyacetone (DHA) involves the dehydration into pyruvaldehyde (PAL), the formation of the hemiacetal and an intramolecular 1,2-hydride shift to form methyl lactate in methanol. The latter step can occur *via* MPV-type redox reaction (Scheme 1.6).<sup>44,163</sup> As discussed for the isomerization of glucose, the coordination of the reactant to the tin active site is still under discussion. Initially, the bidentate coordination was proposed.<sup>44</sup> More recently, DFT calculations have shown that the preferred coordination occurs only on the oxygen of the hydroxy group of PAL hemiacetal on an “open” tin site.<sup>60</sup>

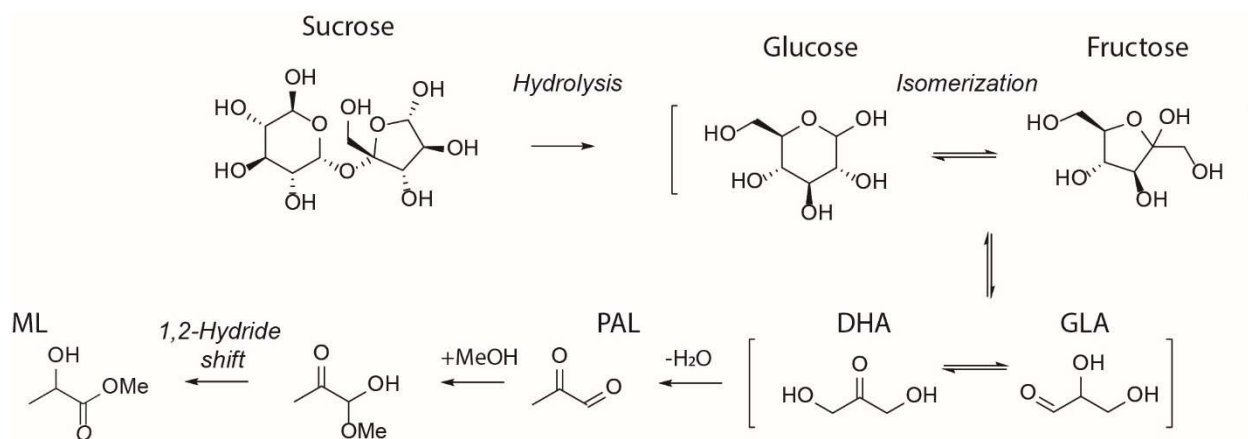
During the conversion of trioses into lactates, the first step of dehydration of DHA has been identified as the rate-determining step. The dehydration can be promoted by weak Brønsted acid sites or Lewis acid sites. On the other hand, strong Brønsted acidity is undesired due to the formation of the acetal forms of PAL.<sup>165</sup> High yields of lactates can be achieved by the use of Lewis acidic catalytic systems.<sup>166</sup> Sn-Beta zeolite catalyzes the rapid isomerization of trioses, resulting in the same yields starting from both DHA or glyceraldehyde (GLA).<sup>44</sup> In 2010, the production of lactates from hexoses at 160 °C was reported for the first time.<sup>111</sup> Hexoses are cheaper and more abundant than trioses, but their conversion involves several competitive pathways, which can produce byproducts, such as humins or furanic compounds derived by the dehydration of carbohydrates.



Scheme 1.6. Mechanism for the MPV-type 1,2-hydride shift leading to methyl lactate during the conversion of trioses in methanol, in agreement with Taarning et al.<sup>44</sup>

## 1.2 Carbohydrates as an Alternative Source of Chemicals

The mechanism for the formation of alkyl lactates from carbohydrates in methanol at 160 °C follows a cascade reaction. The conversion of different carbohydrates occurs *via* the formation of the intermediate fructose derived by the isomerization of glucose, also catalyzed by Sn-Beta zeolites. The catalyst is highly active for the isomerization step and similar yields are obtained starting from both glucose and fructose.<sup>111</sup> Thus, fructose undergoes retro-aldol cleavage resulting in trioses, dihydroxyacetone (DHA) and glyceraldehyde (GLA). The first retro-aldol cleavage of the sugar was identified as the rate-determining step of the process.<sup>111</sup> The reaction is carried out at 160 °C in methanol. Under these conditions, trioses can rapidly react by dehydration into pyruvaldehyde (PAL), addition of methanol and 1,2-hydrate shift resulting in methyl lactate (Scheme 1.7). The optimized system produce 43-44% yields of methyl lactate starting from glucose or fructose and 68% yields starting from sucrose.<sup>111</sup> The reasons for the higher selectivity of sucrose compared to the other initial carbohydrates are still unknown.



Scheme 1.7. Reaction pathway for the formation of methyl lactate from carbohydrates catalyzed by Sn-Beta zeolites at 160 °C in methanol. Formation of the intermediates glyceraldehyde (GLA), dihydroxyacetone (DHA) and pyruvaldehyde (PAL).

Other catalysts have been proposed for the conversion of carbohydrates into lactates,<sup>167</sup> but all have presented lower selectivity and the need for more drastic conditions (i.e. higher temperatures) compared to the use of Sn-Beta catalysts. In 2015, the use of alkali ions in the reactions for the production of methyl lactate from carbohydrates catalyzed by Sn-Beta was reported.<sup>47</sup> The alkali salts both in solution or added to the catalyst during the synthesis act as promoters of the process and 75% yields of methyl lactate are obtained using sucrose as starting substrate. The positive effect of alkali salts has been validated using different stannosilicates and it has been shown that the optimal concentration of the salt for the achievement of the highest selectivity to methyl lactate was different depending on the tin content.<sup>47</sup> Moreover, the effect is different using different salts, where potassium carbonate shows the best activity. Currently, addition of alkali salts in the reaction media is necessary for achieving record yields of methyl lactate. The presence of alkali ions has been observed to suppress the formation of byproducts derived from the dehydration of sugars, which is catalyzed by residual Brønsted acidity, and to promote the C-C cleavage favoring the processes for retro-aldol and epimerization reactions.<sup>168</sup> However, a generally accepted model for the interaction between alkali ions and Sn-Beta zeolite catalysts is still lacking. Different counter ions in the salts have different effects depending on the basicity of the anion. In fact, the use of basic counterions, such as carbonates, suppress side-reactions catalyzed by the Brønsted acidity.<sup>168</sup>

### 1.2.6 Insight into the processes for the conversion of carbohydrates catalyzed by Sn-Beta zeolites

The process for the formation of methyl lactate from carbohydrates catalyzed by Sn-Beta zeolites involves series of pathways leading to complex mixtures of intermediates, products and byproducts. Changes in the reaction conditions can tune the selectivity into the products and the possibility to produce new chemical compounds have been investigated.<sup>169,170</sup> In fact, the process produces several  $\alpha$ -hydroxy acids, which can be applied as building blocks for new bio-based polymers. The monomers obtainable during the conversion of common carbohydrates catalyzed by Sn-Beta in methanol include 2,5,6-trihydroxy-3-hexenoate (THM), methyl vinyl glycolate (MVG), methyl 2,5-dihydroxy-3-pentenoate (DPM), 3-deoxy esters (3DE) and lactones (3DL) (Figure 1.6). Advanced 1D and 2D NMR experiments have been applied in order to elucidate the different mechanisms occurring during the process.<sup>171</sup>

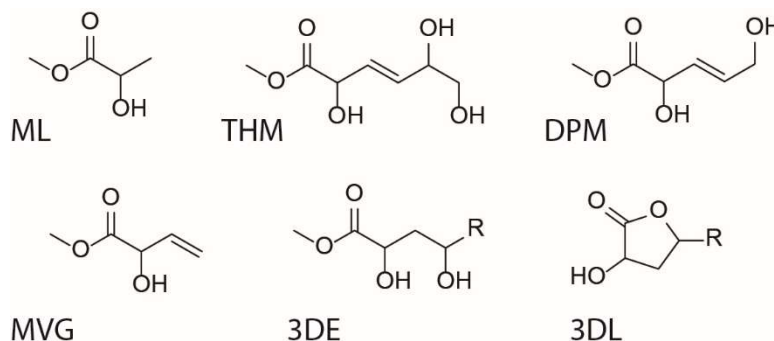
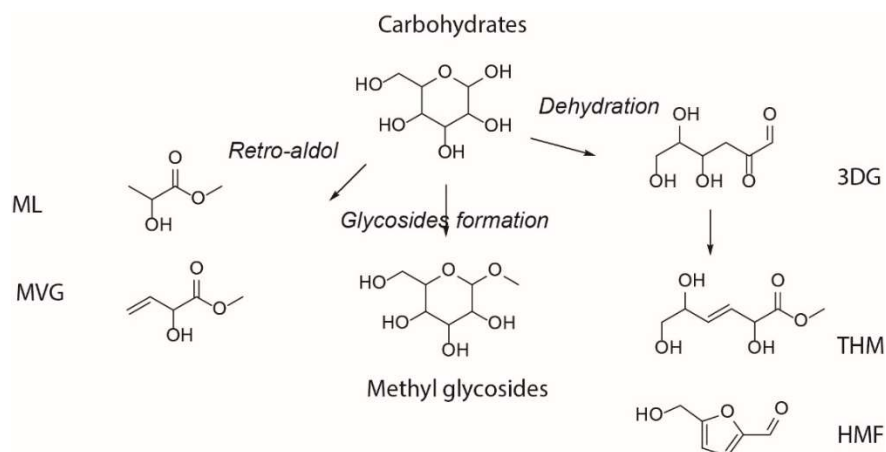


Figure 1.6. Structures of the  $\alpha$ -hydroxy esters obtained during the conversion of common carbohydrates catalyzed by Sn-Beta zeolites in methanol. Methyl lactate (ML), 2,5,6-trihydroxy-3-hexenoate (THM), methyl 2,5-dihydroxy-3-pentenoate (DPM), methyl vinyl glycolate (MVG), 3-deoxy esters (3DE) and lactones (3DL).<sup>172</sup>

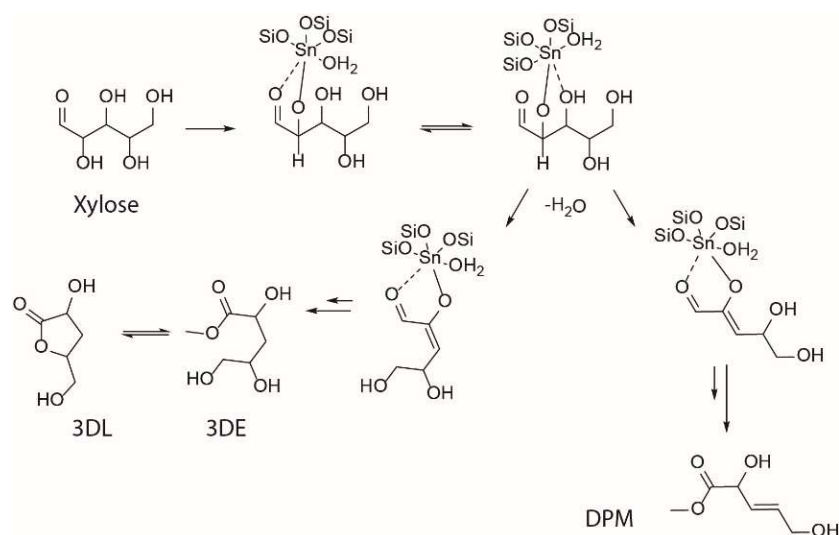
In general, three types of pathways are recognizable during the reactions at 160 °C in methanol. The retro-aldol glycolysis pathway leads to the formation of methyl lactate as already explained. The same process is also responsible to the formation of larger hydroxy esters, such as MVG (Scheme 1.8), derived from the [4+2] retro-aldol cleavage of glucose forming erythrose and glycolaldehyde. On the other hand, the presence of residual Brønsted acidity, derived from the catalyst or from species formed *in situ* during the process, promote the formation of methyl glycosides. Finally, the Brønsted acidity also catalyzes the formation of products derived from the dehydration of sugars, such as furanic compounds.<sup>112</sup> Analysis of the mechanism have shown that the pathway for the conversion of glucose catalyzed by Sn-Beta zeolites is analogous to the biological Embden-Meyerhof-Parnas glycolysis, where glucose is oxidated to gluconic acid and dehydrated to 3-deoxyglucosonic acid, the intermediate that undergoes retro-aldol cleavage to lactate.<sup>173</sup> Analogously, Sn-Beta catalyst promotes the dehydration of glucose leading to the intermediate 3-deoxyglucosone (3DG), which is subsequently converted by further dehydration into THM or HMF. The presence of small amounts of alkali suppresses the dehydration pathway, resulting in a larger amount of substrate available for the retro-aldol cleavage and in higher yield of methyl lactate.<sup>112</sup>





Scheme 1.8. The three main pathways during the conversion of carbohydrates in methanol catalyzed by Sn-Beta zeolites and structure of the intermediate 3DG.

The process has been studied for the conversion of different types of carbohydrates, exploring the possibility to obtain molecules similar to lactates, which, opposite to lactates, are not abundant metabolites and thus could not be obtained by classical fermentation. In general, glycolytic pathways have been observed to form hydroxy esters, which can be applied as building blocks for the production of polyesters.<sup>160</sup> The conversion of pentoses has resulted in the formation of a new chemical, methyl 2,5-dihydroxy-3-pentenoate (DPM) as the main product. DPM has shown good results in the formation of polymers containing functionalities that allow post-synthetic modifications.<sup>174</sup> The mechanism and the intermediates involved in the process for the conversion of pentoses and hexoses have been investigated in detail by the use of advanced NMR techniques<sup>171</sup> and isotope tracking.<sup>172</sup> The study has confirmed the analogy with the mechanism of the glycolysis catalyzed by enzymes, where the keto-forms of the sugars are the reactive species and undergo retro-aldol cleavage. Experimental data have suggested the formation of an enol intermediate strongly coordinated to the catalyst, leading to DPM, 3DG and 3DL in a multistep catalysis (Scheme 1.9). The main side-reactions derive from different rearrangements of unconverted carbohydrates, such as 1,5-hydride shift, 1,2-hydride shift and 1,2-carbon transfer.<sup>172</sup>



Scheme 1.9. Mechanism for the formation of 3DE and 3DL during the conversion of D-xylose catalyzed by Sn-Beta zeolites, in agreement with Elliot et al.<sup>172</sup>

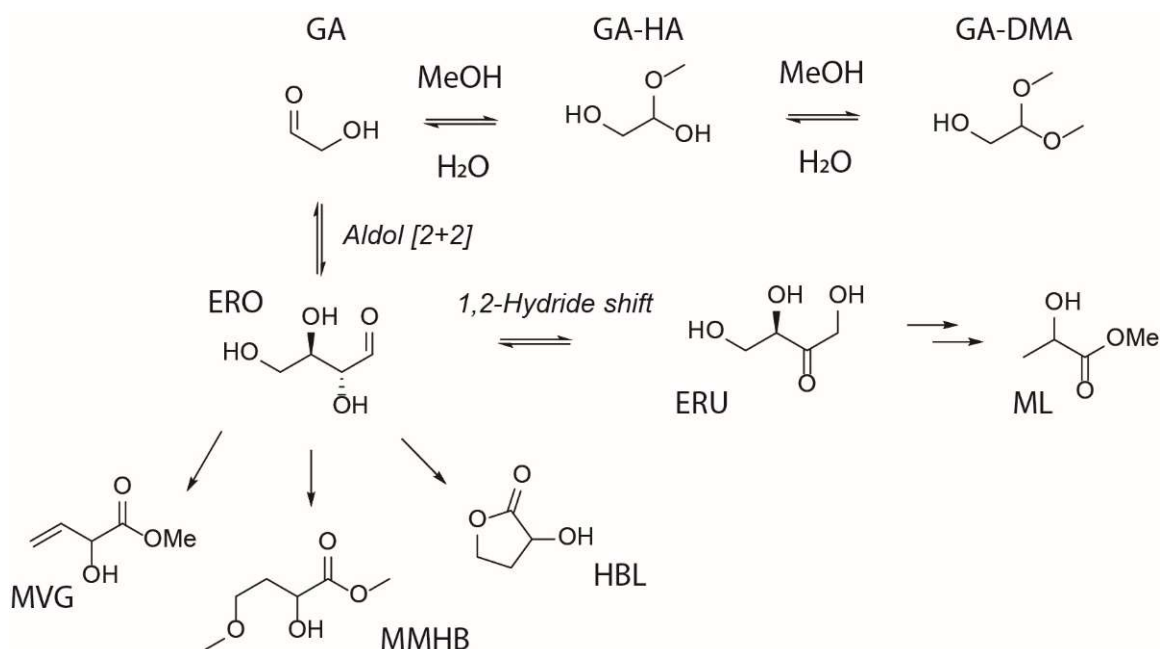
Moreover, C4 hydroxy esters, such as methyl vinyl glycolate (MVG) and methyl-4-methoxy-2-hydroxybutanoate (MMHB), are obtainable from tetroses and glycolaldehyde (GA). The same products have been observed also in the final reactions derived from the conversion of hexoses, as the consequence of the formation of tetroses and glycolaldehyde *in situ* due to retro-aldol cleavage of glucose.<sup>111,165</sup> Thus, cascade-processes from carbohydrates to hydroxy esters catalyzed by Sn-Beta zeolites in methanol allow the application of the reactions in the production of new bio-based building blocks for polyesters.<sup>160</sup>

### 1.2.7 Conversion of glycolaldehyde into methyl vinyl glycolate

Glycolaldehyde (GA) is a two-carbon molecule and, since it is the smallest  $\alpha$ -hydroxy aldehyde available, it can be considered the precursor of the carbohydrate series. Free GA monomer is a gas and it is commercialized as cyclic dimer. Glycolaldehyde is formed during the fast pyrolysis of cellulose<sup>175</sup> and represents one of the major components of the obtained bio-oils.<sup>176,177</sup> The separation of GA from the pyrolysis oil has been extensively optimized, implying the possibility for GA to be among the cheapest available biomass-derived compounds.<sup>178,179</sup> Alternatively, glycolaldehyde can also be produced by retro-aldol cleavage of glucose under subcritical hydrothermal conditions.<sup>180</sup> Saccharides are life-essential compounds and the role of GA in the origin of life has been proposed.<sup>181</sup> The formose process involves cascade-reactions consisting in aldol condensations, which lead to complex mixtures of carbohydrates. The synthetic pathway is unselective and it is stopped by the presence of salts such as borates or silicates that stabilize specific forms of sugars and avoid further condensations.<sup>182</sup>

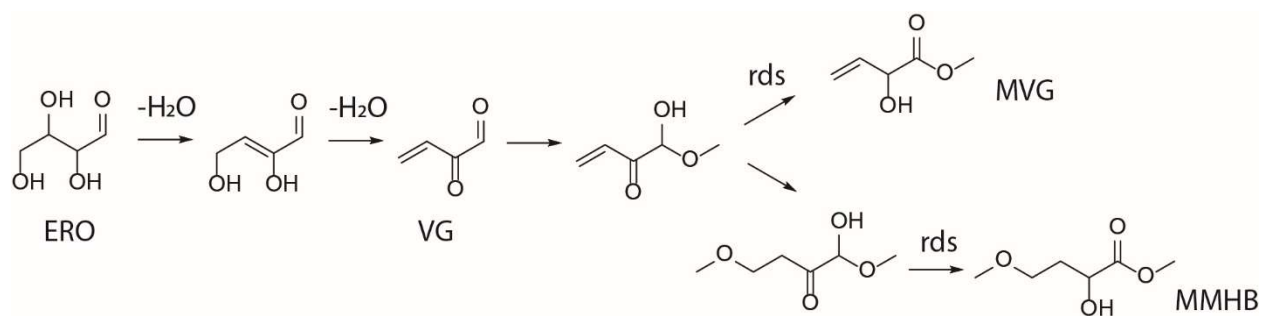
The formose process has inspired researchers to propose bio-mimetic catalytic routes based on cascade aldol condensations for producing new chemical products from glycolaldehyde. The process for the conversion of GA into monomers for polyesters has been first studied using tin halide salts as catalysts in methanol at 90 °C.<sup>183</sup> The reactions lead to the formation of methyl-4-methoxy-2-hydroxybutanoate as the main product, which has been tested for applications in polymers. In contrast, with Sn-Beta zeolite as the catalyst, methyl vinyl glycolate (MVG) is found as the main product.<sup>136</sup> The change in selectivity has been ascribed to shape selectivity due to the greater size of MMHB compared to MVG. Thus, in the process catalyzed by mesoporous stannosilicates, the formation of MMHB is preferred and microporous catalysts favor high yields of MVG.<sup>184</sup> The confinement effects of stannosilicates during the conversion of glycolaldehyde in water at 90 °C has also been studied.<sup>185</sup> Using Sn-MFI catalysts, with smaller pores than Sn-Beta, tetroses are formed as main the products from the aldol condensation of two GA molecules, while the use of zeolites with large porosity lead to the formation of hexoses. Moreover, it has been demonstrated that the conversion of tetrose carbohydrates, promoted by Sn-MFI zeolite, results in high yields of the vinyl glycolic acid (VGA) during prolonged reaction times.<sup>185</sup>

From a mechanistic point of view, the formose-like process resulting in C4 hydroxy esters starting from GA resembles the process for the formation of lactates from trioses. GA can act as both *donor* and *acceptor* in an intermolecular reaction leading to the formation of the erythrose (ERO). Sequentially, ERO can undergo dehydration, addition of methanol and 1,2-hydride shift to form MMHB and MVG using methanol as the solvent (Scheme 1.10). The selectivity between the two products depends on the position of the addition of the methanol.<sup>169</sup> Using alcoholic solvents at 90 °C, GA is rapidly thermally transformed in the hemiacetal (GA-HA), but it takes 24 hours to convert it to the dimethyl acetal (GA-DMA). The study by Dusselier et al.<sup>183</sup> proposed that the balance between the three forms is rate-determining. In fact, the process can be accelerated by the presence of a balanced amount of Brønsted acidity (that catalyzes both acetalization and hydrolysis of GA-DMA) or additional water. After the aldol condensation of GA, erythrose is a central intermediate for the formation of different products.



Scheme 1.10. Proposed reaction pathways for the conversion of glycolaldehyde in methanol promoted by tin-containing catalysts.

The formation of the different products can be explained by considering the mechanisms for the Lewis acid-catalyzed conversion of tetroses. The proposed mechanism follows two consecutive dehydrations to form the intermediate vinylglyoxal (VG) from erythrose (Scheme 1.11). The addition of methanol forms the hemiacetal, which determines the selectivity for the different products.<sup>169</sup> The formal intramolecular Cannizzaro reaction gives MVG. In contrast, the addition of a second molecule of methanol, followed by the formal Cannizzaro reaction forms MMHB. Using tetroses as starting substrates, the last step has been proposed as the rate-determining step (Scheme 1.11).<sup>169,183,184</sup> Methyl lactate has also been observed as a minor product of the reaction. Different routes have been identified using alkaline hydrothermal conditions.<sup>186</sup> Using Lewis acidic catalyst, the mechanism involves the cleavage of the ketose erythrulose leading to formaldehyde and glyceraldehyde.<sup>186</sup> Another route, favored in non-alcoholic solvents (acetonitrile), leads to an intramolecular cyclization, resulting in  $\alpha$ -hydroxy- $\gamma$ -butyrolactone (HBL) (Scheme 1.10).<sup>187</sup> Another bio-based synthesis of the same product can be performed by intermolecular aldol condensation of DHA and formaldehyde derived from the cleavage of carbohydrates.<sup>188</sup> Synthetically, HBL represents a further interesting bio-based product and it can be used as an intermediate for the production of herbicides and pharmaceuticals.<sup>189</sup>



Scheme 1.11. Mechanism for the formation of MVG and MMHB from tetroses, in agreement with Dusselier et al.<sup>169,183,184</sup>

MVG contains a terminal vinyl group, which is critical when the compound is applied as part of polymers because it allows further functionalization and adjustable properties of the derived materials. Thus, considering the two main products derived from the conversion of glycolaldehyde, MMHB is less interesting than MVG for polymer applications. The incorporation of vinyl glycolic acid (VGA) in polylactic acids has been already reported.<sup>183</sup> The terminal vinyl group of VGA has good reactivity and the derived polymeric chains can be modified by addition of thiols. Thus, MVG allows a wide range of applications in the polymer industry. The reaction of homo metathesis of MVG, followed by further modifications, allows producing new bio-based dicarboxylic acids, which have been studied as building blocks for the production of polyesters and polyamides.<sup>190</sup> Transformations of MVG into different compounds with potential commercial applications have been reported in the literature<sup>191</sup> and MVG can be considered a bio-based platform molecule for obtaining different chemical products.

### 1.3 Aim of the thesis

The Ph.D. project was carried out at the Technical University of Denmark in collaboration with Haldor Topsøe A/S and Perstorp AB, with the financial support of the Innovation Fund Denmark. The project aimed to study routes for the production of bio-based monomer polymers. The conversion of carbohydrates into hydroxy esters using Lewis acidic zeolites as catalysts represents a valid alternative to the use of fossil feedstock for the production of polymer building blocks. The work investigated the catalytic pathways for the conversion of different carbohydrates by time-resolved experiments in order to identify intermediates, competitive pathways and parameters relevant for the control of the product selectivity. The project aimed to enhance the current knowledge on the reactions involved during the conversion of hydroxy esters from carbohydrates and the used catalytic systems.

The thesis is divided into different chapters and the results are discussed from Chapter 3 to 6. Chapter 3 considers the conversion of hexoses into intermediates for the production of bio-based chemicals. The discussion explores a new process catalyzed by commercially available zeolites for obtaining fructose. Since zeolites showed improved stability in alcoholic solvents, the reactions were carried out in methanol. Under these conditions, the formation of methyl glycosides assumes a central role in the selectivity and kinetics of the processes. Thus, the role of methyl glycosides during the conversion of carbohydrates in methanol was explored. In particular, the formation of methyl fructosides showed great impact on the kinetics of the process for the conversion of hexoses to methyl lactate in methanol at 160 °C catalyzed by Sn-Beta zeolites. The formation and conversion of substrates, intermediates and products in the reaction mixture was studied at the NMR center DTU using a toolbox of 1D and 2D NMR experiments at high magnetic field (mostly using an 800 MHz instrument equipped with cryogenically cooled probehead).

Chapter 4 focuses on the study of the process for the conversion of glycolaldehyde, a bio-based C2 aldehyde, using Sn-Beta zeolite as the catalyst in methanol at 160 °C. The process leads to the formation of methyl vinyl glycolate (MVG) as the main product, which represents an interesting chemical compound for applications in the polymer industry. Finally, Chapters 5 and 6 discuss the study and the optimization of the stannosilicate catalytic system. The understanding of structure-activity relations is essential in order to achieve high control over the selectivity in the products. The selectivity in processes catalyzed by Sn-Beta zeolites has been affected by the presence of additives, such alkali salts, in the reaction media. Thus, the interaction between the catalyst and additives has been extensively studied. In Chapter 5, the discussion focuses on modifications on the synthesis of the catalytic systems in order to develop zeolites for the selective conversion of carbohydrates into chemical products. Chapter 6 proposes methods for catalyst characterization with the aim to understand the structure-activity relation. Finally, Appendix A reports a complementary study on the mechanism of the conversion of glucose using Lewis acidic salts and Appendix B explores possible applications for methyl vinyl glycolate (MVG) as bio-based reagent for the production of coatings.

# Chapter 2

## Experimental Methods

This chapter includes the detailed descriptions of the experimental methods used for obtaining the results discussed in this thesis. In general, the study included three main fields of experimental work. First, the catalytic materials were studied in order to understand the features required to achieve high catalytic activity and to design optimal systems. Second, the conversion of carbohydrates and the formation of products and intermediates in the reaction mixtures was investigated by NMR spectroscopy. Third, the reactions were studied *ex situ* by time-resolved experiments in order to clarify the catalytic pathways and the effect of different reaction conditions on the selectivity of the processes.

### 2.1 Experimental Methods for the Preparation and the Characterization of the Catalytic Materials

The synthesis of stannosilicate catalysts followed two approaches, the hydrothermal synthesis and the post-synthetic modification of commercial Beta zeolite. The study of the effect of modifications in the synthetic procedure focused on the use of post-synthetic materials, because the ease and the large applicability of the procedures. The effect of different procedures on the catalytic activity is discussed in Chapter 5. Mesoporous materials and modified catalysts were prepared and studied. Moreover, the structural features of the zeolites were characterized using different techniques and the results were used for deducing structure-activity relations.

#### 2.1.1 Procedures for the synthesis of stannosilicates

##### **General procedure for the preparation of Sn-Beta zeolites by hydrothermal synthesis**

Hydrothermal synthesis of Sn-Beta zeolites was performed in the laboratories of Haldor Topsøe A/S under the supervision of Dr. Søren Tolborg. For the preparation of hydrothermal Sn-Beta zeolites, the procedure proposed by Corma et al.<sup>36</sup> was followed using slight modifications.<sup>52</sup> In a typical synthesis, 30.6 g of tetraethyl orthosilicate (TEOS, Sigma-Aldrich, 98%) were mixed to 33.1 g of tetraethylammonium hydroxide (TEAOH, Sigma-Aldrich, 35% aqueous solution) and stirred for 30 minutes at room temperature. Afterwards, 2 mL of a solution of  $\text{SnCl}_4 \cdot 5\text{H}_2\text{O}$  (Sigma-Aldrich, 98%) in water were added dropwise to the mixture in the calculated concentration for obtaining the desired Si/Sn ratio. The mixture was kept under magnetic stirring for one day, until complete evaporation of the ethanol formed during the TEOS hydrolysis and the formation of a thick gel. Then, 3.1 g of hydrofluoric acid (HF, Fluka, 47-51%) diluted in 1.6 g of water were added to the final gel. The compound was gently stirred until reaching a dried white solid. Finally, the product was transferred in a stainless steel autoclave and crystallized at 140 °C for 2-4 weeks, depending on the content of tin.<sup>52</sup> After the crystallization, the zeolite was filtered, washed with abundant water, dried at 80 °C overnight and calcined in air at 550 °C for 6 hours using a temperature ramp of 10 °C/min.

## 2.2 Preparation and Characterization of the Catalysts

---

The hydrothermal synthesis of an aluminum-free Mn-Beta zeolite was explored (Chapter 6.3.5), following the synthesis proposed by He et al.<sup>192</sup>

### General procedure for the preparation of Sn-Beta zeolites by post-synthetic treatment

Post-treated Sn-Beta zeolites were prepared by following the procedure proposed by Hammond et al.<sup>55</sup> A commercial aluminum-containing Beta zeolite (Zeolyst, Si/Al 12.5) was dealuminated in 13 M HNO<sub>3</sub> (VWR, 65%; 20 mL/g(zeolite)) at 100 °C for 20 hours. The zeolite was washed with water until reaching neutral pH and dried overnight at 120 °C. The tin (or other metals in the case of the preparation of M-Beta or Sn-M-Beta zeolites, Chapter 6.3.3) was incorporated inside the framework of the dealuminated Beta zeolite by incipient wetness impregnation of aqueous solutions of the calculated amount of SnCl<sub>4</sub>·5H<sub>2</sub>O (Sigma-Aldrich, 98%) to obtain the desired Si/Sn ratio. Subsequently, the material was dried overnight at 120 °C and calcined in air at 550 °C for 6 hours using a temperature ramp of 10 °C/min.

In Chapter 3.1, the thermally dealuminated Beta zeolite was obtained by treatment at 750 °C in air for 6 hours. In Chapter 5, different modifications to the procedure for the preparation of post-synthetic Sn-Beta zeolites are discussed. The removal of extra-framework tin oxide species was explored following the method reported by Pidko et al.<sup>60</sup> In this case, further methanol washes of the catalyst were added to the procedure for the preparation of post-synthetic Sn-Beta after the impregnation with Sn. Then, the material was dried and calcined as already described. The preparations of post-synthetic stannosilicates using different zeolitic frameworks followed the same procedure as described above. The possibility of preparing Sn-MOR, Sn-MFI and Sn-USY catalysts were explored and described in Chapter 5.2.1.

### Preparation of Sn-Beta catalysts containing different contents of potassium

The interaction between alkali salts and tin active sites in Sn-Beta zeolites was investigated in terms of the catalytic activity and structural changes. Samples for the *ex situ* characterization using ammonia as probe molecule described in Chapter 6.2.2 were prepared by post-treatment. Differently from the preparation described above, samples of the dealuminated zeolite were impregnated with aqueous solutions of SnCl<sub>4</sub>·5H<sub>2</sub>O (Sigma-Aldrich, 98%) and K<sub>2</sub>CO<sub>3</sub> for different concentrations of potassium corresponding values of K/Sn of 0, 0.2, 1 and 2. The catalysts were dried (120 °C, overnight) and calcined (550 °C, 6 h, air).

Alkali-containing Sn-Beta zeolites for the analysis of FT-IR *in situ* adsorption of deuterated acetonitrile were prepared differently in order to simulate the concentration of potassium interacting with the catalyst during the conversion of carbohydrates (Chapter 6.2.3). 400 mg of post-synthetic Sn-Beta (Si/Sn 100) zeolite catalysts were added to 22 mL solutions containing different concentrations of potassium carbonate in water (0.4 mM and 3.0 mM). The suspensions were kept under magnetic stirring for three hours and the catalysts were recovered by filtration and dried overnight at 120 °C.

## 2.1.2 Procedures for the preparation of mesoporous stannosilicates

Synthesis of mesoporous stannosilicates were performed at the Department of Chemistry, Technical University of Denmark, with the help of MSc. Annalisa Sacchetti.

### Procedure for alkaline desilication<sup>104</sup>

The commercial aluminum-containing zeolite was desilicated by alkaline treatment in NaOH 0.2 M, 30 mL g<sup>-1</sup> at 45 °C for 30 minutes. The sample was then filtered and washed with deionized water until reaching neutral pH. The catalyst was dried at 120 °C overnight and used for the preparation of stannosilicates.

**Surfactant templating post-treatment<sup>193</sup>**

The tin-containing zeolite (2.5 g) was added to a solution of cetyltrimethylammonium bromide (CTAB, 1.75 g) in  $\text{NH}_4\text{OH}$  (160 mL, 0.37 M). After 20 minutes of stirring, the suspension was transferred to a Teflon-lined stainless steel autoclave for hydrothermal treatment (150 °C, 10 hours). Afterwards, the sample was filtered, washed with deionized water, dried at 70 °C overnight and calcined in air (550 °C, 6 hours).

**Dissolution-reassembly post-synthesis<sup>194</sup>**

The commercial aluminum-containing zeolite (1 g) was stirred in  $\text{NH}_4\text{OH}$  (64 mL, 0.36 M, 2 hours). Cetyltrimethylammonium bromide (CTAB, 0.7 g) was then added and the final mixture transferred to a Teflon-lined stainless steel autoclave for hydrothermal treatment (150 °C, 48 hours). Afterwards, the sample was filtered, washed with deionized water, dried at 70 °C overnight and calcined in air (550 °C, 6 hours).

**Procedure for the hydrothermal synthesis of mesoporous Beta zeolite<sup>195</sup>**

Fumed silica (4.8 g) was added to a prepared solution of NaOH (0.16 g) and  $\text{NaAlO}_2$  (0.3 g) in tertaethylammonium hydroxide (TEAOH, 32 mL). The mixture was stirred manually to obtain a homogeneous gel and polydiallyldimethylammonium chloride (PDADMA, 3.0 g) was added. The gel was kept under stirring at room temperature (24 hours) and transferred to a Teflon-lined stainless steel autoclave for hydrothermal crystallization (7 days, 140 °C). The obtained aluminum-containing Beta zeolite was then used for the preparation of a post-treated mesoporous Sn-Beta catalyst.

### 2.1.3 Characterization of the catalytic materials

**Ammonia Temperature-Programmed Desorption ( $\text{NH}_3$ -TPD)**

The quantification of the acidity of the samples by  $\text{NH}_3$ -TPD was performed using a Micrometrics AutoChem II 2920 Chemisorption Analyzer. Zeolite powders (100 mg) were inserted into a glass U-tube reactor supported between two quartz wool plugs. In a typical analysis, the sample was pre-treated in helium at 500 °C (ramp of 20 °C/min) for 110 minutes. The adsorption of ammonia was carried out at 150 °C for 30 minutes, the gas flow was changed to helium and the physisorbed ammonia was removed by waiting for 230 minutes. The desorption was carried out between 150 °C and 600 °C using a temperature ramp of 10 °C/min.

**FT-IR experiments of *in situ* desorption of ammonia**

Experiments for the characterization of Sn-Beta zeolites by FT-IR ammonia desorption were performed at the Department of Chemistry, Technical University of Denmark. The experiments were carried out with the help of Principal Scientist Søren B. Rasmussen (Haldor Topsøe A/S). Samples were prepared by pressing 15 mg of zeolite into pellets of 0.8 cm diameter, which fit into the sample holder of a specially designed *in situ* reaction transmission cell equipped with KBr windows (Figure 2.1). Spectra were acquired on a Thermo Scientific Nicolet iS5 spectrometer using Omnia Spectra software. Final elaboration of the data was performed in OriginPro 2018 and processed as described for the experiments of adsorption of deuterated acetonitrile. The reactor was designed for including two compartments dedicated to the acquisition of the background and the sample. During the measurements, it was possible to change *in situ* the position of the holder between the background and sample compartment. The reactor was equipped with a gas-inlet connected to different lines, a water-cooling system and a manual temperature controller.

In a typical experiment, the sample was pre-treated at 500 °C in helium flow for 110 minutes. The adsorption of ammonia was done at 150 °C for 30 minutes and then the physisorbed ammonia was removed in helium flow at 150 °C for 230 minutes. The desorption was carried out step-wise by increasing the temperature manually each 50 °C. Spectra and background were recorded every 50 °C.



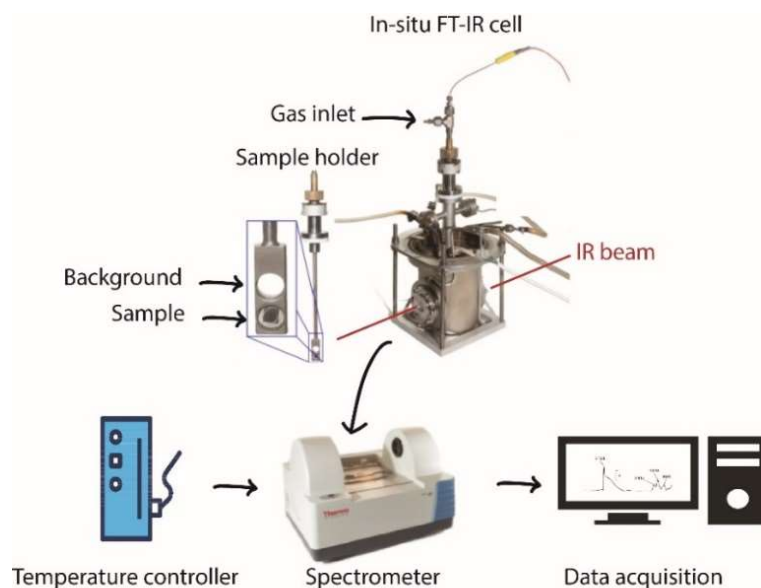


Figure 2.1. FT-IR set-up for experiments of adsorption of ammonia probe molecule, equipped with *in situ* reaction transmission cell.

### FT-IR experiments of *in situ* adsorption of deuterated acetonitrile

FT-IR experiments of adsorption of deuterated acetonitrile were carried out at Haldor Topsøe A/S with the help and under the supervision of Research Scientist Juan S. Martinez-Espin (HTAS). Zeolites were prepared by pressing 20 mg of sample into pellets of 1 cm diameter, which fit into copper envelopes made for the quartz cell shown in Figure 2.2. Samples were connected to a vacuum circulating system and evacuated overnight at room temperature and for 1 hour at 450 °C. After the pre-treatment, the background and blank spectra were acquired. Then, increasing amounts of acetonitriles- $d_3$  were adsorbed *in situ* onto the samples and FT-IR spectra at different pressures were collected (from  $1.5 \times 10^{-2}$  mbar to 4.5 mbar). At the end of the adsorption, the samples were evacuated at room temperature for 20 minutes and the final desorption spectra were recorded. Spectra were recorded on a Vertex 70 spectrometer and analyzed using Bruker OPUS software. Final analysis of the data was performed using OriginPro 2018.

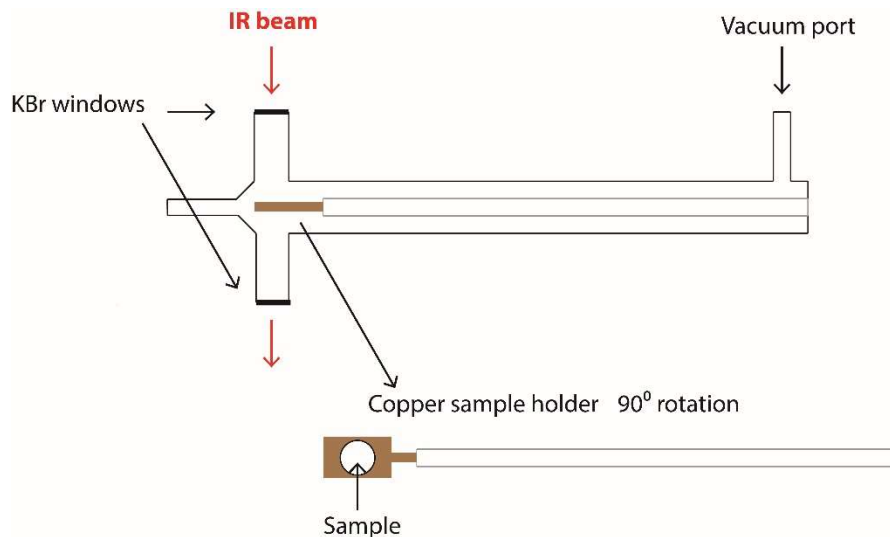


Figure 2.2. Schematic representation of the quartz vacuum cell for *in situ* FT-IR adsorption of probe molecules.

FT-IR spectra were recorded in the range 7500-380  $\text{cm}^{-1}$ , by accumulating 64 scans at 2  $\text{cm}^{-1}$  resolution. The analysis of the collected data was performed using OriginPro 2018 software. The spectra shown in this thesis were baseline-corrected and normalized to the vibrations of the Beta zeolite Si-O-Si stretch band (1700-2100  $\text{cm}^{-1}$ ).

### **Powder X-Ray Diffraction**

The technique was applied to confirm the crystalline structures of the catalytic materials and investigate the formation of crystalline extra-framework metal oxides. The characterization by Powder X-Ray Diffraction (XRD) was carried out both at the Technical University of Denmark (DTU) and at Haldor-Topsøe A/S with the help of specialized technicians. In the first case, diffractograms were collected using a Huber G670 with imaging-plate Guinier powder-diffraction camera using Cu-K $\alpha$  radiation ( $\lambda = 0.154184$  nm). At Haldor Topsøe A/S, the XRD patterns were acquired by X'Pert diffractometer (Philips) with Cu-K $\alpha$  radiation.

### **Elemental analysis**

The elemental composition of the prepared materials was confirmed using different techniques for the different cases. X-Ray Fluorescence (XRF) characterization was carried out using a PANanalytical epsilon3-XL instrument. Samples were analyzed in powder or after preparation of fused glass disk with lithium borate. Preliminary calibration of the signal allowed the determination of Si/Al and Si/Sn ratio. Some samples were characterized at Haldor-Topsøe A/S with the help of specialized technicians. The XRF analyses were carried out on a Supermini 200 (Rigaku) instrument. For element with expected amounts of less than 0.2 wt%, the characterization was performed by Inductively Coupled Plasma-Atomic Emission Spectroscopy (ICP-OES) on a OPTIMA 7300 instrument from Perkin Elmer.

### **Pore and surface analysis**

Isotherms of adsorption and desorption of nitrogen were measured for the investigation of pore volumes and surface area. Analyses were carried out at the Technical University of Denmark and at Haldor-Topsøe A/S. In the first case, the measurements were performed using a Micrometrics ASAP 2020 analyzer for porosity and surface area. In the second case, an Autosorb automatic analyzer from Quantachrome Instruments was used. The samples were prepared by degassing in vacuum at 200 °C for four hours and isotherms of adsorption-desorption were acquired at -196 °C.

### **Scanning Electron Microscopy**

The morphology of the prepared materials was investigated by Scanning Electron Microscopy (SEM). The investigations were carried out at the Center for Electron Nanoscopy of the Technical University of Denmark (CEN DTU). Images were collected on a FEI Quanta 200 ESEM FEG microscope.

## 2.2 Experimental Methods for the Study of the Conversion of Carbohydrates

This work focused on the study of the conversion of different carbohydrates into compounds that can represent platform-molecules for the production of bio-based chemical products. Chapter 3 focuses on the conversion of hexoses, which are cheap and abundant in nature. First, the conversion of sucrose into the high-value keto-hexose fructose was explored. Then, the production of hydroxy esters with potential applications in the polymeric industry was investigated. Reactions for the conversion of hexoses to methyl lactate and the conversion of glycolaldehyde to methyl vinyl glycolate (MVG) were carried out and studied by time-resolved experiments in order to analyze the kinetics of the processes. Using NMR, it was possible to follow the conversion of reagents into intermediates and products. The study allowed the achievement of good understanding of the pathways and the kinetics of the processes.

### 2.2.1 Catalytic conversion of carbohydrates

#### General procedure for the two-step reaction for the conversion of sucrose into fructose

A mixture of 125 mg of sucrose (Sigma-Aldrich, 99.5%) and the catalyst (75 mg) in 5 mL of methanol (Sigma-Aldrich, anhydrous, 99.8%) was prepared and kept under magnetic stirring in a 15 mL Ace glass pressure tube at 100 °C for different times (up to 8 hours). Then, the mixture with the catalyst was used for the second step, reacting the obtained solution after addition of water (5 mL) at 100 °C for different times (up to 4 hours). The highest yields of fructose were obtained by evaporation of the methanol and carrying out the second step in pure water. Samples were collected at different times and analyzed by NMR.

#### General procedure for the conversion of carbohydrates by zeolites at 160 °C

Conversion of carbohydrates at 160 °C were carried out in a Biotage Initiator+ microwave synthesizer. In a typical experiment, the substrate (120 mg), the catalyst (50 mg), the internal standard (DMSO, 80 µL, Sigma-Aldrich, 99.5%) and methanol (5 mL, Sigma-Aldrich, anhydrous, 99.8%) were weighted into a microwave vial. The reaction was carried out at 160 °C for different times and analyzed by NMR.

#### General procedure for the conversion of glycolaldehyde into MVG

In a typical reaction, a mixture of 400 mg of glycolaldehyde dimer and 100 mg of catalyst in 5 mL of methanol was reacted at 160 °C in the presence of 80 µL of mesitylene (Sigma-Aldrich, 99.8%) as internal standard. The reactions were carried out in a microwave synthesizer Biotage Initiator+.

#### Procedure for the *in situ* formation and conversion of MGA-DMA

Methyl glycolaldehyde dimethyl acetal (MGA-DMA) was synthesized from glycolaldehyde dimer with the procedure describe above. A dealuminated ZSM-5 zeolite was used as a heterogeneous Brønsted acidic catalyst. The catalyst was then filtered off and the mixture containing high amount of MGA-DMA was transferred to a 5 mL glass vial for the subsequent reaction with Sn-Beta zeolite catalyst.

#### General procedure for the conversion of glucose catalyzed by CrCl<sub>3</sub>

Glucose (Sigma-Aldrich, 99.5%) was dissolved in 6 mL of water or DMSO (Sigma-Aldrich, 99.5%) and CrCl<sub>3</sub>·6H<sub>2</sub>O (Merck, >96%) was added to the final solution to achieve a concentration of 17 mM. The reactions were carried out in Ace glass pressure tubes at 140 °C under magnetic stirring for different times (up to 6 hours). Samples were collected at different times and analyzed by NMR spectroscopy. The reaction was studied *in situ*: 500 µL of the mixture using D-[1-<sup>13</sup>C]glucose (Sigma-Aldrich, 99 atom% <sup>13</sup>C) and CrCl<sub>3</sub>·6H<sub>2</sub>O in the same

concentration as above was prepared in a NMR tube and reacted at 95 °C in a Bruker Avance III 600 MHz NMR spectrometer equipped with a BBO SmartProbe (Bruker).

## 2.2.2 Analysis of processes for the conversion of carbohydrates

### Analysis of the reaction mixtures by NMR spectroscopy

NMR experiments were performed at NMR center at the Technical University of Denmark with the help and under the supervision of Senior Researcher Sebastian Meier (DTU). Samples for the analyses were prepared by first filtration of the reaction mixture from the catalyst (Nylon Filter 0.22 µm). Subsequently, the NMR tube was prepared by addition of 500 µL reaction solution and 100 µL of deuterated methanol. Spectra were recorded at 25 °C using a Bruker Avance III 800 MHz instrument equipped with a TCI cryoprobe. Products in the mixtures were quantified by the acquisition of quantitative  $^{13}\text{C}$  spectra, sampling 65536 complex data points, using 30 s of recycle delay and acquisition time of 1.36 s. Quantifications were obtained by comparison of the integrated area of the peaks of the products with the area of an internal standard (DMSO). Concentrations of the different products were calculated using the formula:

$$[X] = [\text{DMSO}] \left( \frac{n_{\text{C(DMSO)}}}{n_{\text{C(x)}}} \right) \left( \frac{A_{\text{(x)}}}{A_{\text{(DMSO)}}} \right)$$

where  $n_{\text{C(DMSO)}}$  indicates the number of carbon atoms in DMSO molecule (internal standard) giving the integrated peak,  $n_{\text{C(x)}}$  the number of carbon atoms in the product x giving the integrated peak,  $A_{\text{(x)}}$  the area of the peak integrated for the product x and  $A_{\text{(DMSO)}}$  the area of the peak integrated for DMSO.

The different isomers of the considered carbohydrates were identified and quantified by  $^1\text{H}$ - $^{13}\text{C}$  HSQC spectra, which were used in order to achieve high resolution between the signals.  $^1\text{H}$ - $^{13}\text{C}$  HSQC spectra were recorded using 1024( $^1\text{H}$ ) $\times$ 300( $^{13}\text{C}$ ) complex data points and 62 ppm of  $^{13}\text{C}$  carrier offset (primary alcohols region). Spectra were acquired using a spectral width of 20 ppm and highly-resolved spectra were obtained in short times (30 minutes). Signals for  $^{13}\text{C}$  were also sampled in  $^1\text{H}$ - $^{13}\text{C}$  HSQC spectra for 50 ms with  $^{13}\text{C}$  carrier offset of 102 ppm to better resolve aldose hemiacetal signals. Thus, signals for the different pyrano/furano and  $\alpha/\beta$  isomers of sugars and glycosides were resolved in the two-dimensional spectra. The concentration of the compounds was calculated after construction of calibration curves and extrapolation of a response factor in order to calibrate the signal of the two-dimensional experiment relative to protonated DMSO as internal standard.<sup>196</sup> Spectra were processed and analyzed using TopSpin 4.0.4 software.

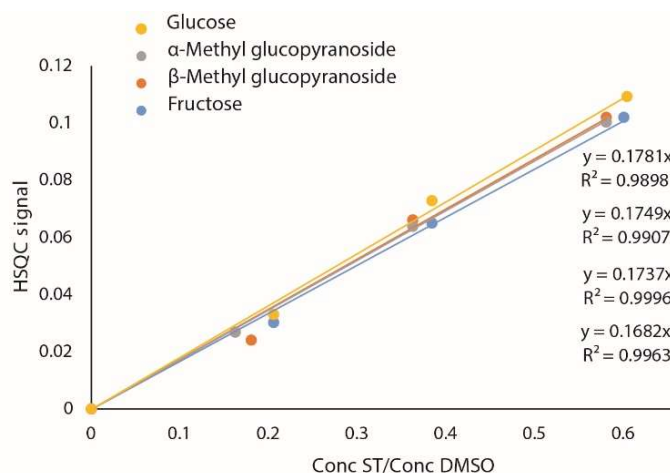


Figure 2.3. Calibration curves of hexoses in  $^1\text{H}$ - $^{13}\text{C}$  HSQC experiments.

## 2.2 Study of the Conversion of Carbohydrates

---

Calibration curves for 2D NMR experiments were built by the analysis of standard samples. In the case of glycosides, response factors were similar due to the similarity in the structures (Figure 2.3). Products not commercially available could be calibrated in the 2D NMR experiments by correlation with the signals in the quantitative 1D  $^{13}\text{C}$  NMR spectra. Thus, the response factor for a compound x is:

$$\text{RF}_{(x)}^{\text{HSQC}} = (A_{(x)}^{\text{HSQC}} / A_{(\text{DMSO})}^{\text{HSQC}}) / (A_{(x)}^{13\text{C}} / A_{(\text{DMSO})}^{13\text{C}})$$

where  $A^{\text{HSQC}}$  is the area integrated in the 2D  $^1\text{H}$ - $^{13}\text{C}$  HSQC spectra and  $A^{13\text{C}}$  the area in the quantitative 1D  $^{13}\text{C}$  NMR spectra. The quantification of the concentration of the compound x can then be calculated:

$$[X] = (A_{(x)}^{\text{HSQC}} / A_{(\text{DMSO})}^{\text{HSQC}}) * [\text{DMSO}] * (nC_{(\text{DMSO})} / nC_{(x)}) / \text{RF}_{(x)}^{\text{HSQC}},$$

where  $nC_{(x)}$  and  $nC_{(\text{DMSO})}$  are the number of carbons giving the integrated signal for the compound x and the internal standard DMSO, respectively. The method allows the quantification of new products formed during the conversion of carbohydrates and is more accurate and faster as compared to the use of only  $^{13}\text{C}$  NMR spectra.<sup>197</sup>

### Fitting and kinetic analysis of the reactions for the conversion of hexoses

Kinetic fittings of the conversion of hexoses was performed by Associate Professor Pernille Rose Jensen and Senior Researcher Sebastian Meier (DTU). Concentrations at different times were obtained by quantitative analysis of the NMR spectra. The data for the conversion of sucrose over time were fitted to exponential decays and the rate constants of pseudo-first order for the methanolysis were obtained using pro Fit 6.2.9 (Quantumsoft, Zurich, Switzerland). The data of the conversion of hexoses to methyl lactate were likewise fitted using proFit 6.29 (Quantumsoft). The formation of methyl lactate over time was fitted using monoexponential and biexponential expressions. The kinetic expression used for the monoexponential fit was  $Y = A(1 - e^{-kt})$ , where A indicates the maximum yield of methyl lactate and k the pseudo-first-order kinetic constant. The expression used for the biexponential fitting was:  $Y = B(1 - e^{-lt}) + C(1 - e^{-mt})$ , where B and C are the maximum yields of methyl lactate derived from fructose and methyl fructosides, respectively, and l and m the two pseudo-first-order kinetic constant. Rate constants for a more involved kinetic model of glucose conversion to fructose and competing irreversible methyl lactate formation and reversible methyl fructoside formation were calculated using Lmfit in the spyder (release 3.2.4) Python environment.

### Kinetic analysis of the reactions for the conversion of glycolaldehyde

Yields of the products and conversion of the starting substrate were calculated from the concentration obtained from quantitative  $^{13}\text{C}$ -NMR analysis using mesitylene as the internal standard. Time-resolved data were fitted with the desired function using OriginPro 2018. The used kinetic expression for describing the MVG yields Y were: for the second-order  $Y = A_0 - 1 / (1/A_0 + k_1t)$ ; for the combined kinetics  $Y = A_0 - 1 / (1/A_0 + k_1t) + A_1 * (1 - \exp(-k_2t))$ ; for the first order  $Y = A_1 * (1 - \exp(-k_2t))$ .

### Yields and selectivity

Yield (Y) and selectivity (S) of different products were calculated as the following.

$$Y (\%) = \text{mol}_{(p)} / \text{mol}_{(s0)} * 100 \quad S (\%) = \text{mol}_{(p)} / (\text{mol}_{(s0)} - \text{mol}_{(st)}) * 100$$

where  $\text{mol}_{(p)}$  indicates mol of the product,  $\text{mol}_{(s0)}$  the initial mol of substrate and  $\text{mol}_{(st)}$  the mol of substrate at the time t.

# Chapter 3

## Conversion of Hexoses Using Zeolite Catalysts

This chapter discusses the results obtained on the study of the conversion of hexoses catalyzed by zeolites. First, an alternative method for the production of fructose starting from sucrose is proposed. Commercial aluminum-containing zeolites were applied for the valorization of the cheap sucrose into the high-value fructose in a two-step two-solvent process. The reactions for the conversion of carbohydrates were carried out in methanol because the catalysts showed improved stability under these conditions. Thus, the formation of methyl glycosides assumed a central importance. In the second section, the role of the formation of methyl glycosides is analyzed with an emphasis on the formation and the conversion of methyl fructoside intermediates. Finally, the process for the conversion of hexoses into methyl lactate was studied by time-resolved experiments and a kinetic model for the process was proposed.

### 3.1 Zeolites with Balanced Brønsted and Lewis Acidity for the Conversion of Sucrose into Fructose

Fructose is a central intermediate in the conversion of biomass feedstock into chemicals.<sup>125</sup> Differently from glucose and other hexoaldoses, it is mainly found in solution in the reactive five-membered ring form. In industry, it is mainly used as sweetener for the preparation of High Fructose Corn Syrup (HFCS) and it is produced by isomerization of glucose promoted by the glucose isomerase enzyme.<sup>126</sup> Alternative methods for the production of fructose are investigated in order to make it competitive as replacement of chemical fossils. Since the isomerization of glucose to fructose catalyzed by heterogeneous Lewis acids directly replaces the existing enzymatic process, it is very attractive for industrial applications.<sup>125</sup> However, the disaccharide sucrose is cheaper and more accessible than glucose. The hydrolysis of sucrose is promoted by Brønsted acidity and it leads to a mixture of glucose and fructose.<sup>198</sup> Reaching high yields of fructose using conventional hydrolysis systems is challenging since acidic conditions also promote the conversion of fructose into products such as furanics and levulinic acid.<sup>130</sup>

In the last years, researchers have applied commercial zeolites to Lewis acid-catalyzed conversions of carbohydrates, such as the isomerization of glucose at 100 °C, using short-chain alcohols as solvents.<sup>149</sup> The use of alcoholic solvents both increases the stability<sup>107</sup> of the catalyst and the selectivity for conversion into fructose because competitive reactions are limited by the immediate formation of methyl fructosides. The proposed method involved the use of two solvents in a two-step process. In the first step, glucose isomerized into fructose, which was immediately converted in methyl fructosides. In the second step, methyl fructosides were hydrolyzed by addition of water (Chapter 1.2.4).<sup>149</sup>

### 3.1 Conversion of Sucrose into Fructose

In this section, a study of the possibility of the use of commercial aluminum-containing zeolites for the production of fructose starting from sucrose is described. The catalytic systems have both Brønsted and Lewis acidity for the catalysis of both the solvolysis of sucrose and the isomerization of glucose to fructose at 100 °C. The use of methanol as the solvent sequestered the formed fructose as methyl fructosides and allowed to reach high selectivity.<sup>1</sup>

#### 3.1.1 Experimental details: NMR spectroscopy for the study of complex mixtures

The analysis of mixtures of carbohydrates is, in general, complex because they have very similar structures and physical properties. Glycosides formed in alcoholic solvents increase the number of detectable compounds and the complexity of the mixtures. Moreover, each hexose is present in solution in different forms, the six-membered (pyrano-) and the five-membered (furano-) ring forms. In addition, each cyclic form can be alpha or beta depending on the spatial arrangement of the anomeric position upon cyclization. Most of the common analytical techniques are not readily able to distinguish all the different forms in solutions and, for this reason, the study was performed by using a two-dimensional NMR experiment, the  $^1\text{H}$ - $^{13}\text{C}$  HSQC spectrum. Signals were resolved and integrated in the region of the primary alcohol and the use of an internal standard (DMSO) in the reaction allowed absolute quantifications (Figure 3.1).<sup>152,199</sup>

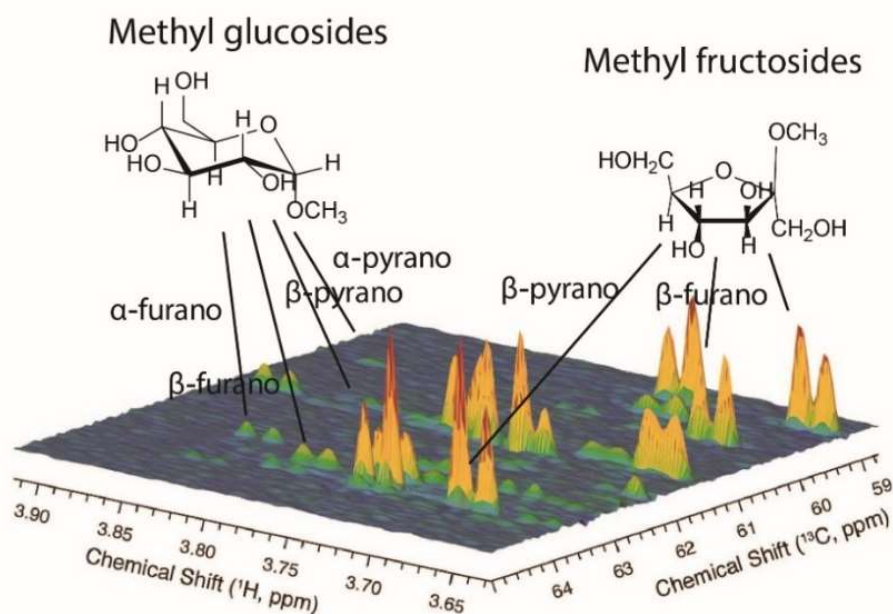
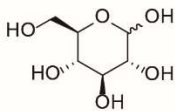
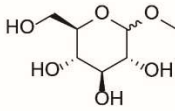
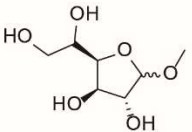
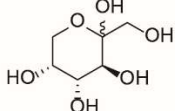
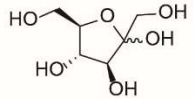
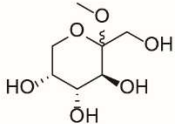
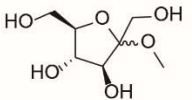


Figure 3.1. Spectral region of the primary alcohols of  $^1\text{H}$ - $^{13}\text{C}$  HSQC spectra, signals of the different forms of methyl fructosides and methyl glucosides.

<sup>1</sup> The section was adapted from the article “Facile and Benign Conversion of Sucrose to Fructose Using Zeolites with Balanced Brønsted and Lewis Acidity” published in *Catalysis Science and Technology*.<sup>200</sup>

Table 3.1. Chemical shifts of the  $-\text{CH}_2\text{-OH}$  group (position C6) of the different forms of glucose, fructose, methyl glucosides and methyl fructosides.

Glucopyranoses				
		<sup>13</sup> C	<sup>1</sup> H	
	α	61.50	3.79/3.84	
	β	61.62	3.85/3.72	
Methyl glucopyranosides				
		<sup>13</sup> C	<sup>1</sup> H	
	α	61.39	3.83/3.68	
	β	61.46	3.89/3.65	
Methyl glucofuranosides				
		<sup>13</sup> C	<sup>1</sup> H	
	α	63.52	3.78/3.61	
	β	64.07	3.83/3.66	
Fructopyranoses				
		<sup>13</sup> C	<sup>1</sup> H	
	β	64.66	3.67/3.51	
Fructofuranoses				
		<sup>13</sup> C	<sup>1</sup> H	
	α	61.34	3.76/3.64	
	β	62.86	3.74/3.61	
Methyl fructopyranosides				
		<sup>13</sup> C	<sup>1</sup> H	
	β	63.77	3.74/3.68	
Methyl fructofuranosides				
		<sup>13</sup> C	<sup>1</sup> H	
	α	59.21	3.72/3.64	
	β	60.19	3.67/3.55	

Reactions were carried out in glass pressure tubes. For kinetic analysis, samples were collected at different times (Chapter 2.2.1).

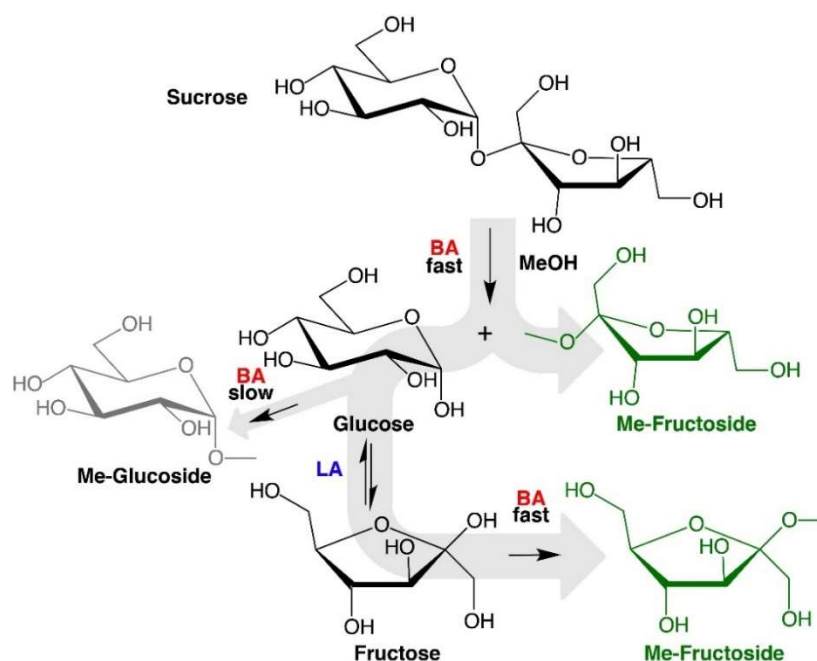
### 3.1.2 Design of a two-step process for the conversion of sucrose into fructose

Starting from the process reported in literature,<sup>149</sup> the same approach for the isomerization of glucose catalyzed by zeolites was used for the design of a two-step process for the conversion of sucrose into fructose in alcohols. The Brønsted acidity catalyzes the solvolysis of sucrose and the Lewis acidity catalyzes the isomerization of glucose. The aim of this study was to find the optimal amount of Brønsted and Lewis acid sites in order to catalyze both the solvolysis of sucrose and the isomerization of the derived glucose. Commercial zeolites contain aluminum, which introduces both types of acidity (Chapter 1.1.1). However, acidity and catalytic behavior can be influenced by several factors, such as Si/Al ratio or the type of framework. The Lewis acidity of aluminum-containing zeolites is suppressed in aqueous solutions<sup>164</sup> and the conversion of sucrose in water at 120 °C using H-USY (6) zeolite as the catalyst resulted in only 43% yield of fructose. Isomerization was not observed in water and the reactions were carried out using methanol as the solvent. Under these conditions, the reaction of glycosylation of the substrate with the alcoholic solvent became highly relevant. Methyl fructosides were kinetically favored and they were directly formed by solvolysis of sucrose. Methyl glucosides were absent using catalysts with balanced weak Brønsted acidity. Methyl glucosides are the thermodynamically preferred products, they were stable and they represented unconvertable byproducts. Using strong Brønsted acidic catalysts, the formation of methyl glucosides became fast and competitive with the formation of methyl fructosides.



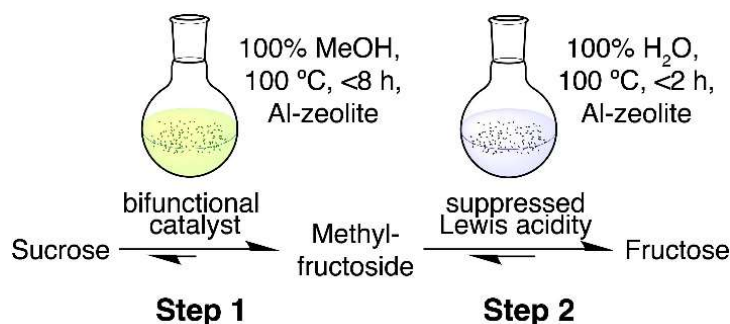
### 3.1 Conversion of Sucrose into Fructose

The proposed process for the production of fructose from sucrose is a two-step reaction with the use of a unique catalyst. At the beginning, the hydrolysis of sucrose and the isomerization of glucose in pure methanol resulted in high yields of methyl fructosides. Balanced Brønsted acidity was essential for reaching high yield of methyl fructosides in this initial step. The Lewis acidity was able to promote the isomerization of glucose formed by hydrolysis of sucrose, giving fructose, which was readily transformed into methyl fructosides in methanol. Therefore, the process required two steps. In the first step, high yields of methyl fructosides were achieved from sucrose in methanol. In the second phase, the hydrolysis of methyl fructosides occurred by promotion with addition of water and the same catalyst as in the first step (Scheme 3.1).



Scheme 3.1. Scheme of the interconversion between different sugars in the reaction starting from sucrose using zeolite catalysts in methanol (BA: Brønsted acidity, LA: Lewis acidity). Reproduced from Ref. 200 with permission from The Royal Society of Chemistry.

Two-step reactions were performed in order to test the activity of different commercial zeolites as catalysts for the process. Furthermore, optimal reaction conditions were studied and optimized. The purely Brønsted acidic sulphonic resin Amberlyst 36 was used as a reference for a purely Brønsted acidic heterogeneous catalyst. The conversion of sucrose was performed at 100 °C in methanol and the subsequent hydrolysis of methyl fructosides was promoted by addition of water.



Scheme 3.2. Two-step process for the conversion of sucrose into fructose. Reproduced from Ref. 200 with permission from The Royal Society of Chemistry.

### 3.1.3 Zeolites with balanced Brønsted and Lewis acidity

Different commercial zeolites were studied and the results of their catalytic activity were compared with the acidic properties. The reaction conditions were studied considering temperature, time, catalyst loading and sucrose concentration. Hydrolysis of sucrose, isomerization and formation of methyl fructosides occurred at slow rate at 100 °C and it was necessary to carry out the reaction over eight hours for reaching high yields (>70%) of methyl fructosides. Further conversion of unreacted glucose was possible in prolonged reaction times, but eight hours was chosen in order to avoid the formation of byproducts during prolonged times. Increasing the reaction temperature, the formation of methyl fructosides accelerated and maximum yields were reached within the first few minutes. Nevertheless, high temperatures reduced selectivity and increased the amount of different products. The final optimal conditions were decided based on a compromise between highest yields and applicability of the system (125 mg sucrose, 75 mg catalyst, 5 mL methanol, 100 °C, 8 hours).

Figure 3.2 shows the distribution of carbohydrates after eight hours of reaction at 100 °C using different catalysts. Only for Amberlyst 36, yields are reported after one hour, since prolonged reaction times led to the formation of products derived from the dehydration of fructose (5-hydroxymethyl furfural and other furanic compounds) catalyzed by Brønsted acidity. Aluminum-containing zeolites formed methyl fructosides in yields higher than 70%. Catalysts without marked Lewis acidity, Amberlyst 36 and H-USY (30), were insufficiently active for isomerization and methyl fructosides were only derived by direct solvolysis of sucrose (Scheme 3.1). On the other hand, the NMR spectra showed glucose accumulation and the formation of methyl glucosides due to the Brønsted acidic behavior. Using H-USY (30), the low amount of aluminum did not provide the Lewis acidity necessary for promoting isomerization and the formation of methyl glucosides became competitive to the formation of methyl fructosides.

For the other catalytic systems, differences in activity were minimal. The Sn-Beta (12.5) catalyst showed the best performance in terms of high methyl fructoside yields and low methyl glucoside yields. The thermally dealuminated Beta zeolite also presented the capability to isomerize glucose to fructose by stabilizing high yields of methyl fructosides. The extra-framework aluminum remaining on the surface of the material after thermal dealumination behaved as a Lewis acidic center. However, the formation of methyl glucosides using DeAl-Beta and H-Beta (12.5) was slightly higher than for Sn-Beta (12.5) and H-USY (6) (Figure 3.2) and the latter catalysts were chosen as the optimal systems for the study of the second step of methyl fructoside hydrolysis. Amberlyst 36 was also explored as purely Brønsted acidic counterpart in order to understand the benefits of balanced Brønsted and Lewis acidity.

### 3.1 Conversion of Sucrose into Fructose

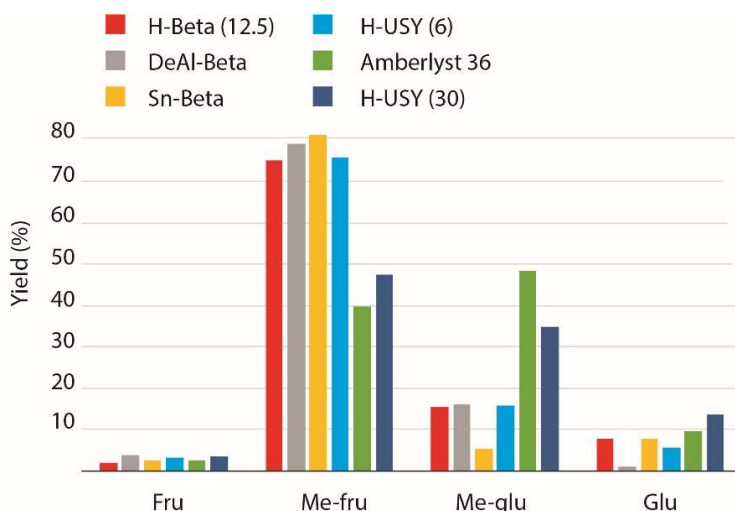


Figure 3.2. Distribution of carbohydrates after the first reaction step. Reaction conditions: 125 mg sucrose, 75 mg catalyst, 5 mL methanol, 100 °C, 8 hours. Only in the case of Amberlyst 36, yields are calculated after 1 hour in order to avoid excessive degradation. Adapted from Ref. 200 with permission from The Royal Society of Chemistry.

Table 3.2 summarizes the total amount of acid sites measured by  $\mu\text{mol}$  of ammonia desorbed per gram of zeolite during the  $\text{NH}_3$ -TPD experiments and the temperature of desorption indicates their strength. Although it is not possible to distinguish between Lewis and Brønsted acid sites using ammonia as probe molecule, TPD profiles of all catalyst samples presented two characteristic desorption peaks. The first peak between 100 °C and 270 °C was related to weak acid sites, the second peak between 270 °C and 500 °C was due to more persistent acid sites. Assuming that Brønsted acid sites are strong and desorb at higher temperature compared to Lewis acidic sites, the quantification of the TPD peaks followed the trend of activity just discussed. Optimal acidity for the formation of methyl fructosides as main products was not dependent on the total amount of acid sites, but required that the weak-type acid sites desorbing at low temperatures exceeded the strong sites responsible for the formation of byproducts. In fact, solvolysis occurred when using catalysts with some character of Brønsted acidity, while prominent Lewis acidity was needed for the isomerization.

Table 3.2. Physical characterization of the different catalysts.

<sup>a</sup> The number in bracket in aluminum-containing zeolites indicates the Si/Al ratio

Entry	Catalyst	Acid sites type 1 (100-270 °C) ( $\mu\text{mol/g}$ ) <sup>c</sup>	Acid sites type 2 (270-500 °C) ( $\mu\text{mol/g}$ ) <sup>c</sup>	Total acid sites ( $\mu\text{mol/g}$ ) <sup>c</sup>	BET area ( $\text{m}^2/\text{g}$ ) <sup>d</sup>	Pore volume ( $\text{cm}^3/\text{g}$ ) <sup>d</sup>
1	H-USY (6) <sup>a</sup>	488	539	1027	708	0.2436
2	H-USY(30) <sup>a</sup>	140	226	366	792	0.2504
3	H-Beta(12.5) <sup>a</sup>	693	395	1088	579	0.1631
4	DeAl-Beta	128	91	219	526	0.1492
5	Sn-Beta (12.5) <sup>b</sup>	196	95	291	492	0.1446
6	Amberlyst 36	-	-	>5400	33	0.2

<sup>b</sup> The number in bracket in Sn-Beta zeolite indicates the Si/Sn ratio <sup>c</sup> Measured by  $\text{NH}_3$ -TPD <sup>d</sup> Measured by nitrogen physisorption

It is noteworthy that the two best performing catalysts, H-USY (6) and Sn-Beta (Table 3.1 entry 1 and 5), presented opposite situations considering the total amount of acid sites. H-USY (6) has a high Si/Al ratio, which determined the high acidity (1027  $\mu\text{mol/g}$ ) and activity for both Lewis and Brønsted catalysis. Sn-Beta does not contain aluminum and the total amount of acid sites was low (291  $\mu\text{mol/g}$ ). However, the presence of tin introduced Lewis acidic properties and high activity for both solvolysis and isomerization. When the strong acid sites (type 2) were predominant, high formation of methyl glucosides were obtained. These products derived directly from glycosylation of glucose in methanol (Scheme 3.1) and were thermodynamically stable. Using catalysts able to promote the quick interconversion between glucose and fructose, the formation of glucosides did not occur since the substrate was preferably sequestered from the mixture as methyl fructosides upon quick conversion of fructose. However, when the Lewis acidic behavior was not prevalent and the isomerization was slow, methyl glucosides formation became competitive.

The formation of methyl glucosides was strongly undesired because the stability of methyl glucosides stopped the process. The possible conversion of  $\alpha$  and  $\beta$  methyl glucopyranosides was explored starting from the commercial compounds and using different reaction conditions. Using Lewis acidic zeolites, the conversion of methyl glucosides and the presence of traces of products were observed only at high temperatures ( $>160^\circ\text{C}$ ) and in the presence of a large amount of water ( $> 50\%$  (v/v)) for both anomers ( $\alpha$ - and  $\beta$ -glucopyranose). These conditions were not relevant for the process and the stability of the catalysts. Hence, methyl glucosides need to be considered as unreactive byproducts. In all cases, the predominant amount of acid sites type 2 was not beneficial for the process. Amberlyst 36 is an organic resin with sulphonic acid groups and cannot be characterized by using the same techniques as for inorganic materials, such as zeolites. For this reason, the results obtained with the zeolite catalytic systems were not directly comparable with Amberlyst 36. However, it could be used as a qualitative reference for the effect of Brønsted acid sites in the process.

The NMR spectra showed also the formation of other hexoses. Mannose, sorbose, methyl mannosides and methyl sorbosides were present in the reaction mixture in small amounts ( $<1\%$  yield) due to concurrent reactions starting from glucose. In all cases, prolonged times led to the degradation of the sugars, as proved by the decrease of fructosides and the appearance of other products. In the case of marked Brønsted acidity (Amberlyst 36), derivatives of levulinic acid were formed, while for increased proportion of Lewis acid sites, traces of products derived by retro-aldol pathways appeared, i.e. methyl lactate, hydroxy esters and lactones. Free fructose was barely visible in the reaction mixtures and free glucose was present only at short reaction times.

### 3.1.4 Investigations on the formation and the hydrolysis of methyl fructosides

Considering the low abundance of free fructose, methyl fructosides represented central products of the first step in the two-step process converting sucrose to fructose. Therefore, the formation of methyl fructosides over time using Sn-Beta, H-USY and Amberlyst 36 catalysts was explored. Figure 3.3 shows the kinetics of the conversion of sucrose for the three investigated catalytic systems. H-USY (6) and Sn-Beta showed similar trends with high yields of methyl fructosides (80%) and no accumulation of glucose or fructose. However, H-USY (6) showed a slower reaction progression and the conversion of sucrose was complete after about 150 minutes, while only 50 minutes were necessary using Sn-Beta zeolite. A further acceleration occurred when using Amberlyst 36 as the catalyst, which provided a complete consumption of the starting substrate in only 20 minutes. The hydrolysis led to methyl fructosides, glucose and methyl glucosides, but, over time, the amount of methyl glucosides from glucose and products from the degradation of methyl fructosides increased.

### 3.1 Conversion of Sucrose into Fructose

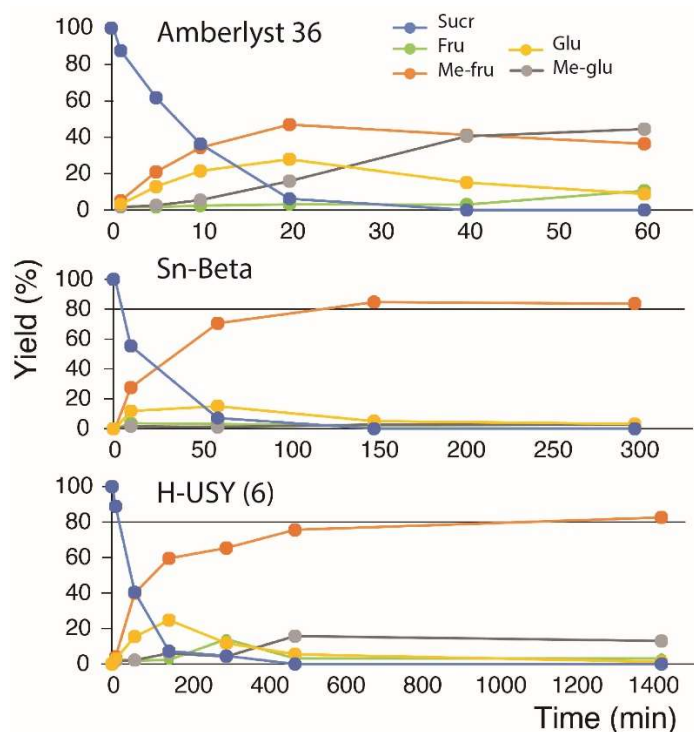


Figure 3.3. Distribution of carbohydrates during the progression of the reaction for the catalyst Amberlyst 36 (top), Sn-Beta (middle) and H-USY (6) (bottom). Note different time axes for the three catalysts. Reaction conditions: 125 mg sucrose, 75 mg catalyst, 5 mL methanol, 100 °C, DMSO as internal standard. Reproduced from Ref. 200 with permission from The Royal Society of Chemistry.

The fitting of the data for the solvolysis of sucrose for the different catalysts during the first 150 min is presented in Figure 3.4. The data followed a pseudo-first-order kinetic as methanol,  $H^+$  and catalyst concentration were constant over the progression of the reaction. Under these conditions, the fitted rate constants for the hydrolysis of sucrose were  $0.10 \text{ min}^{-1}$ ,  $0.06 \text{ min}^{-1}$  and  $0.02 \text{ min}^{-1}$  for the catalysis by Amberlyst 36, Sn-Beta (12.5) and H-USY (6), respectively. Methyl fructofuranosides and methyl glucofuranosides were the main forms of glycosides identified by  $^1H$ - $^{13}C$  HSQC. The majority of the five-member ring forms indicated that the formation of methyl glycosides under such conditions occurred under kinetic control on a short timescale at 100 °C.

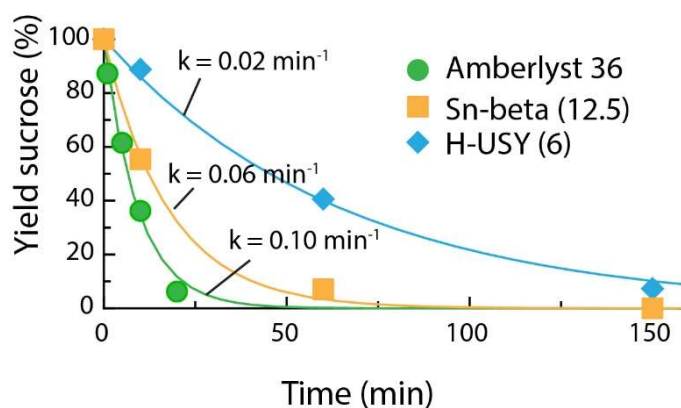


Figure 3.4. Curve fitting for the conversion of sucrose. Reaction conditions: 125 mg sucrose, 75 mg catalyst, 5 mL methanol, 100 °C, 80  $\mu\text{L}$  DMSO as internal standard. Adapted from Ref. 200 with permission from The Royal Society of Chemistry.

The hydrolysis of methyl fructosides to fructose could be performed in water using the same catalysts as used in the first step. Optimal fructose yields (80%) and stable distribution of products were obtained by evaporation of the methanol and addition of the same volume of water (5 mL). The reported results were achieved after 2 hours at 100 °C. The hydrolysis of methyl fructosides was carried out for the same duration for the different catalytic systems. However, using Sn-Beta (12.5) as the catalyst, the composition of the mixtures was not stable. After 30 minutes of reaction, the consumption of methyl fructosides was complete and the yield of fructose reached a maximum of 80%. For longer reaction times, fructose was further converted due to the high Lewis acidity of the catalyst, which allowed the isomerization of glucose in water. Therefore, fructose yields decreased and glucose yields increased over time using Sn-Beta (12.5) catalyst (Figure 3.5). On the other hand, the Lewis acidic character of H-USY (6) was completely suppressed in the second step, as generally known for aluminum-containing zeolites in aqueous solutions.<sup>164</sup> Thus, the use of H-USY (6) catalyst produced 80% fructose yields from sucrose in the two-step process (Figure 3.6).

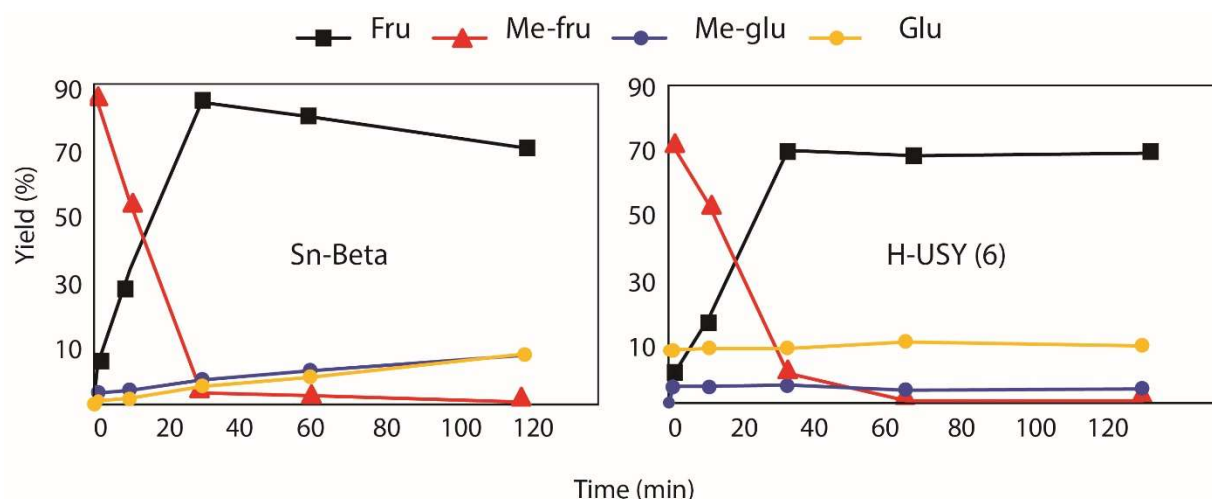


Figure 3.5. Hydrolysis of methyl fructosides in water using Sn-Beta (12.5) (left) and H-USY (6) (right) as catalysts. Reaction conditions: products and catalyst (50 mg) mixture obtained from the first step after evaporation of the solvent, 5 mL water, 100 °C, 80  $\mu$ L DMSO as internal standard. Adapted from Ref. 200 with permission from The Royal Society of Chemistry.

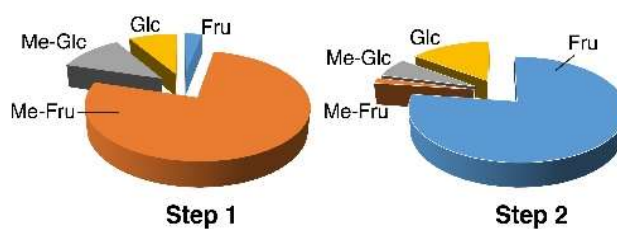


Figure 3.6. Distribution of carbohydrates for the two different steps of the process using H-USY (6) as catalyst. Adapted from Ref. 200 with permission from The Royal Society of Chemistry.

The hydrolysis of methyl fructosides occurred also without the need of evaporation of the solvent after the first step. Small volumes of water were sufficient to promote the hydrolysis and to stabilize the free fructose. Figure 3.7 A shows the evolution of the reaction over time, if water was added 1:1 (v/v) to the reaction mixture. The formation of fructose was slower compared to the use of pure water and 50% yields were obtained after 2 hours. The use of 50% water 50% methanol (v/v) preserved the activity of the catalyst, which showed high stability over five cycles of recycle and reuse even at 120 °C (Figure 3.7 B).

### 3.1 Conversion of Sucrose into Fructose

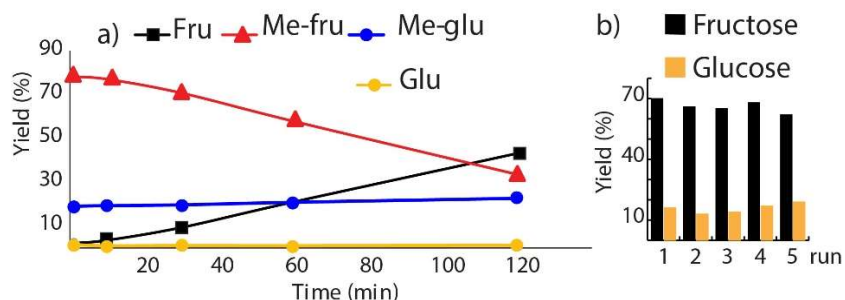
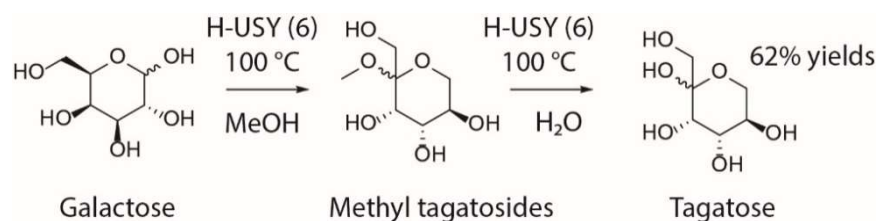


Figure 3.7. a) Hydrolysis of methyl fructosides into fructose by H-USY (6) in a mixture of water and methanol and b) stability of the catalytic system over five runs. Reaction conditions: product, catalyst (H-USY (6) 50 mg) and methanol (5 mL) from the first step, 5 mL water, 100 °C, 80  $\mu$ L DMSO as internal standard.

The applicability of the system to the isomerization of different sugars was studied in the conversion of galactose into tagatose. Tagatose is a rare sugar with low calorie content and it is used as sweetener with beneficial effects for lowering the blood glucose content.<sup>201</sup> The two-step process using H-USY (6) catalyst allowed to achieve around 62% yields in 2 hours. During the first step, galactose was isomerized in methanol and methyl tagatosides were obtained. Successively, the alcoholic solvent was evaporated and the water used in the second step promoted the hydrolysis of the glycosides leading to tagatose (Scheme 3.3). Hence, the process can be generally used for the valorization of common sugars via isomerization into rare isomers.



Scheme 3.3. Conversion of galactose into tagatose using the two-step two-solvent approach.

#### 3.1.5 Conclusions on the study for the conversion of sucrose into fructose catalyzed by zeolites

In this section, the approach for the isomerization of carbohydrates in alcohols by a two-step reaction catalyzed by aluminum-containing zeolites was applied to the conversion of sucrose into fructose in methanol. The process involved the solvolysis of sucrose into glucose and methyl fructosides catalyzed by weak Brønsted acidity. In the presence of Lewis acidity in the heterogeneous catalyst, the formed glucose isomerized into fructose, which accumulated as methyl fructosides. Finally, methyl fructosides could be easily hydrolyzed in a second step by addition of water. The optimal catalyst for the process required balanced Brønsted and Lewis acidity. Excessive Brønsted acidity promoted the formation of methyl glucosides, which represented unreactive byproducts. Different zeolites were screened as catalysts for the process and most of them were able to promote the accumulation of methyl fructosides in high yields. After characterization of the acidity by NH<sub>3</sub>-TPD, the most active catalysts were the samples presenting a prevalent desorption of ammonia at low temperatures. Results indicated that the active sites of the catalyst required weak acidic behavior. Sn-Beta and H-USY (6) zeolites presented the best activity for the formation of methyl fructosides in the first step and they were further studied and compared to Amberlyst 36, as a purely Brønsted acidic reference material. Finally, H-USY (6) showed the best result in the final formation of fructose after both steps. Differently from Sn-Beta zeolite, the Lewis acidity was suppressed in water and it was possible to stabilize fructose in the final mixture in high yields.



## 3.2 The Role of Methyl Glycosides during the Conversion of Hexoses in Methanol

The conversion of carbohydrates in industry is mainly performed by enzymatic processes. The use of zeolites as catalysts for the conversion of carbohydrates allows a wide range of applications for the production of bio-based chemicals. Industrially, the processes would be carried out in alcoholic solvents since the catalytic materials have shown improved stability under these conditions.<sup>107</sup> Thus, the study of the glycosylation of carbohydrates in short-chain alcoholic solvents needs to receive particular attention. As discussed in the previous section, alkyl glycosides can represent reactive intermediates or unreactive byproducts and they have great influence on rates and selectivity of the different processes. In the previous section, the formation of methyl fructosides from sucrose in methanol at 100 °C using aluminum-containing zeolite catalysts was utilized to sequester the masked product from the reaction mixture.<sup>200</sup> However, using temperatures higher than 100 °C, the formed methyl fructosides were activated for the production of different compounds. The selectivity into the different reaction pathways depended on the balanced amount of Brønsted and Lewis acidity in the catalyst. The use of increased temperatures and different zeolite catalysts could promote the formation of different products and the approach could be studied as a method for the production of bio-based platform chemicals from carbohydrates. In this section, formation, hydrolysis and reactivity of methyl glycosides in the reactions of hexoses in methanol using zeolite catalysts at 160 °C is presented and discussed.

### 3.2.1 The role of the formation of methyl fructosides in the conversion of hexoses in methanol catalyzed by solid acids

The analysis of the reaction mixtures by  $^1\text{H}$ - $^{13}\text{C}$  HSQC showed the formation and the conversion of the different isomers (Figure 3.8). Free fructose was present mainly as  $\alpha$ - and  $\beta$ -fructofuranose and only minor amount of  $\beta$ -fructopyranose was formed. Analogously, methyl fructosides were formed in high amount as furanosides and only low yields of  $\beta$ -pyranosides were visible. On the other hand, glucose was only visible as  $\alpha$ - and  $\beta$ -glucopyranose. In contrast, methyl glucosides were formed in all the possible forms.

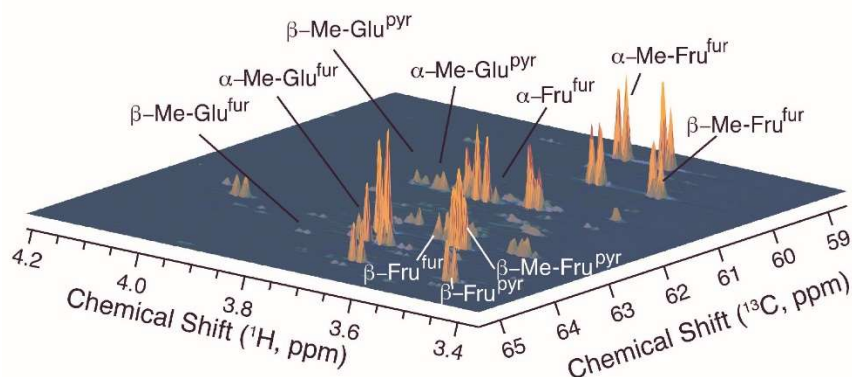


Figure 3.8.  $^1\text{H}$ - $^{13}\text{C}$  HSQC spectra, in the region of the primary alcohols.

The conversion of carbohydrates in methanol at 160 °C using catalysts with different balanced acidity was studied by time-resolved experiments. Figure 3.9 shows the conversion of glucose in methanol promoted by catalysts with poor Lewis acidity. Using the purely Brønsted acidic Amberlyst 36, methyl glucosides were the only products at 160 °C. In this case, the absence of Lewis acidity did not allow the isomerization to the reactive



### 3.2 The Role of Methyl Glucosides

fructose and the only pathway available was the glycosylation to methyl glucosides. Differently, H-Beta (12.5) contains aluminum, which is a Lewis acidic center. Thus, the isomerization to fructose and the sequential formation of methyl fructosides in methanol was promoted (Figure 3.9 b). During the first hour, methyl fructosides were also hydrolyzed and converted into different products. In particular, furanic products appeared in the mixtures after 15 minutes, when the consumption of methyl fructosides started. In this work, the term of “furanics” indicates the sum of furfural, 5-hydroxymethylfurfural (HMF) and derivative compounds. Nevertheless, H-Beta (12.5) zeolite is prevalently Brønsted acidic and methyl glucosides were the favored products in methanol.

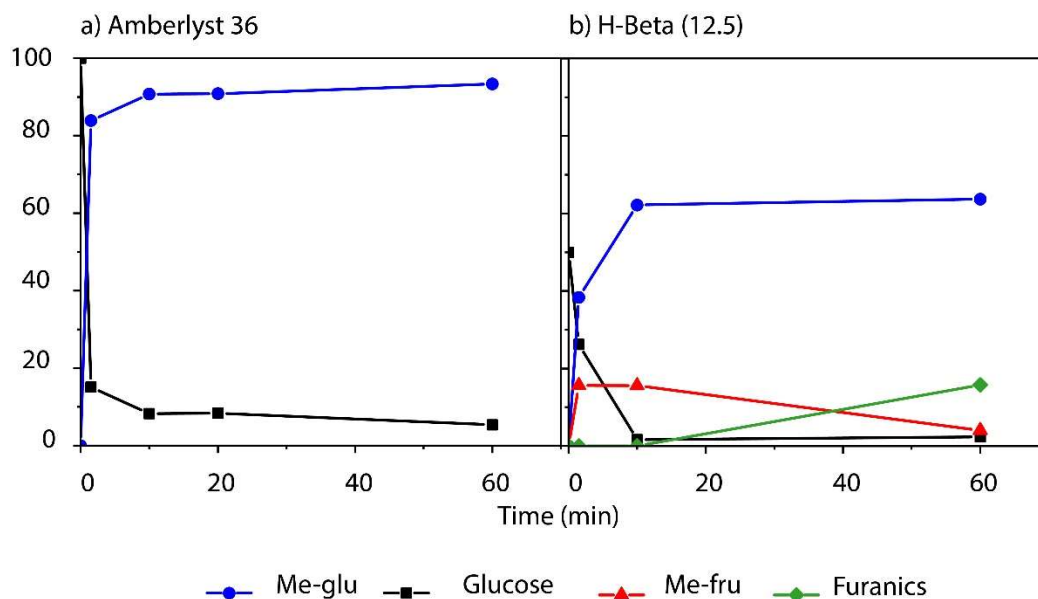


Figure 3.9. Conversion of glucose by a) Amberlyst 36 and b) H-Beta (12.5). Reaction conditions: 120 mg glucose, 50 mg catalyst, 5 mL methanol, 160 °C, 80  $\mu$ L DMSO as internal standard.

Methyl glucosides are stable compounds and they were not converted into different products under the studied conditions. Thus, the results indicated the requirement of the first isomerization step for converting glucose into the reactive fructose in order to obtain the desired products. Fructofuranoses and fructofuranosides are in dynamic equilibrium with the open-chain form and they were prone to react in solution. In contrast, glucose and glucosides are present in the thermodynamically stable pyrano-forms and they did not undergo any reaction pathway.<sup>202</sup> Consequently, the reactions starting from fructose in methanol showed different trends over time compared to the use of glucose as substrate (Figure 3.10). The main products consisted in furanic compounds derived from the dehydration of fructose. Using both Amberlyst 36 and H-Beta (12.5) as catalysts, methyl fructosides were initially formed from fructose as reactive intermediates. Then, they were rapidly hydrolyzed and converted into different products. Using H-Beta (12.5) zeolite, the consumption of methyl fructosides yielded high amounts of furanic compounds. Differently, the use of the strong Brønsted acidic resin Amberlyst 36 produced furanics at short times, which were converted further. Subsequently, furanics were consumed and derivatives of the levulinic acid were formed from their rehydration.

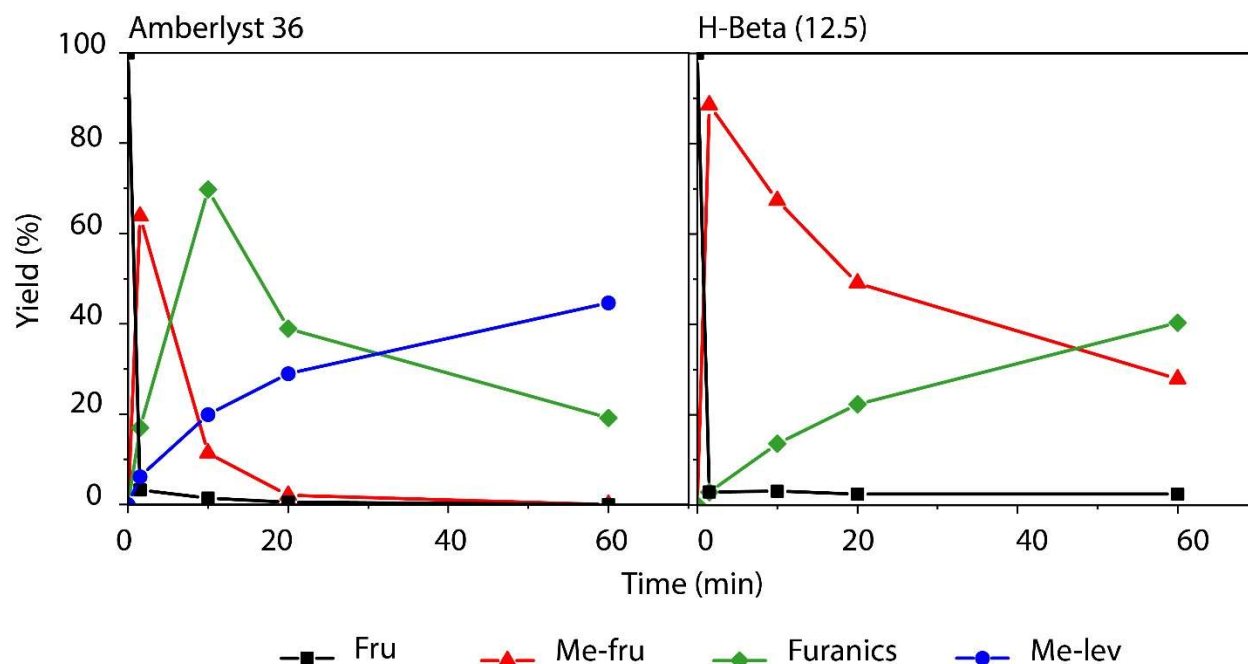


Figure 3.10. Conversion of fructose by Amberlyst 36 (left) and H-Beta (12.5) (right). Reaction conditions: 120 mg fructose, 50 mg catalyst, 5 mL methanol, 160 °C, 80  $\mu$ L DMSO as internal standard.

Fructose was converted into different products under the considered conditions. Methyl fructosides were the first intermediates in all cases. They were rapidly formed, but they were then hydrolyzed back to fructose and converted to other products for prolonged reaction times. In the reactions starting from glucose, the first isomerization to fructose catalyzed by the Lewis acidity was an essential requirement to enter catalytic pathways beyond glucosides formation.

### 3.2.2 Formation of methyl fructosides from glucose at 160 °C using post-treated Sn-Beta zeolite catalysts

Methyl fructosides are key intermediates for the conversion of glucose in methanol.<sup>152</sup> Glucose cannot undergo reactive pathways into desired products without the presence of a Lewis acidic catalyst promoting the isomerization into fructose.<sup>202</sup> Using zeolite catalysts in methanol, fructose was quickly converted into methyl fructosides as first intermediates. Thus, the formation of methyl fructosides promoted by Lewis acidic zeolites could be used as an activation of the starting glucose. For this purpose, post-treated Sn-Beta zeolites presented optimal catalytic properties. The tin conferred high Lewis acidity for promoting the fast isomerization between glucose and fructose. Moreover, the presence of defects in the structure due to the post-synthetic preparation introduced the weak Brønsted acidic behavior for the rapid formation of glycosides. The formation of methyl fructosides from glucose at 160 °C in methanol was studied by short-time experiments (five minutes). As seen in the previous section, free fructose was hardly observed as it was immediately sequestered as fructosides. The increased temperature promoted a great acceleration of the process. Using a Sn-Beta with Si/Sn ratio 50 at 160 °C, the conversion of glucose was complete within the first two minutes and methyl fructosides reached maximum yields. In contrast, methyl fructosides required two hours in order to reach 70% yields from sucrose at 100 °C. The correlation between amount of tin and progress of the formation of methyl fructosides from glucose was also explored (Figure 3.11), further corroborating the dependence on sufficient Lewis acidic sites for efficient isomerization.

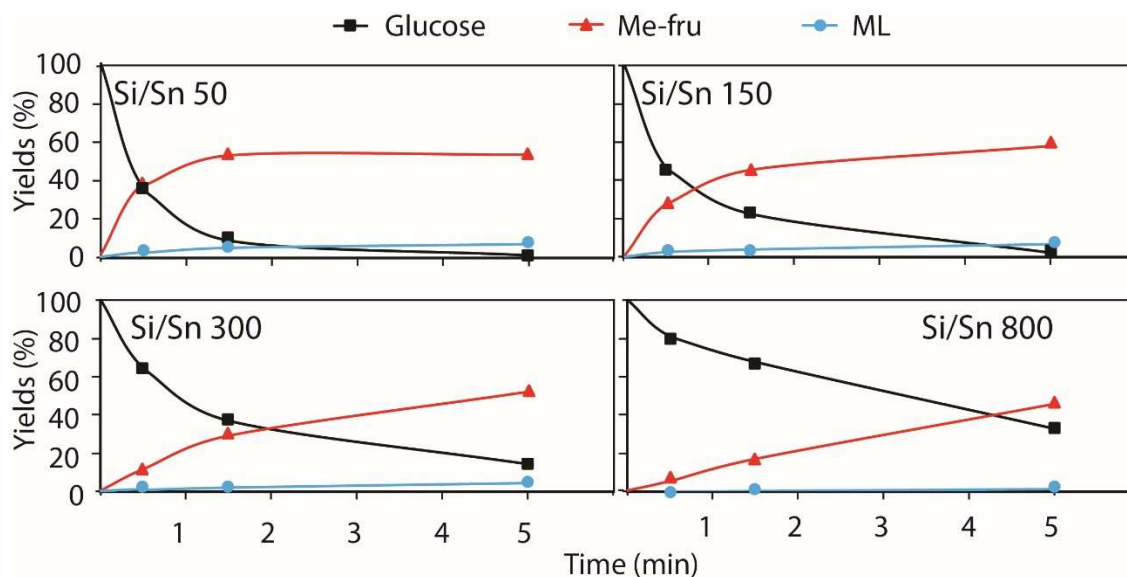


Figure 3.11. Formation of methyl fructosides in the first 5 minutes of reaction using Sn-Beta catalysts containing different amounts of tin: a) Si/Sn = 50 b) Si/Sn = 150 c) Si/Sn = 300 d) Si/Sn = 800. Reaction condition: 120 mg glucose, 50 mg Sn-Beta catalyst, 160 °C, 5 mL methanol, 80  $\mu$ L DMSO as internal standard.

Yields of methyl fructosides after five minutes at 160 °C were around 60% for all the catalysts containing different amount of tin. However, the formation of methyl fructosides during the first minute decelerated using the catalysts containing lower amount of tin. The reaction blank without any catalyst did not present glycosylation products under the same conditions. The formation of methyl fructosides from glucose required acidic catalysis and both Lewis and Brønsted acidity promoted the reaction. On the other hand, the amount of acidic sites required for the catalysis was extremely low under the used conditions and by application of small tin contents (Si/Sn = 800) yields of methyl fructosides still reached 60% yields after five minutes. The process forming methyl fructosides from glucose at 160 °C by post-treated Sn-Beta zeolites could be used as activation of the substrate by the creation of a pool of reactive intermediates in few minutes. In a second step, the accumulated glycosides could undergo transformation by different catalytic pathways. In the next paragraph, the sequential hydrolysis and conversion of methyl fructosides promoted by different zeolites are explored.

### 3.2.3 The reactivity of methyl fructosides in the presence of different zeolites

Methyl fructosides are the reactive intermediates in the conversion of glucose in methanol.<sup>152</sup> Once they are formed in the reaction media, they can be hydrolyzed and they can be converted into different products using zeolite catalysts. Methyl fructosides could be synthesized in high yields from glucose, fructose or sucrose using post-treated Sn-Beta zeolites. Consequently, the prepared solutions could be reacted using different catalysts and different products can be obtained. Using aluminum-containing zeolites with main Brønsted acidic behavior, furanic compounds and derivatives of levulinic acid were formed in high yields. Furanic compounds derived from the dehydration of sugars and include furfural and 5-hydroxymethylfurfural (HMF), which represent attractive bio-based chemicals. In fact, furfural and its derivatives can be used for the production of a wide variety of fuels, solvents, polymers and other chemical products.<sup>203</sup> Levulinic acid derives from the rehydration of HMF and it has been also applied as precursor for many chemical products. Processes for the conversion of sugars in alkyl levulinates using zeolites have been previously studied.<sup>154</sup>

The reactivity of methyl fructosides at 160 °C using different heterogeneous catalysts and methanol as the solvent was explored. A stock-solution of methyl fructosides was synthesized from fructose at 100 °C for five hours in methanol using post-treated Sn-Beta (150) catalyst. Although the high temperature allowed the production of the intermediates in short times, a temperature of 100 °C was chosen for the synthesis in order to avoid the formation of different byproducts. The catalyst was then filtered off and the resulting stock-solution analyzed by NMR. The final composition resulted in 70% of methyl fructosides and 30% of unreacted fructose. No other products were visible in the mixture. Portions of the solution containing methyl fructosides were reacted at 160 °C for two hours using different catalysts. Reference reactions were carried out starting from the pure fructose. All tested catalytic systems showed same catalytic activity in the reactions starting from fructose or methyl fructosides at 160 °C for two hours (Figure 3.12). In all cases, the two final mixtures had the same products distribution. Catalysts with different types of acidity influenced the reactivity and allowed to obtain different products. The presence of aluminum in commercial zeolites introduces Brønsted acidity, which promoted the dehydration of fructose forming furanics and the further rehydration leading to methyl levulinates as main products. The ratio of these two products depended on the balanced Brønsted acidity. Yields of methyl levulinates higher than 70% were obtained using H-USY (30) as the catalyst.

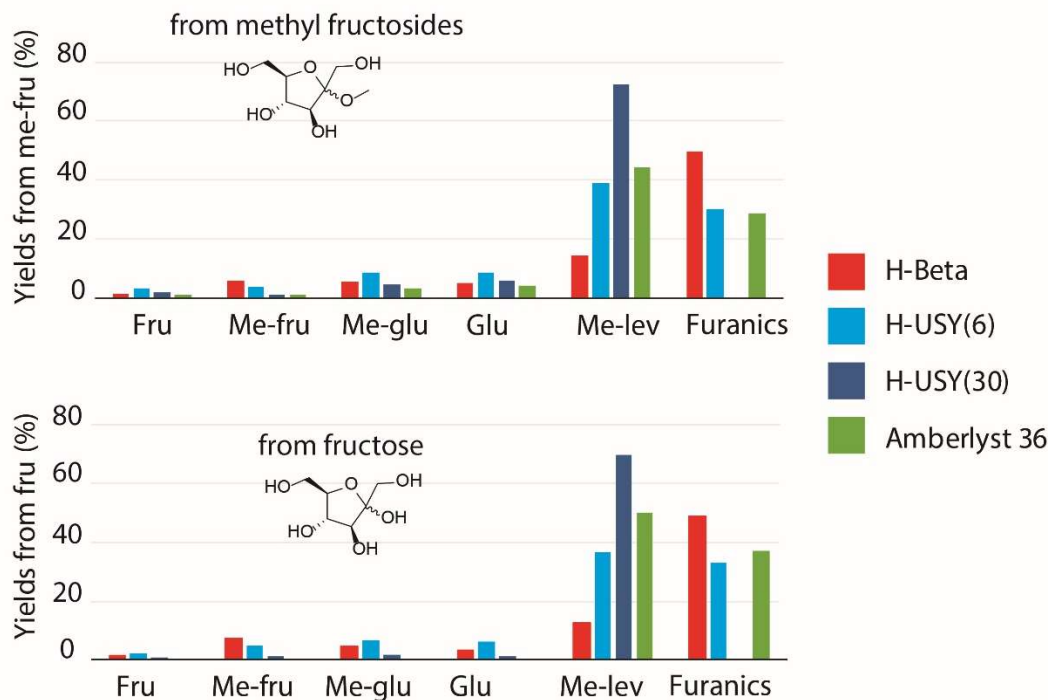


Figure 3.12. Distribution of products in the reactions starting from methyl fructosides and fructose using different commercial aluminum-containing zeolite. Reaction conditions: 120 mg fructose in 5 mL methanol or 5 mL of methanol solution containing 70% of methyl fructosides and 30% of fructose, 50 mg catalyst, 160 °C, 2 hours, 80  $\mu$ L DMSO as internal standard.

Small amounts of glucose and methyl glucosides derived from the isomerization and the glycosylation of glucose were also present in the mixtures. Using Sn-Beta catalyst, the products distribution changed, as expected for the absence of the aluminum Brønsted acid center (Figure 3.13). The retro-aldol pathway was promoted and methyl lactate was formed as the main product. In addition, only negligible differences were observed starting from fructose or from a mixture of methyl fructosides as the substrates. The results indicated that using either Brønsted or Lewis acidic conditions, methyl fructosides were rapidly converted into other products without relevant changes in the reactive behavior compared to unmasked fructose.

### 3.2 The Role of Methyl Glycosides

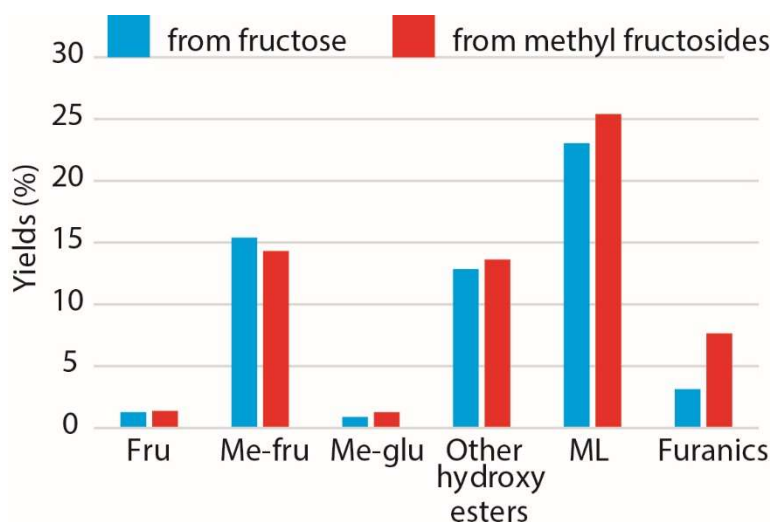


Figure 3.13. Distribution of products in the reaction starting from methyl fructosides and from fructose using Sn-Beta catalyst. Reaction conditions: 120 mg fructose in 5 mL methanol or 5 mL of methanol solution containing 70% of methyl fructosides and 30% of fructose, 50 mg catalyst, 160 °C, 2 hours, 80  $\mu$ L DMSO as internal standard.

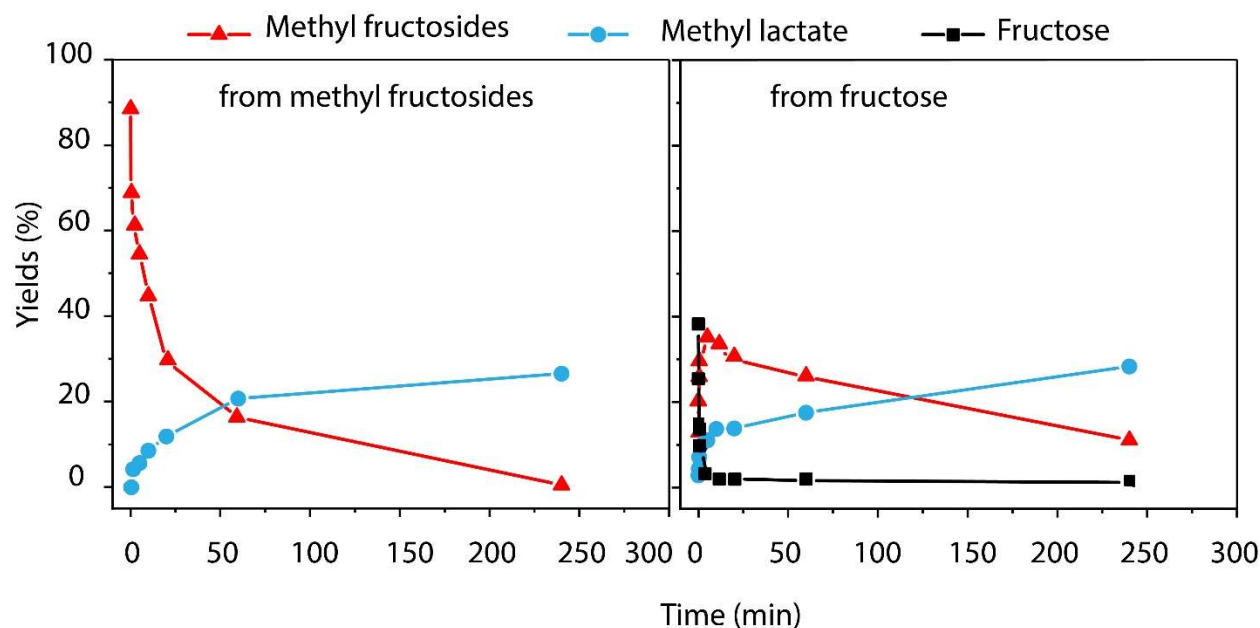


Figure 3.14. Time-resolved conversion of fructose (left) and methyl fructosides (right) using Sn-Beta catalyst. Reaction conditions: 120 mg fructose in 5 mL methanol or 5 mL of methanol solution containing 70% methyl fructosides 30% fructose, 50 mg catalyst, 160 °C, *ex situ* analysis by NMR, 80  $\mu$ L DMSO as internal standard.

The comparison of the kinetics starting from fructose and from methyl fructosides using Sn-Beta zeolite catalysts was explored by time-resolved experiments (Figure 3.14). Methyl fructosides were the first intermediates in the reaction for the conversion of fructose at 160 °C in methanol catalyzed by Sn-Beta. They were rapidly formed and then further converted. The reaction pathway starting from a mixture of methyl fructosides did not present relevant differences and led to identical distribution of products. Using methanol as the solvent, the formation of methyl fructosides was kinetically preferred from fructose and occurred quickly. Thus, the trend using fructose or methyl fructosides as starting substrates was the same.

### 3.2.4 Conclusions on the study of the role of methyl glycosides during the conversion of carbohydrates in methanol

In this section, the differences in reactivity between glucose and fructose was first explored. The identification of the different isomers in  $^1\text{H}$ - $^{13}\text{C}$  HSQC spectra confirmed the correlation between reactive behavior and different cyclic forms. Fructose was highly reactive and it was present in solution mainly as five-membered ring, which was instable and prone to react. In contrast, glucose was present in solution mainly as pyranose and underwent glycosylation with the solvent to furanosides under kinetic control and to pyranosides under thermodynamic control. However, glucose could be channeled into the reaction pathways by initial isomerization to fructose catalyzed by Lewis acidity. In the reactions starting from both glucose and fructose catalyzed by zeolites in methanol, methyl fructosides are the first intermediates. Thus, the formation of methyl fructosides in methanol could be used as first activation step of glucose using Lewis acidic zeolites. Subsequently, the accumulated methyl fructosides could undergo the different reaction pathways catalyzed by zeolites with different acidity. Methyl fructosides could be synthesized from glucose in very short times at 160 °C using post-treated Sn-Beta zeolites. Furthermore, they showed the same reactivity as fructose and they produced different attractive bio-based chemicals, such as 5-hydroxymethylfurfural (HMF) and alkyl levulinates.

## 3.3 Kinetic Analysis of the Production of Methyl Lactate from Hexoses Catalyzed by Sn-Beta Zeolites

In 2010, the process for the production of methyl lactate using Sn-Beta zeolite catalysts was reported for the first time.<sup>111</sup> Since then, the reaction for the conversion of carbohydrates into methyl lactate using Sn-Beta zeolites has been extensively studied<sup>160</sup> and, currently, it represents an important possibility for the production of bio-based biodegradable materials, i.e. polylactic acids (PLA). However, an in-depth understanding of the kinetics of the process still misses. Understanding kinetic details has an important role in the optimization of processes and applications. In this section, the study of the process for the conversion of hexoses by Sn-Beta is discussed by the analysis of time-resolved experiments. The evolution of products and intermediates over time was followed *ex situ* by NMR. The technique allowed the identification and quantification of the intermediate species. All the reactions studied in the section were carried out using a hydrothermal Sn-Beta (150) zeolite. The effect of the use of a post-treated catalyst is compared and discussed separately.

The formation and the reactivity of methyl glycosides in the reactions of carbohydrates in methanol using zeolite catalysts is discussed in the previous sections. Thus, the interconversion into methyl glycosides occurred also in the process for the production of methyl lactate from hexoses catalyzed by Sn-Beta zeolites. In particular, methyl fructosides represented central intermediates and had a great impact on the kinetics. In this section, a kinetic model for the process is proposed and the effect of changes in the reaction conditions, such as the addition of small amounts of water, on the kinetics are explored.<sup>2</sup>

### 3.3.1 Conversion of hexoses into methyl lactate using hydrothermal Sn-Beta catalyst

As reported in the previous sections, the use of two-dimensional NMR experiments, such as <sup>1</sup>H-<sup>13</sup>C HSQC, allowed high-resolved analysis of the species in the reaction mixtures. The technique allowed the identification and quantification of all the different forms of the studied carbohydrates. Thus, the conversion of hexoses catalyzed by hydrothermal Sn-Beta (150) zeolites was studied *ex situ* by time-resolved experiments. Reactions were carried out in a microwave reactor (Chapter 2.2.1), which permitted the controlled repetition of the heating ramp for all the experiments, eliminating experimental variables due to the manual settings control. Moreover, the microwaves heating occurs rapidly without temperature fluctuations and allowed the study of the process at very short times (few seconds).<sup>204</sup> Figure 3.15 reports the distributions of products in the conversion of hexoses catalyzed by Sn-Beta zeolite.

---

<sup>2</sup> The section was adapted from the article “Kinetic Analysis of Hexose Conversion to Methyl Lactate by Sn-Beta: Effects of Substrate Masking and of Water” published in *Catalysis Science and Technology*.<sup>196</sup>



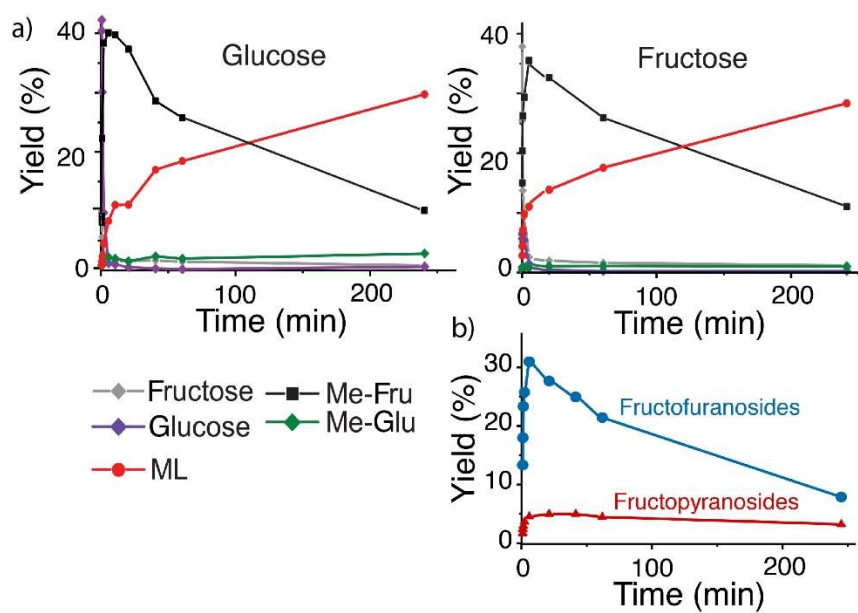


Figure 3.15. a) Distribution of products during the conversion of hexoses catalyzed by Sn-Beta zeolite. b) Methyl fructosides forms (furanosides and pyranosides) during the conversion of fructose catalyzed by Sn-Beta zeolite. Reaction conditions: substrate 120 mg, catalyst 50 mg, methanol 5 mL, DMSO as internal standard 80  $\mu$ L, 160  $^{\circ}$ C. Adapted from Ref. 196 with permission from The Royal Society of Chemistry.

In the case of the conversion of both glucose and fructose, the starting substrate was converted rapidly and it was consumed in the first few minutes. Concurrently, methyl fructosides were formed in high yields. The highly-resolved  $^1\text{H}$ - $^{13}\text{C}$  HSQC spectra showed that methyl fructofuranosides were the main fructoside species formed. Pyranosides were present in small amounts during the entire process and they seemed to be as stable as methyl glucosides (Figure 3.15 b). On the other hand, fructofuranosides were reactive in the mixture and they were slowly converted. Methyl glucosides and furanic compounds were also formed in the process, but only in small yields. Thus, it was decided to neglect the formation of these byproducts from the analysis of the process. Figure 3.15 a illustrates that small differences were observed in the distribution of products starting from either glucose or fructose. The result indicated that the isomerization between the two substrates occurred rapidly and there were no differences in using the two substrates under the considered reaction conditions.

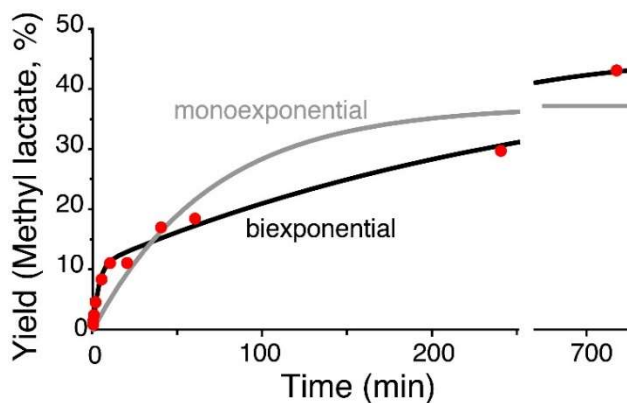


Figure 3.16- Yields of methyl lactate over time and fitting of data with monoexponential and biexponential functions. Reaction conditions: glucose 120 mg, catalyst 50 mg, methanol 5 mL, DMSO as internal standard 80  $\mu$ L, 160  $^{\circ}$ C. Reproduced from Ref. 196 with permission from The Royal Society of Chemistry.



### 3.3 Kinetic Analysis of the Production of Methyl Lactate

The yields of methyl lactate over time followed two trends (Figure 3.16). At the beginning of the process, the starting substrate was rapidly consumed and the yields of methyl lactate started to increase. However, the majority of methyl lactate was produced slowly during the conversion of methyl fructosides making the yields of methyl lactate follow a biexponential kinetics, given by the sum of two first-order regimes (Figure 3.16).

#### 3.3.2 Kinetic analysis of the process for the conversion of hexoses into methyl lactate

Data from time-resolved experiments were used for obtaining and testing a kinetic model.<sup>3</sup> The proposed model is shown in Figure 3.17. The isomerization between glucose and fructose occurred rapidly. Fructose behaved as central reactive species and it could undergo two different competitive pathways. The first route was the Lewis acid-catalyzed irreversible retro-aldol process leading to methyl lactate. The formation of methyl fructosides as acetals of the substrate due to the presence of weak residual Brønsted acidity was the second competitive reaction.

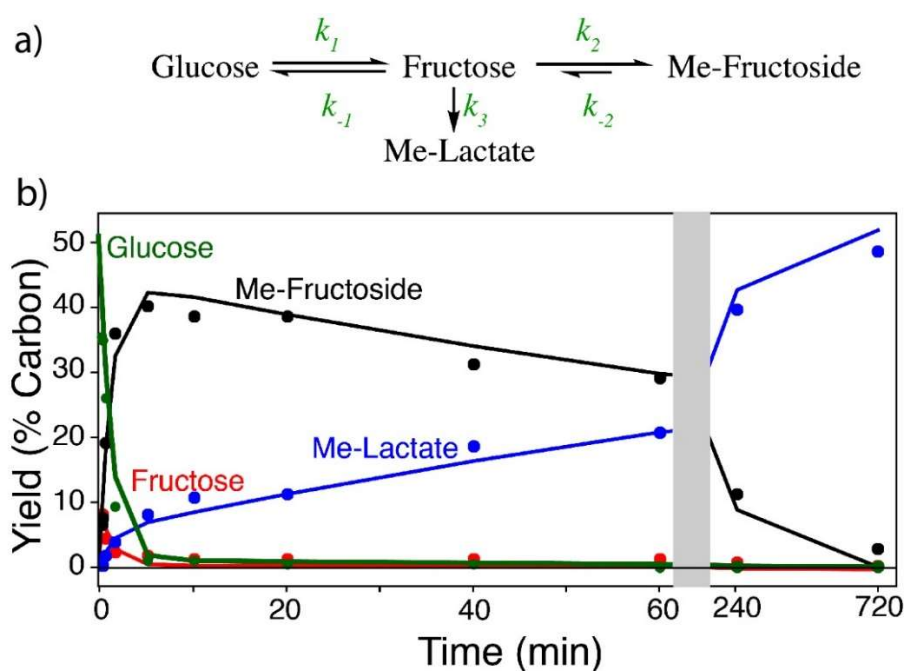


Figure 3.17. a) Scheme for the proposed kinetic model and b) fit of the concentration of the products in time-resolved experiments with the functions for the proposed model. Reaction conditions: substrate 120 mg, catalyst 50 mg, methanol 5 mL, DMSO as internal standard 80  $\mu$ L, 160  $^{\circ}$ C. Adapted from Ref. 196 with permission from The Royal Society of Chemistry.

Under the considered reaction conditions, the second pathway was highly favored and methyl fructosides were formed in high yields at the beginning of the process. However, methyl fructosides were reactive compounds, they accumulated in this first step as masked substrates and then they were hydrolyzed back to fructose. Thus, the formation of methyl lactate followed two kinetic regimes. In the first regime, methyl lactate derived directly from the retro-aldol pathway of fructose at the beginning. Afterwards, in a second kinetic regime, methyl lactate was formed by the slow hydrolysis of methyl fructosides.

<sup>3</sup> The project was carried out in collaboration with Senior Researcher Sebastian Meier and Associate Professor Pernille Rose Jensen (DTU) for the kinetic fits and the calculations of reaction rate constants.

Table 3.3. First-order rate constants of the different reactions occurring in the process for the formation of methyl lactate from hexoses.

	Reaction	Constant ( $\text{min}^{-1}$ )
$k_1$	Isomerization glucose-fructose	1.8
$k_{-1}$	Isomerization fructose-glucose	1.8
$k_2$	Formation of methyl fructosides	3.6
$k_{-2}$	Hydrolysis of methyl fructosides	0.036
$k_3$	Retro-aldol to methyl lactate	0.72

In Table 3.3 the calculated first-order rate constants of the different reactions occurring in the process are listed. Considering  $k_2$  and  $k_3$ , the rate for the formation of methyl fructosides occurred faster than the pathway leading to methyl lactate. Thus, the formation of methyl fructosides was favored at the beginning of the process. On the other hand, the hydrolysis of methyl fructosides with a rate constant ( $k_{-2}$ ) of  $0.036 \text{ min}^{-1}$  was the rate-determining step. The kinetics for the formation of methyl lactate was strongly dependent on the Fischer glycosylation of the substrate catalyzed by the weak residual Brønsted acidity. Balanced Brønsted and Lewis acidity of the catalyst was essential for the control of the productivity of the process.

### 3.3.3 Improving the productivity in methyl lactate by the addition of small amounts of water

In the reaction model proposed, methyl fructosides assumed a central role in determining the production of methyl lactate. In fact, they were the first intermediates formed in the process and their consumption was the rate-determining step. Thus, a possible acceleration of the production of methyl lactate could be obtained by addition of water to reaction media in order to facilitate the hydrolysis of methyl fructosides to fructose. The use of water as the solvent was previously avoided due to the instability of Sn-Beta catalysts in aqueous solutions.<sup>105</sup> However, the addition of few percent water in the alcoholic solvent could act as promoter of the hydrolysis maintaining the properties of the catalyst unaltered.

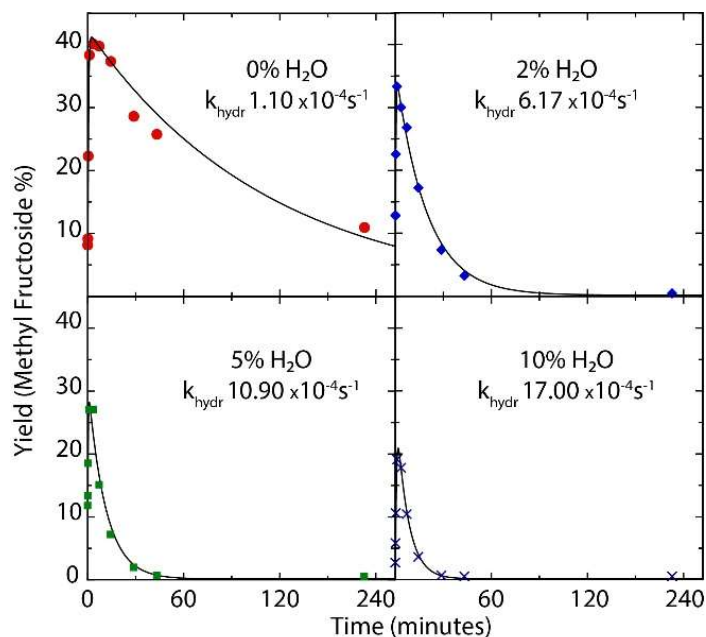


Figure 3.18. Time-resolved experiments in mixtures containing different percentages of water. Reaction conditions: substrate 120 mg, catalyst 50 mg, methanol 5 mL, DMSO as internal standard 80  $\mu\text{L}$ , 160  $^{\circ}\text{C}$ .

### 3.3 Kinetic Analysis of the Production of Methyl Lactate

Figure 3.18 illustrates the effect of the addition of small volumes of water to the reaction. Water drastically affected the formation of methyl fructosides and the kinetics of the formation of methyl lactate. The water had two main effects on the methyl fructoside intermediates. First, it prevented the glycosylation of fructose and the maximum yields of methyl fructosides decreased in reactions containing increased amounts of water (Figure 3.19 a). Second, their hydrolysis was accelerated and no traces of methyl fructosides were present after two hours in all the reactions containing water. Thus, hydrolysis of methyl fructosides was accelerated by factors of 5.6, 9.9, 15.5 in the case of 2, 5 and 10% (v/v) of water, respectively. The promoted hydrolysis released free fructose (Figure 3.19), which rapidly entered the retro-aldol pathway leading to methyl lactate. Thus, the presence of water accelerated the formation of methyl lactate (Figure 3.19 b).

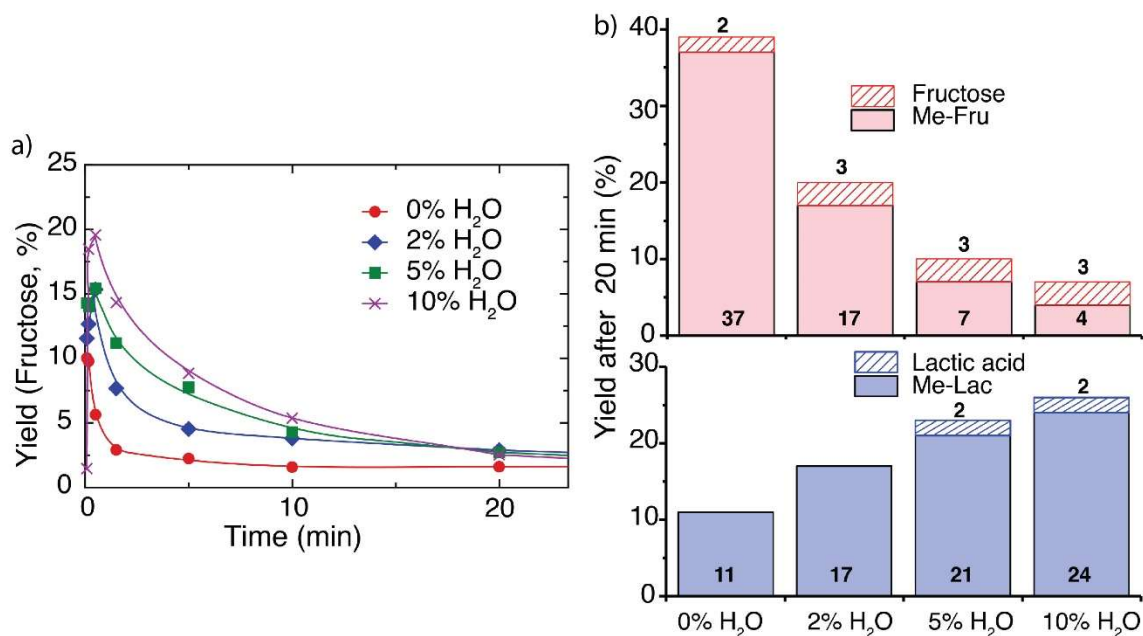


Figure 3.19. a) Formation and consumption of fructose in time-resolved experiments for the conversion of glucose in the presence of different amounts of water and b) yields of methyl fructosides, fructose, methyl lactate and lactic acid after 20 minutes of reaction in the presence of different amounts of water. Reaction conditions: substrate 120 mg, catalyst 50 mg, methanol 5 mL, DMSO as internal standard 80  $\mu$ L, 160  $^{\circ}$ C. Adapted from Ref. 196 with permission from The Royal Society of Chemistry.

The presence of water also affected the formation of the methyl glucosides byproduct, which showed decreased yields upon addition of water. These products were formed in very small amounts in all the reactions and they were neglected for the general process. Results indicated the possibility to increase the rate for the formation of methyl lactate by simple addition of water to the reaction media. The acceleration of the production can represent an important improvement for the application of the process in continuous operations.<sup>110</sup> Moreover, water has been shown to affect the stability of Sn-Beta catalysts in continuous operations.<sup>109</sup>

#### 3.3.4 Comparison in the production of methyl lactate using different starting substrates

The distribution of products in the reactions converting fructose or glucose revealed only minor differences due to the fast isomerization between the two carbohydrates catalyzed in the presence of Lewis acidic catalysts at high temperature. However, small differences were measurable when comparing the conversion of the substrate in the first ten minutes of reaction (Figure 3.20 b). Both substrates were completely consumed within the first five minutes, but fructose was consumed faster than glucose. The effect was due to the additional pre-equilibrium of glucose into fructose before reacting, while fructose directly entered the reactive pathways.

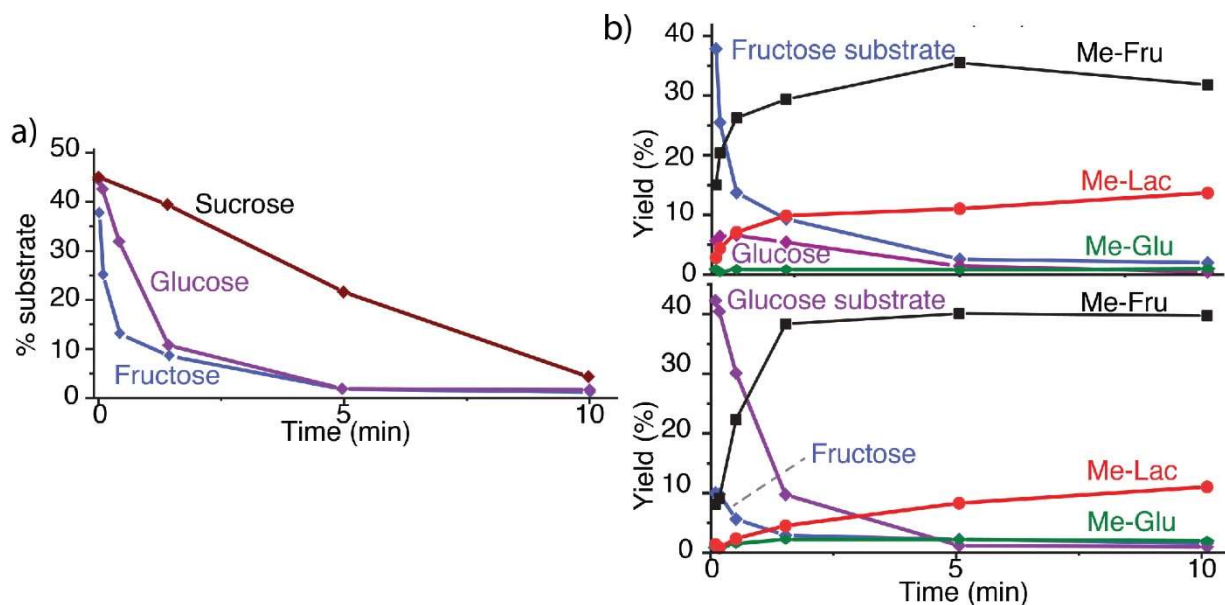


Figure 3.20. a) Comparison of the conversion of fructose, glucose and sucrose during the first ten minutes of reaction and b) products distribution during the first ten minutes of reaction using fructose (top) and glucose (bottom) as starting substrate. Reaction conditions: substrate 120 mg, catalyst 50 mg, methanol 5 mL, DMSO as internal standard 80  $\mu$ L, 160  $^{\circ}$ C. Adapted from Ref. 196 with permission from The Royal Society of Chemistry.

The trends for the conversion of fructose and glucose were then compared with the consumption of the disaccharide sucrose over time (Figure 3.20 a). In contrast to fructose and glucose, sucrose was only completely converted after ten minutes of reaction due to the further necessary step of solvolysis of the substrate before conversion into the reactive species. The solvolysis of sucrose in methanol gave glucose and methyl fructosides, as seen previously in this chapter. Therefore, methyl fructosides were accumulated in higher yields starting from sucrose compared to the other substrate. Thus, hydrolysis and slow release of the reactive species were necessary in this case and the process starting from sucrose presented slightly different features compared to glucose and fructose.<sup>111</sup> All substrates presented the general effect of acceleration of methyl lactate production by addition of water. In all cases, the promotion of the hydrolysis of the accumulated methyl fructosides led to increased rates in the formation of methyl lactate.

### 3.3.5 Comparison between hydrothermal and post-synthetic Sn-Beta zeolites

All the results previously considered in this section were obtained by the use of a hydrothermal Sn-Beta (150) zeolite as the catalyst. The hydrothermal synthesis of zeolites leads to large-crystal defect-free materials<sup>52</sup> and, in this case, high Lewis acidity. Differently, Sn-Beta zeolites prepared by post-synthetic treatments have many structural defects present in the samples as large silanol nests. The use of post-treated catalysts in the process for the conversion of hexoses to methyl lactate was studied and the results compared with the data obtained using hydrothermal samples. Table 3.4 reports the physical characterization of the prepared post-treated and hydrothermal Sn-Beta. The post-synthetic modification produced a material with higher amounts of acid sites, measured by  $\text{NH}_3$ -TPD. Moreover, the presence of defects was reflected in lower crystallinity and higher surface area compared to the hydrothermal catalyst.

### 3.3 Kinetic Analysis of the Production of Methyl Lactate

Table 3.4. Physical properties of the studied hydrothermal Sn-Beta (150) and post-treated Sn-Beta (150).

	Hydrothermal Sn-Beta (150)	Post-treated Sn-Beta (150)
Crystallinity (%) <sup>a</sup>	93.66	59.60
SBET (m <sup>2</sup> /g) <sup>b</sup>	602	722
Sn (wt%) <sup>c</sup>	1.189	0.977
Si/Sn <sup>c</sup>	130.36	152.80
V <sub>micropore</sub> (mL/g) <sup>d</sup>	0.24	0.30
Total acid sites (μmol/g) <sup>e</sup>	56	108

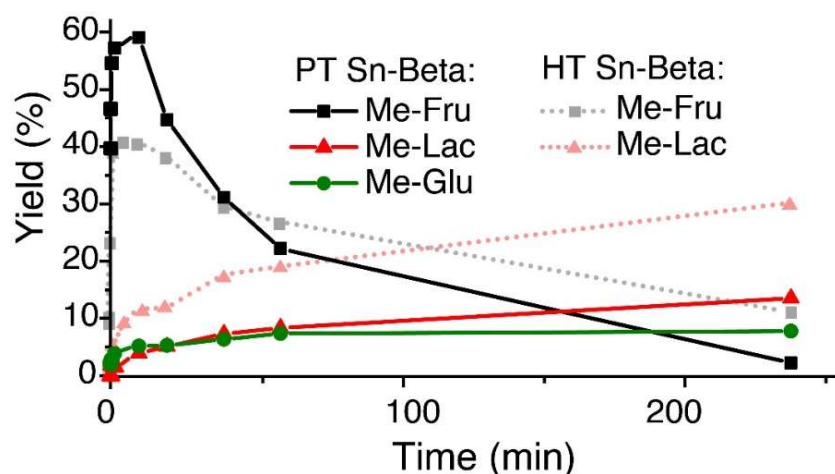


Figure 3.21. Comparison of the distributions of products in time resolved-experiments for the conversion of hexoses catalyzed by post-treated or hydrothermal Sn-Beta (150) zeolites. Reaction conditions: substrate 120 mg, catalyst 50 mg, methanol 5 mL, DMSO as internal standard 80 μL, 160 °C. Adapted from Ref. 196 with permission from The Royal Society of Chemistry.

Notably, the Lewis acidity of post-treated Sn-Beta was sufficient for promoting both the isomerization of glucose and the retro-aldol pathway to methyl lactate. However, the higher amount of acid sites in post-treated zeolites catalyzed higher yields of methyl fructosides at the beginning of the process. Methyl glucosides and furanic byproducts were also produced in larger amount in this case. The increased Brønsted acidity was reflected in decreased yields of methyl lactate formed during the process due to the competitive reaction pathways catalyzed by the Brønsted acidity. Thus, a proper balanced between Lewis and Brønsted acidic properties of the catalyst was still essential for achieving high productivity in methyl lactate.

#### 3.3.6 The role of methyl glycosides in the conversion of different substrates catalyzed by post-treated Sn-Beta zeolite

Methyl fructosides are central intermediates during the conversion of glucose, fructose and sucrose in methanol.<sup>152</sup> They were formed in high yields at the beginning of the reaction prior to being hydrolyzed and converted into the different products. Thus, hydrolysis of methyl fructosides was the step controlling the rate of the processes catalyzed by Sn-Beta zeolites in methanol.<sup>196</sup> Methyl fructosides had a high impact on the rate of the conversion of hexoses catalyzed by hydrothermal Sn-Beta. Nevertheless, post-synthetic catalysts promoted increased formation of methyl glycosides and the step of hydrolysis assumed great importance. This paragraph includes a short analysis of the role of methyl glycosides in the conversion of different carbohydrate substrates, i.e. pentoses and tetroses, catalyzed by post-synthetic Sn-Beta zeolites.

Figure 3.22 illustrates the time-resolved experiments for the conversion of xylose. Xylose is an aldo-pentose and its conversion by Sn-Beta zeolites gave methyl 2,5-dihydroxy-3-pentenoate (DPM) and methyl lactate (ML) as the main products.<sup>174</sup> The pattern over time followed the same steps as the conversion of hexoses. The conversion of the starting pentose substrate occurred rapidly and the consumption of xylose was completed at the very beginning of the process. Concurrently, methyl xylosides were formed in high yields (50%). The slow hydrolysis of methyl glycosides over prolonged reaction times led to the increased formation of the products, i.e. methyl lactate and DPM. Thus, methyl glycosides seemed to assume a central role for the general conversion of carbohydrates in methanol.

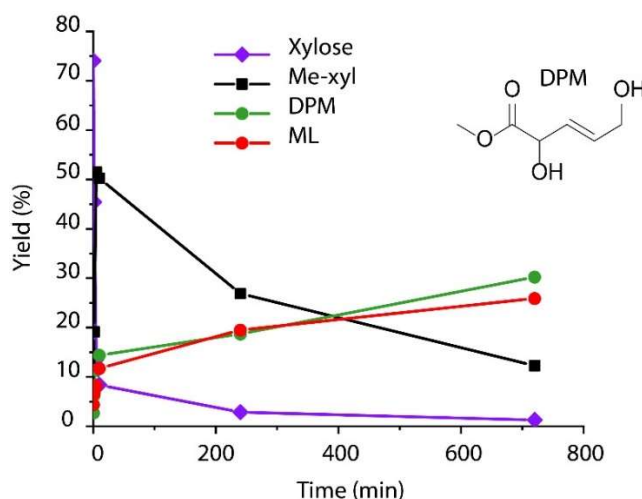


Figure 3.22. Time-resolved experiments for the conversion of xylose catalyzed by post-treated Sn-Beta catalysts. Reaction conditions: xylose 120 mg, catalyst 50 mg, methanol 5 mL, DMSO as internal standard 80  $\mu$ L, 160  $^{\circ}$ C.

The impact of the formation of methyl glycosides in the reactions catalyzed by post-treated Sn-Beta zeolites in methanol was further studied by comparison with the conversion of erythrulose under the same conditions (Figure 3.23). Erythrulose is a keto-tetrose and the derived methyl glycosides were not observed during the reaction in methanol. The conversion of erythrulose using Sn-Beta zeolites gave methyl vinyl glycolate (MVG) as the main product. The process for the production of MVG and is discussed in detail in Chapter 4.1.6.

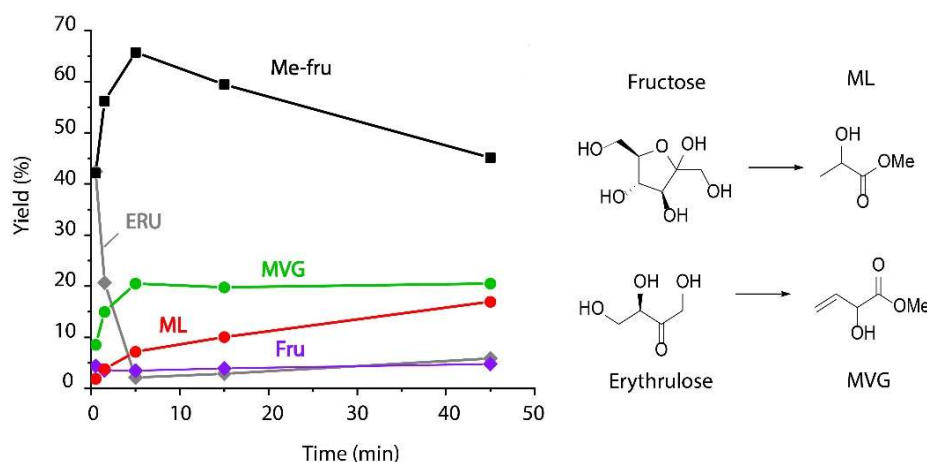


Figure 3.23. Distribution of products during the first hour of reaction for the conversion of a mixture of erythrulose and fructose catalyzed by post-treated Sn-Beta zeolite. Reaction conditions: erythrulose 60 mg, fructose 60 mg, catalyst 50 mg, methanol 5 mL, DMSO as internal standard 80  $\mu$ L, 160  $^{\circ}$ C.



### 3.3 Kinetic Analysis of the Production of Methyl Lactate

In this section, erythrulose was used as reference substrate for the analysis of the kinetic impact of the formation of methyl glycosides on the process. A mixture of fructose and erythrulose was reacted in methanol at 160 °C using Sn-Beta zeolite as the catalyst. Figure 3.23 shows the distribution of products derived from the conversion of both substrates during the first hours. Fructose was rapidly converted and the yields of methyl fructosides reached 40% in the first two minutes. The maximum yields of methyl fructosides at the beginning of the process exceeded 60% using a post-treated Sn-Beta catalyst. On the other hand, erythrulose was converted slightly slower compared to fructose and it was completely consumed after the first five minutes. However, erythrulose did not form glycoside intermediates and the reagent was immediately converted into the product. The formation of MVG occurred in the first five minutes and yields were not increased further for prolonged reaction times. In contrast, methyl lactate was only slowly formed without the presence of water and 45% of unreacted methyl fructosides was still present in the reaction mixture after 45 minutes. The results confirmed the role of methyl fructosides as intermediates during the conversion of fructose in methanol. The absence of methyl glycosides formation during the conversion of erythrulose had a great impact on the kinetics of the process, leading to an immediate formation of the final product.

#### 3.3.7 Conversion of different keto-hexoses: comparison between fructose and sorbose

The experimental data showed that the ketose fructose was the reactive species in the process for the formation of methyl lactate from glucose and initially rapid isomerization between fructose and glucose occurred. The use of reactive substrates leading to high selectivity into the desired product and minor amounts of byproducts would simplify the design of downstream processes and the purification of the product. Different ketoses, such as tagatose, sorbose and psicose, have previously shown different reactivity from fructose in the formation of 5-hydroxymethylfurfural (HMF) catalyzed by mineral acids.<sup>205</sup> Although L-sorbose is available in nature and it presents a structure similar to D-fructose, the application of sorbose in chemical reactions is rare. The main application of sorbose in industry is in the synthesis of vitamin C.<sup>140</sup> In this paragraph, the reactivity of sorbose for producing methyl lactate in methanol at 160 °C using post-treated Sn-Beta zeolite catalysts is investigated and compared to the conversion of fructose. The conversion of a mixture of fructose and sorbose was studied by time-resolved experiments (Figure 3.24).

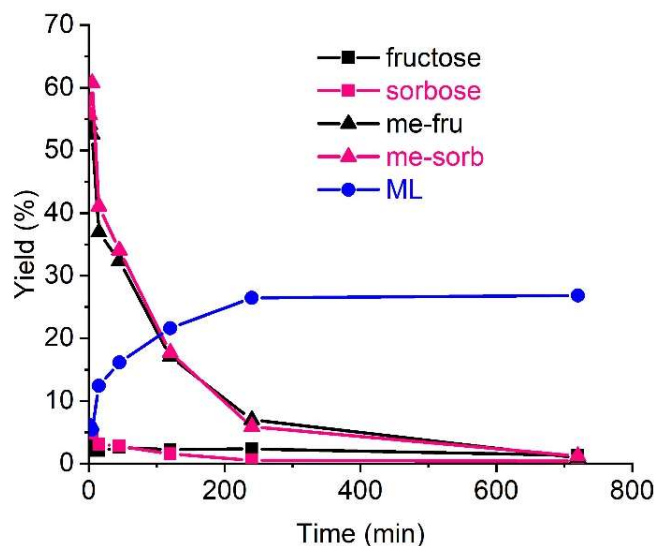


Figure 3.24. Conversion of a mixture of sorbose and fructose into methyl lactate. Reaction conditions: sorbose 60 mg, fructose 60 mg, catalyst 50 mg, methanol 5 mL, DMSO as internal standard 80  $\mu$ L, 160 °C.

The trends of the reactions for the conversion of fructose and sorbose were identical (Figure 3.24). Sorbose was rapidly consumed in the first few minutes of reaction under the considered conditions. Concurrently, methyl sorbosides were formed in yields over 60% and then hydrolyzed and converted into other products in prolonged reaction times. Similar reaction profiles were observed for fructose and methyl fructosides. Methyl lactate was formed following the same pattern as for the conversion of only fructose. Thus, the results indicated that there was no difference between fructose and sorbose in the conversion into methyl lactate catalyzed by Sn-Beta zeolite catalysts.

### 3.3.8 Conclusions on the kinetic analysis of the production of methyl lactate from carbohydrates catalyzed by Sn-Beta zeolites

In this section, the kinetics of the conversion of hexoses into methyl lactate was analyzed by series of time-resolved experiments. The formation and conversion of methyl glycosides was followed by  $^1\text{H}$ - $^{13}\text{C}$  HSQC NMR. The reactions starting from fructose, glucose and sucrose showed similar trends, the initial isomerization was promoted and there was no difference in the products distribution for the reactions starting from the different substrates. In all cases, the initial reagent was consumed in the first few minutes concurrently to the formation of high yields of methyl fructosides. Afterwards, methyl fructosides were hydrolyzed and converted. Thus, a biexponential kinetic model for the formation of methyl lactate was proposed involving two kinetic regimes. The first regime involved the direct retro-aldol pathway from fructose and the second pathway proceeded with the hydrolysis of methyl fructosides.

The majority of methyl lactate was produced in the second step. Moreover, calculated rate constants indicated that the hydrolysis of methyl fructosides was the rate-determining step of the process. Thus, the production of methyl lactate was drastically accelerated by the addition of small amounts of water (2-10% (v/v)). The results were used for further analysis of the process starting from different substrates and the differences between post-treated and hydrothermal zeolites. In general, residual weak Brønsted acidity was enhanced in post-synthetic samples due to the presence of high amounts of defects. Thus, post-treated catalysts showed increased formation of methyl fructosides at the beginning of the process, in association with decreased selectivity for the products derived from the Lewis acid-catalyzed pathways. The study was also extended to the conversion of different substrates, resulting in analogous findings and confirming the proposed model.



# Chapter 4

## Conversion of Glycolaldehyde into Bio-Based Chemicals

Glycolaldehyde is an abundant product formed during the pyrolysis of cellulose and it represents a renewable resource for the production of bio-based chemicals. Using homogeneous tin halides or heterogeneous stannosilicates as catalysts, cascade reactions leading to C4 hydroxy esters are catalyzed.<sup>183</sup> In particular, methyl vinyl glycolate (MVG) was produced using Sn-Beta catalysts for applications in the polymer industry.<sup>191</sup> This chapter includes the study of the conversion of glycolaldehyde into MVG. The catalytic process was investigated by time-resolved experiments and the data were analyzed in order to propose a kinetic model in comparison with the kinetics of the conversion of hexoses and tetroses under the same conditions. The effect of water and additives such as alkali was also considered.

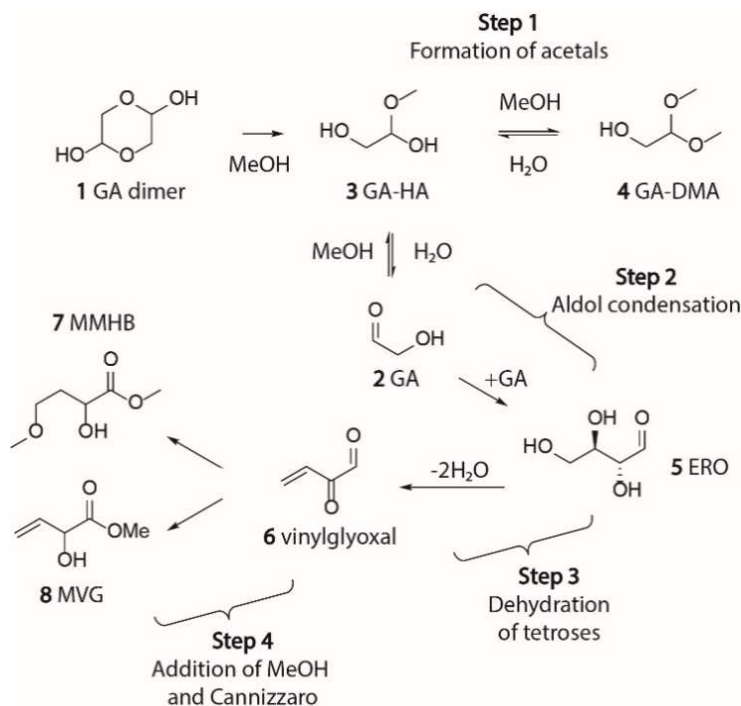
### 4.1 Conversion of Glycolaldehyde Using Sn-Beta Catalysts

Glycolaldehyde (GA) is a useful bio-based feedstock for the production of chemicals. Mixtures of oxygenate compounds containing high concentration of glycolaldehyde can be produced from the pyrolysis of cellulose.<sup>175</sup> In the study of the conversion of carbohydrates catalyzed by Sn-Beta zeolites, GA represents one of the smallest compounds formed by retro-aldol cleavage. However, using hexoses as starting substrates, the [3+3] retro-aldol pathway, leading to the cascade process to form methyl lactate, is preferred.<sup>111</sup> Glycolaldehyde can be used as the starting reagent for the formation of hydroxy esters promoted by Sn-Beta catalysts. The process from GA gives methyl vinyl glycolate (MVG) as the main product, which can represent a new green monomer for the production of polyesters.<sup>183</sup> As the terminal double bond of MVG allows the insertion of additional functionalities and the possibility to modulate the physical properties in the final materials, the process for the conversion of glycolaldehyde to MVG has lately received much attention.<sup>191</sup> On the other hand, the use of a small molecule as starting reagent complicates the available pathways of transformation and the mechanisms of the reaction. Thus, the study of the process still misses fundamental understanding.

The process for the conversion of glycolaldehyde using Sn-Beta catalysts was explored in order to understand the involved reaction pathways and to control selectivity. Under optimized conditions, the production of MVG could represent a new route for the development of sustainable building blocks for polymers and this section had the purpose to improve the knowledge on the process. The screening of the reaction parameters aimed to optimize the conditions and to increase yields and selectivity into the desired products. The comparison with the reaction using a larger starting substrate and mechanistic insight are discussed in the following section.

### 4.1.1 The process for the formation of MVG from glycolaldehyde

Glycolaldehyde is a small molecule and the study of the different pathways during its conversion is extremely complex. The available reaction pathways are numerous and the main mechanism of the formation of products can change by modification of the reaction conditions. A comprehensive overview of the reaction pathways has been reported by Dusselier et al. for the study of the formation of MVG and methyl-5-methoxy-2-hydroxybutanoate (MMHB) from glycolaldehyde<sup>183</sup> or tetroses<sup>169</sup> using tin halide catalysts. The proposed mechanism starting from GA is shown in Figure 4.1. First, GA can undergo acetalization leading to the reversible<sup>206</sup> formation of the hemiacetal (**3** GA-HA) or the dimethyl acetal (**4** GA-DMA). On the other hand, 2 molecules of GA can react by aldol condensation to form erythrose (**5** ERO) as central intermediate for the sequential formation of hydroxy esters. The tetrose **5** undergoes dehydration by two sequential retro-Michael reactions forming the intermediate vinylglyoxal **6**. The final step involves the addition of the solvent and formal intramolecular Cannizzaro reaction to form the products. This latter reaction has been considered as the responsible step for the discrimination between formation of MVG and MMHB. However, no experimental evidences have been available for the identification of the mechanism during the last step.<sup>183</sup> The authors have identified the last intramolecular Cannizzaro reaction as the rate-determining step for the process starting from tetroses<sup>169</sup> and the hydrolysis of GA-DMA to free GA as the rate-determining step in the case of the use of GA as the starting substrate.<sup>183</sup>

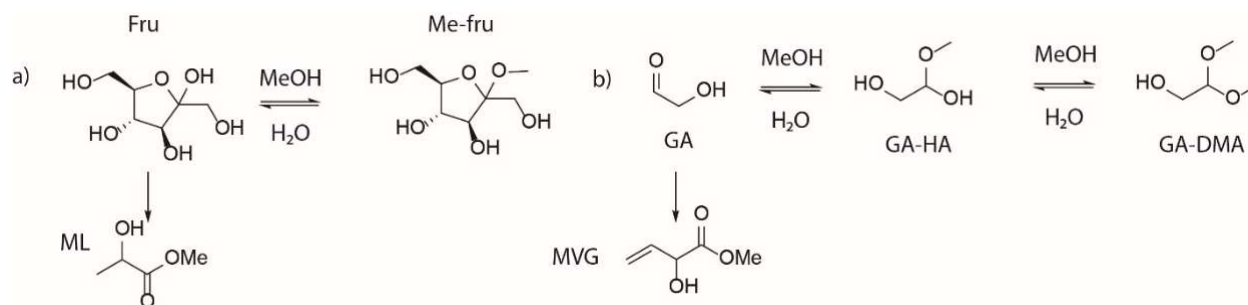


Scheme 4.1. Simplified scheme for the cascade reactions during the process for the conversion of GA into MVG and MMHB proposed by Dusselier et al.<sup>183</sup>

First, the process was studied considering the similarity with the reaction for the conversion of hexoses to methyl lactate promoted by Sn-Beta catalysts. In both cases, the process was carried out in methanol at 160 °C and the starting reagents could undergo two competitive reactions. The first pathway involved the aldol condensation of two molecules of GA or the retro-aldol cleavage of fructose and they both led to cascade processes resulting into the desired hydroxy esters (MVG or methyl lactate, respectively). Concurrently, the competitive acetalization of the substrate with methanol occurred. As discussed in Chapter 3.3.1, fructose in

## 4.1 Conversion of GA Using Sn-Beta Catalysts

methanol at 160 °C preferably formed methyl fructosides, whereas the majority of methyl lactate derived from further hydrolysis of methyl fructosides (Scheme 4.2 a). This second step of hydrolysis was determined to be the rate-determining step of the process. The kinetics for formation of methyl lactate from hexoses followed a biexponential model composed of two apparent first order reactions.<sup>196</sup> Analogously in the case of glycolaldehyde (GA), the reaction could proceed by formation of the hemiacetal (GA-HA) and dimethyl acetal (GA-DMA) or to the aldol condensation of two molecules of glycolaldehyde giving erythrose (ERO). Also in this case, the acetalization of the starting substrate occurred quickly at the beginning of the process and the dimethyl acetal was the main form of glycolaldehyde formed after few minutes. Free glycolaldehyde was never observed in the mixtures under these conditions. The conversion of GA-DMA was therefore used as representation for the consumption of the starting substrate (Scheme 4.2 b).



Scheme 4.2. Similarity between the process for the conversion of a) hexoses and b) GA in methanol at 160 °C catalyzed by Sn-Beta zeolites.

The process was studied by *ex situ* time-resolved experiments in order to extrapolate the order of the reaction from the experimental data. As for the kinetic study of the conversion of hexoses by Sn-Beta catalysts, the crude mixtures were analyzed by <sup>13</sup>C-NMR and quantification was performed by the use of an internal standard (mesitylene).

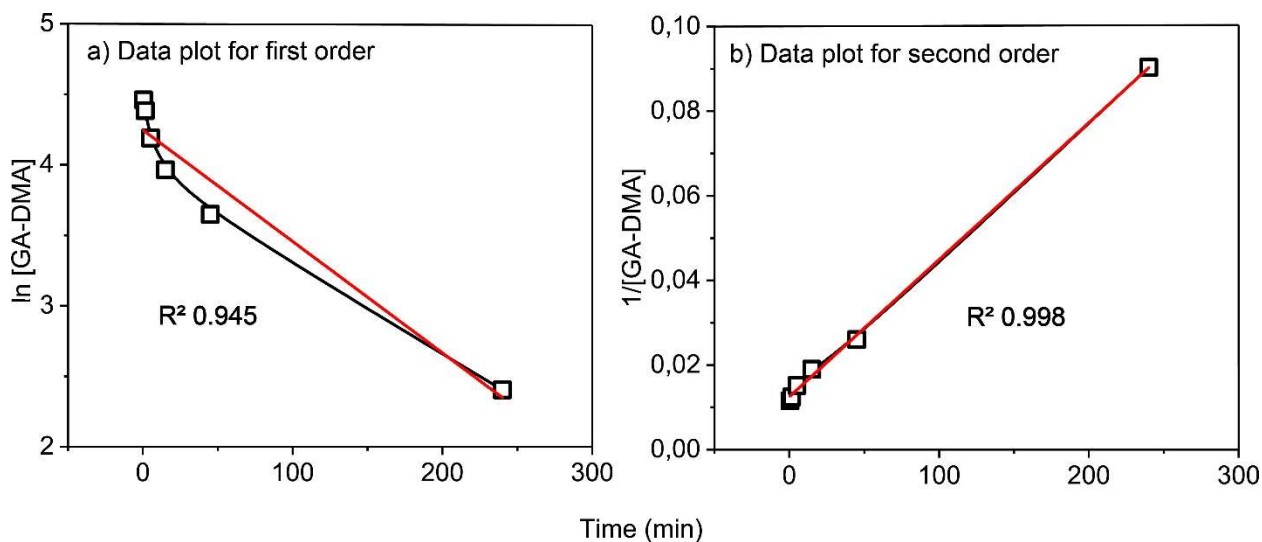
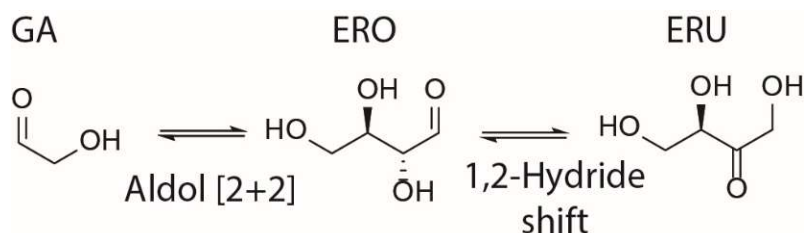


Figure 4.1. Data plot for the conversion of GA-DMA during the time using Sn-Beta catalysts.

The plots of the data for the conversion of GA-DMA over time are shown in Figure 4.1. The integrated rate law for a first-order reaction is  $\ln[A] = \ln[A_0] - kt$ . Thus, the correlation between logarithm of the concentration of the substrate and time is linear in first-order reactions. On the other hand, the integrated rate law for a second-order reaction is  $1/[A] = 1/[A_0] + kt$  and the concentration is linear between time and reciprocal of the concentration of the substrate. The experimental data followed the trend of a second-order reaction (Figure 4.1), which was consistent with the aldol condensation of two molecules of glycolaldehyde as the determining step. Figure 4.2 shows the distribution of products over time. The acetalization of glycolaldehyde under these conditions occurred immediately and GA-DMA was the main product at the beginning of the process, whereas the hemiacetal (GA-HA) was present in the mixtures only in small amounts. Blank reactions showed that the acetalization of glycolaldehyde was also thermally promoted in the absence of a catalyst, as also reported in literature.<sup>183</sup> MVG was the main product, while methyl-5-methoxy-2-hydroxybutanoate (MMHB), methyl-2,4-dihydroxybutanoate (MHMB), methyl lactate (ML) and  $\alpha$ -hydroxy- $\gamma$ -butyrolactone (HBL) were formed as minor byproducts. Moreover, erythrulose (ERU) was an identified intermediate formed by 1,2-hydrate shift of erythrose (ERO), which is the product of the aldol condensation of two molecules of glycolaldehyde (Scheme 4.3).



Scheme 4.3. Formation of the intermediate erythrulose (ERU) from glycolaldehyde (GA) *via* erythrose (ERO)

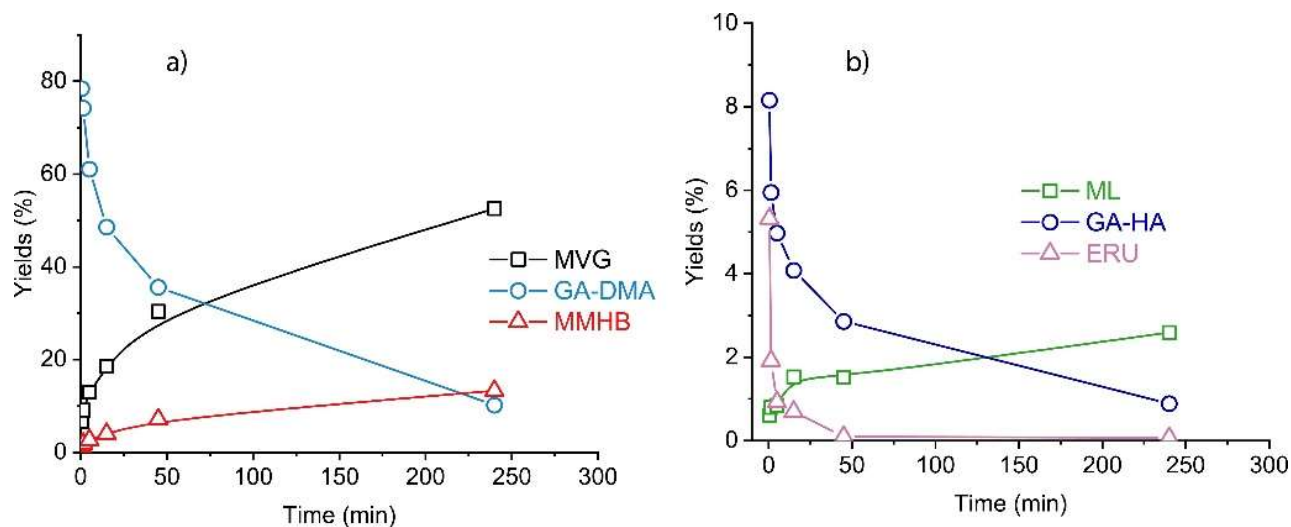


Figure 4.2. General distribution of products and intermediates in the conversion of glycolaldehyde by Sn-Beta catalysts. Reaction conditions: glycolaldehyde 400 mg, catalyst 50 mg, methanol 5 mL, mesitylene 80  $\mu$ L as internal standard, 160  $^{\circ}$ C.

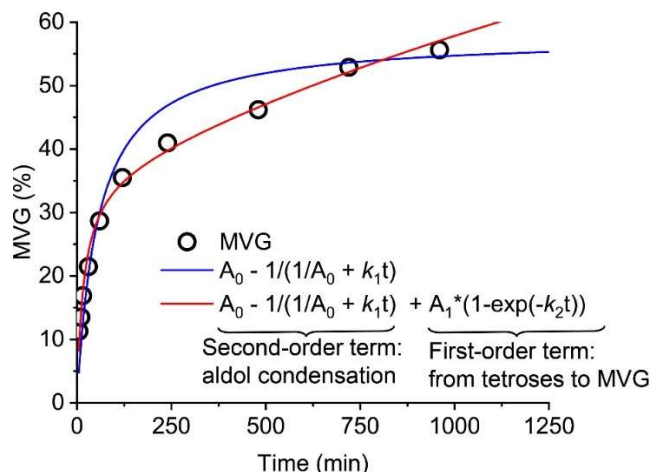


Figure 4.3. Formation of MVG from glycolaldehyde using Sn-Beta catalysts, fitting of time-resolved experiments.

Fitting of the data for the formation of MVG was not consistent with a second-order reaction kinetics (Figure 4.3). Instead, as for the production of methyl lactate from glucose, the trend for the formation of MVG over time showed the presence of two kinetic regimes. The red trend-line for the formation of MVG in Figure 4.3 was given by the combination of a second-order kinetic function (the first term) and a first-order function (the second term). The kinetic law for the second-order fit of the yields of MVG ( $Y$ ) was  $Y = A_0 - 1/(1/A_0 + k_1t)$ , where  $A_0$  is the maximum yield of MVG and  $k_1$  the apparent second-order rate constant. The expression of the combination of a second-order and first-order kinetics was defined as  $Y = A_0 - 1/(1/A_0 + k_1t) + A_1*(1 - \exp(-k_2t))$ , where  $A_1$  represented the maximum yields of MVG during the second regime and  $k_2$  the apparent first-order constant. It could be assumed that the first term indicated the formation of MVG derived from the direct aldol condensation of GA and represented correctly the beginning of the process. The second part of the expression could be referred to the hydrolysis of the acetals, the dehydration of tetroses or the intramolecular Cannizzaro reaction.

Hypothetically, the process for the formation of MVG was determined by the aldol condensation of two molecules of GA at short times. During the reaction progress, when all the starting substrate reacted, the process followed the same kinetics as for the conversion of the formed erythrose. As reported previously for the formation of MMHB from tetroses,<sup>169</sup> the final Cannizzaro reaction was the rate-determining step. On the other hand, the same authors proposed the hydrolysis of the acetals as the rate-determining step for the conversion of GA catalyzed by homogeneous tin salts.<sup>183</sup> Nevertheless, more experimental evidences were necessary in order to elucidate the determining step during this second kinetic regime and hydrolysis of the acetals, dehydration of tetroses or intramolecular Cannizzaro reaction were all possible candidates for the rate-determining step. Thus, the kinetic model for the formation of MVG from GA catalyzed by Sn-Beta zeolites has not been clarified yet and the conclusions of the kinetic model are currently under elaboration.

### 4.1.2 The study of the reaction conditions for the conversion of glycolaldehyde

The study of the conversion of glycolaldehyde into MVG started with the optimization of the reaction conditions. The effect of different parameters on the selectivity for the desired products and on the rate of the formation of MVG was analyzed. First, the effect of the concentration of the starting substrate was investigated, resulting in the acceleration of the process for high concentration of the initial reactant, as expected for a second-order reaction. In the same way, the use of catalysts containing different amounts of tin induced

acceleration in the formation of MVG (Chapter 5.1.3). Thus, optimal conditions for the study of the process in batch reactions were defined as 400 mg GA in 5 mL methanol using 100 mg of Sn-Beta (150) at 160 °C.

Among the parameters studied for optimizing the selectivity for MVG, the use of different stannosilicate catalysts was explored. In this case, the hydrothermal Sn-Beta showed similar activity to the post-treated catalyst (Figure 4.4). Thus, the use of the post-treated catalysts was chosen for the ease of the synthetic procedure. The MFI framework was recalcitrant to the acidic dealumination process and the resulting post-treated Sn-MFI (150) presented a marked Brønsted acidity leading to GA-DMA and methyl glycolaldehyde dimethylacetal (MGA-DMA) as the only products of the conversion of GA in methanol. Hydrothermal Sn-MFI (150) was tested in order to understand the effect of the porosity of the catalyst on the formation of different products. The small pores of the MFI framework can give beneficial confinement effects for the small substrate in the pores.<sup>185</sup> However, Sn-MFI did not show improved activity compared to Sn-Beta. In contrast, the reaction seemed to proceed at lower rate, tetrose intermediates accumulated and MVG was formed only in 18% yield after two hours compared to 36% yield obtained with the use of Sn-Beta under the same conditions (Figure 4.4). The formation of lactone byproducts was suppressed using Sn-MFI as catalyst, probably because of steric effects in the small pores for the large compounds. Sn-USY (150) zeolite was also tested as a catalyst for the conversion of GA to MVG, resulting in the deceleration of the process and higher yield of GA-DMA compared to the use of Sn-Beta were found after two hours (Figure 4.4.).

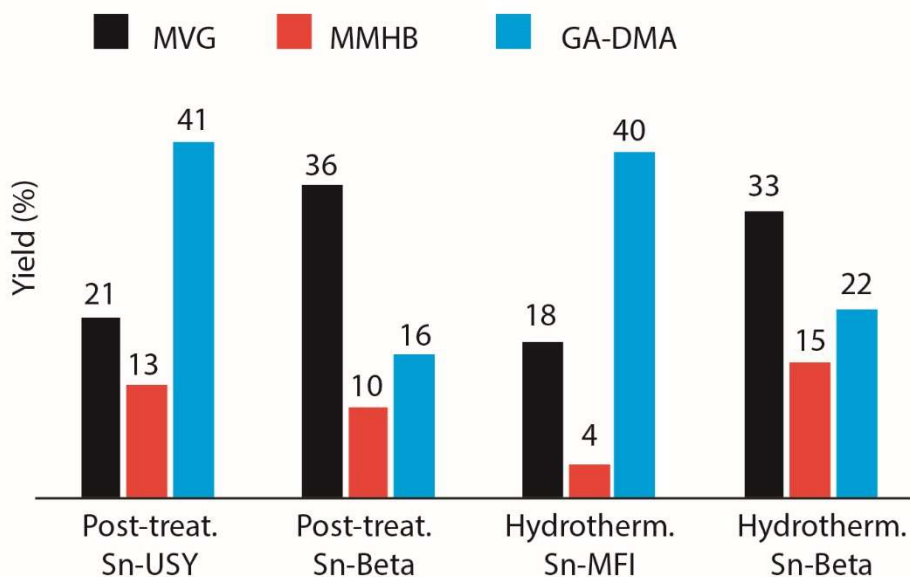
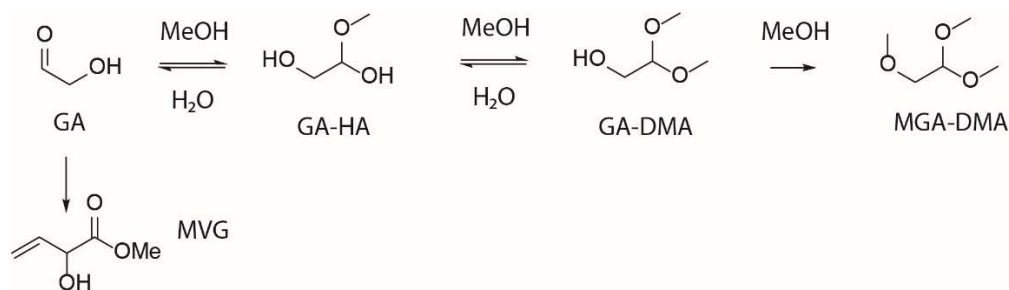


Figure 4.4. Distribution of main products in the conversion of glycolaldehyde using Sn-USY and Sn-Beta, Sn-MFI and hydrothermal Sn-Beta zeolite catalysts. Reaction conditions: glycolaldehyde 400 mg, catalyst 100 mg, 5 mL methanol, mesitylene 80  $\mu$ L as internal standard, 160 °C, 2 hours.

#### 4.1.3 Effect of water on rate and MVG formation

In the proposed model for the formation of MVG from glycolaldehyde in methanol,<sup>183</sup> the product derived both from the direct aldol condensation of two molecules of glycolaldehyde and from the hydrolysis of the dimethyl acetal intermediate. Thus, the presence of water could promote the hydrolysis of GA-DMA and accelerate the formation of MVG (Scheme 4.4). The effects of small amounts of water on the reaction kinetics and on the distribution of products were therefore studied.

## 4.1 Conversion of GA Using Sn-Beta Catalysts



Scheme 4.4. Equilibria of glycolaldehyde in methanol. In the presence of a catalyst or at high temperatures, the formation of the hemiacetal and the dimethyl acetal forms is favored.

Scheme 4.4 shows the equilibria of glycolaldehyde in methanol. In the presence of a catalyst or at high temperatures, the formation of the hemiacetal (GA-HA) and the dimethyl acetal (GA-DMA) forms was favored.<sup>183</sup> A further reaction with methanol led to the formation of the methyl glycolaldehyde dimethyl acetal (MGA-DMA). This last compound was formed only in small amount in the reaction mixtures, the reactivity is further discussed in this chapter. As described for hexoses in Chapter 3, the acetalization was the preferred pathway under the used reaction conditions. Thus, the effect of small amounts of water as a promoter for the hydrolysis of GA-DMA was investigated.

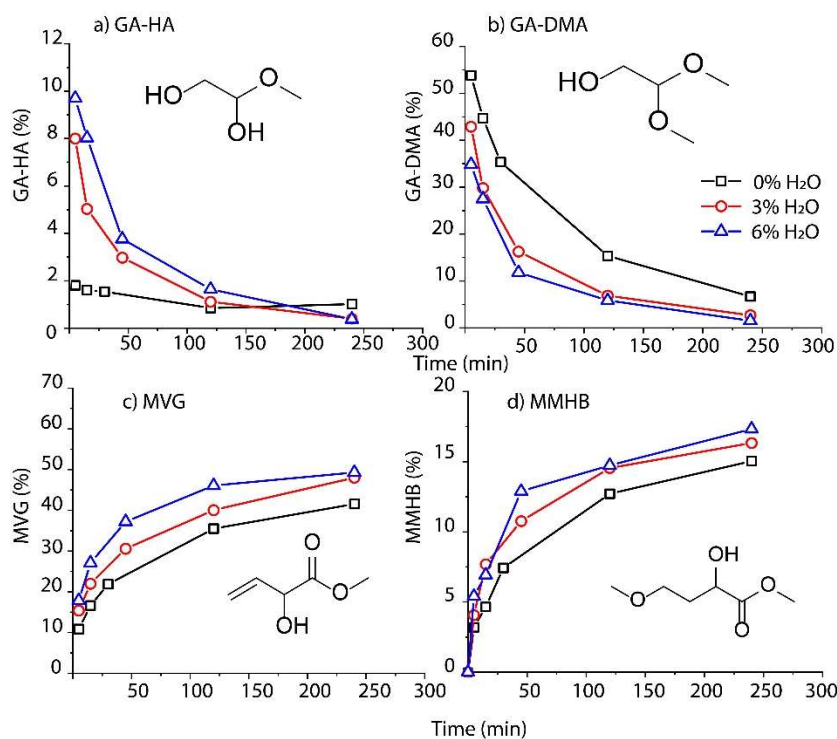


Figure 4.5. Conversion of glycolaldehyde by Sn-Beta with and without water, different methylated forms (a and b) and formation of main products (c and d). Reaction conditions: glycolaldehyde 400 mg, catalyst 100 mg, 5 mL methanol, mesitylene 80  $\mu$ L as internal standard, 160  $^{\circ}$ C.

Figure 4.5. shows the conversion of glycolaldehyde in the presence of 3 and 6% (v/v) of water. Compared to the reaction in the absence of water (black line), the water accelerated the conversion of GA-DMA. As previously described for methyl fructosides from fructose, the presence of water both promoted the hydrolysis and avoided the formation of the acetal intermediate resulting in lower maximum yields of GA-DMA at the



beginning of the reaction. The reduced formation of GA-DMA was associated with increased population of GA-HA. However, the hemiacetals hydrolysis occurred quickly and the effect of this product on the kinetics could be neglected. Moreover, the addition of small amounts of water completely suppressed the formation of the byproduct MGA-DMA. The trend for the formation of the main products, MVG and MMHB, was accelerated in the presence of water (Figure 4.5 c and d). The absence of the formation of GA-DMA needed to be correlated to a favored aldol condensation and an accelerated process at the beginning, when the kinetics was determined by the aldol condensation (first term of the function corresponding to a second-order kinetics) as described in Chapter 4.1.1. The results indicated the kinetic role of the hydrolysis in the process and the possibility to adjust the productivity in MVG by addition of water.

#### 4.1.4 The role of MGA-DMA

1,1,2-Trimethoxyethane (methyl glycolaldehyde dimethyl acetal, MGA-DMA) derived from the further reaction of GA-DMA with methanol (Scheme 4.4). This compound exhibited high stability and it accumulated in the mixtures as a stable byproduct. For this reason, the formation and the reactivity of MGA-DMA was explored. In the studied reactions, MGA-DMA was formed only in small amounts and it seemed to disappear over prolonged reaction times. However, the formation of byproducts in small amounts can be problematic during the upgrade of processes in continuous operations. Thus, the possibility to avoid the formation of MGA-DMA or to convert it into useful products was explored. Firstly, the commercial reagent for MGA-DMA was reacted using a post-treated Sn-Beta catalyst and different conditions. The compound was very stable in all cases and no conversion was observed. The presence of water did not help to promote the reactivity of this compound, which hence is an unreactive byproduct.

The formation and the conversion of MGA-DMA was also studied simulating the process conditions. MGA-DMA was synthesized *in situ* by using a slightly Brønsted acidic catalyst (dealuminated ZSM-5) from glycolaldehyde in methanol. The final reaction mixtures resulted in 50% of MGA-DMA and large amount of dehydration products, such as humins, due to the use of a Brønsted acidic catalyst and no initial reagent was visible (Figure 4.6 a). The heterogeneous Brønsted acidic catalyst was then removed and the mixtures reacted using a Sn-Beta zeolite as the catalyst. The conversion of MGA-DMA was observed, in association with the formation of MVG and increased yields of MMHB (Figure 4.6 b). In the presence of small amounts of water, the conversion of MGA-DMA and the formation of products increased (Figure 4.6 c).

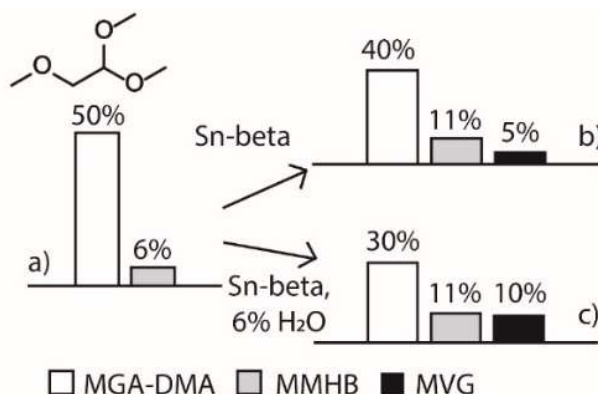


Figure 4.6. *In situ* formation and conversion of MGA-DMA. Reaction conditions: a) glycolaldehyde 400 mg, catalyst deAl-ZSM-5 100 mg, 5 mL methanol, mesitylene as internal standard 80  $\mu$ L, 160  $^{\circ}$ C, 2 hours. b) 5 ml of the mixture derived from (a), catalyst Sn-Beta 100 mg, mesitylene as internal standard 80  $\mu$ L, 160  $^{\circ}$ C, 2 hours. c) 5 ml of the mixture derived from (a), water 6% (v/v), catalyst Sn-Beta 100 mg, mesitylene as internal standard 80  $\mu$ L, 160  $^{\circ}$ C, 2 hours.



## 4.1 Conversion of GA Using Sn-Beta Catalysts

The results suggested the conversion of MGA-DMA *in situ* due to the presence of acidic species formed in the mixture. The increased yields of MVG and MMHB could also be caused by the accumulation of undetectable intermediates between the two steps, so it was not possible to prove that MGA-DMA was converted into useful products. Nevertheless, the results confirmed the possibility to consume MGA-DMA *in situ* under the considered reaction conditions and to avoid its accumulation from GA, as observed experimentally during prolonged reaction times.

### 4.1.5 The presence of alkali salts in the reaction mixtures

The effect of alkali on Sn-Beta catalysts has been studied extensively and discussed as an interaction with the tin active sites. The use of low concentrations of alkali salts in the reaction mixtures or as modifiers of the catalyst has been largely applied for the production of methyl lactate from carbohydrates.<sup>47</sup> However, analysis of the consequences of the presence of alkali salts on reactions starting from different substrates are lacking. The effect of alkali salts on the kinetics and selectivity of the process for the conversion of GA to MVG was investigated by time-course experiments.

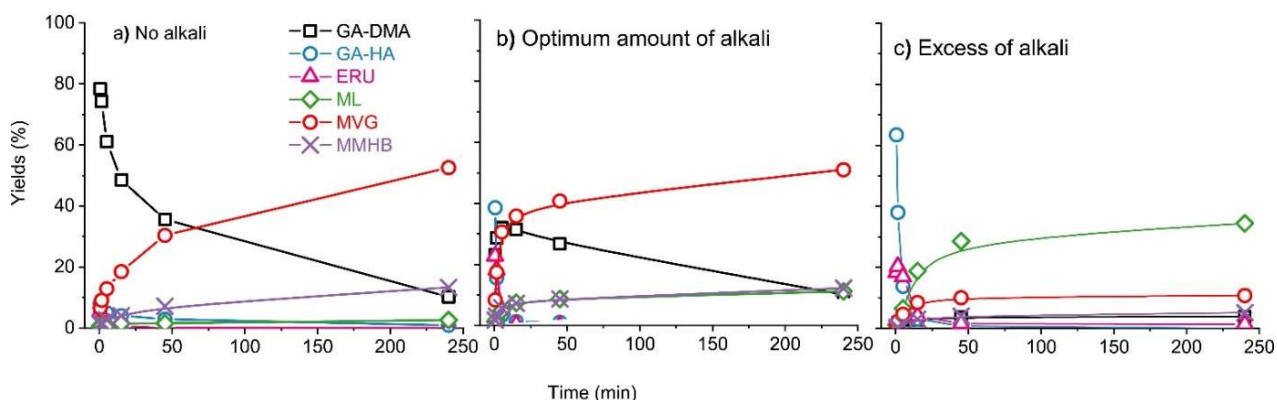


Figure 4.7. Products distribution of the reaction for the conversion of glycolaldehyde by Sn-Beta (150) a) in the absence of alkali, b) in the presence of a 0.24 mM and c) 1.2 mM of  $K_2CO_3$ . Reaction conditions: glycolaldehyde 400 mg, 100 mg Sn-Beta (150), 5 mL methanol, mesitylene 80  $\mu$ L as internal standard, 160  $^{\circ}C$ .

In the reaction for the conversion of hexoses to methyl lactate, alkali salts increased the yields of the desired product.<sup>47</sup> The amount of alkali salts needed to achieve the maximum yields of methyl lactate was different for different catalysts and it was strictly correlated to the amount of tin contained in the sample. The study for the titration by potassium carbonate of the active sites in Sn-Beta zeolites is discussed in detail in Chapter 6.2.4. Starting from the results obtained by studying the interaction between alkali ions and the active sites in the process for the formation of methyl lactate from hexoses, three different concentrations were compared: no  $K_2CO_3$ , optimum amount of  $K_2CO_3$  (related to the maximum yields obtained in ML in Chapter 6.2.4), excess of ML (deactivation of the catalyst, Chapter 6.2.4). Since optimal concentrations of the salt depended on the content of tin, the absolute amounts were adjusted based on the catalyst used and the kinetic effects using Si/Sn ratio of 25, 150, 400 were studied by time-resolved experiments. Results underlined the same effect for the different catalysts with different kinetics due to the different amount of active tin. An overview of the distribution of products is given in Figure 4.7 using a post-treated Sn-Beta (150) as the catalyst.

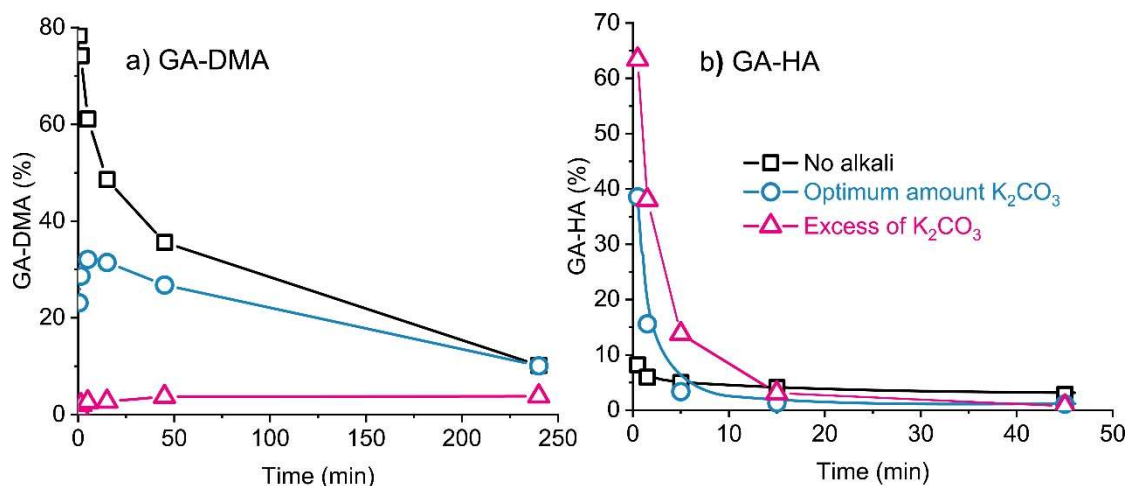


Figure 4.8. Consumption of a) glycolaldehyde dimethyl acetal and b) hemiacetal in reactions containing different amounts of potassium carbonate. Reaction conditions: glycolaldehyde 400 mg, catalyst 100 mg, 5 mL methanol for no alkali (black line), 5 mL solution of 0.24 mM  $K_2CO_3$  in methanol for the optimum amount of alkali (blue line), 5 mL solution of 1.2 mM  $K_2CO_3$  in methanol for excess of alkali (pink line), mesitylene 80  $\mu$ L as internal standard, 160  $^{\circ}C$ .

Figure 4.8. shows the effect of the presence of potassium carbonate on the conversion of the substrate. The presence of alkali salts avoided the formation of GA-DMA at the beginning of the reaction. Concurrently, the yields of GA-HA increased, meaning that the acetalization of GA to form GA-DMA was reduced and the balance was shifted to the hemiacetal. In the mixture containing potassium carbonate, the formation of GA-DMA and the consumption of GA-HA over time could be followed (Figure 4.8 b). This effect could be explained by the neutralization of residual Brønsted acidity that promoted the formation of acetals, due to addition of a basic salt. At the same time, free GA was available in larger amount compared to the case in the absence of potassium carbonate and the aldol condensation between two molecules of GA was favored leading to the tetrose sugars that are the central intermediates for the cascade processes to the different C4 products. Therefore, the acceleration of the formation of erythrose was associated with the acceleration of the formation of MVG and MMHB (Figure 4.9).

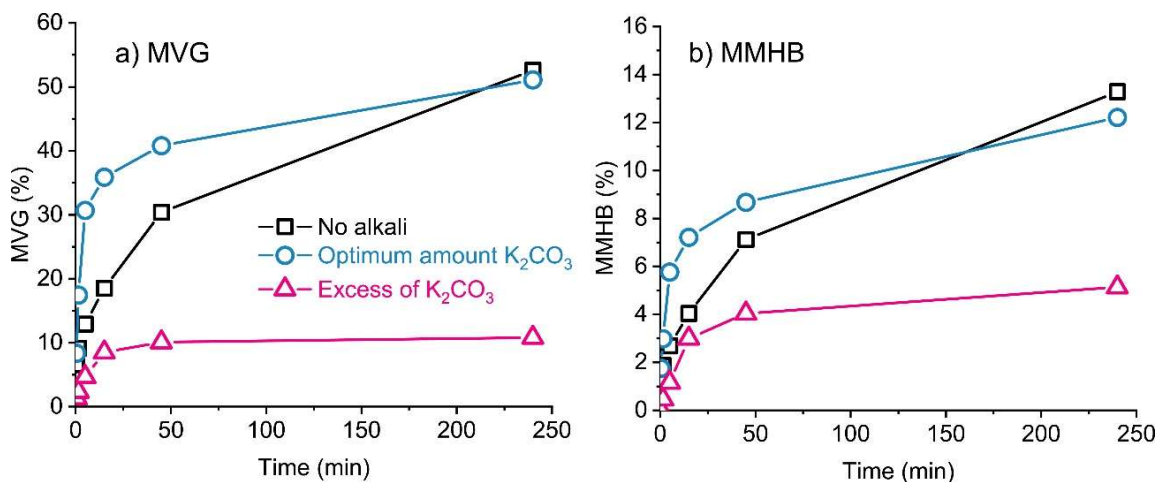


Figure 4.9. Formation of MVG and MMHB from glycolaldehyde using Sn-Beta catalyst and different amounts of alkali. Reaction conditions: glycolaldehyde 400 mg, catalyst 100 mg, 5 mL methanol for no alkali (black line), 5 mL solution of 0.24 mM  $K_2CO_3$  in methanol for the optimum amount of alkali (blue line), 5 mL solution of 1.2 mM  $K_2CO_3$  in methanol for the excess of alkali (pink line), mesitylene 80  $\mu$ L as internal standard, 160  $^{\circ}C$ .

## 4.1 Conversion of GA Using Sn-Beta Catalysts

On the other hand, the yields of MVG decreased when using an excess of alkali salts. In the reaction with a large excess of potassium carbonate, alkaline decomposition of sugars occurred, leading to a large amount of insoluble undetectable products (humins), as suggested by the dark color of the final mixtures. In Figure 4.9, it is possible to notice the change in the curve shape for the formation of MVG over time. The plot suggests a different pathway for the reaction containing potassium carbonate. The elimination of GA-DMA formation favored the aldol condensation and avoided the need for hydrolysis of GA-DMA, similar to the case of the presence of water. In this case, the kinetics of the process was modified by the presence of alkali salts. The curves of the formation of MVG with and without alkali ions were fitted using the combined function for two kinetic regimes previously explained in Chapter 4.1.1 (Figure 4.10).

Increasing the amount of alkali salts, the formation of the intermediate compound GA-DMA was suppressed and the aldol condensation of free GA was favored. Thus, the first term of the expression determined by the aldol condensation step decreased and an acceleration for the formation of MVG at short times was observed from the absence of alkali salts (Figure 4.10 a) to the presence of alkali salts (Figure 4.10 b). In the case of an excess of potassium carbonate, the presence of GA-DMA was almost completely suppressed and the shape of the curve for the formation of MVG over time changed (Figure 4.10 c). The curve of the yield of MVG ( $Y$ ) resembled the trend of an ordinary first-order kinetics described as the monoexponential function  $Y = A_1 \cdot (1 - \exp(-k_2 t))$  with  $A_1$  as the maximum yield of MVG and  $k_2$  as the apparent first-order constant. The results supported that the process in the presence of abundant basic alkali salt proceeded similar to the conversion of tetroses due to the favored initial aldol condensation. However, the fitting of the different expressions (first-order, second-order and the combination of the two) were similar and the data supporting the kinetic model for the formation of MVG in the presence of excess of potassium carbonate were not evident.

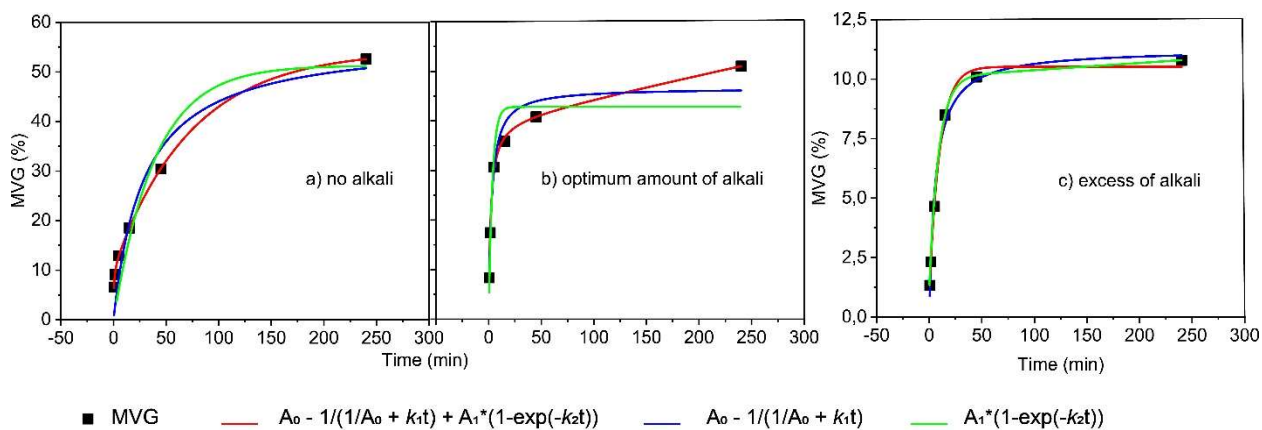
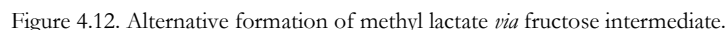
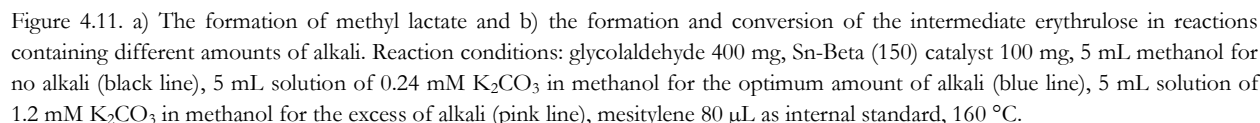
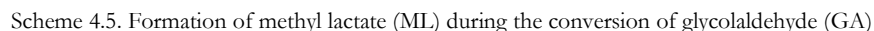


Figure 4.10. Data fit for the formation of MVG from glycolaldehyde in reactions containing different amounts of alkali.

The presence of alkali salts increased yields of methyl lactate, similar to results from more detailed studies for the conversion of hexoses. Starting from glycolaldehyde, methyl lactate was only a minor product without alkali salts (2-3% yield), but in solutions containing potassium carbonate, the final concentration increased (up to 35% yield). This result was associated with the high amounts of erythrulose found in the reaction mixtures (Figure 4.11). In a hypothetical mechanism (Scheme 4.5), erythrulose was an intermediate in the pathway for the formation of methyl lactate and it was not an immediate precursor in the formation of MVG. The formation of erythrulose (ERU) in high yields was observed at the beginning of the reactions containing alkali salts. ERU derived from the 1,2-hydride shift of erythrose (ERO), the central intermediate produced after the aldol condensation of two molecules of glycolaldehyde.



## 4.1.6 Formation of MVG using erythrulose as starting reagent

Erythrulose is a keto-tetrose carbohydrate. Commercially, it is produced by enzymatic fermentation and, since its natural abundance is limited, it is an expensive feedstock for the production of chemicals. In general, tetroses are rare sugars and their conversion into monomers is not industrially relevant.<sup>207</sup> However, tetroses represent an intermediate in the process for the conversion of glycolaldehyde to MVG<sup>183</sup> and the study of its reactivity can help to understand the reaction pathways and achieve a high control of the process. For this reason, time-resolved experiments for the conversion of erythrulose by Sn-Beta catalyst were carried out and the resulting distribution of products were compared to the use of glycolaldehyde as the starting substrate.

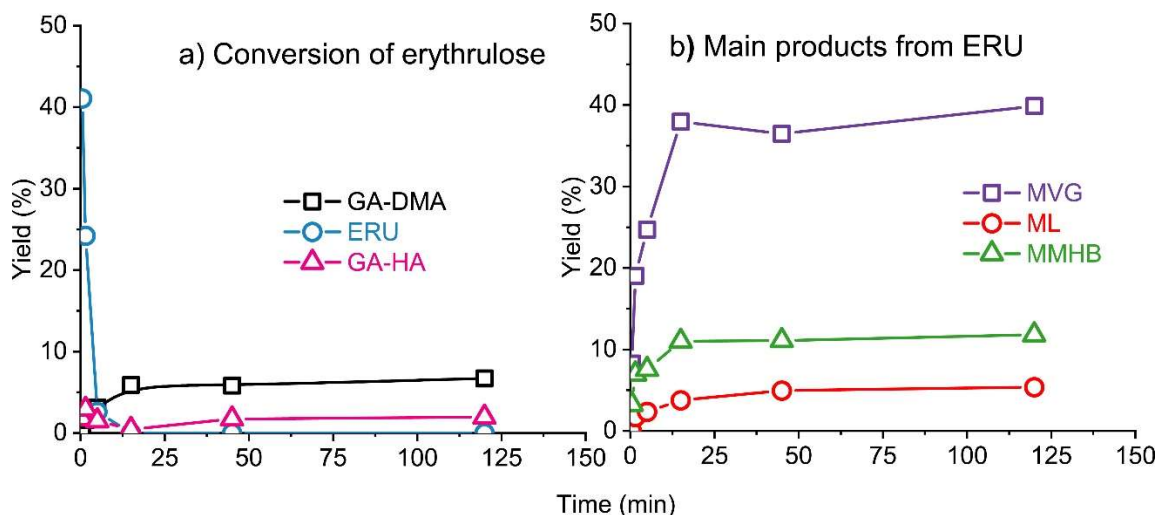
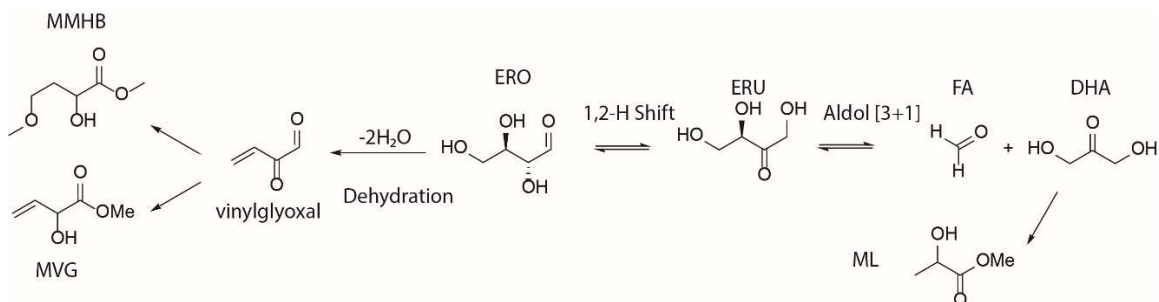


Figure 4.13. Distribution of products in the conversion of erythrulose by Sn-Beta zeolite catalyst. Reaction conditions: erythrulose 120 mg, catalyst 50 mg, methanol 5 mL, mesitylene 80  $\mu$ L as internal standard, 160  $^{\circ}$ C.

Figure 4.13 shows the trend for the conversion of erythrulose over time using Sn-Beta catalyst and the main products formed in the reaction. The consumption of the starting sugar occurred quickly and the conversion was complete after the first ten minutes. To a minor extent, erythrulose underwent retro-aldol cleavage forming glycolaldehyde, as shown by the presence of GA-HA and GA-DMA in the reaction mixtures. The trend of GA-DMA (Figure 4.13a black line) showed an accumulation over time (yield 6%) without any apparent conversion within two hours. Thus, the behavior of GA-DMA in the reactions starting from ERU differed from the conversion of glycolaldehyde. Erythrulose gave MVG as main product, together with MMHB and methyl lactate (Figure 4.13 b). The yields of MVG and MMHB after two hours of reaction at 160  $^{\circ}$ C corresponded to 40 and 12%, respectively. The results indicated the quick isomerization between erythrulose and erythrose and the favored formation of MVG compared to the retro-aldol cleavage leading to methyl lactate (Scheme 4.6). Nevertheless, methyl lactate was produced in a yield of 6% after two hours compared to the 2% yields obtained from glycolaldehyde. The increased formation of methyl lactate was an indication of the formation of this product *via* erythrulose intermediate. The kinetics of the formation of MVG from erythrulose was different from both conversion of glycolaldehyde to MVG and from the conversion of hexoses to methyl lactate.



Scheme 4.6. Competitive dehydration leading to MVG and MMHB and retro-aldol leading to ML pathways using erythrulose (ERU) as starting substrate.

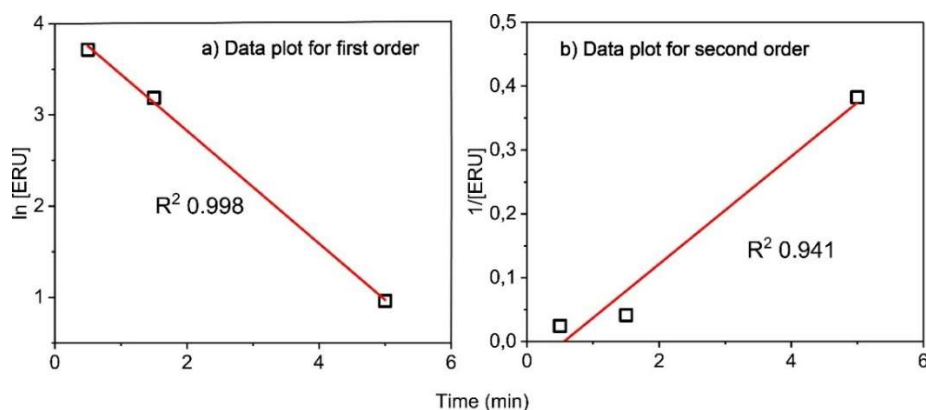


Figure 4.14. Data plot for the conversion of GA-DMA over time using Sn-Beta zeolites.

Experimental data indicated the linear correlation of the exponential decrease of the concentration of ERU over time (Figure 4.14), as occurring in first-order reactions. The results reflected a first-order kinetic process, as expected in the absence of the aldol condensation step. In the case of erythrulose as the starting substrate, the data were fitted to a monoexponential first-order kinetics (Figure 4.15). The absence of the aldol condensation step changed the mechanism into a first-order reaction and the data described a monoexponential trend. The data were in-line with the kinetic model indicating the final intramolecular Cannizzaro reaction as the rate limiting step, proposed previously by Dusselier et al.<sup>169</sup>

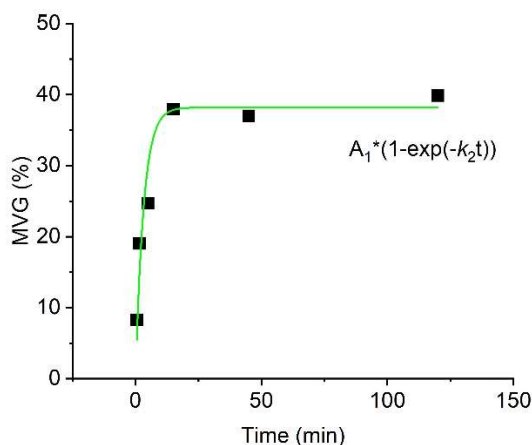


Figure 4.15. Data fit for the formation of MVG from erythrulose.



## 4.1 Conversion of GA Using Sn-Beta Catalysts

The effect of small amounts of water in the conversion of erythrulose using Sn-Beta catalyst was investigated. The conversion of the starting substrate and the distribution of products in the reaction of erythrulose by Sn-Beta in the presence of 6% water reflected the trend observed in the absence of water and the conversion of erythrulose was unchanged by the presence of water (Figure 4.16). However, the formation of MVG was slightly increased by the presence of water (Figure 4.16). This result could indicate the contribution to the formation of MVG from GA-DMA derived from retro-aldol cleavage of the tetroses. GA-DMA was present in lower amounts in the reactions containing water. However, the formation of GA-DMA from erythrulose presented low yields also in the case of the absence of water. Therefore, it is possible that the results suggested the possible beneficial influence of water on a different step than the hydrolysis of GA-DMA for the formation of MVG. Differently from MVG, the formation of all the other products were not influenced by the presence of water.

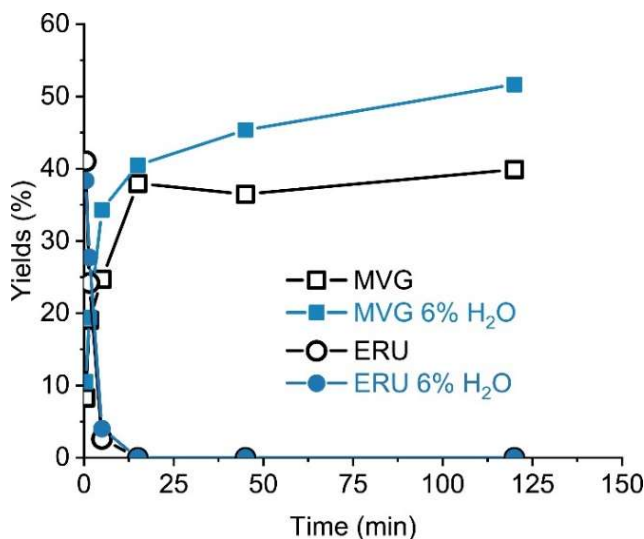


Figure 4.16. Comparison of the conversion of erythrulose into MVG in the presence and in the absence of water. Reaction conditions: erythrulose 120 mg, catalyst 50 mg, methanol 5 mL, 6% (v/v) water, mesitylene 80  $\mu$ L as internal standard, 160  $^{\circ}$ C.

The effect of the presence of alkali salts in the conversion of erythrulose by Sn-Beta was also considered in order to better understand the pathway for the formation of methyl lactate from glycolaldehyde. Potassium carbonate in the reaction mixture promoted the retro-aldol [3+1] route to methyl lactate. The retro-aldol [2+2] reaction giving glycolaldehyde from erythrulose was not visible and the formation of GA-DMA was suppressed by alkali ions. Fructose was not identified as an intermediate for the formation of methyl lactate. Supposedly also in the case of the use of glycolaldehyde as a starting reagent, methyl lactate was mainly formed by erythrulose and only traces of fructose were present due to aldol condensation [4+2]. Differently from the case of glycolaldehyde, the optimum amount of potassium carbonate did not accelerate the formation of MVG and, in contrast, yields dropped in the presence of small concentrations of potassium carbonate (Figure 4.17). The results confirmed that the effect of alkali salts on the conversion of GA to MVG was mainly determined by the suppression of the formation of the acetal GA-DMA.

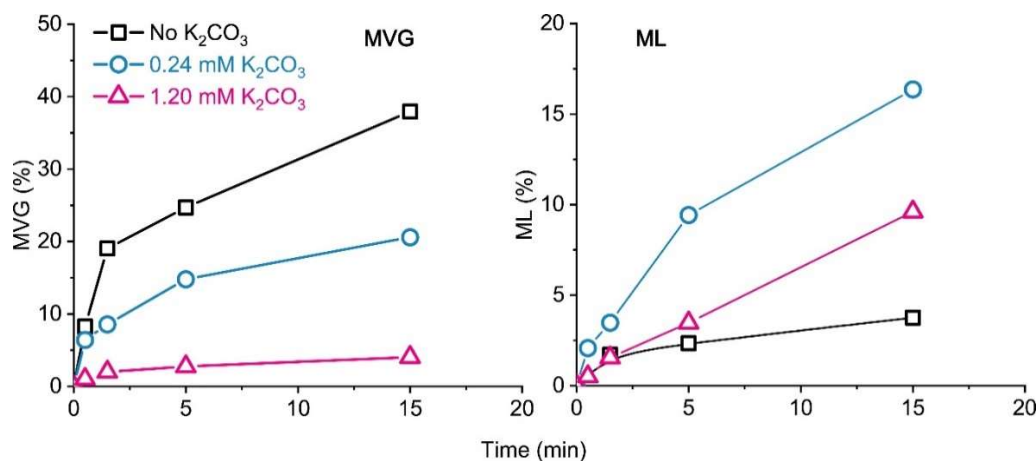


Figure 4.17. Formation of MVG from erythrulose by Sn-Beta catalyst in the presence of different amounts of potassium carbonate. Reaction conditions: erythrulose 120 mg, catalyst 50 mg, 5 mL methanol for no alkali (black line), 5 mL solution of 0.24 mM  $K_2CO_3$  in methanol for the optimum amount of alkali (blue line), 5 mL solution of 1.2 mM  $K_2CO_3$  in methanol for the excess of alkali (pink line), mesitylene 80  $\mu$ L as internal standard, 160  $^{\circ}C$ .

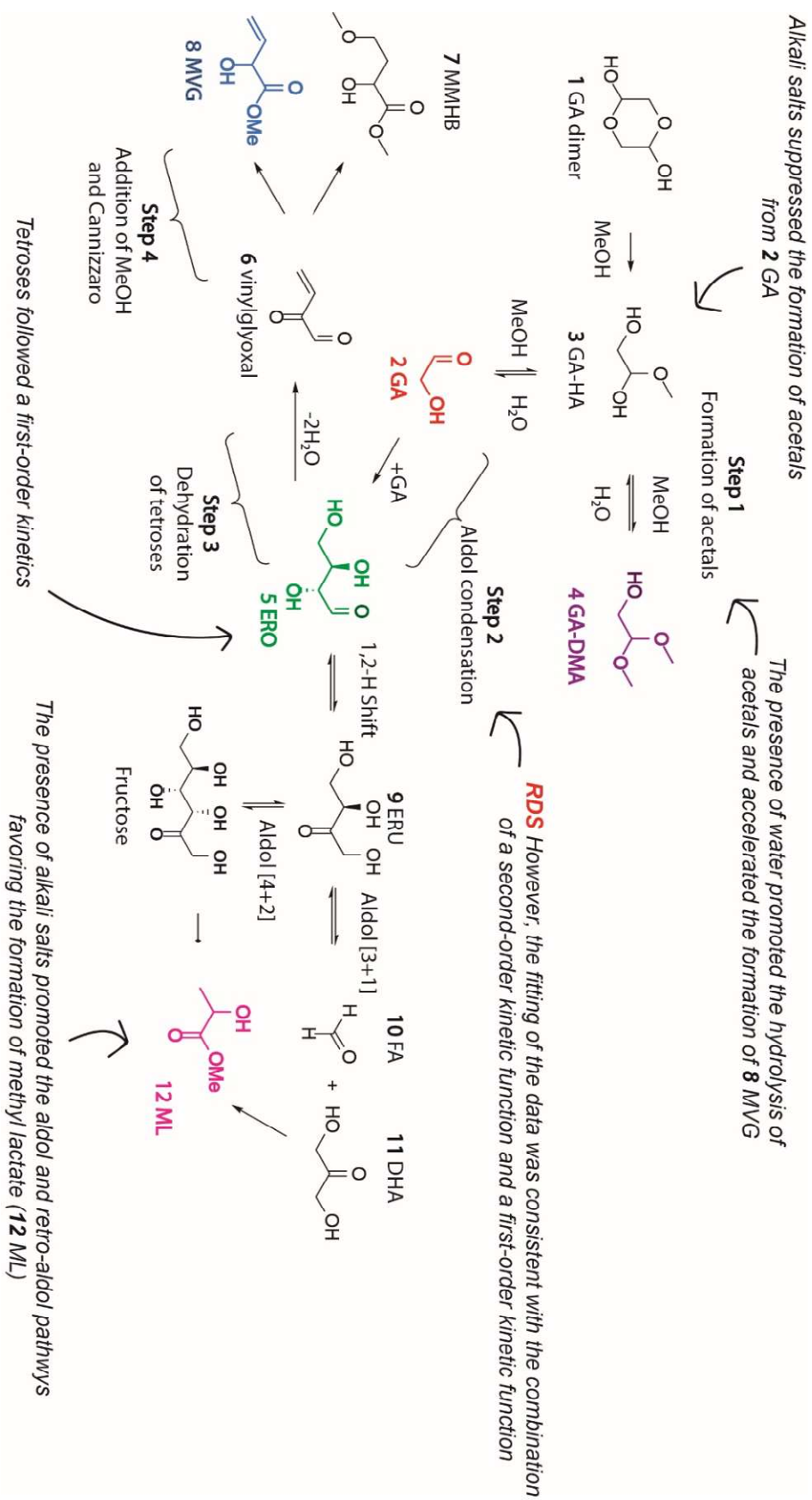
In the case of the use of erythrulose as starting reagent, the beneficial effect of the presence of potassium carbonate in avoiding the acetalization step was lacking. In this case, the predominant effect of the presence of potassium carbonate was the alkaline degradation of sugars leading to high carbon loss and to decreased yields of MVG.

#### 4.1.7 Conclusions on the study for the conversion of glycolaldehyde catalyzed by Sn-Beta zeolites

This section discussed the investigation of Sn-Beta zeolites as catalysts for the conversion of glycolaldehyde (GA) into methyl vinyl glycolate (MVG), which has great potential for applications as bio-based monomer for the production of polyesters. The mechanism of the conversion of glycolaldehyde (**2** GA) involved an initial [2+2] aldol condensation resulting in the main intermediate erythrose (**5** ERO), as represented in Scheme 4.7. The experimental time-resolved data showed that the process followed a second-order kinetics, suggesting the determining step of aldol condensation of two molecules of GA (Step 2). The data for the formation of MVG presented two kinetic regimes and yields of MVG over time were fitted with an expression given by the combination of two different terms. The first term indicated a second-order reaction, corresponding to the aldol condensation of two molecules of GA and the second term indicated a first-order reaction, corresponding to either the hydrolysis of acetals (Step 1), the dehydration of tetroses (Step 3) or the intramolecular Cannizzaro reaction (Step 4). The effect of different parameters on the reaction rate and selectivity into the different products was studied in order to define optimal reaction conditions.

The effect of the presence of water and alkali salts on the reaction kinetics was explored. In both cases, the formation of GA-DMA was suppressed and the formation of MVG was accelerated. The use of an excessive amount of potassium carbonate (3.0 mM) led to high carbon loss due to the alkaline degradation of sugars resulting in large amounts of humins. However, the complete suppression of GA-DMA resulted in the change of the kinetics and the elimination of the two regimes for the formation of MVG. The conversion of erythrulose into MVG catalyzed by Sn-Beta was also investigated in order to confirm the proposed model. Erythrulose showed different kinetics compared to the conversion of glycolaldehyde. The data followed a first-order kinetics due to the lack of the aldol condensation step and the formation of MVG could be fitted to a monoexponential function.





Scheme 4.7. Overview of the findings obtained herein on the conversion of glycolaldehyde using Sn-Beta zeolite catalyst.

# Chapter 5

## Development of Synthetic Procedures for the Preparation of Tin-Containing Zeolite Catalysts

This chapter presents a study of the procedures for the preparation of stannosilicates as catalysts for the conversion of carbohydrates into bio-based chemical products. The project focused on the preparation of post-synthetic materials because of the ease of the procedures and their large applicability. First, the different steps involved during the synthesis of post-treated Sn-Beta zeolites were considered, studying the effect of modifications in each step on the activity and the physical properties of the catalysts. Furthermore, different frameworks were studied for the preparation of tin-containing zeolites. Beta and USY were chosen as optimal for obtaining stannosilicates and these frameworks were used for the preparation of mesoporous materials. The effect of introducing mesoporosity was studied by the conversion of substrates with different sizes.

### 5.1 Exploring the Parameters for the Synthesis of Sn-Beta Zeolites

The synthesis of stannosilicates has received much attention during the last decades. Different synthetic routes lead to different materials and catalytic activity. Hydrothermally prepared Sn-Beta zeolites are defect-free large-crystals materials.<sup>52</sup> However, the synthetic procedure presents several disadvantages, which do not allow industrial-scale applications (e.g. long crystallization times and the use of HF as mineralizing agent). More recently, post-synthetic procedures have been proposed in order to overcome these problems.<sup>55</sup> Post-treated catalysts contain more defects than hydrothermal samples. The general understanding of the impact of the parameters employed during the synthesis on the final material can help the design of optimal catalytic systems. Thus, this section explores the effect of modifications in the synthetic procedure on the catalytic material and on the activity in the conversion of carbohydrates. The analysis of synthetic modifications and their effect on the final catalytic properties can bring useful information for the design of modified catalysts with high selectivity in the specific processes.

## 5.1 Parameters of the Synthesis of Sn-Beta Zeolites

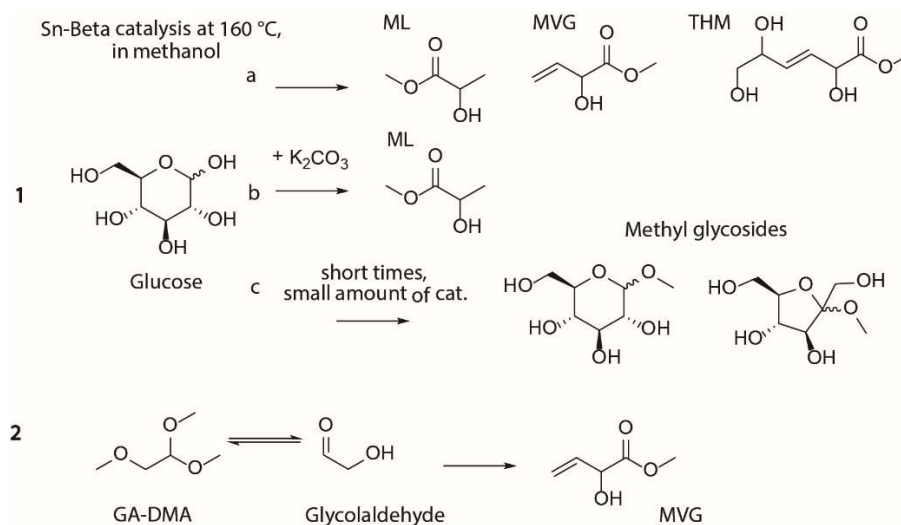


Figure 5.1. Reactions for testing the performances of the synthesized Sn-Beta catalysts in the conversion of bio-based feedstock. 1-Conversion of glucose to a) different hydroxy esters, b) methyl lactate using alkali salts in solution, c) methyl glycosides intermediates and byproducts using short times and low amounts of catalyst. 2- Conversion of glycolaldehyde into MVG. All the reactions were performed at 160 °C in methanol solution.

In this part of the project, parameters affecting the preparation of Sn-Beta and the effect on the resultant materials were explored. Catalysts were tested in different reactions for the conversion of carbohydrates (Figure 5.1). Different reaction conditions in the conversion of glucose allowed to study the selectivity for specific products. The conversion of glucose was carried out at 160 °C in methanol for two hours for analyzing retro-aldol pathways leading to methyl lactate and other hydroxy esters, such as trans-2,5,6-trihydroxy-3-hexenoic acid methyl ester (THM) and methyl vinyl glycolate (MVG), as main products. The addition of small amounts of alkali salts (usually K<sub>2</sub>CO<sub>3</sub>) in the reaction mixtures allowed to maximize the methyl lactate selectivity and yields. In order to study the formation of intermediates, experiments using low amounts of catalyst and short times (30 minutes) were used. Finally, the conversion of glycolaldehyde into MVG at 160 °C in methanol was also considered. Characterization of the prepared materials and results from the different catalytic tests allowed to give a correlation between parameters employed for the synthesis, material features and activity in the conversion of carbohydrates for obtaining different products. The section starts with a comparison of Sn-Beta zeolites prepared by hydrothermal synthesis and post-treatment in order to elucidate the differences between the two materials. Afterwards, the steps for the preparation of post-synthetic stannosilicates are analyzed and the influence of different protocols for dealumination and tin incorporation on the final material are discussed.

### 5.1.1 Comparison between hydrothermal and post-treated Sn-Beta catalysts

The preparation of Sn-Beta zeolites by hydrothermal synthesis yields large defect-free crystals, but the use of HF as mineralizer and the need of long times for the crystallization makes the method inconvenient for large-scale applications. Thus, alternative studies have focused on *top-down* methodologies for the introduction of tin in already crystallized zeolites.<sup>55</sup> This paragraph explores the characteristic and catalytic properties of post-synthetic materials compared to their hydrothermal counterparts and aims to elucidate the differences between the two catalytic materials.

Initially, the comparison between catalysts prepared by the two routes was performed. Subsequently, the effect of several parameters in the preparation of post-synthetic catalysts was studied in order to optimize the

procedure and the characteristic of the final material. Figure 5.2 displays the SEM images of two Sn-Beta catalysts with Si/Sn ratios of 200 prepared via the hydrothermal (left) and post-treated (right) route. The pictures show different crystal sizes: hydrothermal crystals were large and monodisperse. Although post-synthetic crystals maintained regular shapes and dimensions of the parental aluminum-containing Beta zeolite, they were ten times smaller compared to the material prepared by the *bottom-up* procedure. The formation of small crystals could bring advantages in terms of diffusion control.<sup>208</sup> Moreover, hydrothermal Sn-Beta crystals prepared with the use of HF as crystallization agent presented a capped bipyramidal morphology.<sup>52</sup> In contrast, the appearance of the crystals in post-treated Sn-Beta strictly depended of the starting zeolite. In this case, the SEM image in Figure 5.2 shows the formation of round-shape crystals.

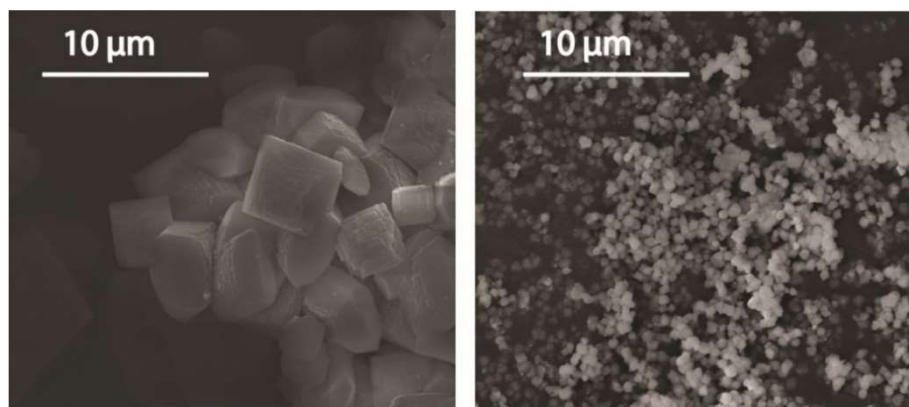


Figure 5.2. Scanning Electron Microscopy images of hydrothermal (left) and post-synthetic (right) Sn-Beta (200) zeolites. The hydrothermal synthesis resulted in material with large crystals.

Table 5.1 illustrates the characteristic physical properties of the two samples. Post-synthetic procedures involved the partial dissolution of the zeolite at 100 °C, but the process was not followed by any recrystallization. As a result, the post-treated material had lower crystallinity. In contrast, the hydrothermal Sn-Beta was crystallized for forty days and exhibited high crystallinity. Both samples had a good incorporation of the tin and microporosity. The increased surface area of the post-synthetic material was due to the smaller size of the crystals compared to the other sample. Also in the case of the acidity, the post-synthetic material had a higher value than the hydrothermal sample, reflecting the presence of defects containing slightly acidic O-H groups. The different acidity of the samples reflects the different catalytic activity and the presence of different active sites in the two materials.<sup>62</sup>

Table 5.1. Physical characteristics of hydrothermal and post-treated Sn-Beta zeolites.

	Hydrothermal Sn-Beta	Post-treated Sn-Beta
Crystallinity (%) <sup>a</sup>	93.66	59.60
Tin (wt%) <sup>b</sup>	1.189	0.977
Si/Sn <sup>b</sup>	130.36	152.80
S <sub>BET</sub> (m <sup>2</sup> /g) <sup>c</sup>	602	722
V <sub>micropore</sub> (mL/g) <sup>c</sup>	0.24	0.30
Total acid sites (µmol/g) <sup>d</sup>	56	108
Methyl lactate yield (%) <sup>e</sup>	29	15

<sup>a</sup>X-Ray Diffractometry, <sup>b</sup>X-Ray Fluorescence, <sup>c</sup>Nitrogen physisorption, <sup>d</sup>Ammonia Temperature-Programmed Desorption, <sup>e</sup>Reaction conditions: glucose 120 mg, catalyst 50 mg, 5 mL methanol, DMSO 80 µL as internal standard, 160 °C, 2 hours.

The two zeolites showed different catalytic activity. The catalysts were tested in the reaction for the conversion of glucose into methyl lactate at 160 °C in methanol. The production of methyl lactate tested under standard

## 5.1 Parameters of the Synthesis of Sn-Beta Zeolites

conditions gave 15% yield in the case of the post-synthetic material and 29% yield using the hydrothermal catalyst. Thus, optimizations of the features of the post-treated catalyst were necessary in order to increase methyl lactate. Further comparison in the production of methyl lactate between the post-synthetic and hydrothermal Sn-Beta is discussed in Chapter 3 with an emphasis on kinetic and mechanistic findings. The following discussion aimed to understand the parameters of the synthesis influencing the catalytic activity in order to increase the efficiency of post-synthetic materials.

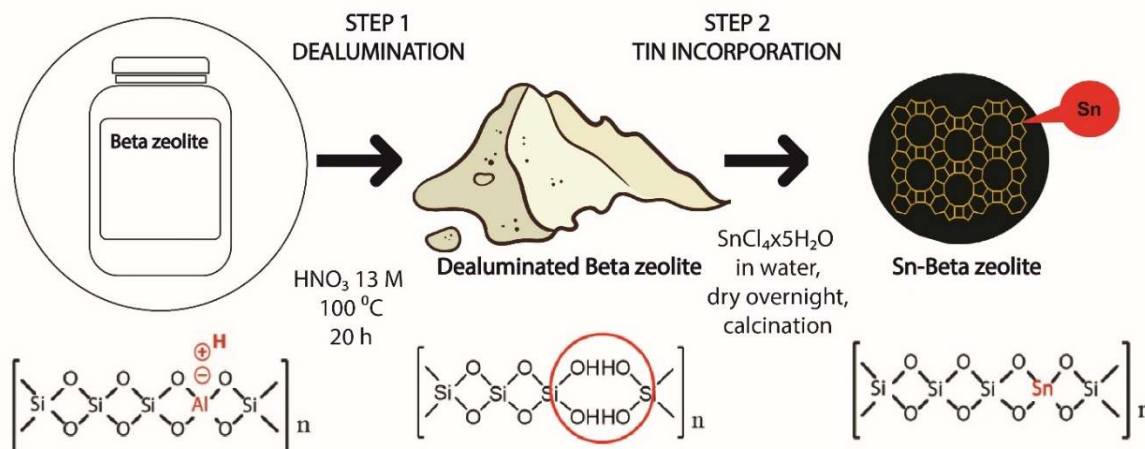
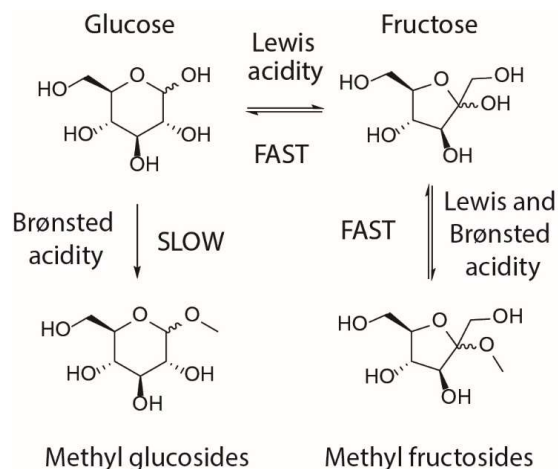


Figure 5.3. Schematic representation of the procedure for the preparation of post-synthetic Sn-Beta zeolites.

Figure 5.3 represents a simplified scheme of the preparation of post-synthetic stannosilicates. The procedure involved two main steps. The first step consisted in the dealumination of the starting commercial Beta zeolite. The acid treatment overnight led to dealuminated Beta zeolite, which had free silanols available for the incorporation of other metal ions. The second step was the incorporation of the tin into the dealuminated material leading to the final Sn-Beta zeolite, which was thoroughly washed, dried and calcined.<sup>55</sup> In the following sections, the different steps of the procedure for the preparation of Sn-Beta zeolites are described. Specifically, the effects of using different durations for the dealumination treatment leading to the presence of residual aluminum and the amount of tin incorporated are discussed.

### 5.1.2 Sn-Beta catalysts containing residual aluminum

The presence of residual aluminum has different impacts depending on the considered reaction. In general, the aluminum introduces Brønsted acid sites, which can have positive, concerted effects in bifunctional catalysis as reported by Dikjimans et al.<sup>56</sup> in the reaction for the production of methyl lactate starting from dihydroxyacetone (DHA). Using hexoses as starting substrates, the presence of Brønsted acidity led to the formation of byproducts in the process for the formation of methyl lactate. The Brønsted acidity promoted the dehydration of sugars giving furanic compounds, such as furfural or 5-hydroxymethylfurfural (HMF), which were undesired byproducts during the production of methyl lactate (Chapter 3.2.1). Using glucose as the starting reagent, the Brønsted acidity introduced by the presence of residual aluminum was also responsible for the formation of methyl glucosides. Methyl glucosides were stable compounds and they did not convert further under the considered reaction conditions. However, their formation was usually suppressed by the use of highly Lewis acidic catalysts. In fact, the Lewis acidity promoted the fast isomerization equilibrium between glucose and fructose and the reactive methyl fructosides were the preferred products (Scheme 5.1). Methyl fructosides could then be further converted into other products. In Chapter 3, the effect of balanced Brønsted and Lewis acidity on the conversion of hexoses is discussed in detail.



Scheme 5.1. Formation of methyl glycosides from hexoses, competition and roles of Brønsted and Lewis acidity.

The introduced Brønsted acidity could have either positive or negative effects on the selectivity of a process. The role of residual aluminum in Sn-Beta catalysts was investigated for the conversion of glycolaldehyde into methyl vinyl glycolate (MVG). Beta zeolites were dealuminated in nitric acid solutions (13 M) for different durations and the resultant materials presented different level of dealumination and contained different Si/Al ratio. The dealuminated zeolites were used for preparing Sn-Beta samples containing the same amount of tin (1.3 wt%, Si/Sn ratio of 150) and they were tested as catalysts for glycolaldehyde conversion. The acidic treatment was highly effective and high levels of aluminum removal were obtained for the samples treated at short times. Therefore, only the extreme cases are discussed in this chapter. The treatment did not affect the crystallinity of the materials, as observed by XRD analysis and reported in literature.<sup>89</sup> The acidity measured by  $\text{NH}_3$ -TPD was high in samples that were dealuminated for short times, as the aluminum introduced acidic centers (Table 5.2).

Table 5.2. Acidity of samples dealuminated for different times. Measurements by XRF<sup>a</sup> and  $\text{NH}_3$ -TPD<sup>b</sup> analysis

Time of dealumination (h)	Si/Al <sup>a</sup>	Acidity ( $\mu\text{mol/g}$ ) <sup>b</sup>
1	65	96
24	126	59
48	152	39

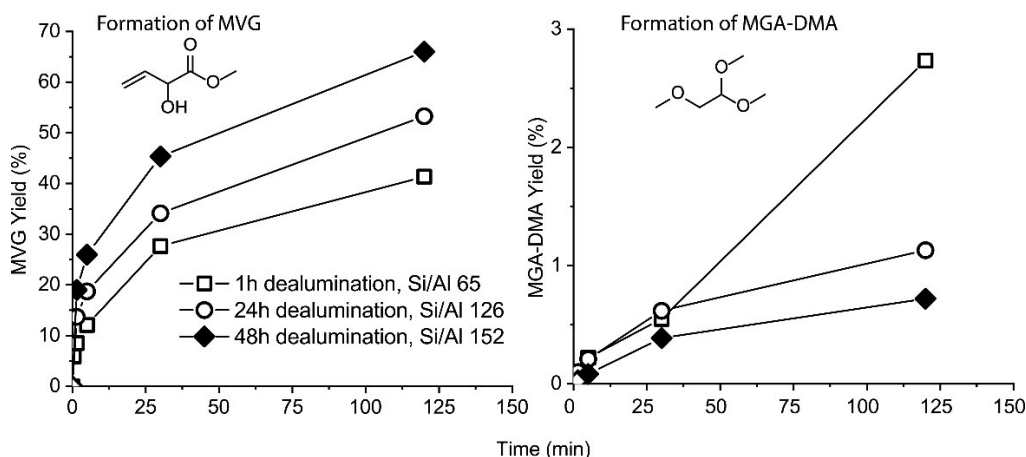


Figure 5.4. Trend of formation of MVG (left) and MGA-DMA (right) using catalysts with different Si/Al ratio. Reaction conditions: glycolaldehyde 400 mg, catalyst 100 mg, methanol 5 mL, mesitylene 80  $\mu\text{L}$  as internal standard, 160  $^{\circ}\text{C}$ .



Figure 5.4 shows the trends for the formation of MVG using catalysts dealuminated for 1 hour, 24 hours and 48 hours. Following the process by time-resolved experiments, the negative influence of residual aluminum on the formation of MVG was evident. Samples dealuminated for longer times performed better in the production of MVG from glycolaldehyde compared to the partially dealuminated catalysts. The introduced Brønsted acidity mainly led to the formation of byproducts. In particular, the amounts of the methyl glycolaldehyde dimethyl acetal (MGA-DMA) increased considerably using catalysts containing residual aluminum, i.e. Brønsted acidity (Figure 5.4). This latter product was stable and had a reduced rate of conversion, as is discussed in more detail in Chapter 4.

### 5.1.3 Synthesis of Sn-Beta zeolites containing different amounts of tin

The second step considered in the preparation of post-synthetic Sn-Beta zeolites was the incorporation of the tin inside the dealuminated framework. The tin incorporated in the zeolite is the Lewis acid center and forms the active site of the catalyst. However, the amount of active tin that can be incorporated inside the structure is limited for both hydrothermal and post-synthetic synthesis and the addition of excessive concentrations of tin salts leads to the formation of inactive extra-framework species.<sup>60</sup> The extra-framework material can obstruct the pores and limit the access of reactants to the active sites.<sup>89</sup> The possibility to incorporate large amounts of active tin in Beta zeolites was studied. Post-treated Sn-Beta catalysts were prepared by impregnation of different amounts of tin and tested for the conversion of carbohydrates.

In Supplementary Information SI.1, the full characterization of the physical properties for the prepared catalysts is enclosed. Samples with higher tin content presented higher acidity in the  $\text{NH}_3$ -TPD measurements, but all the other features were not significantly affected. QBET surface areas decreased slightly for high tin content, as also reported in literature.<sup>62</sup> The impregnation did not change the crystal structure, as shown in the XRD diffractograms. The peaks relative to crystalline extra-framework  $\text{SnO}_2$  species were well visible in samples with Si/Sn ratio equal or lower than 50. Moreover, amorphous oxides or nanoparticles may be formed also in samples with higher Si/Sn ratio and they are invisible to the XRD technique. Zeolites impregnated with different amounts of tin were tested in the conversion of glucose for maximizing yields of methyl lactate (ML), methyl glycosides (Me-Fru and Me-Glu) and other hydroxy esters (MVG and THM) (Table 5.3). All the Sn-Beta catalysts were prepared starting from the same dealuminated Beta zeolite, meaning that the physical properties were constant and the only variable among the samples was the tin content.

Table 5.3. Catalytic tests of post-treated Sn-Beta containing different amount of Sn (three standard reaction conditions for testing ML, MVG/THM, methyl glycosides)

Si/Sn	ML (%) <sup>a</sup>	Me-Fru (%) <sup>b</sup>	Me-Glu (%) <sup>b</sup>	THM (%) <sup>c</sup>	MVG (%) <sup>c</sup>
<b>12.5</b>	47	26	6	4	3
<b>50</b>	29	25	4	4	3
<b>100</b>	25	41	4	3	4
<b>150</b>	15	37	4	2	3
<b>200</b>	15	57	4	2	3

Reaction conditions: glucose 120 mg, catalyst 50 mg, methanol 5 mL, DMSO 80  $\mu\text{L}$  as internal standard, 160  $^\circ\text{C}$ , 2 hours. <sup>a</sup> In the assays for the optimization of the formation of methyl lactate, a solution of  $\text{K}_2\text{CO}_3$  in methanol was used. The concentration of the solution was calculated for having a Sn/K ratio of 0.1. <sup>b</sup> In the assays for the optimization of the formation of methyl glycosides, 25 mg of catalyst and 30 minutes reaction time were used. <sup>c</sup> Standard reaction conditions.

The catalytic results presented in Table 5.3 indicate that the formation of methyl lactate increased for higher tin content in the reaction with alkali, while no significant yields of MVG and THM were observed in the test without alkali. However, the increase was not proportional to the tin content and it was combined with an opposite trend in the amount of methyl fructosides in the short-time tests. Methyl fructosides were formed in

high yields using catalysts with low tin content. Therefore, considering methyl fructosides as intermediates to the formation of methyl lactate, higher tin content accelerated the process as the main effect. The effect of different tin contents in the formation of methyl fructosides from glucose at 160 °C in methanol is discussed in detail in Chapter 3.2.2. The non-linear correlation between tin content and final yields has been already reported for Sn-Beta catalysts.<sup>62,89</sup> The effect could be explained by the presence of extra-framework tin in samples containing high amounts of tin or to the change of the distribution of the T sites.<sup>69</sup>

Samples containing different amounts of tin were also tested in the conversion of glycolaldehyde into MVG. Figure 5.5 shows the yield of MVG and glycolaldehyde dimethyl acetal (GA-DMA) after four hours. GA-DMA is the main form of glycolaldehyde in methanol solution in the presence of an acidic catalyst, therefore, it could be used as representation of the conversion of the starting substrate. Also in the case of the conversion of glycolaldehyde, the tin content affected the kinetics of the reaction. The yield of the main product MVG increased for high amounts of tin, while at low tin content the conversion of GA-DMA was still incomplete after four hours.

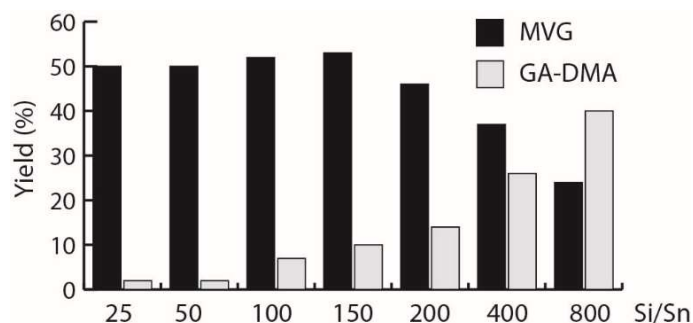


Figure 5.5. Yields of MVG and GA-DMA using Sn-Beta containing different amount of Sn. Standard reaction conditions for the conversion of glycolaldehyde after 4 hours. Reaction conditions: GA dimer 400 mg, catalyst 100 mg, 5 mL methanol, mesitylene as internal standard 80  $\mu$ L, 160 °C, 4 hours.

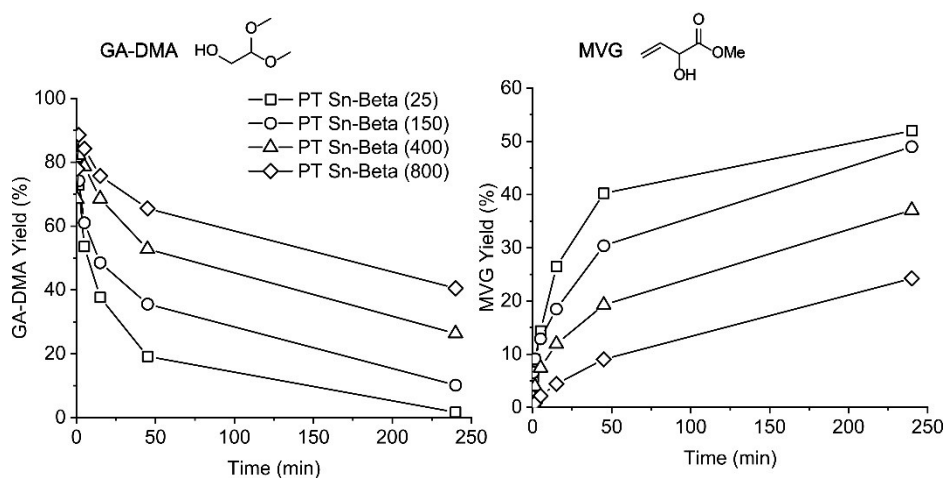


Figure 5.6. Time-resolved experiments for the conversion of glycolaldehyde using catalysts containing different amounts of tin. Reaction conditions: GA dimer 400 mg, catalyst 100 mg, 5 mL methanol, mesitylene as internal standard 80  $\mu$ L, 160 °C.

The acceleration of the formation of MVG starting from glycolaldehyde was then confirmed by time-resolved experiments (Figure 5.6). The conversion of GA-DMA by post-treated Sn-Beta (800) followed the same trend as the other high tin content counterparts with a decreased rate in MVG formation. Considering the formation



of MVG over time (Figure 5.6), the presence of high tin contents seemed to affect the kinetics of the process mainly at the beginning. On the other hand, the slope of the curves in Figure 5.6 at longer reaction times were similar. As discussed in Chapter 4.1.1, the formation of MVG followed two kinetic regimes and the presence of high tin contents mainly acted on the first part determined by the aldol condensation of two molecules of GA. Thus, the increased amount of tin affected the kinetics of the first regime of the formation of MVG.

### 5.1.4 The addition of a washing step in the procedure for the removal of extra-framework species

Extra-framework tin oxides can be deposited on the surface and inside the porosity of the zeolite when the impregnation procedures are performed with high concentrations of tin salts.<sup>60</sup> Tin oxides are mostly inactive in the conversion of sugars and can block the pores with consequent negative effects on the catalytic activity.<sup>89</sup> Recently, van der Graaff et al. have proposed a method for removing extra-framework deposits by additional methanol washing during the preparation of post-synthetic Sn-Beta zeolites.<sup>60</sup> The obtained catalysts have shown improved activity in the formation of methyl lactate from dihydroxyacetone.<sup>60</sup> The method was applied to the Sn-Beta samples containing Si/Sn ratios of 50 and 12.5, because the XRD characterization showed the presence of high amounts of crystalline tin oxide in these samples. The zeolites were repeatedly washed with methanol after the impregnation with the aqueous solution of tin in order to remove the non-incorporated species. As shown in Figure 5.7, the washed catalysts presented slightly improved activity in the formation of methyl lactate from glucose at full conversion.

The amount of tin determined by XRF decreased after washing, from Si/Sn 20 to Si/Sn 23 in the case of the sample having Si/Sn nominal ratio of 12.5 and from Si/Sn 45 to Si/Sn 49 in the case of the sample with Si/Sn nominal ratio of 50. However, the XRD diffractograms of the washed samples after calcination still indicated presence of some crystalline SnO<sub>2</sub>. It is possible that the washing procedure removed amorphous tin species not visible in the XRD and had no effect on the crystalline oxides. As already reported for reactions using different substrates,<sup>60</sup> the washing procedure had a beneficial effect on catalyst activity. However, no drastic improvement was obtained in the final yields of methyl lactate from glucose. Therefore, the method was not investigated further.

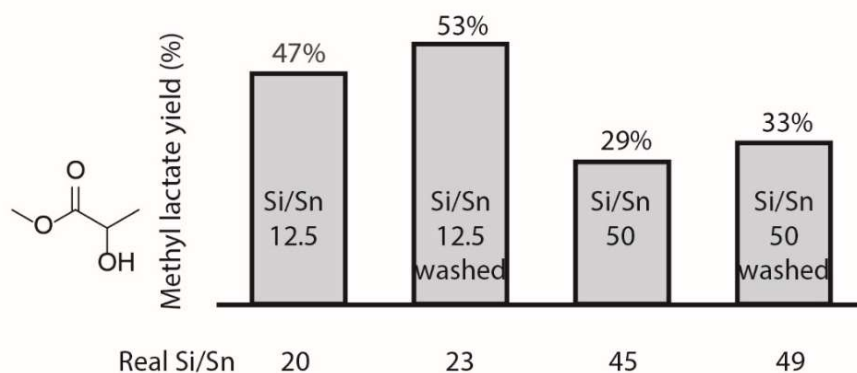


Figure 5.7. Formation of methyl lactate using post-treated Sn-Beta (12.5) and (50) prepared with and without methanol washes. Reaction conditions: glucose 120 mg, catalyst 50 mg, 5 mL solution of K<sub>2</sub>CO<sub>3</sub> in methanol (to a concentration that corresponds to a K/Sn ratio of 0.1), DMSO 80  $\mu$ L as internal standard, 160  $^{\circ}$ C, 2 hours.

### 5.1.5 Conclusions on the study of the parameters for the synthesis of Sn-Beta zeolites

This section aimed to probe the effect of systematic changes in the procedures for the preparation of Sn-Beta zeolites on the catalyst. The study focused on the development of post-synthetic procedures because they allow easy catalyst synthesis and many applications. The preparation of post-synthetic Sn-Beta zeolites involved the initial dealumination of the commercial aluminum-containing zeolite, followed by the incorporation of tin by incipient wetness impregnation. The effect of the presence of residual aluminum was studied by the preparation of catalysts derived from Beta zeolites, which were dealuminated for different times. The residual aluminum introduced Brønsted acidity, which had a negative impact on the production of methyl lactate from glucose and MVG from glycolaldehyde. Different from using dihydroxyacetone as starting substrate,<sup>56</sup> residual aluminum needed to be avoided for the processes considered herein (the conversion of both hexoses and glycolaldehyde) and a complete dealumination led to optimal performances of the catalysts.

Table 5.4. Effect of residual aluminum in Sn-Beta catalysts on the conversion of different substrates.

Reaction	Effect of residual aluminum
Conversion of DHA into lactates	Positive: promotion of the dehydration of DHA into PAL <sup>56</sup>
Conversion of glucose into lactates	Negative: formation of glucosides and furanic byproducts
Conversion of GA into MVG	Negative: formation of MGA-DMA byproduct

The maximum amount of active tin incorporated in the structure by impregnation was also considered. The tin forms the active sites of the catalyst, but excessive amounts cannot be incorporated and result in the obstruction of the porosity due to the formation of extra-framework tin oxides.<sup>60</sup> Increased tin contents resulted in an acceleration of the production of MVG from glycolaldehyde at the beginning of the process. The preparation of samples containing different amounts of tin were probed by XRD and were found to contain extra-framework species in some instances. The possibility to remove the oxides by washings steps during the synthesis was explored, but resulted in only marginally improved catalytic activity and was therefore not studied further considering that the additional step increased the times for the preparation of the catalysts.

## 5.2 Synthesis and Use of Mesoporous Stannosilicates for the Production of Methyl Lactate

In this section, the preparation of stannosilicates with different porous systems is explored.<sup>4</sup> The use of microporous materials as catalysts can lead to several disadvantages for industrial applications. The deactivation of the catalyst due to the formation of coke has a large impact on micropores because of the ease of obstruction in these systems.<sup>17</sup> Moreover, in biorefinery applications, the ability to convert large natural molecules that can find diffusional limitations in small pores systems is often required. The enlargement of the porous structure can facilitate the access of oligo- and polysaccharides. For this reason, the synthesis of hierarchical zeolite catalysts has become a central topic in the research for the use of biomass as a source for the production of chemicals.<sup>209</sup> Strategies for the preparation of mesoporous systems can be classified as *top-down* and *bottom-up* (Chapter 1.1.3). The first approach involves post-synthetic modification of already crystallized materials.<sup>19</sup>

Post-synthetic treatments have received much interest because of the ease of the procedures that allow many applications. Traditionally, the cavities in zeolites have been enlarged by treatments with a basic solution of NaOH.<sup>21</sup> However, the procedure has low level of control and can lead to the formation of irregular structures. More recently, procedures involving the use of surfactants as templates for post-synthetic reorganizations of the zeolites structures have been proposed. The hydrothermal restructuring can be performed after the first dissolution<sup>23</sup> of the sample in basic media or directly by hydrothermal treatment.<sup>24</sup> The methodologies allow obtaining organized and controlled hierarchical materials using a simple and broadly applicable post-synthetic treatment. On the other hand, direct *bottom-up* procedures can be used for the preparation of mesoporous catalysts. The approach involves classical hydrothermal synthesis with the use of specific templates, such as large organic polymers.

In this section, the preparation of stannosilicates starting from different commercial zeolites is discussed. Beta and USY frameworks showed the best results for the dealumination and incorporation of tin. Therefore, those zeolites were used for studying the modification of microporous systems into hierarchical systems. Several post-synthetic procedures were applied for the preparation of mesoporous stannosilicates. Finally, a large-pore hydrothermal Sn-Beta was synthesized for comparison with the post-synthetic catalysts. All the samples were characterized and tested for the conversion of substrates with different dimensions, namely glucose, sucrose and inulin.

### 5.2.1 Synthesis and characterization of stannosilicates with different porous systems

In this work, the possibility of the use of different porous systems in the preparation of stannosilicates for the conversion of carbohydrates into methyl lactate was explored. In a first preliminary screening, the preparation of stannosilicates by post-synthetic modifications of different commercial zeolites was studied. Among the Beta, USY, MOR and MFI zeolite frameworks, only Beta and USY were successfully dealuminated. The dealumination was not dependent on the initial Si/Al ratio, therefore, the dealuminated USY resulted in similar materials starting from both H-USY (6) and H-USY (30). All the frameworks were impregnated with tin and tested for the conversion of glucose to methyl lactate. Sn-Beta (100) and Sn-USY (25) presented the best activity

---

<sup>4</sup> Synthesis of the zeolites and tests of reactivity were carried out with the help of MSc. Annalisa Sacchetti during the project for her final thesis. The section was adapted from the article “Exploring the Synthesis of Mesoporous Stannosilicates as Catalysts for the Conversion of Mono- and Oligosaccharides into Methyl Lactate” published in Topics in Catalysis.<sup>212</sup>

and they were chosen for the preparation of mesoporous catalytic systems. Table 5.4 lists the procedures explored for the preparation of tin-containing zeolites. Alkaline desilication<sup>104</sup> and surfactant templating<sup>22</sup> were applied as post-synthetic modifications. Moreover, a hydrothermal Sn-Beta was synthesized using polydiallyl dimethylammonium chloride (PDADMA) and tetraethyl ammonium hydroxide (TEAOH) as templates.<sup>195</sup>

Table 5.5. Synthetic procedures for the preparation of modified stannosilicates.

Catalysts	Preparation
Sn-Beta (100)/Sn-USY (25)	Dealumination of the commercial zeolite and impregnation of tin <sup>55</sup>
[deSi] Sn-Beta (100)/ [deSi] Sn-USY (25)	Alkaline desilication, dealumination and impregnation of tin <sup>104</sup>
[ST] Sn-Beta (100)/ [ST] Sn-USY (25)	Surfactant templating of Sn-beta (100)/Sn-USY (25) <sup>193</sup>
[DR] Sn-Beta (100)/ [DR] Sn-USY (25)	Dissolution in alkaline media and surfactant reassembly of the commercial zeolites, dealumination and impregnation of tin <sup>194</sup>
[HT] Sn-Beta (100)	Hydrothermal synthesis of mesoporous Sn-beta zeolite <sup>195</sup>

Numbers in brackets indicate the Si/Sn ratio

Opposite to the dealumination procedure, the alkaline treatment introducing mesoporosity was strongly dependent on the Si/Al ratio.<sup>104</sup> Therefore, the method was applied on the aluminum containing zeolites before the dealumination step. However, the H-USY zeolite was recalcitrant to the basic treatment and underwent a collapse of the structure. Thus, only the Beta mesoporous framework was obtained by desilication. On the other hand, it was possible to obtain mesoporous Sn-USY zeolites following surfactant templating procedures and using cetyltrimethylammonium bromide (CTAB) as surfactant agent. Finally, a mesoporous Sn-Beta was also synthesized by hydrothermal *bottom-up* methodology by the use of polydiallyl dimethylammonium chloride (PDADMA) together with tetraethyl ammonium hydroxide (TEAOH) as structure directing agents.

Table 5.5 reports the physical properties of the prepared samples. Materials presenting amorphous structures in the XRD characterization were omitted from Table 5.5. It was not possible to modify USY zeolites by desilication in alkaline media, nor to apply the surfactant restructuring to Beta zeolites. In Supplementary Information SI.1, the SEM images of the samples shows that the morphology of the crystals were not modified after post-treatment. However, evident clusters of extra-framework species were visible on the surface of the crystals in Sn-USY (25) (Figure 5.8). The deposit corresponds to an improper incorporation of the tin inside the structure, giving external amorphous oxides or tin nanoparticles, invisible to the XRD technique. However, the material still had a catalytic activity that was comparable to the other samples.

Table 5.6. Characterization of the physical properties of mesoporous stannosilicates.

Catalyst	Framework	BET (m <sup>2</sup> /g)	Average pore width (Å)	Si/Sn ratio	Si/Al ratio	Acidity (μmol NH <sub>3</sub> /g)
Sn-Beta (100)	BEA	592.4	21.8	102.5	134.8	71
Sn-USY (25)	USY	757.6	25.6	33.7	67.8	69
[deSi] Sn-Beta (100)	BEA	637.7	48.0	129.0	137.0	95
[ST] Sn-USY (25)	USY	539.7	25.0	28.5	126.0	-
[DR] Sn-USY (25)	USY	626.0	34.0	52.0	70.0	58
[HT] Sn-Beta (100)	BEA	568.0	70.0	95.7	11.3	76

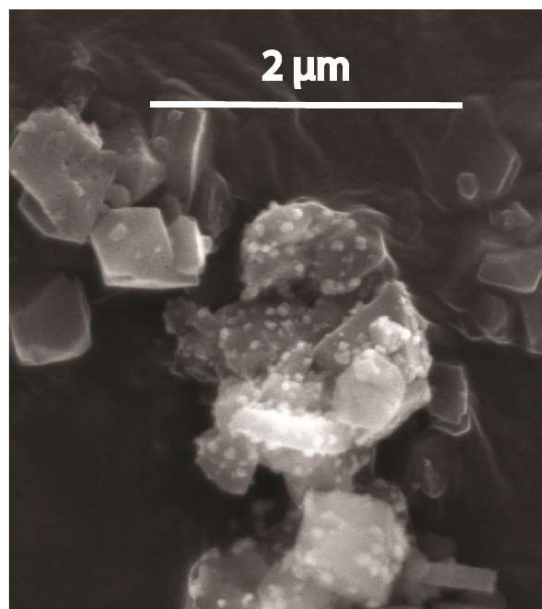


Figure 5.8. SEM image of Sn-USY (25). Adapted from Ref. 212.

Results from nitrogen physisorption characterization confirmed the enlargement of the pores in the modified samples. Only the sample [ST] Sn-USY (25) did not result in the dimensions between 30 Å and 75 Å. Therefore, it was not investigated further. The hydrothermal synthesis was the most efficient in terms of width of pores, leading to average dimension of 70 Å. As expected for hydrothermal Sn-Beta, the material presented large crystals and the absence of the use of HF as mineralizing agent led to spherically shaped crystals. However, the SEM images showed the presence of amorphous material, indicating the incomplete crystallization (Supplementary Information SI.1.8). Synthesized catalysts did not show drastic changes in the acidity measured by  $\text{NH}_3$ -TPD (Table 5.5), indicating comparable tin incorporation and activity among the samples.

### 5.2.2 The activity of mesoporous stannosilicates in the conversion of carbohydrates into methyl lactate

The activity for the conversion of carbohydrates was studied for the different catalytic systems using substrates with different dimensions. Large pores should reduce diffusional limitations and promote a faster conversion of large compounds compared to micropores.<sup>18</sup> Glucose, sucrose and inulin were used as starting substrates in the process for the production of methyl lactate at 160 °C in methanol and the reaction mixtures were analyzed by quantitative 2D NMR. Reactions carried out at full conversion (two or four hours) did not present a clear trend between porosity and distribution of products. However, indications for the effect of enlarged porosity could be noticed in the trends of initial rates. Glucose is a small substrate and its conversion (Figure 5.9) was not improved by the use of large pore catalytic systems. In contrast, microporous Sn-Beta and Sn-USY presented a faster conversion of glucose and formation of methyl lactate. This outcome could be ascribed to the beneficial effect of confinement<sup>210</sup> or to the higher concentration of active tin in micropores compared to the mesoporous counterparts.

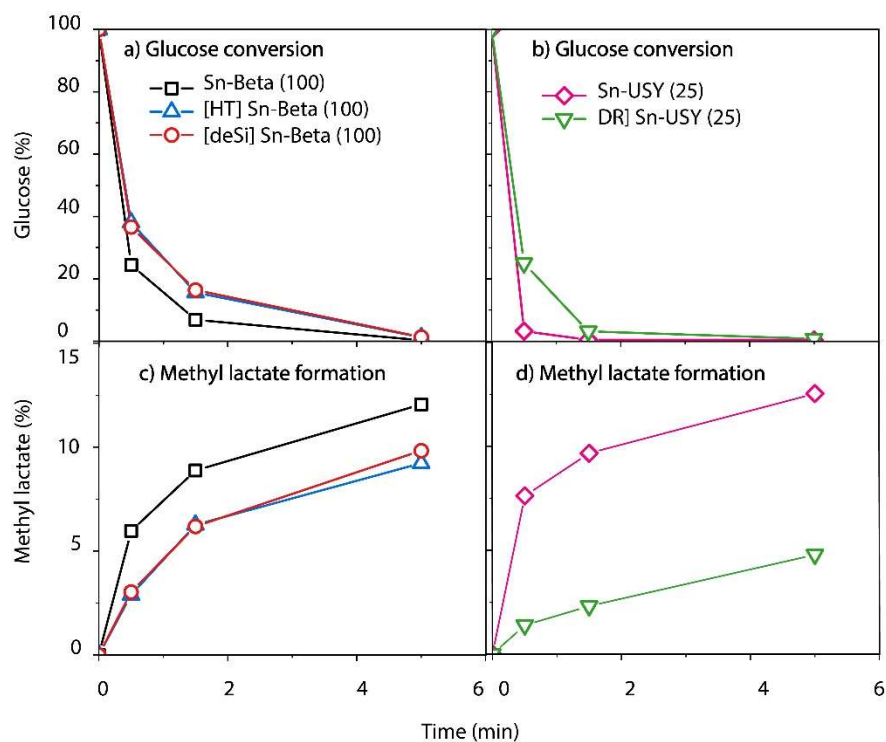


Figure 5.9. Conversion of glucose (a, b) and formation of methyl lactate (c, d) using different Beta (a, c) and USY (b, d) catalytic systems. Reaction conditions: glucose 120 mg, catalyst 50 mg, methanol 5 mL, DMSO as internal standard 80  $\mu$ L, 160  $^{\circ}$ C. Adapted from Ref. 212.

Analogous to the use of glucose, the conversion of sucrose was not affected by the modified porosity. In general, the disaccharide sucrose requires an initial step of Brønsted acid-catalyzed hydrolysis before it enters the retro-aldol catalytic pathway catalyzed by Lewis acidity. This additional step complicated the interpretation of results and made the general formation of methyl lactate slower compared to the use of glucose or other monomers.<sup>196</sup> However, sucrose did not show diffusional limitations and microporous stannosilicates were able to catalyze a slightly faster formation of methyl lactate than mesoporous catalysts (Figure 5.10). All the studied systems formed negligible amounts of furanic byproducts, indicating minor contribution of Brønsted acid catalysis in the reaction.

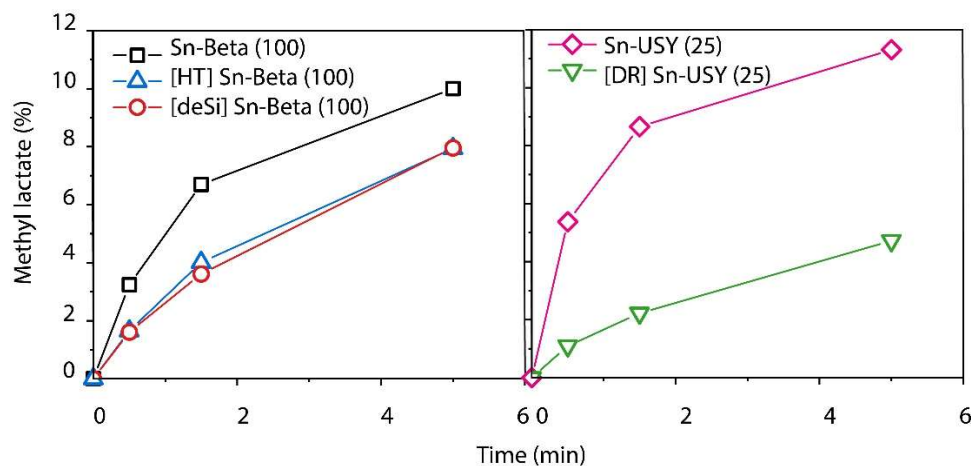
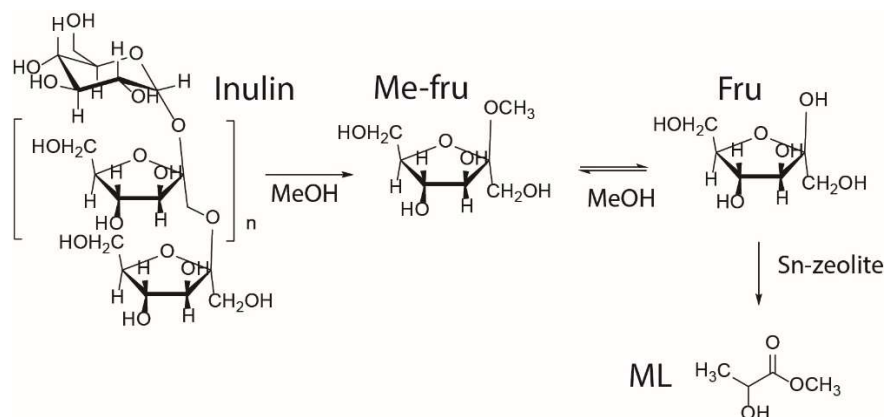


Figure 5.10. Formation of methyl lactate from sucrose using different Beta and USY catalytic systems. Reaction conditions: sucrose 120 mg, catalyst 50 mg, methanol 5 mL, DMSO as internal standard 80  $\mu$ L, 160  $^{\circ}$ C. Adapted from Ref. 212.

## 5.2 Mesoporous Stannosilicates

Inulin is an oligosaccharide found in nature as carbon storage for different types of plants. It is formed by fructose units linked by  $\beta$ -(1,2)-glycosidic bonds and it is rather easily hydrolyzed in water.<sup>211</sup> Using methanol as solvent, the solvolysis of inulin gives methyl fructosides, which can be hydrolyzed further to fructose and enter retro-aldol pathways to form methyl lactate in the presence of a Lewis acidic catalyst (Scheme 5.2).<sup>196</sup> The conversion of inulin into methyl lactate showed slower reaction rates compared to the conversion of glucose and fructose due to the additional steps required using this substrate. The use of the bulky starting substrate inulin resulted in the initial formation of methyl fructosides and methyl lactate. Catalysts with larger porosity were affected less by diffusional limitations compared to the microporous counterparts and the process was faster in mesopores (Figure 5.11). For both mesoporous Sn-USY and Sn-Beta the solvolysis of inulin occurred rapidly, resulting in the formation of methyl fructosides.



Scheme 5.2. Scheme of the reaction pathway for the conversion of inulin into methyl lactate. Adapted from Ref. 212.

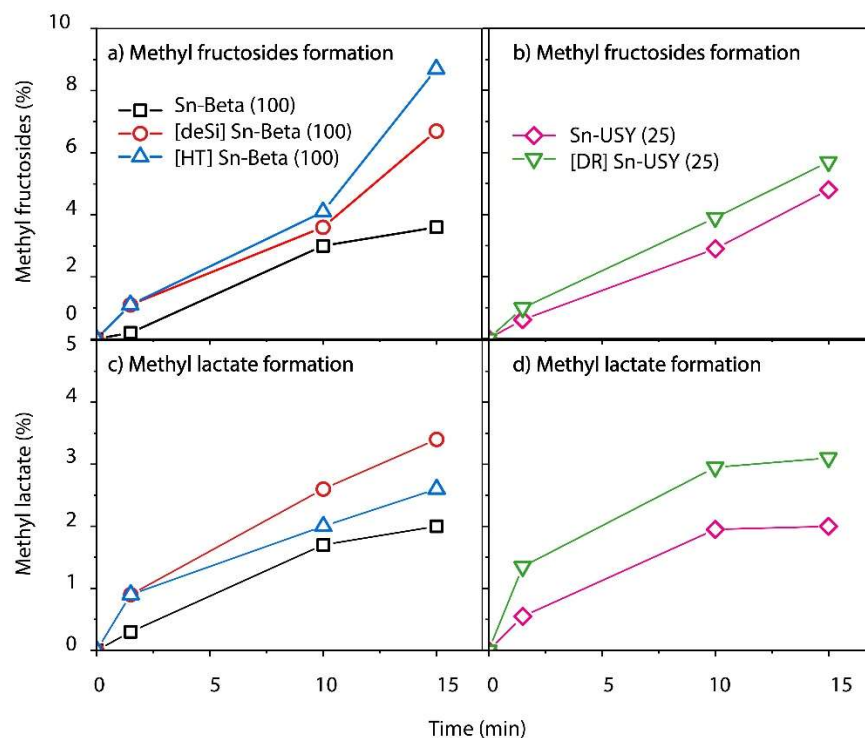


Figure 5.11. Formation of methyl fructosides (a, b) and methyl lactate (c, d) from inulin using different Beta (a, c) and USY (b, d) catalytic systems. Reaction conditions: inulin 120 mg, catalyst 50 mg, methanol 5 mL, DMSO as internal standard 80  $\mu\text{L}$ , 160  $^{\circ}\text{C}$ . Adapted from Ref. 212.

On the other hand, yields of methyl lactate from inulin were not improved when taking the distribution of products after four hours as an indicator (Figure 5.12). Only the Beta framework presented slightly increased formation of methyl lactate using mesoporous catalysts. However, yields in Figure 5.14 were not the only relevant parameter for considering the catalytic activity of one particular systems. The products distribution after four hours showed a large quantity of methyl fructosides left in the final mixtures. As discussed in Chapter 3.2.2, methyl fructosides were intermediates in the process and could be further converted into methyl lactate by changing the reaction conditions, for instance by using prolonged reaction times. Therefore, the pore sizes were not limiting for the conversion of inulin during long periods, but it affected conversion at the beginning of the process. The final product distribution was dependent only on the amount of active tin in the catalyst.

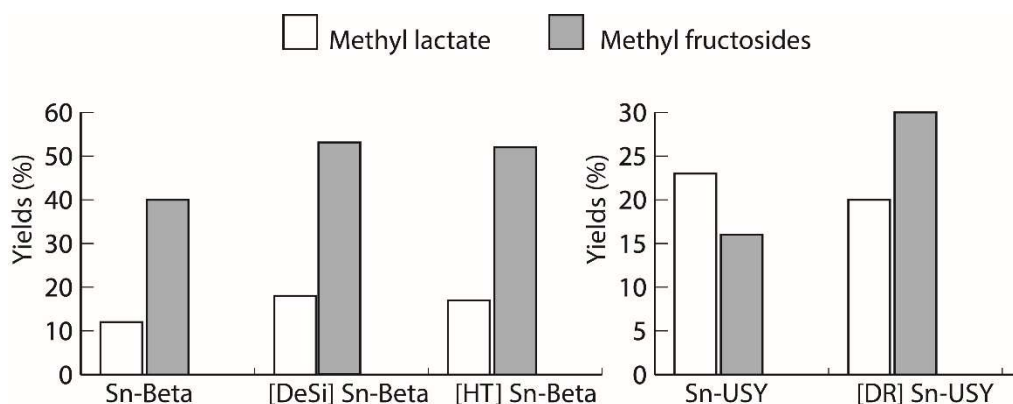


Figure 5.12. Yields of methyl lactate and methyl fructosides in the conversion of inulin using catalysts with different porosity. Reaction conditions: inulin 120 mg, catalyst 50 mg, methanol 5 mL, DMSO as internal standard 80  $\mu$ L, 160  $^{\circ}$ C, 4 hours. Adapted from Ref. 212.

The prepared catalytic systems presented good stability over three cycles of reuse without regeneration (Figure 5.13). The removal of the inactive tin oxide species from the surface after the first catalytic run may be the cause of the increased yields of methyl lactate for Sn-USY.

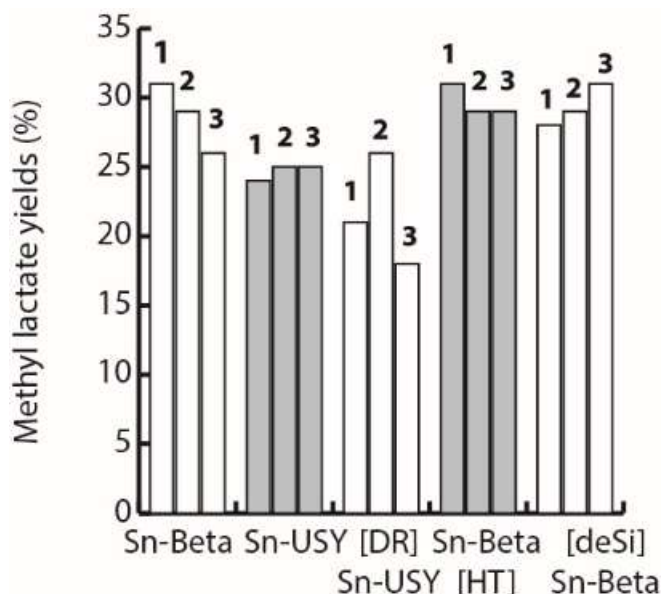


Figure 5.13. Reuse of the mesoporous catalysts over three cycles. Reaction conditions: glucose 120 mg, catalyst 50 mg, 5 mL methanol, DMSO 80  $\mu$ L as internal standard, 160  $^{\circ}$ C, 2 hours. Adapted from Ref 212.



### 5.2.3 Conclusions on the study of mesoporous stannosilicates as catalysts for the production of methyl lactate

This part of the project investigated the use of stannosilicate catalysts with different pore systems in order to avoid diffusional limitations during the conversion of carbohydrates into methyl lactate. In a preliminary screening, the framework Beta and USY were selected as the best frameworks for the preparation of tin-containing zeolites by acidic dealumination and tin incorporation. Beta and USY were then used for the preparation of hierarchical porous structures. Different synthetic approaches were followed. Mesoporous Sn-USY were successfully synthesized by a *top-down* method of surfactant templating of original Sn-USY zeolites. In contrast, mesoporous Beta zeolites were prepared by alkaline desilication of a commercial Beta zeolite. Finally, hierarchical Sn-Beta was synthesized by hydrothermal *bottom-up* procedure using polydiallyl dimethylammonium chloride (PDADMA) and tetraethyl ammonium hydroxide (TEAOH) as templates. All the samples showed physical properties similar to the original microporous systems, except for the width of the pores. The effect of pore size was studied in the conversion of glucose, sucrose and inulin to methyl fructosides and methyl lactate. Using glucose and sucrose as starting reagents, mesoporous systems did not improve the initial formation of methyl lactate, indicating low impact of diffusional limitations in the reactions. On the other hand, the initial formation of methyl lactate from a large oligomer like inulin was accelerated using mesoporous stannosilicates. The catalytic materials were stable over three cycles of reuse. Results indicated the possibility to improve the activity of Sn-Beta catalysts for conversion of biomasses by modifications in the porosity. Mesoporous systems could overcome diffusional limitations of large substrates without changing the intrinsic activity of the catalysts.

# Chapter 6

## Characterization of the Structure-Activity Relation of Sn-Beta Zeolites

This chapter discusses the characterization of Sn-Beta zeolite catalysts. FT-IR spectroscopy was applied for the investigation of the structural modifications in the material resulting from different synthetic procedures. The effect of a thermal treatment for the regeneration of the catalyst was also explored. The FT-IR *in situ* adsorption of deuterated acetonitrile as a probe molecule resulted in an efficient technique for the characterization of the structure of Sn-Beta catalysts. Ammonia was also applied as a probe molecule for the characterization of the catalyst acidity by TPD and FT-IR spectroscopy for quantitative and qualitative information. These methods of characterization were used for the determination of the acidity in Sn-Beta in the absence and in the presence of alkali ions. The interaction between Sn-Beta catalysts and alkali salts was studied by titration with potassium carbonate. Moreover, the interaction with different additives was considered. Salts of different metals were incorporated into the structure of Beta zeolites and the effect on the reaction for the conversion of glucose into methyl lactate was analyzed.

### 6.1 Characterization of Sn-Beta Zeolites Using FT-IR Spectroscopy with *In Situ* Adsorbed Deuterated Acetonitrile as a Probe Molecule

In stannosilicates, tin can be incorporated into different coordinative environments,<sup>69</sup> influencing the catalytic properties of the final material. Thus, the characterization of the active sites can give important information for the design of optimal catalytic systems. Vibrational spectroscopic techniques represent relevant methods for the characterization of zeolitic materials and different methods have been developed and applied to study tin-containing catalysts.<sup>93</sup> Among the explored procedures, the use of FT-IR experiments of *in situ* adsorption of deuterated acetonitrile represents a powerful method for the analysis of active sites acidic properties. In this section, the FT-IR spectroscopic characterization of different Sn-Beta zeolites is presented. The technique was applied for studying the connection between catalytic properties, characteristics of the materials and procedures of preparation. The acidity of each sample was studied by adsorption of deuterated acetonitrile. This section aimed to understand the structure of the catalytic material and the parameters affecting the acidity and the

activity in order to bring useful information for future development of the catalytic system. Finally, the techniques were used to characterize a Sn-Beta sample that was spent and regenerated. The study aimed to probe how processes of deactivation and regeneration modify the physical properties of the catalytic material.<sup>5</sup>

### 6.1.1 FT-IR characterization of zeolites and the use of deuterated acetonitrile as a probe molecule for active sites Lewis acidity

In general, FT-IR spectra of zeolites are most informative in two main regions: 3000-4000  $\text{cm}^{-1}$  and 1500-2100  $\text{cm}^{-1}$ . The bands at high frequencies appear in the spectral region of the O-H vibrations. The sharp peak at 3733  $\text{cm}^{-1}$  (Figure 6.1) is related to the stretching of the O-H group in terminal silanols. It is followed by a broad tail at lower frequencies, indicating the hydrogen-bonded internal silanol nests.<sup>87</sup> The O-H stretching frequency is also indicative of the Brønsted acidic behavior: at higher frequency, the O-H bond is stronger and the proton is not easily released, corresponding to weaker acidity. Isolated Brønsted acidic sites usually creates bands around 3600  $\text{cm}^{-1}$ .<sup>213</sup> The other signals at lower frequencies (Figure 6.1) are related to the framework vibrations and are specific for each zeolite type. In general, zeolites show a stretching band between 2000  $\text{cm}^{-1}$  and 1800  $\text{cm}^{-1}$ , connected to the stretching modes of T-O, where T indicates silicon or aluminum.<sup>213</sup> Spectra are usually normalized to these signals in order to compare different samples of the same zeolite. However, for absolute quantifications, it is necessary to take into account the amount of sample and the thickness of the pellets. These parameters are not easily controllable and, in this work, only relative comparisons are discussed. Figure 6.1 shows the FT-IR spectra of a Sn-Beta sample. Bands related to the vibrations of tin are not visible since they overlap with other intense signals (the stretching of stannanol is reported in literature at 3664  $\text{cm}^{-1}$ ).<sup>214</sup>

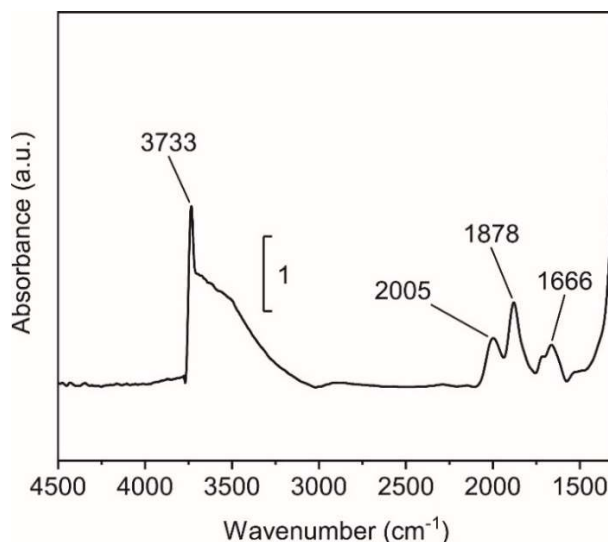


Figure 6.1. FT-IR spectra of Sn-Beta zeolite.

Probe molecules are widely used for exploring the acidity of solids by spectroscopy, especially NMR and FT-IR spectroscopy. In the case of Lewis acidity, deuterated acetonitrile was applied as the probe molecule and the adsorption was followed by FT-IR spectroscopy. Acetonitrile adsorbed on Sn-Beta is able to distinguish Lewis and Brønsted acidic sites, but also to identify the tin in different environments. The technique has been recently

<sup>5</sup> Experiments discussed in this section were performed in the laboratories of Haldor Topsøe A/S with the help and under the supervision of Research Scientist Juan S. Martinez-Espin.

applied to correlate the intensity of the different peaks to specific catalytic behavior.<sup>93</sup> This characterization method is thus an attractive tool for predicting the activity of synthesized catalytic materials.

In a general experiment of acetonitrile adsorption, the sample was first pre-treated to completely remove water. The probe molecule was adsorbed *in situ* and spectra were recorded at different pressures of acetonitrile (between  $2 \times 10^{-2}$  and 4 mbar). In the first spectra at low pressure, bands related to the probe interacting with strong acid sites were visible. The interactions with weak sites appeared later in spectra at relative high pressures. The overall area of the peaks was proportional to the amount of bonds in the sample giving the same signal, i.e. the quantity of sites. Although normalization for the vibrations of the framework allowed the comparison between different samples, the technique was challenging to be used for absolute quantifications due to the difficulty in controlling samples preparation. The peaks of acetonitrile adsorbed on Sn-Beta appeared in the region between  $2150\text{ cm}^{-1}$  and  $2400\text{ cm}^{-1}$  and above  $3000\text{ cm}^{-1}$ . The main signals observed in this type of experiment are summarized in Table 6.1.

Table 6.1. Signals of acetonitrile interacting with Sn-Beta zeolites.<sup>93, 97</sup>

Vibration frequency (wavenumber $\text{cm}^{-1}$ )	Detected group	Group interacting with acetonitrile
2265	$\nu(\text{C}\equiv\text{N})$	None (physisorbed)
2276	$\nu(\text{C}\equiv\text{N})$	Silanols
2290	$\nu(\text{C}\equiv\text{N})$	Tin oxide
2301	$\nu(\text{C}\equiv\text{N})$	Alumina
2308	$\nu(\text{C}\equiv\text{N})$	Tin closed sites
2316	$\nu(\text{C}\equiv\text{N})$	Tin open sites
3300-3600	-OH	Hydrogen-bonded silanols

From the adsorption of deuterated acetonitrile, it is possible to distinguish open and closed tin sites.<sup>70</sup> Open sites are stronger than the closed counterparts, thus the signals have higher wavenumbers. At higher pressures, the peak is shifted to a lower frequency, indicating the interaction with the weaker closed sites. Recently, Sushkevich et al. have contradicted the correlation of the peak at  $2308\text{ cm}^{-1}$  to closed sites in a study using combined spectroscopic techniques.<sup>97</sup> The authors have proposed that the signal derives from the interaction of acetonitrile with weak Brønsted acidic sites, probably silanols affected by the presence of tin.

### 6.1.2 Sn-Beta catalysts with different tin content

Tin content is a crucial parameter for the activity of the catalyst, since it constitutes the active site. The effects of the tin content on the activity are discussed in the previous chapters. High contents of tin accelerated the formation both of intermediates and products, such as methyl fructosides during the conversion of hexoses in methanol at  $160\text{ }^{\circ}\text{C}$  (Chapter 3.2.2) and MVG during the conversion of glycolaldehyde (Chapter 5.1.3). However, the correlation between activity and tin content was not completely proportional. The tin could be positioned in different coordination environments in the zeolite framework, leading to active sites with different strength and activity.<sup>69</sup> Moreover, the amount of active tin, which can be incorporated inside the structure, is limited and synthetic routes for the incorporation of high active tin content are still under investigation.<sup>60</sup> Catalysts containing different tin contents were characterized by FT-IR adsorption of deuterated acetonitrile, in order to study the relation between incorporation of tin in the framework and acidity.

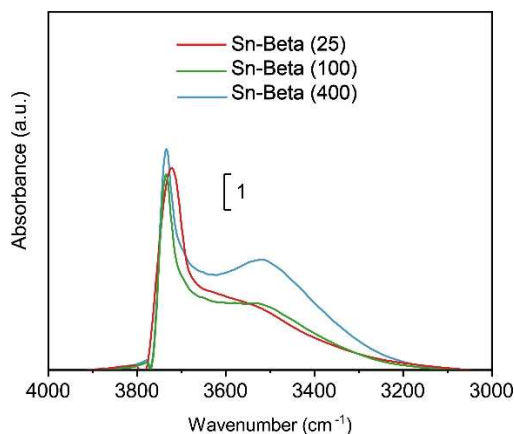


Figure 6.2. FT-IR spectra of Sn-Beta zeolites containing different amounts of tin.

The blank spectra, obtained upon water removal at 450 °C under vacuum overnight, of the samples containing different amounts of tin showed different intensity of the bands related to the O-H stretching (Figure 6.2). The process of dealumination of H-Beta zeolites removed aluminum and created free silanols inside the framework. The tin was then incorporated into the vacant T-sites by closing the formed silanol nests.<sup>55</sup> For high tin contents, the amount of free silanols was small and the O-H band in the FT-IR spectra was less intense than for samples containing low amounts of tin (Figure 6.2). The adsorption of acetonitrile (Figure 6.3) clearly showed that the ratio between silanols and tin changed for different Si/Sn nominal ratios. The band around 2310 cm<sup>-1</sup> related to the interaction between probe and framework tin was barely visible in the Si/Sn 400 catalyst (Figure 6.3 a), but became predominant in the case of Si/Sn ratio 25 (Figure 6.3 c). Unfortunately, it was not possible to separate the peaks at 2308 cm<sup>-1</sup> and 2316 cm<sup>-1</sup> for these samples and no indication about the relation between level of incorporation and different coordination environments was obtained.

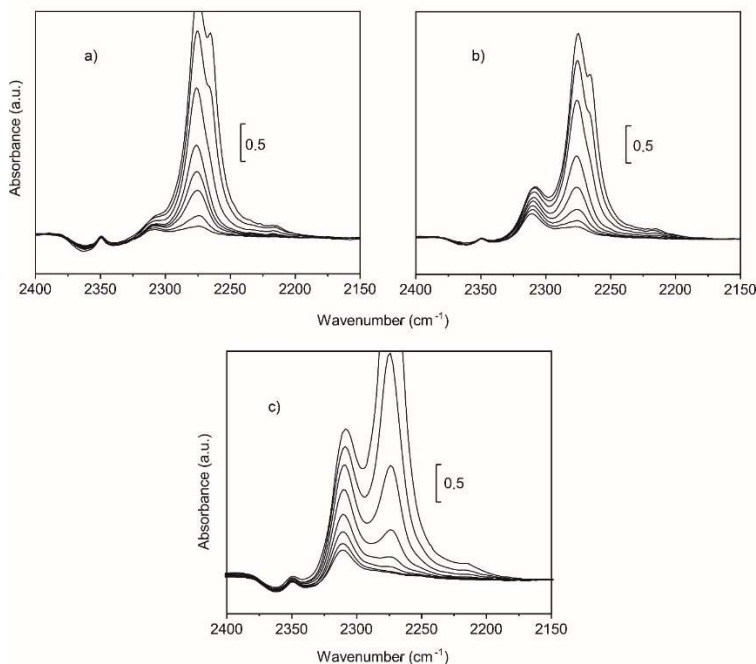


Figure 6.3. FT-IR spectra of *in situ* adsorption of deuterated acetonitrile on Sn-Beta containing different amounts of tin: a) Si/Sn 400, b) Si/Sn 100, c) Si/Sn 25.

Table 6.2. Properties of Sn-Beta catalysts with different tin content.

Sample Si/Sn	Sn wt%	Si wt%	Area <sup>a</sup> 2310 cm <sup>-1</sup>	Area <sup>a</sup> 2276 cm <sup>-1</sup>	NH <sub>3</sub> -TPD (μmol/g)
25	7.3	40.6	44	62	184
100	1.89	43.7	16	23	71.9
400	0.46	44.7	7	26	27.2

<sup>a</sup>Integrated in the spectra recorded after 20 minutes of desorption of deuterated acetonitrile under vacuum at room temperature

Table 6.2 reports the elemental composition, the integrated area in the FT-IR spectra of the peak of acetonitrile interacting with the zeolites and the NH<sub>3</sub>-TPD acidity. The area of the peak was integrated in the FT-IR spectra after desorption of deuterated acetonitrile under vacuum at room temperature for 20 minutes. The area of the peak had a linear correlation with the number of groups in the sample giving the signal. Nevertheless, the area of the peaks at 2310 cm<sup>-1</sup> did not show an exact linear correlation with tin content (Table 6.2). This deviation was probably caused by the presence of tin that was not incorporated in the framework, which did not contribute to the signal. The area of the peak could be properly correlated to the acidity measured by NH<sub>3</sub>-TPD (Figure 6.4). The values of acidity gave quantitative information on the activity of the sample, as discussed in the following section. The linear correlation between the total acidity of the catalyst and the area of the signal also showed that the activity and the acidity of the samples were derived from the tin incorporated in the framework.

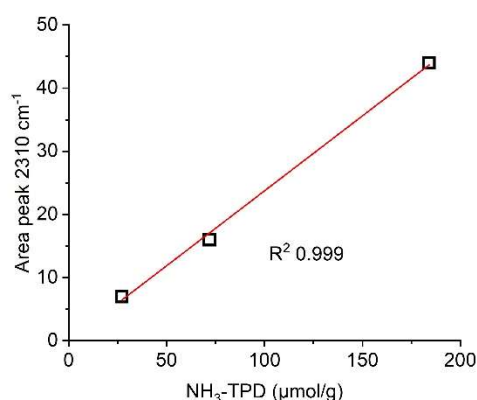


Figure 6.4. Linear correlation between acidity of samples measured by NH<sub>3</sub>-TPD and area of the peak at 2308 cm<sup>-1</sup> in the FT-IR spectra of zeolites after *in situ* desorption of deuterated acetonitrile under vacuum at room temperature for 20 minutes.

### 6.1.3 Calcination of the dealuminated Beta zeolite precursor

The preparation of Sn-Beta catalysts was performed by post-synthetic procedure starting from the acidic dealumination of a commercial Beta zeolite. Zeolites were treated with nitric acid overnight leading to the dealuminated material. Samples of dealuminated Beta zeolite were calcined at different temperatures before impregnation with tin and studied by FT-IR spectroscopy. This step was not carried out for samples generally used herein and calcinations were performed only at the end of the synthetic procedure. The calcination in air after dealumination can change the structure of the sample, mainly due to condensation of silanols that typically occurs at 400-700 °C.<sup>215</sup> This process of elimination of water can “close the silanol nests”, which are essential for the incorporation of tin into the framework.<sup>57</sup> In this paragraph, the effect of the calcination of dealuminated Beta zeolites on the final catalytic material is discussed. The effect of intermediate calcination was investigated in order to optimize parameters for the preparation of Sn-Beta zeolite catalysts. Figures 6.5 and 6.6 report

## 6.1 FT-IR Experiments of Deuterated Acetonitrile Adsorption

FT-IR experiments on dealuminated Beta zeolites calcined at 450 and 650 °C and reflect the effect of silanol condensation after dealumination and subsequent calcination.

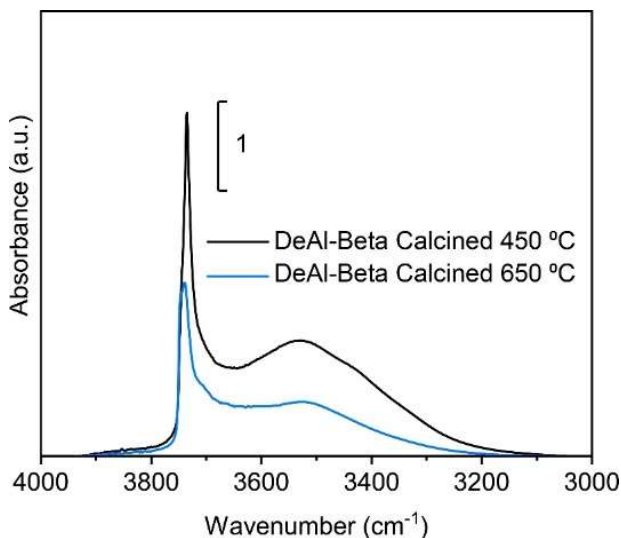


Figure 6.5. Different -OH region in the FT-IR spectra (blank) of dealuminated Beta zeolites calcined at 450 °C and at 650 °C.

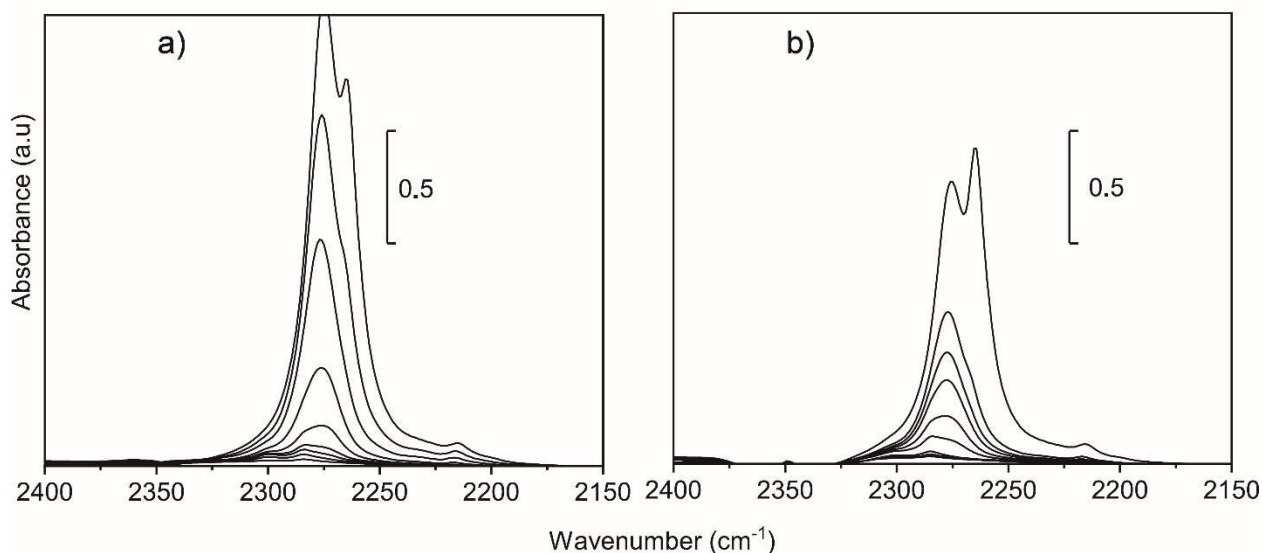


Figure 6.6. *In situ* adsorption of deuterated acetonitrile on dealuminated Beta zeolites: a) calcined at 450 °C, b) calcined at 650 °C.

The blank spectra in Figure 6.5 showed the silanols peak decreasing upon increased calcination temperature. The same results were found during the experiments of adsorption of deuterated acetonitrile on the dealuminated samples. For calcination at 650 °C (Figure 6.6b), the band related to acetonitrile adsorbed on silanols had lower intensity than for the sample calcined at 450 °C. Four samples of dealuminated Beta zeolite calcined at temperatures between 350 and 650 °C were impregnated with tin at 1.5 wt%. Figure 6.7 shows the same trend as Figure 6.5. When increasing the calcination temperature, the amount of silanols decreased.

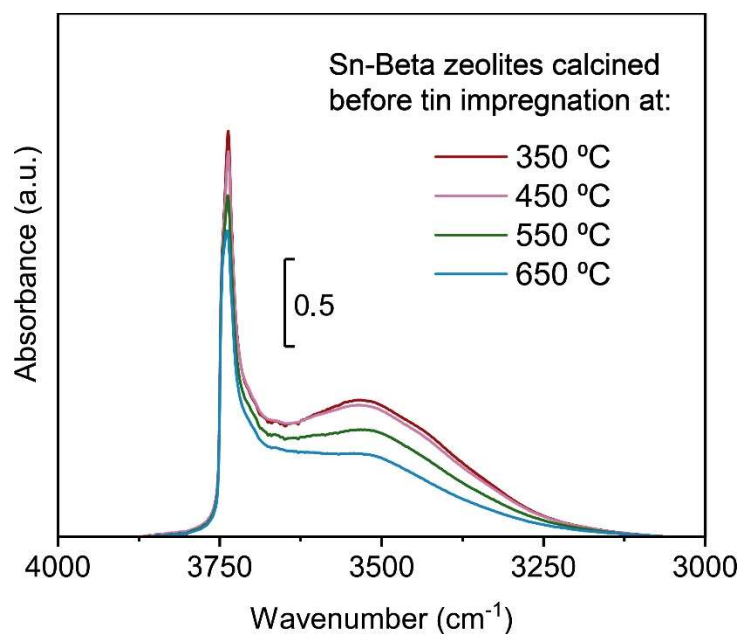


Figure 6.7. Sn-Beta zeolites calcined at different temperatures before tin incorporation.

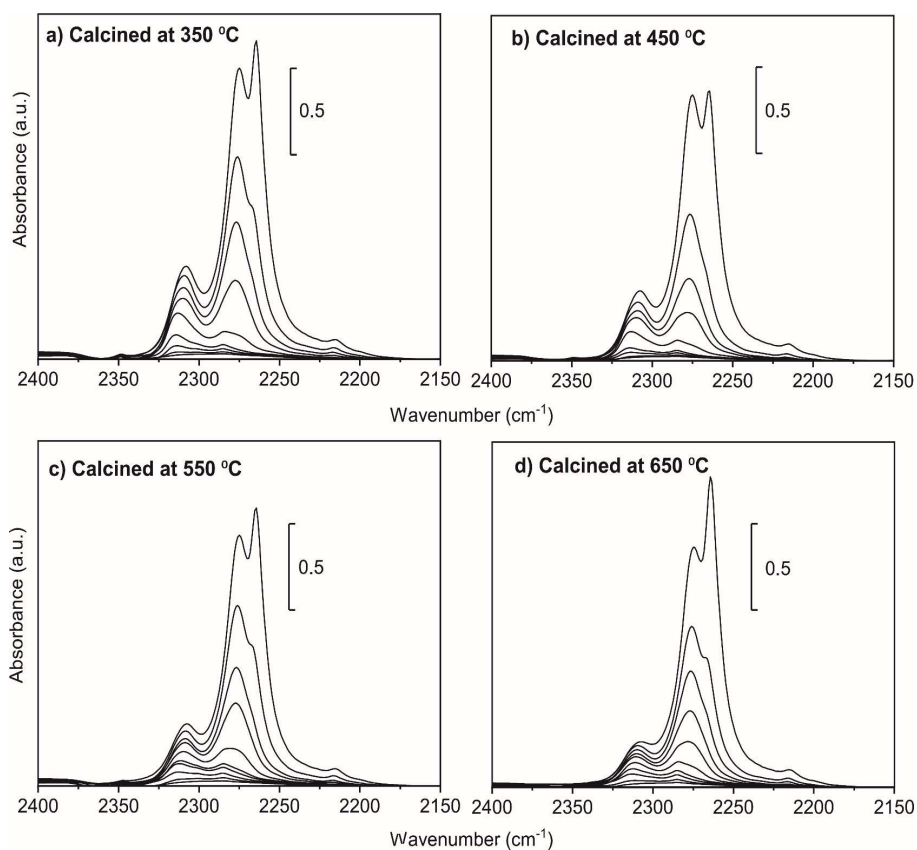


Figure 6.8. FT-IR spectra of *in situ* adsorption of deuterated acetonitrile on Sn-Beta catalysts prepared from dealuminated Beta zeolites calcined at different temperatures: a) 350 °C, b) 450 °C, c) 550 °C, d) 650 °C.

Results shown in Figure 6.8 for the adsorption of the probe molecule on the final catalysts (after incorporation of tin) were more relevant. The intermediate calcination reduced the silanols available in the dealuminated Beta



## 6.1 FT-IR Experiments of Deuterated Acetonitrile Adsorption

precursors and different levels of incorporation of tin in the framework were obtained depending on the temperature of calcination. The peaks of acetonitrile in the spectra recorded after desorption under vacuum for 20 minutes were deconvoluted and integrated using OriginPro 2018 (Table 6.3). The values of the area of the peak related to the interaction with the framework tin reflected the availability of silanols for the incorporation. The sample calcined at low temperature (350 °C) showed an intense peak for the framework tin, with an integrated area of 4.56. In contrast, the value of the area decreased to 2.47 in the sample calcined at 650 °C. The integration of the peaks at 2276 cm<sup>-1</sup> and 2290 cm<sup>-1</sup> related to the interaction of the probe with the silanols and extra-framework tin, respectively, did not show a clear trend probably due to the difficult deconvolution of the two overlapped peaks, which created a large error in the integration at low acetonitrile pressures.

Table 6.3. Properties of Sn-Beta catalysts calcined at different temperatures before tin incorporation.

Sample calcination (°C)	Sn wt%	Al wt%	Si wt%	Area <sup>a</sup> 2308 cm <sup>-1</sup>	Area <sup>a</sup> 2276 cm <sup>-1</sup>	Area <sup>b</sup> 2290 cm <sup>-1</sup>
350	1.35	0.087	44.9	4.6	6.2	2.7
450	1.23	0.086	45.2	3.5	4.8	2.3
550	1.32	0.085	45.2	2.6	5.1	5.5
650	1.29	0.086	45.0	2.5	4.5	3.7

<sup>a</sup>Peak integrated in the spectra acquired after 20 minutes of *in situ* desorption of deuterated acetonitrile <sup>b</sup>Peak integrated in the spectra acquired at pressure of 5x10<sup>-2</sup> mbar of deuterated acetonitrile

The study of samples calcined before tin impregnation showed the importance of the presence of the silanol nests during the preparation of post-synthetic Sn-Beta zeolites. The effective incorporation of tin in the zeolitic framework was achieved for samples calcined at low temperatures. Above 400 °C, the dehydroxylation of the silanols occurred and the final materials presented a high amount of extra-framework (inactive) tin. A condensed rigid dealuminated structure did not allow the insertion of the tin into the framework which is indispensable for active Sn-Beta catalysts, but it led to the formation of inactive extra-framework tin species. Thus, the presence of free silanols was an essential parameter for the preparation of active Sn-Beta zeolites and calcination at high temperatures before the impregnation of tin led to undesired modifications of the catalytic material.

### 6.1.4 Characterization of regenerated catalysts

Stability of the catalyst is an important parameter for industrial applications. Catalysts can deactivate temporarily or permanently. The first case often occurs when the formation of deposit obstructs the access to active sites.<sup>100</sup> Thermal treatments can be carried out for removing organic deposit materials and reactivating the materials. However, thermal treatments could also ruin the catalytic material and cause irreversible damages. In this section, the effect of the thermal treatment for the regeneration of a spent Sn-Beta catalysts is analyzed. Fresh and regenerated samples were characterized by FT-IR spectroscopy in order to understand the structural modifications occurring during the process of deactivation and thermal regeneration. The regenerated catalyst was obtained after deactivation during the conversion of glycolaldehyde into MVG for prolonged times and regeneration in air at 550 °C. The section focuses on the analysis of the structural changes of the materials after regeneration and samples were characterized by FT-IR spectroscopy of deuterated acetonitrile *in situ* adsorption. As observed for freshly calcined samples (Chapter 6.1.3), the spectra in the region of O-H vibrations showed that the thermal treatment partially removed silanols by dehydration (Figure 6.9). The broad band of the silanols decreased in the sample regenerated at 550 °C. Experiments of *in situ* adsorption of deuterated acetonitrile also had different patterns in the regenerated catalyst compared to the fresh sample (Figure 6.10).

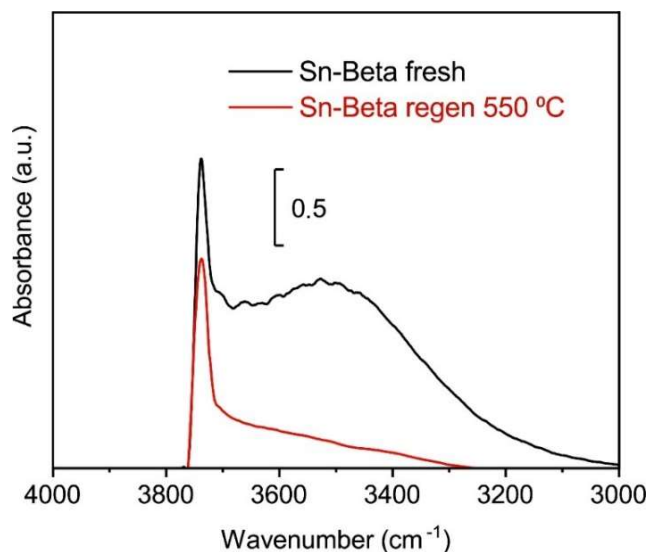


Figure 6.9. Spectral region of O-H vibrations in FT-IR spectra of fresh and regenerated Sn-Beta catalysts.

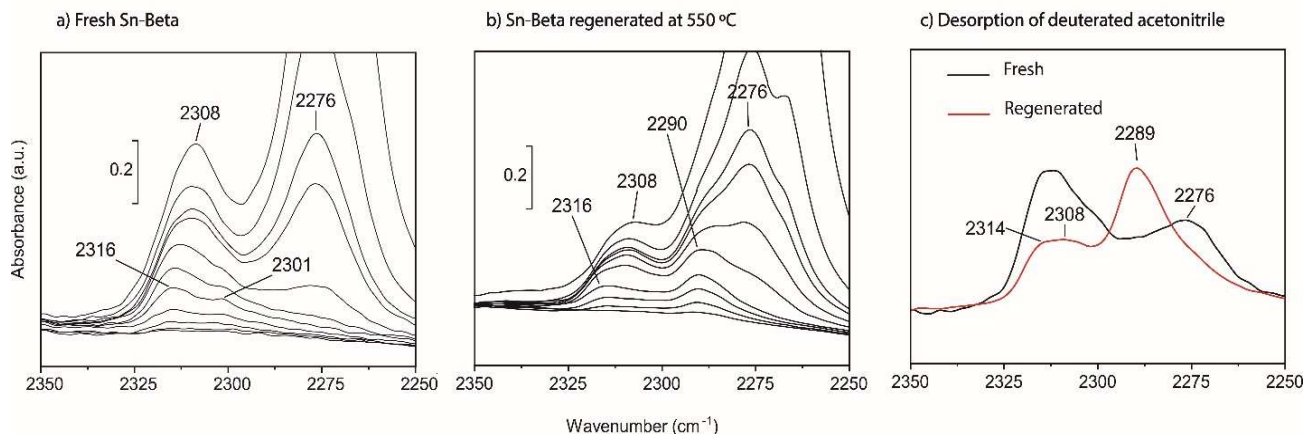


Figure 6.10. FT-IR spectra of *in situ* adsorption and desorption of deuterated acetonitrile on Sn-Beta zeolites a) fresh and b) regenerated at 550 °C, c) comparison between the desorption from the fresh and regenerated samples.

Changes in the FT-IR peaks occurred when comparing fresh and regenerated samples, corresponding to changes in the acidic properties. In the adsorption on fresh Sn-Beta, the peaks at 2316  $\text{cm}^{-1}$  and 2301  $\text{cm}^{-1}$  related to the probe interacting with open tin sites and residual aluminum, respectively, appeared as first, indicating the strong acidic behavior of these sites. At higher pressure, the high band at 2276  $\text{cm}^{-1}$  for the adsorption of acetonitrile on silanols was visible and the band related to the framework tin was shifted from 2316  $\text{cm}^{-1}$  to 2308  $\text{cm}^{-1}$  (Figure 6.10 a). After 20 minutes of desorption under vacuum at room temperature, the fresh Sn-Beta still showed probe molecules adsorbed on tin sites at 2308  $\text{cm}^{-1}$  and on silanols at 2276  $\text{cm}^{-1}$ , indicating the high number of these sites in the material (Figure 6.10 c). The regenerated catalyst presented a different pattern. The peak at 2301  $\text{cm}^{-1}$  was absent, meaning that the residual aluminum was lost during the reaction or the regeneration procedure. At the same time, the new peak at 2290  $\text{cm}^{-1}$  of tin oxide was present at the beginning of the experiment (Figure 6.10 b). The interaction of the probe with the oxide gave information of the strong influence of these new sites on the acidic behavior of the catalyst. The formation of tin sites in a highly-defective coordination is an important pathway toward the loss of activity in regenerated catalysts,<sup>105</sup> but it has not been reported as the main cause of Sn-Beta catalyst deactivation.<sup>109</sup>

## 6.1 FT-IR Experiments of Deuterated Acetonitrile Adsorption

The interaction with framework tin sites was less abundant in the experiment on the regenerated sample than on fresh Sn-Beta. The tin peak around  $2310\text{ cm}^{-1}$  appeared at high pressures and led to scarcely intense bands. In addition, the acetonitrile adsorbed on silanols was also less intense in the regenerated sample compared to fresh Sn-Beta. After desorption, the regenerated catalyst showed the peak at  $2290\text{ cm}^{-1}$ , as the most intense signal remained, meaning that the formed tin oxide was an abundant acidic species in this sample. The active tin in fresh Sn-Beta was incorporated in the framework leading to two signals in the FT-IR spectra when interacting with deuterated acetonitrile, at  $2308\text{ cm}^{-1}$  and  $2316\text{ cm}^{-1}$ . A large amount of this framework tin leached and formed extra-framework oxides, which had different acidic behavior and were catalytically inactive. These results may contribute to explain part of the mechanism of deactivation of the catalyst. However, still it was not possible to determine if the leaching of tin from the framework and the formation of the oxides occurred during reaction or regeneration. In fact, the dark deposit (humins) on the catalyst surface and porosity made the application of spectroscopic techniques directly to the spent materials impossible. A further study on the mechanism of formation of tin oxide in used Sn-Beta could give important information for future process optimization. Small changes in the reaction conditions or in the regeneration treatment could maintain the tin inside the framework and greatly prolong the catalyst lifetime.<sup>109</sup>

Table 6.4. Properties of Sn-Beta catalysts calcined at different temperatures before tin incorporation.

Sample	Sn wt%	Area <sup>a</sup>	Area <sup>b</sup>
		$2308\text{ cm}^{-1}$	$2290\text{ cm}^{-1}$
fresh	1.37	9.9	0.0
Regen. $550\text{ }^{\circ}\text{C}$	1.22	4.3	3.5

<sup>a</sup>Peak integrated in the spectra acquired at pressure of 4 mbar of deuterated acetonitrile

<sup>b</sup>Peak integrated in the spectra acquired at pressure of  $4 \times 10^{-2}$  mbar of deuterated acetonitrile

The integrals and elemental analysis of fresh and regenerated materials are listed in Table 6.4. The catalyst showed loss of tin during the reaction. The integration of the peaks related to the adsorption on silanols at  $2276\text{ cm}^{-1}$  was not completely reliable due to the interference with the intense band of physisorbed acetonitrile at  $2267\text{ cm}^{-1}$ . On the other hand, the area of the peak at  $2310\text{ cm}^{-1}$ , measured at the maximum intensity of 4 mbar of deuterated acetonitrile pressure, decreased after the regeneration treatment. The value of the integral dropped from 9.9 for the fresh catalyst to 4.3 for the sample regenerated at  $550\text{ }^{\circ}\text{C}$ . These results indicated a correlation between the change in coordination of framework tin and the processes of deactivation and regeneration.

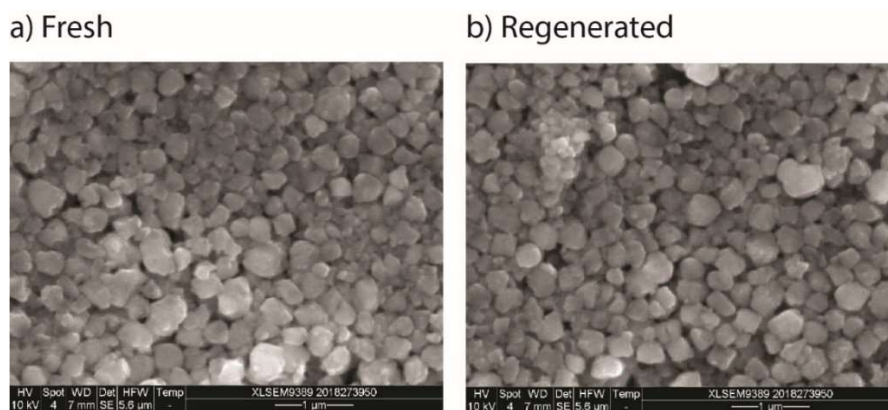


Figure 6.11. SEM images of the Sn-Beta zeolites a) fresh and b) regenerated.

In Figure 6.11, SEM images show unchanged morphology upon regeneration and no extra-framework species were visible on the zeolite surface. The XRD patterns also reported the stability of the crystalline structure. The extra-framework tin species were invisible to the XRD technique, therefore they had amorphous structures or they formed nano-clusters. Despite the results obtained from the SEM and XRD characterization, the FT-IR analysis of adsorbed deuterated acetonitrile clearly showed the changes in the structure of the catalytic material during deactivation and regeneration. Thus, the FT-IR technique represented a powerful method for the characterization of the catalysts and gave information invisible to other commonly used techniques. However, further studies are necessary in order to understand and prevent the mechanism of degradation of the catalyst structure during deactivation and regeneration.

### 6.1.5 Conclusions on the study for the characterization of Sn-Beta zeolites by FT-IR spectroscopy and *in situ* adsorbed deuterated acetonitrile probe molecule

FT-IR spectroscopy is a powerful tool for the characterization of zeolites and deuterated acetonitrile can be used as a probe molecule for studying the Lewis acidity by *in situ* adsorption experiments. The technique was applied for the characterization of Sn-Beta zeolites. From the spectra, qualitative information on the species in the samples and relative quantifications were obtained. The section explored the differences in the final materials for catalysts derived from impregnation of different tin contents. The results indicated that the integrated area for the peak of acetonitrile interacting with the tin in the framework in the spectra recorded after desorption of acetonitrile under vacuum for 20 minutes had a linear correlation with the total acidity of the sample. Thus, the peak could be considered as representative for the acidic behavior of the catalyst. Moreover, the trend indicated that the acidity of the samples derived mainly from the tin incorporated in the framework.

The effect of the calcination step before tin impregnation was investigated. The calcination can close the silanol nests needed for the incorporation of tin in the framework, leading to inactive final materials. Samples prepared from dealuminated zeolites calcined at different temperatures were characterized by adsorption of deuterated acetonitrile. Although the samples presented the same content of tin measured by XRF elemental analysis, the spectra clearly showed different interaction between probe molecule and tin in the framework within the different samples. Samples calcined at higher temperatures, i.e. 650 °C, presented lower intensity for the peak of the acetonitrile interacting with framework tin at 2308  $\text{cm}^{-1}$  compared to samples calcined at lower temperatures, i.e. 350 °C. Results indicated that the calcination of dealuminated Beta zeolites led to the condensation of the silanol nests and avoided the incorporation of active tin in the framework. Finally, FT-IR spectroscopy was applied to study the changes of the structural features of Sn-Beta catalysts over deactivation and regeneration in air at 550 °C. Upon regeneration, the sample showed tin leaching and the intense peak at 2290  $\text{cm}^{-1}$  related to the interaction of acetonitrile with tin oxide appeared. The technique represented a powerful tool for the characterization of the structural modifications in the catalytic material and allowed information undetectable using other techniques.

## 6.2 Characterization of the Interaction between Sn-Beta Catalysts and Alkali Salts

During the last years, the beneficial effect of the presence of alkali salts in the reactions for the conversion of carbohydrates to methyl lactate has been studied.<sup>47</sup> The performance of the catalyst in the production of methyl lactate has increased the yields from 20-25% to 65-70%. The increased activity has been observed for either alkali salts in solutions or for hydrothermal catalysts prepared in the presence of alkali ions.<sup>47</sup> Thus, the use of alkali salts has been shown to be essential for achieving high yields of methyl lactate. Different alkali ions and counter ions have exhibited slightly different effects and the use of potassium carbonate has been identified as the best for producing methyl lactate. For this reason, in this work potassium carbonate was the only salt studied.

The mechanism for the effect of alkali ions on Sn-Beta catalysts is still unclear; the model proposed for Na-exchange Sn-Beta zeolite during the catalysis of epimerization of glucose involves the interaction with the environment of active sites by ion-exchange with a proton in the silanol nests.<sup>82</sup> The change in activity has been first studied at temperatures around 100 °C. Under these conditions, Sn-Beta catalysts usually promote the isomerization of glucose to fructose in both aqueous and alcoholic media *via* 1,2-hydride shift. In the presence of alkali salts, the epimerization into mannose is preferred *via* 1,2-carbon transfer.<sup>81</sup> Thus, the favored catalytic pathways are modified by the presence of alkali. However, a clear model for the interaction of alkali ions with Sn-Beta catalysts is still missing. In this section, a comprehensive study of spectroscopic analysis and reactivity data on the interaction between alkali salts and Sn-Beta catalysts is presented. The study aimed to understand how alkali salts change the active sites in order to extend the knowledge on the best catalytic structures and help the future design of highly active and selective catalytic systems.

### 6.2.1 Ammonia as probe molecule for the characterization of solid acids

Although many studies have been carried out for the analysis of the physical properties of Lewis acidic zeolites,<sup>25</sup> routine methods of characterization are still lacking. Ammonia Temperature-Programmed Desorption (NH<sub>3</sub>-TPD) is a technique commonly applied for quantitative analysis of the acidity in solids.<sup>92</sup> The ease of the procedure and the automation of the technique allowed the use of TPD measurements as routine analytical technique. However, ammonia is not a selective probe and does not allow the distinction between Brønsted and Lewis acid sites. Using different titrants, it is possible to achieve a generally good overview of the acidity of the solid sample.<sup>93</sup> Otherwise, spectroscopic techniques, such as FT-IR, are available for the distinction of the type of acid sites. The use of probe molecules allows insights in the mechanism of interaction between reactants and acid sites as detailed above.<sup>93</sup>

Currently, ammonia is not commonly applied as a probe molecule in FT-IR experiments for the characterization of the acidity of stannosilicate catalysts. However, the availability and the ease of use make ammonia an attractive compound for investigating the acidic properties of solid acid by FT-IR. Ammonia absorbs on both Lewis and Brønsted acid sites and the use of FT-IR spectroscopy as detection method allows to identify the different interactions by monitoring of the vibration of adsorbed NH<sub>3</sub> (Lewis) or NH<sub>4</sub><sup>+</sup> (Brønsted).<sup>216</sup> In Table 6.5, frequencies for the vibrations of NH<sub>3</sub> and NH<sub>4</sub><sup>+</sup> are listed.

Table 6.5. Frequencies of the vibrations of  $\text{NH}_3$  and  $\text{NH}_4^+$ .<sup>216,217</sup>

	Molecular $\text{NH}_3$ Wavenumber ( $\text{cm}^{-1}$ )	$\text{NH}_4^+$ ions Wavenumber ( $\text{cm}^{-1}$ )
$\nu_1$	3290-3340	2890
$\nu_2$	930-960	1690
$\nu_3$	3800	3050
$\nu_4$	1620	1440

For molecular ammonia, the band of the vibration  $\nu_4$  is commonly considered indicative for the presence of Lewis acidic centers. Since it is not dependent on the adsorption environment, it can be found at a fixed wavenumber of  $1620\text{ cm}^{-1}$ .<sup>216</sup> In contrast, the vibration  $\nu_2$  is very sensitive to the coordination environment and the signal in the FT-IR spectra is shifted depending on the electron-acceptor character of the interacting metal. Thus, the shift of the band can give information on the electronegativity of the metal.<sup>218</sup> Wavenumbers around  $1300\text{--}1340\text{ cm}^{-1}$  have been reported for  $\nu_2$  in ammonia adsorbed on aluminum containing zeolites.<sup>217</sup> The bending mode at  $1620\text{ cm}^{-1}$  is overlapped with the water vibration in the same spectral region.<sup>217</sup> Regarding the ammonium ion, the peak at  $1440\text{ cm}^{-1}$  can be shifted up to  $1490\text{ cm}^{-1}$  due to the solvation with other ammonia molecules at high pressures. Moreover, in the spectra of adsorbed ammonia, it is often possible to observe bands at  $3740\text{ cm}^{-1}$  and between  $3520$  and  $3430\text{ cm}^{-1}$ . The former signal is formed by the shift of the silanols peak around  $3050\text{ cm}^{-1}$  when interacting *via* hydrogen-bonds with the ammonia. The latter signal between  $3520$  and  $3430\text{ cm}^{-1}$  is indicative of the consumption of Al-OH groups on the surface of the material and the formation of Al-NH<sub>2</sub> during the heating treatment of the experiment.<sup>217</sup>

In the current work, the possibility to use ammonia as a probe molecule for *in situ* adsorption during FT-IR experiments for the characterization of Lewis acidic zeolites was explored because of the ease of use, availability and direct correlation with the TPD as quantitative reference. The experiments of adsorption of ammonia were carried out using an *in situ* FT-IR cell (Chapter 2.1.3). The comparison with results obtained by adsorption of deuterated acetonitrile was performed. The experiments of ammonia TPD involved a first pretreatment of the sample under inert atmosphere at  $500\text{ }^\circ\text{C}$  to complete dehydration, followed by saturation with gaseous ammonia. The step of adsorption was carried out at  $150\text{ }^\circ\text{C}$  in order to avoid the interference of physisorbed ammonia. Desorption of chemisorbed ammonia occurred in inert gas flow under programmed increase of the temperature and it was measured as a change in the thermal conductivity of the flow by a Thermal Conductivity Detector (TCD). The detected signal gave indications of the amount of acid sites in the sample, but it also indicated the acid strength, since stronger sites desorbed ammonia at higher temperatures.<sup>92</sup> In order to correlate qualitative information on the type of desorbing sites with the quantitative information of TPD, the steps of the TPD analysis were reproduced using FT-IR spectroscopy as the detection method.

### 6.2.2 Ammonia as a probe molecule for studying the acidity of Sn-Beta modified by alkali ions

Samples containing different concentrations of alkali salts were prepared with the post-synthetic procedure for Sn-Beta zeolites (Si/Sn nominal ratio of 150), using aqueous solutions of  $\text{SnCl}_4$  and  $\text{K}_2\text{CO}_3$  during the impregnation of the dealuminated zeolites. Moreover, hydrothermal Sn-Beta zeolites (Si/Sn nominal ratio of 150) were impregnated after calcination with aqueous solutions at different concentrations of potassium carbonate. The materials were studied in their activity and acidic properties. The characterization by FT-IR spectroscopy aimed at discovering the structural features modified by the presence of alkali ions in the catalyst. The effect of potassium carbonate on the conversion of glucose into methyl lactate was analogous for catalysts

## 6.2 Characterization of the Interaction between Sn-Beta and Alkali Salts

containing alkali ions or using alkali salts in solution in the reaction mixture, as already reported in literature.<sup>47</sup> The presence of potassium carbonate in the conversion of glucose catalyzed by Sn-Beta zeolites resulted in increased yields of methyl lactate and suppressed formation of products derived from the dehydration of sugars (furanics) and glycosides. The selectivity into methyl lactate increased by increasing the amount of potassium in the sample to an optimum amount. Increasing the concentration beyond the optimum led to a drop in methyl lactate yields (Figure 6.12). The specific amount of potassium needed for the optimum was different for each synthesized sample. Generally, hydrothermal Sn-Beta zeolites needed lower concentrations of potassium carbonate for reaching the optimum yields of methyl lactate compared to post-treated catalysts.

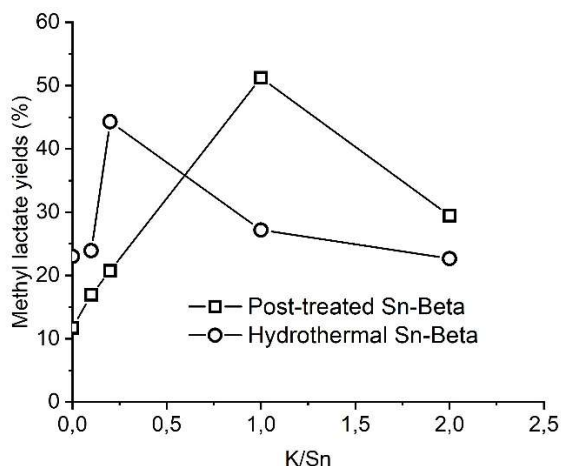


Figure 6.12. Change in the yields of methyl lactate using Sn-Beta (150) catalysts impregnated with solutions containing different concentrations of  $K_2CO_3$ . Reaction conditions: glucose 120 mg, catalyst 50 mg, 5 mL methanol, 80  $\mu$ L DMSO as internal standard, 160  $^{\circ}C$ , 2 hours.

The considered catalysts gave different  $NH_3$ -TPD profiles. In general, post-treated samples had higher acidity values compared to the hydrothermal materials. Probably, this effect was due to the presence of numerous defects in the post-synthetic materials leading to the formation of weakly acidic hydroxy groups. In both cases, the addition of potassium decreased the value of the total acidity of the samples. The effect could be explained by the interaction of potassium with a silanol group by ion-exchange with the weakly acidic proton. This mechanism could also explain the need of higher amounts of potassium carbonate for post-treated Sn-Beta for reaching the optimum compared to hydrothermal catalysts. The acidity decreased up to a characteristic value of K/Sn and subsequently remained unchanged for the further increase of K/Sn.

Table 6.6. Acidic properties of post-treated and hydrothermal Sn-Beta zeolites measured by  $NH_3$ -TPD.

Post-treated Sn-Beta K/Sn	Area desorption peak at 185 $^{\circ}C$	Area desorption peak at 250 $^{\circ}C$	Total acidity ( $\mu$ mol/g)
0	3.97	5.37	128
0.2	3.46	3.75	75
1	6.22	1.17	77
2	5.56	1.30	73
Hydrothermal Sn-Beta K/Sn	Area desorption peak at 157 $^{\circ}C$	Area desorption peak at 202 $^{\circ}C$	Total acidity ( $\mu$ mol/g)
0	1.38	3.17	67
0.2	1.57	2.33	45
1	1.80	0.46	22
2	1.93	0	22

It is possible that the salt acted as a base for the neutralization of the weak residual Brønsted acidity, suppressing competitive reaction pathways catalyzed by Brønsted acidity and leaving the substrate available to form the desired product. The TPD profiles gave precise information on the decrease of the acidity in materials modified by impregnation with alkali salts. The curve of the desorption of ammonia presented the combination of two or more peaks with maximum intensity around 190 and 250 °C in the case of post-treated samples and 160 and 210 °C for hydrothermal materials. The peaks were deconvoluted and the obtained area was compared (Table 6.6). While the area of the peak centered at 190 °C was almost stable for all samples, the desorption at 250 °C decreased during increasing of the amount of potassium in the sample. The samples containing the amount of potassium carbonate corresponding to the maximum production of methyl lactate presented the smallest area of the second desorption peak centered at 250 °C. The further increase of the content of potassium carbonate did not lead to an additional decrease of the peak. Thus, the results suggested that the ammonia interacted with at least two different types of acidic sites of the catalyst and only the strongest acidic sites seemed affected by the presence of alkali ions. However, qualitative information on the type of sites required the correlation with other characterization techniques.

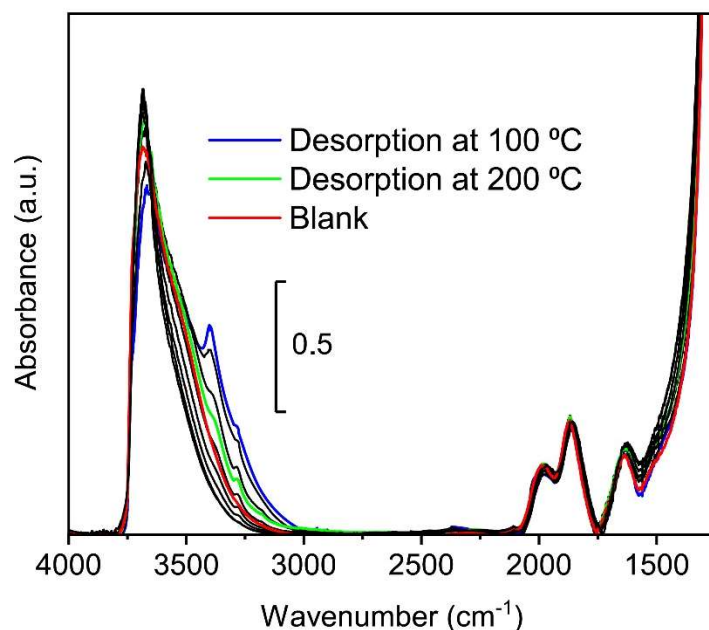


Figure 6.13. FT-IR spectra of Sn-Beta zeolite recorded during ammonia desorption between 100 °C and 400 °C. Analysis condition: 15 mg PT Sn-Beta (200) pellet, temperature ramp to 450 °C, sample drying at 500 °C for 1 h,  $\text{NH}_3$  absorption at 100 °C for 1 h, removal of physisorbed  $\text{NH}_3$  in He at 100 °C for 1 h, temperature ramp in He from 100 °C to 450 °C and spectra acquisition each 50 °C.

Experiments of  $\text{NH}_3$ -TPD were correlated with FT-IR analysis of *in situ* desorption of ammonia. The aim of the study was to correlate the same TPD experiment to a different analytical method of detection. FT-IR spectroscopy was able to distinguish ammonia interacting with different types of sites and gave qualitative information about the tin active sites. A typical experiment of *in situ* desorption of ammonia is presented in Figure 6.13. Spectra were collected at different temperatures and the desorption of ammonia at increased temperatures was followed *in situ*. In order to study the ammonia vibrations in detail, the subtraction of the blank spectra recorded at each temperature was needed to remove the overlap from the intense bands of the zeolitic framework. The corrected spectra showed that the ammonia interacts with different acidic sites (Figure 6.14). Unfortunately, for low intensity bands (Figure 6.14 b), the interference of gaseous water was visible due to the humidity between the windows of the reactor when using high temperatures.



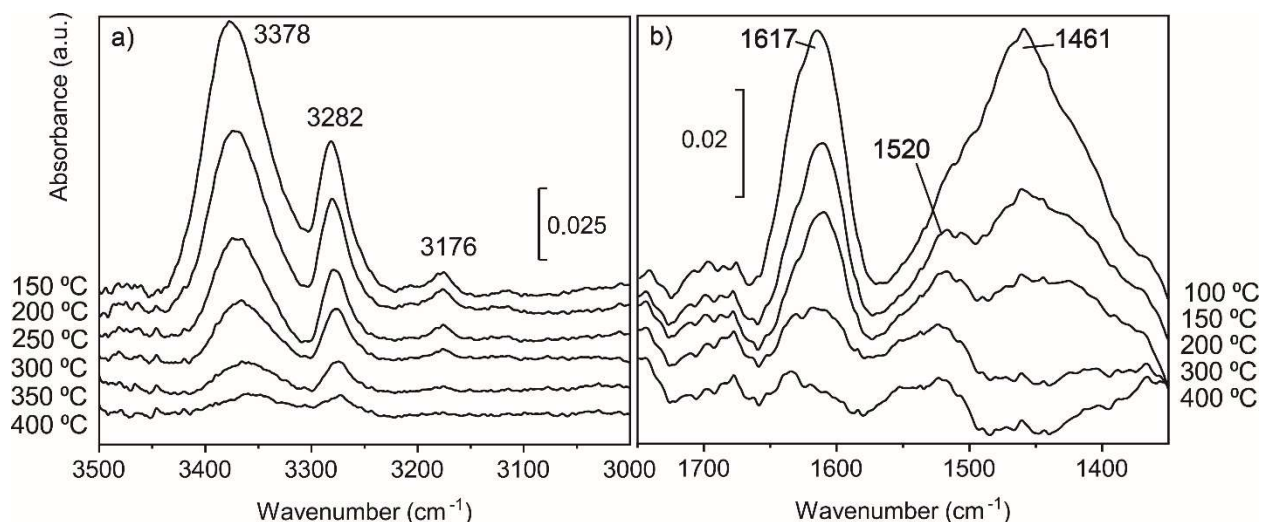


Figure 6.14. FT-IR spectra of ammonia adsorbed on Sn-Beta zeolite recorded during desorption between 100 °C and 400 °C. Subtraction of the blank (Sn-Beta zeolite FT-IR spectra) from the experiments of desorption.

Figure 6.14 b shows the bands of ammonia adsorbed on Sn-Beta zeolite between 1350 and 1750  $\text{cm}^{-1}$ . In the current case, the interferences with the small bands due to the presence of vapor and the vicinity of the subtracted vibrations of the zeolitic framework made the interpretation difficult. The peak at 1617  $\text{cm}^{-1}$  was related to the presence of molecular ammonia interacting with a Lewis acid site. The interaction was persistent up to 300 °C meaning the strong adsorption of the probe on the site. The peak at 1461  $\text{cm}^{-1}$  indicated the adsorption of ammonia on a Brønsted acid site. However, the band was barely visible for temperatures higher than 200 °C, indicating the weakness of the interaction. The signal at 1520  $\text{cm}^{-1}$  was related to the presence of gaseous water outside the reactor since the signal was constant in all spectra. Thus, Sn-Beta zeolites contained both Lewis and Brønsted acidity. However, the Lewis acidity was dominant and the Brønsted acidity assumed a weak character.

Considering the subtracted spectra at high frequencies, between 3500 and 3000  $\text{cm}^{-1}$ , three peaks of adsorbed ammonia were visible, at 3378, 3282 and 3176  $\text{cm}^{-1}$  (Figure 6.13 a). Comparing them with the values reported in literature,<sup>216</sup> all the three were connected to ammonia adsorbed on Lewis acidic sites. The peaks at 3378 and 3282  $\text{cm}^{-1}$  were both connected to the interaction with Lewis tin sites, but their behavior in desorbing ammonia was different. In fact, the peak at 3378  $\text{cm}^{-1}$  lost 80% of its area at 300 °C, while the peak at 3282  $\text{cm}^{-1}$  was more persistent and lost only the 65% of the integrated area at the same temperature. Different behavior in the interaction with ammonia could be caused by the different coordination of the tin or the different environment in the zeolite framework.<sup>69</sup> Since the maximum of the desorption of the peak at 3282  $\text{cm}^{-1}$  was more persistent compared to the other signal, it was correlated to the second desorption peak in the TPD experiment centered at 250 °C.

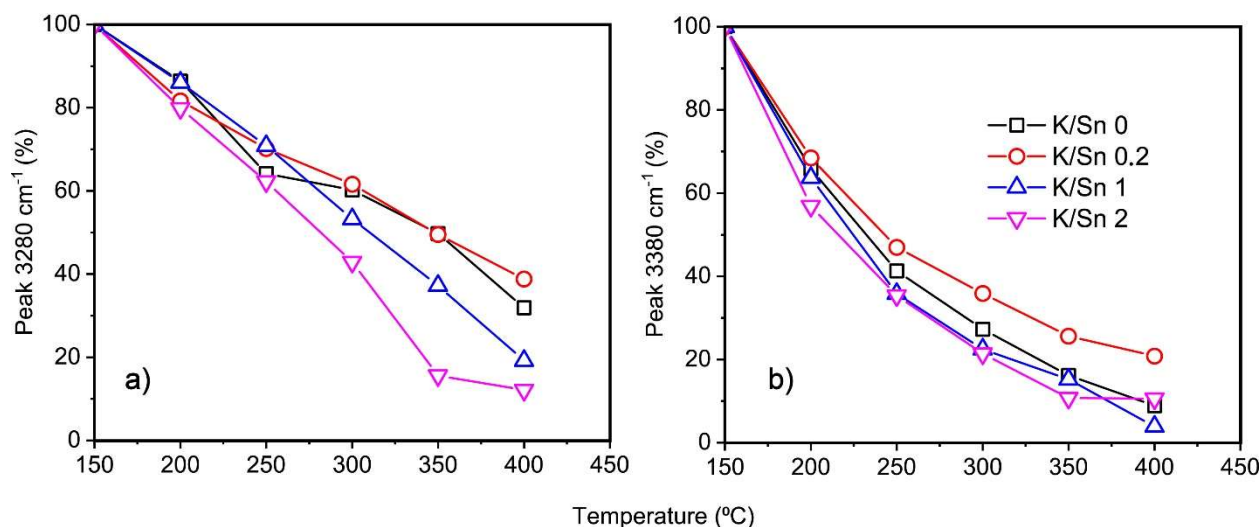


Figure 6.15. Percentage decrease of the ammonia peaks during desorption between 150 °C and 400 °C from samples containing different amounts of alkali.

Figure 6.15 indicates the decrease in the area of the ammonia peaks at  $3282\text{ cm}^{-1}$  (Figure 6.15 a) and at  $3378\text{ cm}^{-1}$  (Figure 6.15 b). Desorption of ammonia from the two sites followed different patterns. The ammonia on the site with signal at  $3282\text{ cm}^{-1}$  was desorbed following a linear trend over increased temperature. On the other hand, the curve connected to the desorption from the site at  $3378\text{ cm}^{-1}$  resembled an exponential decay. The latter peak was not found at high temperature and it could represent the TPD peak not affected by the presence of potassium. Thus, the characterization showed the presence of two Lewis acidic sites with different acidic behavior. Clear proof for the structural role of alkali ions could not be obtained from the data of the desorption from samples containing different amounts of potassium carbonate. Using FT-IR as detection method, qualitative information on the type of site (Lewis and Brønsted) were correlated with the quantitative information obtained by TPD. However, the interaction of alkali salts with the catalyst remained unclear and the use of different probe molecules was necessary for a realistic interpretation of the modifications of the acidity in Sn-Beta catalysts by alkali ions.

### 6.2.3 Deuterated acetonitrile as a probe molecule for studying the acidity of Sn-Beta zeolites modified by alkali ions

Deuterated acetonitrile was used as the probe molecule in order to study the change of the acidity in samples containing alkali ions by FT-IR spectroscopy. The use of acetonitrile for studying the acidity in Sn-Beta catalysts is discussed in detail in Chapter 6.1. As simplification, this paragraph only considered post-treated Sn-Beta zeolites. Samples containing different amounts of potassium carbonate were prepared using concentration above and equal to the optimum amount of potassium carbonate (3.0 and 0.4 mM) for the production of methyl lactate starting from glucose. Optimal yields refer to the experiments of titration by potassium carbonated discussed in Chapter 6.2.4. The effect of the presence of different amounts of alkali salts in the reaction mixtures was examined by experiments of FT-IR *in situ* adsorption of deuterated acetonitrile. Samples of the already prepared post-treated catalyst containing a Si/Sn ratio of 100 were stirred at room temperature for three hours in aqueous solution of potassium carbonate at different concentrations.

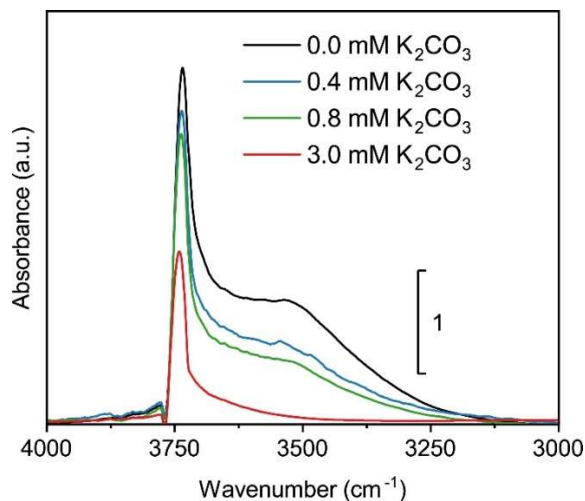


Figure 6.16. FT-IR spectra of Sn-Beta zeolites containing different amounts of  $K_2CO_3$  in the spectral region of the O-H stretching.

Samples containing different amounts of potassium presented different features in the spectral region of the O-H stretching. The large band connected to the vibrations of silanols decreased with increasing concentration of potassium carbonate for both the sharp peak at  $3752\text{ cm}^{-1}$  connected to the terminal silanols and the broad band of the internal silanol nests (Figure 6.16). Potassium could interacted with the silanol group by ion-exchange with the proton.<sup>82</sup> Thus, the O-H signal decreased, resulting in a low intensity band around  $3500\text{ cm}^{-1}$ . The experiments of adsorption of deuterated acetonitrile and the values for the integrated area of the peak at  $2310\text{ cm}^{-1}$  connected to the acetonitrile interacting with the tin in the framework are shown in Figure 6.17 and Table 6.7. Increasing the concentration of potassium carbonate less molecules of acetonitrile interacted with the tin and the intensity of the signal decreased. Thus, when increasing the concentration of potassium carbonate from  $0.0\text{ mM}$  to  $3.0\text{ mM}$ , the area of the peak was reduced from 15 to 6.

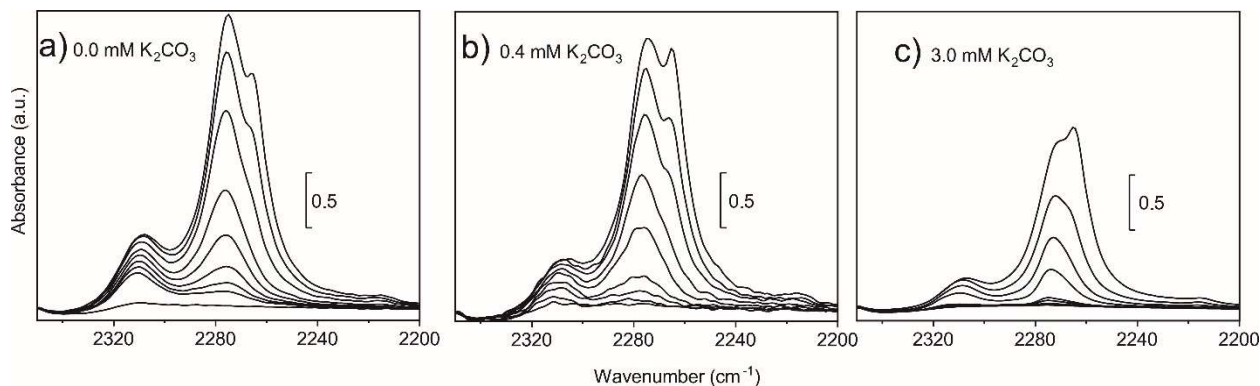


Figure 6.17. FT-IR experiments of *in situ* adsorption of deuterated acetonitrile on samples impregnated with different concentrations of  $K_2CO_3$ , a)  $0.0\text{ mM}$ , b)  $0.4\text{ mM}$  and c)  $3.0\text{ mM}$ . the table reports the integrated area of the peak at  $2308\text{--}2316\text{ cm}^{-1}$  related to vibrations of deuterated acetonitrile interacting with tin in the zeolite framework for samples containing different amounts of  $K_2CO_3$ .

Table 6.7. Integrated area of the peak at  $2308\text{--}2316\text{ cm}^{-1}$  related to the interaction of deuterated acetonitrile with tin in the zeolitic framework.

Sample (mM $K_2CO_3$ )	0	0.2	0.4	0.8	3
Area peak $2310\text{ cm}^{-1}$	15	11	11	10	6

Results indicated the possibility that potassium exchanged with a proton of a silanol group of the zeolite, but it also affected the tin in the framework and the acidity of the final material. Exchange of potassium with a proton of a stannanol group was also possible but not visible in the experiments due to the interference with the intense silanols bands.<sup>87</sup> Minor amount of probe molecule was able to interact with the tin site in samples modified by potassium carbonate. Small amounts of alkali salts were able to increase the activity of the catalyst in the production of methyl lactate, but an excess led to deactivation.<sup>168</sup> Thus, the sample treated with a solution of 3.0 mM of  $K_2CO_3$  yielded a low intensity peak at  $2310\text{ cm}^{-1}$ . The experiments of adsorption of deuterated acetonitrile gave relevant information on the acidic behavior of Sn-Beta zeolites modified by alkali ions. In fact, the presence of potassium carbonated affected the interaction between the probe and both silanols and framework tin sites.

#### 6.2.4 Titration of Sn-Beta active sites by potassium carbonate

All the results on the characterization of Sn-Beta zeolites modified by the presence of alkali suggested that the interaction with potassium carbonate occurred by titration of the hydroxy groups near tin Lewis acid sites. The presence of alkali ions affected the acidity of framework tin and a quantitative effect correlated with the amount of tin in the sample could be expected. Therefore, the study proceeded with the analysis of the stoichiometric effect of alkali salts in samples containing different amounts of tin.<sup>6</sup> Catalysts with different Si/Sn nominal ratios were tested for the conversion of glucose into methyl lactate in the presence of different concentration of potassium carbonate. Each catalyst presented the highest yield of methyl lactate at full conversion (four hours) at a different concentration of potassium carbonate. As previously reported in the literature,<sup>168</sup> the use of basic counter ions resulted in the deactivation of the material for an excess of alkali salts. As in the case of catalysts impregnated with alkali salts, the presence of potassium had the general effect of avoiding the formation of furanic byproducts and methyl glycosides. Thus, yields for all the catalysts increased by increasing the concentrations of potassium carbonate up to an optimum. Increasing the concentration further above the optimum, yields of methyl lactate dropped. The optimum amount of potassium carbonate needed for the highest yield of methyl lactate was different for each catalyst, indicating the stoichiometric correlation between content of tin and alkali ions (Figure 6.18).

The suggested stoichiometric binding of the potassium to the active site was confirmed after normalization of the potassium carbonate concentration for the acidity of each catalyst experimentally measured by  $NH_3$ -TPD (Figure 6.18). After normalization, all the catalysts containing different amount of tin followed the same trend and the optimal concentrations of potassium carbonate were identical for all the catalysts. All the catalysts with Si/Sn ratios between 25 and 400 presented the highest yields of methyl lactate in a range of concentrations of potassium carbonate corresponding to values of  $K/NH_3$  between 0.6 and 1. Some deviations for the Si/Sn ratio of 400 were observed because of the nonlinear response of the TPD instrument in the case of minor acidity. Deviations were also observed in the case of Si/Sn ratio of 25 due to the presence of tin not incorporated in the zeolite framework, but present as inactive tin oxide species.

<sup>6</sup> The study of this paragraph was carried out in collaboration with Ph.D. Samuel G. Elliot (DTU).

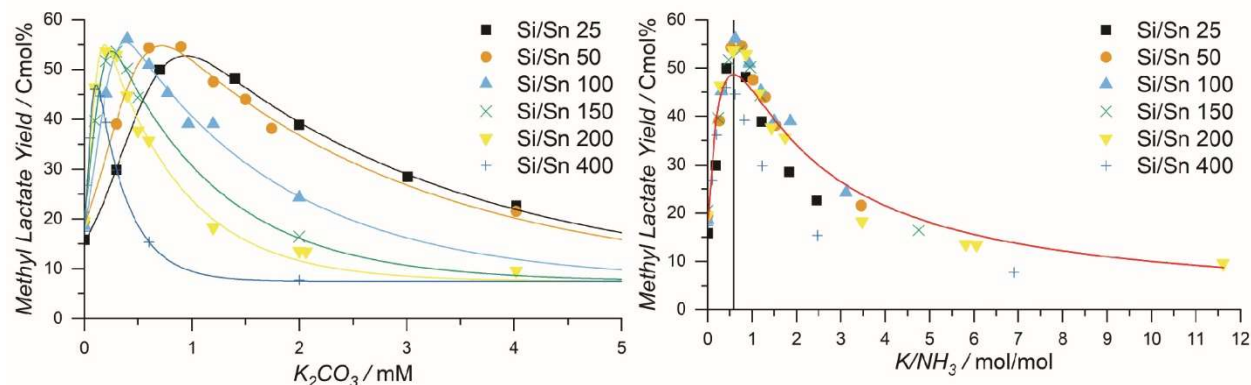


Figure 6.18. Production of methyl lactate from glucose using Sn-Beta catalysts with different amounts of tin at different concentrations of added potassium carbonate (left), and normalization by the acidity of the catalysts measured by  $NH_3$ -TPD analysis (right). Reaction condition: 360 mg glucose, 90 mg catalyst, 55 mg DMSO as internal standard, 5 mL solution of potassium carbonate in methanol, 160 °C, 4 hours.

$NH_3$ -TPD experiments can be used as a quantitative analytical tool for predicting the amount of alkali salts in solution required for maximizing the formation of methyl lactate from glucose. In the current case, all the samples had the optimum value of normalized potassium content between 0.6 and 1  $K/NH_3$ . However, absolute values were dependent on the specific characteristic of the zeolite material and only samples with the same features could be compared. In this case, all the catalysts were prepared from the same batch of dealuminated Beta zeolite in order to eliminate deviations due to different residual aluminum contents.

Starting from the assumption that in polar solvent the incorporated tin assumes preferentially an “open” configuration,<sup>80</sup> FT-IR analysis showed that the modification of the OH in silanol groups upon alkali addition affected the tin acidity. Thus, the hydroxy groups adjacent to the tin sites had central roles. In the absence of alkali ions, the fully protonated form of the site (stage A in Figure 6.19) had a weakly Brønsted acidic behavior and promoted the dehydration of sugars as a competitive reaction to the formation of methyl lactate. The furanic byproducts were formed in the reaction mixture. In the case of excess alkali salts, the double titration of the site occurred and the absence of the synergistic effect of hydroxyls adjacent to the tin<sup>81</sup> (stage C) led to deactivation of the site. Reactions in the presence of excessive concentration of alkali salts resulted in high formation of undetectable byproducts (humins). The intermediate situation (B), corresponding to the single titration of the site, represented the optimal configuration for the production of methyl lactate starting from glucose.

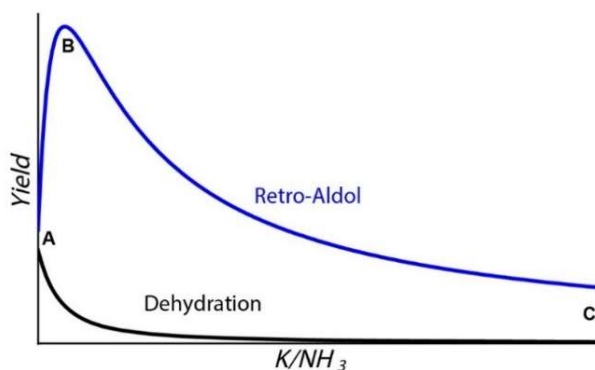


Figure 6.19. The three stages of the active sites in Sn-Beta catalysts titrated with alkali and the preferred catalytic pathways.

### 6.2.5 Conclusions on the study for the characterization of the interaction between Sn-Beta zeolites and alkali salts

In this section, the mechanism for the interaction of alkali salts with Sn-Beta zeolites was investigated by different characterization techniques correlated to the activity in the production of methyl lactate from glucose. The use of ammonia as a probe molecule for studying the acidity in Lewis acidic zeolites was optimized and presented.  $\text{NH}_3$ -TPD was applied for the quantification of the acidity of the catalyst. In addition, ammonia was also used as a probe molecule for studying the acidity by FT-IR spectroscopy, indicating the presence of two Lewis acidic sites in the material. The two sites had different acidic behavior and were affected differently by alkali salts. More detailed qualitative information was obtained by the use of acetonitrile as the probe molecule for *in situ* FT-IR analysis. In the presence of potassium, the broad silanol band decreased, indicating the possibility of the interaction of potassium by ion-exchange with silanol protons. At the same time, increasing the amount of potassium carbonate the peak of acetonitrile interacting with framework tin decreased. When the concentration of alkali is excessive the exchange in proximity of tin sites limited the interaction of reactants with the active sites. The results from the characterization were correlated to experiments on the titration of the active sites. The amount of potassium carbonate required for achieving maximum yields of methyl lactate had a linear correlation with the amount of tin and the acidity measured by  $\text{NH}_3$ -TPD. The stoichiometric interaction between alkali and tin active sites was proposed. The tin interacting with alkali ions showed three stages with different activity, consistent with a double titration of the hydroxy groups in the octahedral coordination of an open site.

## 6.3 Conversion of Carbohydrates Using Sn-Beta Catalysts in the Presence of Additional Metals

The presence of alkali salts during the conversion of hexoses was able to increase drastically the production of methyl lactate.<sup>47</sup> Alkali ions interact with the active sites in the catalyst and modify the activity. The possibility of the interaction between Sn-Beta catalyst and other external species during the conversion of hexoses was investigated. In a preliminary screening, different homogeneous additives were tested in the reaction. The work focused on the use of additional metals in order to introduce co-catalysts or modifiers of the catalyst. Zinc was studied for the potential catalytic activity in the conversion of glucose to methyl lactate.<sup>219</sup> Moreover, zinc has a central role in biological aldol transformations in nature, forming the active site in class II fructose-bisphosphate aldolase enzymes.<sup>220</sup> Beyond the use of homogeneous additives, the study proceeded with the investigation of the possibility to incorporate additional metals in the catalyst framework and create bifunctional heterogeneous Sn-M-Beta catalysts. In this section, the results of the use of homogeneous metal additives and their incorporation into the zeolitic framework are discussed.

### 6.3.1 Modification of Sn-Beta catalysts with metals

The positive effect of the presence of alkali salts in the reaction for the production of methyl lactate has been confirmed for both homogeneous and heterogeneous introduction of the alkali salts.<sup>47</sup> Among all the salts, potassium carbonate has shown the most effective interaction with the catalyst. Since the use of homogeneous additives is not attractive for industrial production, the possibility to incorporate potassium in the framework during the synthesis has been studied. However, the interaction of alkali ions with the zeolite is labile and the catalysts showed a rapid leaching of the additional metals.<sup>47</sup> Moreover, several studies have been presented about the introduction of different additional metals into a Sn-Beta framework, in order to introduce bifunctionality and new types of catalytic activity. The incorporation of lead<sup>221</sup> and zinc<sup>222</sup> has been proposed for increasing the yields of methyl lactate from glucose. Different hypotheses have been proposed as explanations for the increased activity, for instance the role of a second promoter of the reaction from lead<sup>221</sup> and the introduction of zinc as a basic site.<sup>222</sup> In this work, bifunctional catalysts were also prepared and their activity in the reaction for the conversion of glucose into methyl lactate was explored. In particular, the possibility to use a catalytic system containing both acid and basic sites was investigated. Zinc was largely investigated for the potential to introduce both Lewis acidity and basic sites.<sup>222</sup> Analogously, the incorporation of manganese into the framework was studied. In addition, basicity could be introduced by incorporation of calcium<sup>223</sup> or magnesium.<sup>224</sup>

### 6.3.2 Homogeneous additives during the conversion of glucose to methyl lactate

Since the presence of alkali salts in the reaction mixtures had a great impact on the production of methyl lactate, the possibility of using additives able to interact with the catalyst and thus to modify the catalytic properties was explored. A preliminary screening of salts as homogeneous additives for the conversion of glucose into methyl lactate was carried out. In general, many metal salts had a positive effect on the production of methyl lactate using post-treated Sn-Beta catalysts. Using hydrothermal Sn-Beta zeolites, however, the impact decreased and final yields of methyl lactate were similar to the reaction without additives. Therefore, the project focused on the study of post-treated Sn-Beta zeolites.



The general effect of salts in solution seemed comparable to the effect of alkali ions, deriving from the ion-exchange with the weak Brønsted acidic hydroxyl protons. The formation of furanic compounds and byproducts derived by Brønsted acidic competitive pathways was suppressed and more substrate was available for the formation of methyl lactate. Thus, yields of the final product were generally enhanced. Here, the salts with the best reaction performances are discussed. Metal chlorides were initially chosen due to their large availability. The effect of different counter ions was considered only for specific compounds. Finally, results were compared with the yields of methyl lactate obtained without additives and in the presence of potassium carbonate as a reference for the traditional effect of alkali salts. Figure 6.20 presents the cases of most significantly increased methyl lactate yields, specifically potassium carbonate, zinc acetate and manganese chloride in solution compared to the reaction containing Sn-Beta without additives.

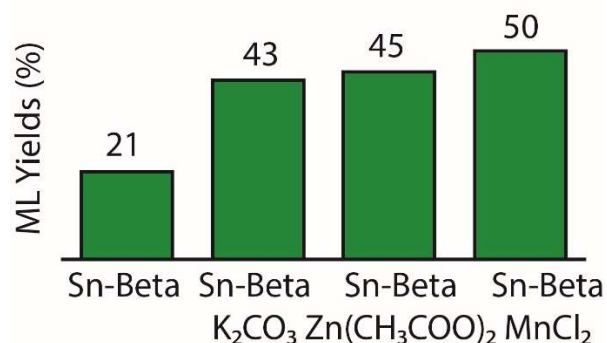


Figure 6.20. Yields of methyl lactate using catalytic systems containing only Sn-Beta and Sn-Beta together with additive salts, potassium carbonate, zinc acetate and manganese chloride. Reaction conditions: Glucose 120 mg, catalyst 50 mg, 5 mL methanol, M/Sn = 1 (M=  $K^+$ ,  $Zn^{2+}$ ,  $Mn^{2+}$ ), DMSO 80  $\mu$ L as internal standard, 160  $^{\circ}C$ , 2 hours.

The addition of the salts in Figure 6.20 had a positive impact on the production of methyl lactate and the yields increased from 21% to 43-50%. The use of divalent manganese in solution was not considered further because the paramagnetic character of the metal interfered with NMR analysis. Zinc has Lewis acidic properties and is part of the active sites in aldolase enzymes.<sup>220</sup> However, divalent zinc showed different behavior in function of the counter ion of the salts. In the blank reactions using the additive salts in a solution of glucose in methanol without catalyst, zinc acetate showed the ability to promote the Lewis acidic-catalyzed pathways and 7% of methyl lactate was found after two hours at 160  $^{\circ}C$  together with unconverted sugars. On the other hand, zinc chloride was not active by itself and only unconverted sugars were present in the final mixture. The ability of Zn (II) to convert sugars into alkyl lactates was already reported for zinc chloride at 200  $^{\circ}C$ .<sup>219</sup> Results indicated that the presence of different counter ions had different effect on the activity and the process was already promoted at 160  $^{\circ}C$  with zinc acetate. Using the zinc salts as additives in the reaction containing Sn-Beta, the formation of methyl lactate and furanic compounds was changed, as shown in Figure 6.21.



### 6.3 Conversion of Carbohydrates Using Sn-Beta Catalyst and Additives

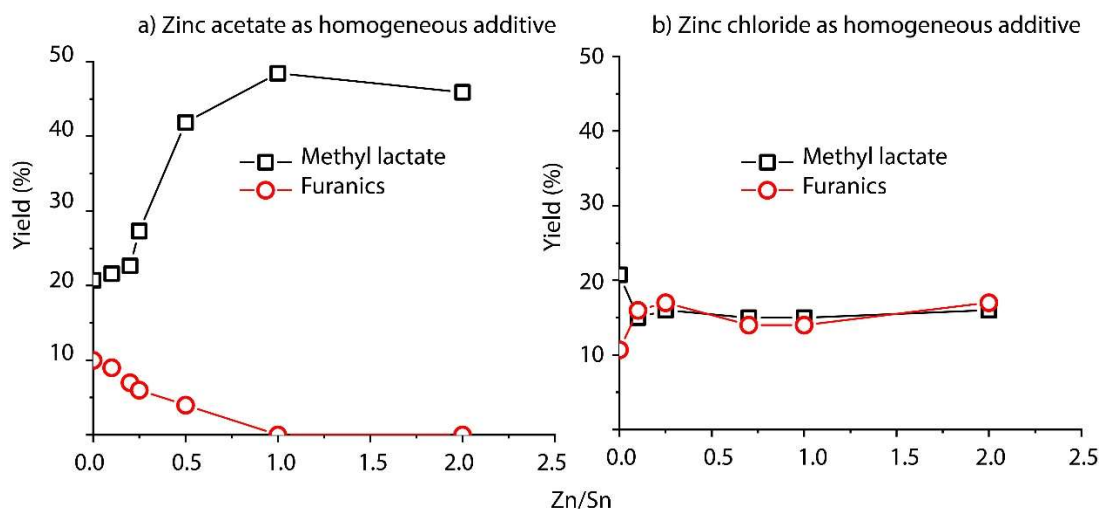


Figure 6.21. Formation of methyl lactate and furanic compound using different concentration of a) zinc acetate and b) zinc chloride. Concentrations are reported as ratio between metals, Zn/Sn. Reaction conditions: Glucose 120 mg, catalyst 50 mg, 5 mL methanol, DMSO 80  $\mu$ L as internal standard, 160  $^{\circ}$ C, 2 hours.

The use of zinc acetate improved the production of methyl lactate and decreased the formation of furanics, eliminating the competition of dehydration pathways catalyzed by residual Brønsted acidity (Figure 6.21 a). As seen for the use of potassium carbonate, the yields of methyl lactate increased for high concentrations of the salts up to an optimum (Zn/Sn 1). Increasing the concentration further, the yields of methyl lactate decreased. In contrast to zinc acetate, the use of zinc chloride did not affect the reaction greatly and the yields of methyl lactate remained similar for the additions of different concentrations of the salt (Figure 6.21 b). The trend for the formation of methyl lactate in the presence of zinc chloride seemed to indicate the absence of a co-catalysis and the need of high temperature for the activation of the salt.<sup>219</sup> In this case, the metal did not show the activity for a co-catalysis nor a positive interaction with the Sn-Beta catalyst.

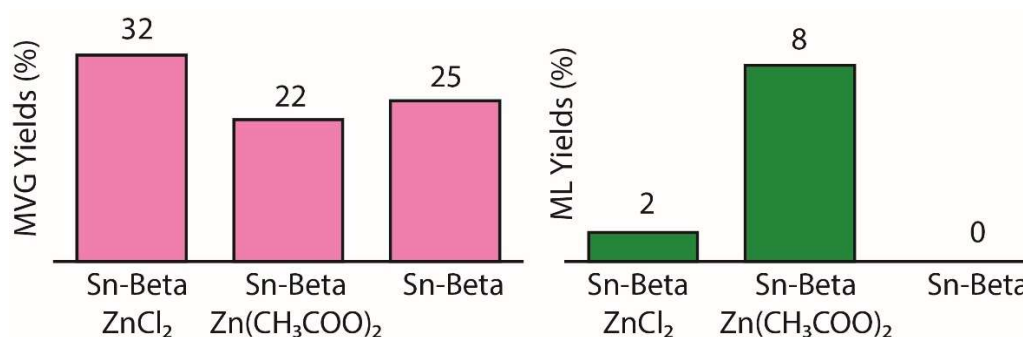


Figure 6.22. Formation of MVG and ML from glycolaldehyde using only Sn-Beta catalyst and Sn-Beta in the presence of zinc salts. Reaction conditions: glycolaldehyde 120 mg, catalysts 50 mg, methanol 5 mL, DMSO 80  $\mu$ L as internal standard, Zn/Sn ratio of 1, 160  $^{\circ}$ C, 2 hours.

The effect of homogeneous salts in the reactions catalyzed by Sn-Beta zeolite was explored also for the conversion of glycolaldehyde into methyl vinyl glycolate (MVG). In general, yields of MVG at full conversion were not greatly increased using alkali salts, but the presence of the salts increased methyl lactate yields also in this case. The effect of potassium carbonate on the conversion of glycolaldehyde is discussed in detail in Chapter 4.1.5. Figure 6.22 shows the yields of MVG during the conversion of glycolaldehyde using zinc salts as additives. The activity of the catalyst did not undergo drastic changes. However, some differences were still

present. In this case, zinc acetate did not affected drastically the reaction, but zinc chloride improved the production of MVG. The poor yields of MVG in the reaction containing zinc acetate needed to be explained as analogous to the effect of potassium carbonate. In fact, increased formation of methyl lactate was observed in this case. On the other hand, zinc chloride was not active for promoting the formation of methyl lactate and the available substrate entered the pathway leading to MVG.

### 6.3.3 Sn-M-Beta catalysts for the conversion of sugars

The interaction of salts with Sn-Beta catalysts was further studied and different metals were attempted to be incorporated into heterogeneous catalytic systems. This paragraph includes the study for the preparation of bifunctional Sn-M-Beta catalysts for the conversion of glucose into methyl lactate.<sup>7</sup> All samples were prepared from the same batch of dealuminated Beta zeolite in order to eliminate structural variability in the starting materials. Thus, residual aluminum and Brønsted acidity were fixed for all the compared systems. Manganese, potassium, zinc, calcium and magnesium were used for the preparation of catalysts containing different metals. The preparation followed the procedure of the incipient wetness impregnation for obtaining Si/M final ratios of 200.

M-Beta samples were first prepared without the insertion of tin. However, the absence of tin led to inactive materials for the conversion of carbohydrates, indicating the need of tin as active site. Therefore, Sn-M-Beta zeolites were prepared using M/Sn ratio of 1 and tested as catalysts for the conversion of glucose into methyl lactate. Structural properties were not modified by the insertion of different metals and the characteristic of BET surface area and XRD were the same for Sn-Beta and Sn-M-Beta zeolites. As seen for samples modified by impregnation with potassium carbonate, the modification decreased the acidity measured by NH<sub>3</sub>-TPD compared to original Sn-Beta zeolite. The sample Sn-K-Beta presented the lowest acidity of 22 μmol/g compared to the value of 128 μmol/g for the parent Sn-Beta (Table 6.8).

Table 6.8. Acidity of Sn-M-Beta catalysts measured by NH<sub>3</sub>-TPD analysis.

Catalyst	Acidity (μmol NH <sub>3</sub> /g)
Sn-Beta	128
Sn-Mn-Beta	71
Sn-K-Beta	22
Sn-Zn-Beta	74
Sn-Ca-Beta	61
Sn-Mg-Beta	69

In order to investigate the catalytic behavior of the incorporated metals, samples were characterized also by CO<sub>2</sub>-TPD. The experiment was analogous to the NH<sub>3</sub>-TPD analysis, but carbon dioxide was adsorbed instead of ammonia on the material surface in order to detect basic sites. Two or more desorption peaks were present in the CO<sub>2</sub>-TPD profiles of Sn-M-Beta zeolites, but the integrated areas of the peaks corresponded to extremely low values and it was not possible to correlate the results to basic properties of the materials. The catalytic systems were tested in methanol using glucose as the substrate at 100 °C and 160 °C. Using low temperatures, the activity of the samples for the catalysis of the isomerization of glucose was explored and the results are reported in Figure 6.23.

<sup>7</sup>The project was carried out with the help of MSc. Luca Piccirilli during the final project for his thesis.

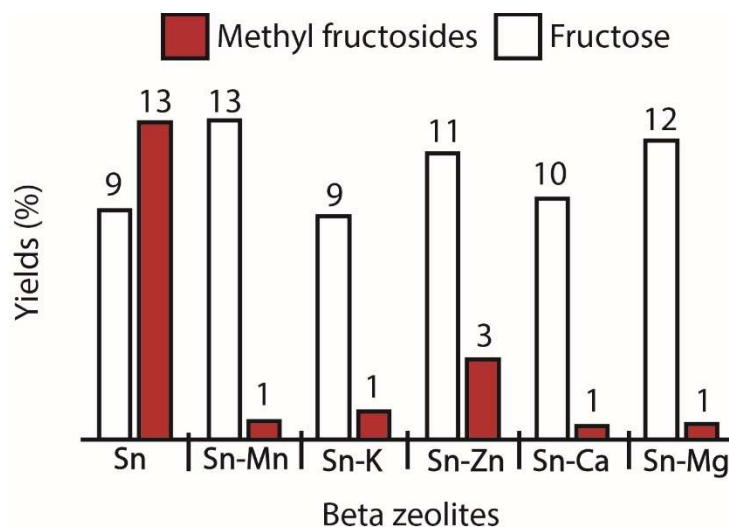


Figure 6.23. Isomerization of glucose into fructose using Sn-M-Beta zeolites as catalysts. All the carbon loss corresponds to unreacted glucose. Reaction conditions: glucose 120 mg, catalyst 50 mg, 5 mL methanol, DMSO 80  $\mu$ L as internal standard, 100  $^{\circ}$ C, 2 hours.

The isomerization catalyzed by Lewis acidic zeolites proceeded at slow rates and resulted in high amount of unconverted glucose after two hours, as reported previously under these reaction conditions.<sup>200</sup> Surprisingly, methyl fructosides were formed only using tin or zinc as active metals. Sn-Beta zeolite was the best catalyst of the series. Methyl glucosides and other products were detected only in minor amounts. Mannose derived from the epimerization of glucose was also visible in traces in all the reaction mixtures. Results from the conversion of glucose into methyl lactate at 160  $^{\circ}$ C are reported in Figure 6.24. All the modified catalysts showed better activity in the production of methyl lactate than the original Sn-Beta zeolite. Increased methyl lactate yields were associated with the suppression of the formation of furanic compounds derived by the dehydration of sugars. Only the reference catalyst, Sn-Beta without additional metals, promoted the formation of furanics in 8% yields after two hours of reaction. In contrast, the decreased acidity of Sn-M-Beta zeolites avoided dehydration reactions leading to furanic byproducts.

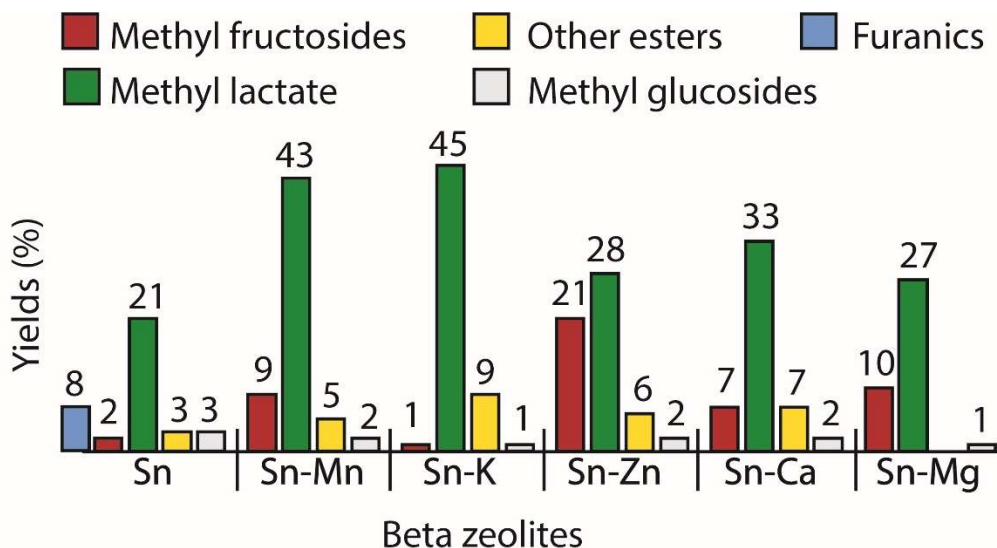


Figure 6.24. Conversion of glucose into methyl lactate using Sn-M-zeolites as catalysts. Reaction conditions: glucose 120 mg, catalyst 50 mg, 5 mL methanol, 80  $\mu$ L DMSO as internal standard, 160  $^{\circ}$ C, 2 hours.

### 6.3.4 The time-resolved formation of methyl lactate over Sn-M-Beta catalysts compared to the kinetic model proposed for Sn-Beta zeolites

Modified catalysts showed increased activity in the production of methyl lactate from glucose after two hours at 160 °C. Therefore, the reaction was studied by time-resolved experiments in order to understand the differences between Sn-M-Beta and Sn-Beta catalysts in promoting the catalytic pathways. Figure 6.25 shows the formation over time of methyl fructosides (a) and methyl lactate (b) using different Sn-M-Beta zeolites as the catalysts. The presence of additional metals changed the reaction pathway. In the conversion of glucose catalyzed by Sn-Beta zeolite, methyl fructosides are the first products formed in high yields after few minutes at 160 °C. Afterwards, they were slowly converted and yields of methyl lactate increased. Thus, the formation of methyl lactate followed a biexponential kinetics, as discussed in Chapter 3.3.2. First, methyl lactate was formed directly from fructose, but the majority of the product derived from the hydrolysis and conversion of the intermediate methyl fructosides.

In contrast, the pathway in the presence of potassium showed an immediate formation of methyl lactate with only little amount of methyl fructosides during the whole reaction. The potassium-modified zeolite did not promote the formation of methyl fructosides and methyl lactate was the main product since the beginning of the process. In this case, the formation of the product from methyl fructosides was negligible and the kinetic for the production of methyl lactate followed a monoexponential trend. Sn-Mn-Beta and Sn-Zn-Beta zeolites had intermediate behavior. In the case of the catalyst containing zinc, methyl fructosides were formed in lower amounts compared to the zeolite without zinc, but methyl fructosides showed slower consumption. Manganese showed a pattern very similar to the trend derived by the use of potassium. Methyl fructosides were stable and formed in small amounts and methyl lactate was immediately formed as the main product of the process. Different from the use of potassium, Sn-Mn-Beta zeolite showed a less sharp slope in the formation of methyl lactate at the very beginning, indicating the lower activity compared to the Sn-K-Beta catalyst in the production of methyl lactate (Figure 6.25).

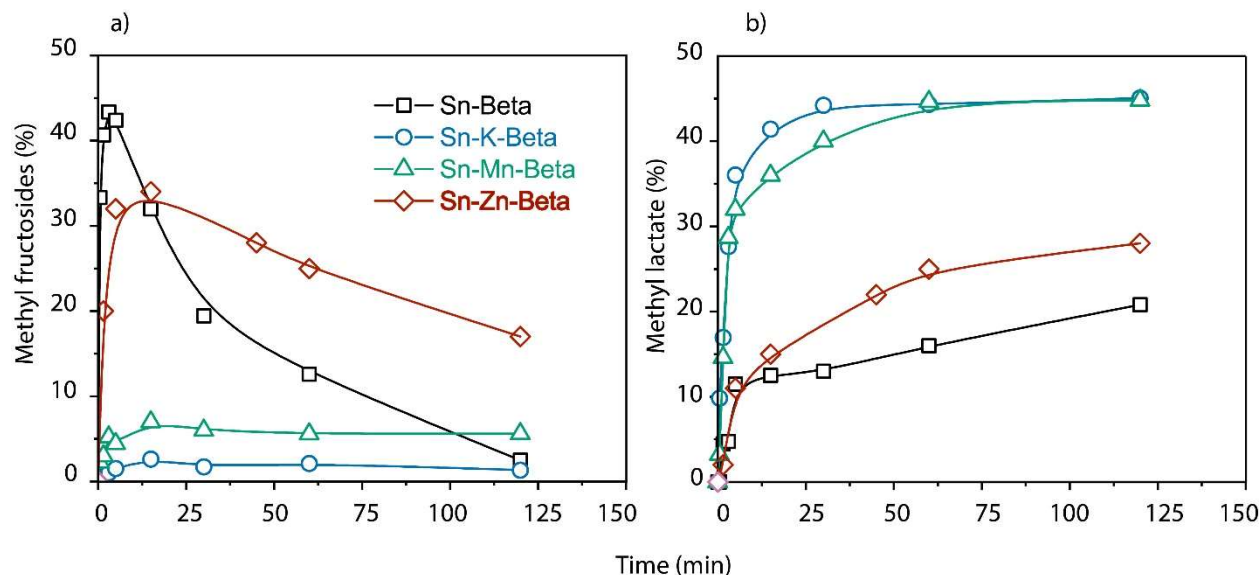


Figure 6.25. Time-resolved formation of a) methyl fructosides and b) methyl lactate using different Sn-M-Beta zeolite catalysts. Reaction conditions: glucose 120 mg, catalyst 50 mg, 5 mL methanol, 80  $\mu$ L DMSO as internal standard, 160 °C.

### 6.3.5 The use of Sn-Mn-Beta zeolite for replacing the addition of homogeneous potassium carbonate in the production of methyl lactate

Manganese-modified catalyst showed catalytic properties similar to the use of Sn-K-Beta zeolite. Therefore, the possibility of applying it in converting sugar-based feedstock was investigated further. As already reported, the process for the production of methyl lactate from glucose requires the use of homogeneous alkali salts in order to achieve high yields of the final product.<sup>47</sup> Nevertheless, the use of homogeneous additives is inconvenient for large-scale processes and the substitution with heterogeneous alternatives is highly desired. Potassium-modified Beta zeolites presented the same activity as Sn-Beta catalysts in potassium carbonate solutions, but the bond between potassium and the zeolite structure is labile, giving rapid leaching of the potassium and deactivation of the catalytic material. In this paragraph, the study of Sn-Mn-Beta zeolite as alternative for the potassium modified catalyst is presented. The study shows results analogous to the use of Sn-K-Beta zeolites, for both activity and deactivation. Mn-Beta zeolite synthesized following post-treated and hydrothermal procedures<sup>192</sup> was inactive for the conversion of glucose, implying the need of tin as active site. The optimal tin to manganese ratio for the production of methyl lactate was approximately 1:1, resulting in yields of methyl lactate of 42.6%. In Table 6.9 are reported the methyl lactate yields using different ratios, the activity of the catalyst decreased with decreasing amounts of manganese.

Table 6.9. Yields of methyl lactate for different manganese to tin ratios in Sn-Mn-zeolites (Si : Mn+Sn ratio of 100). Reaction conditions: glucose 120 mg, catalyst 50 mg, methanol 5 mL, DMSO 80  $\mu$ L as internal standard, 160  $^{\circ}$ C, 2 hours.

Mn : Sn	Methyl lactate yields (%)
1	42.6
0.5	27.4
0.3	22.3
0.1	20.5

However, catalysts containing manganese showed reduced or comparable activity compared to the use of alkali salts. Unfortunately, it did not show stable incorporation and the yields of methyl lactate decreased over time in recycling experiments. Figure 6.26 shows the reduction in methyl lactate formations for Sn-K-Beta and Sn-Mn-Beta zeolites over three cycles. In contrast, Sn-Beta zeolites were stable under the studied conditions and no deactivation was observed in the considered reactions over three cycles. Therefore, additional metals did not show catalytic properties useful for the conversion of sugars, nor stable incorporation and the increased activity was rapidly lost as in the case of the impregnation by potassium.

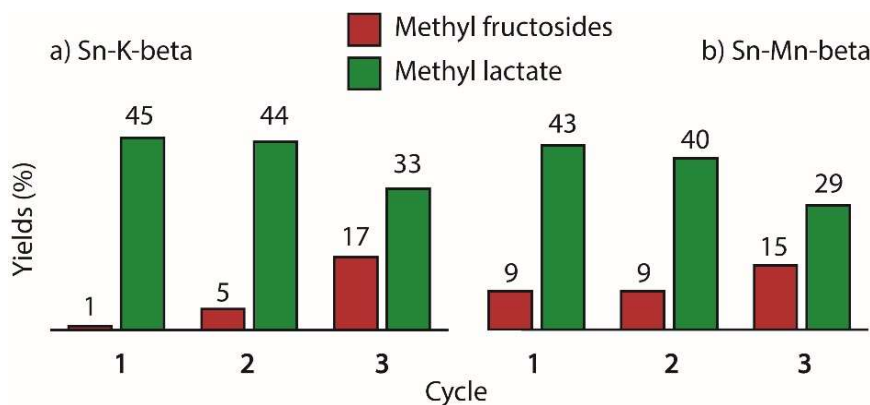


Figure 6.26. Yields of methyl lactate and methyl fructosides using a) Sn-K-Beta and b) Sn-Mn-Beta zeolites during three recycles of the catalysts. Reaction conditions: glucose 120 mg, catalyst 50 mg, methanol 5 mL, DMSO 80  $\mu$ L as internal standard, 160  $^{\circ}$ C, 2 hours.

### 6.3.6 Conclusions on the study of the conversions of sugars by Sn-Beta in the presence of additional metals

In this section, the possibility of the use of additional metals in the conversion of carbohydrates catalyzed by Sn-Beta catalysts was explored. Several metals showed beneficial effects when present in the solutions for the production of methyl lactate from glucose. The use of zinc as co-catalysts was then investigated, finding different results based on the nature of the counter ions. Even if the presence of homogeneous additives led to increased production of methyl lactate, the use of heterogeneous systems is attractive. Thus, the possibility to incorporate different active metals in the zeolite framework and to obtain Sn-M-Beta bifunctional catalysts was explored. The modification of Sn-Beta zeolite with calcium, magnesium, manganese and potassium led to increased yields of methyl lactate from glucose. The metals did not show intrinsic activity and the presence of the tin was indispensable for promoting the reaction. The modified samples presented different reaction pathways analyzed by time-resolved experiments. In particular, the formation of methyl fructosides in high yields as first intermediates was suppressed using Sn-K-Beta and Sn-Mn-Beta zeolites. The latter catalysts presented the best catalytic activity in producing methyl lactate and their stability was studied over three cycles of reuse. Unfortunately, the experiments of recycling showed a fast deactivation of the materials, due to the weak bonds between the impregnated metals and the zeolite structure.

# Chapter 7

## Conclusions

The work explored the development of zeolite-based catalytic systems for the conversion of carbohydrates into promising bio-based chemicals and developed, implemented and used spectroscopic tools to investigate further the characterization of catalyst structure and function. Results and discussion are described in Chapters 3 to 6. These chapters include investigations on the catalytic processes (Chapter 3 and 4) and on the catalytic materials (Chapter 5 and 6). The processes for the conversion of carbohydrates were studied in detail in order to understand kinetics, reaction pathways and parameters that can affect the selectivity into the desired products. The work aimed especially at identifying material properties that are central to the formation of new chemical building blocks for the development of innovative materials. The main conclusions of the study are summarized in the following.

- Chapter 3 explored the conversion of hexoses using zeolite catalysts. In the chapter, a new method for the valorization of sucrose into fructose at 100 °C in methanol was proposed. Fructose is a central intermediate for the synthesis of bio-based chemicals from carbohydrates and chemocatalytic procedures for its production are currently investigated. The procedure was based on the formation of methyl fructosides as masked substrates, which could easily be hydrolyzed to fructose by addition of water. The formation and the reactivity of methyl glycosides during the conversion of hexoses in methanol was explored and methyl fructosides had a central role for the general conversion of hexoses. The balance between Brønsted and Lewis acid sites in zeolites was essential for the conversion of glucose into useful products. In the absence of Lewis acidity, the unreactive methyl glucosides were formed from glucose in methanol and no formation of different products occurred. On the other hand, the Lewis acidity promoted the isomerization resulting in high yields of methyl fructosides, which were reactive and could be transformed into different platform chemicals. Methyl fructosides were the central intermediates also in the process for the formation of methyl lactate from glucose, fructose and sucrose. The use of highly-resolved 2D NMR experiments allowed the study of the formation and conversion of the different forms of the sugars in the reaction mixtures over time. The results were used to propose a kinetic model for the formation of methyl lactate starting from hexoses. The addition of small amounts of water promoted the hydrolysis of the methyl fructoside intermediates and affected drastically the kinetics of the process.
- In Chapter 4, the conversion of glycolaldehyde (GA) into methyl vinyl glycolate (MVG) catalyzed by Sn-Beta zeolites at 160 °C in methanol was investigated by time-resolved experiments. The process was compared with the formation of methyl lactate from hexoses in methanol and the time-resolved data were used for kinetic analysis. The formation of MVG, as well as methyl lactate from hexoses, presented two kinetic regimes. Different from the conversion of hexoses or tetroses, the reaction starting from GA followed a second-order kinetics, determined by the aldol-condensation of two molecules of GA. The process was compared to the formation of MVG starting from erythrulose, which presented a first-order

kinetics. The effect of the addition of alkali and water in the reaction mixture was also explored. The study aimed to understand the reaction pathways leading to the formation of MVG and the parameters affecting the selectivity in order to design optimal processes for the production of a new bio-based hydroxy ester.

- Chapter 5 and 6 include the study of the catalytic materials. In Chapter 5, the synthesis of stannosilicates with different properties was explored and the effect of the different procedures was studied on the selectivity of the processes for the conversion of carbohydrates. Post-synthetic Sn-Beta zeolites are active catalysts for the conversion of carbohydrates, but the catalytic material can be optimized further. Thus, modifications to the synthesis were explored in order to understand how the different synthetic steps can be modified for improving the activity of the catalysts. Mesoporous catalytic systems were prepared and tested as catalysts for the conversion of different carbohydrates into methyl lactate, resulting in the initial acceleration of the conversion of large substrates like inulin and in unchanged activity in the cases of the use of small substrates, such as glucose and sucrose.
- Chapter 6 focused on the characterization of the structure-activity relation of Sn-Beta zeolites. The adsorption of deuterated acetonitrile was studied *in situ* by FT-IR spectroscopy and it represented an efficient method for studying the structure of catalytic materials. The technique was applied to study materials calcined before tin impregnation and to explore the changes in the structure in regenerated catalysts. In both cases, extra-framework tin species, invisible to other characterization techniques, were formed. Thus, the method was an useful tool for understanding structural changes occurring in the catalyst under different conditions. Ammonia was also applied as a probe molecule for quantitatively determining the acidity by TPD and qualitatively by FT-IR spectroscopy. The data correlated with functional experiments of titration of the tin in the catalysts by potassium carbonate and allowed to propose three stages of the active sites in Sn-Beta zeolites in the presence of alkali salts. The addition of small amounts of alkali salts inhibited the formation of furanic compounds due to the neutralization of the residual Brønsted acidity given by the presence of defects in the catalyst structure. The suppression of the competitive reaction resulted in increased yields of methyl lactate. However, an excess of alkali salts led to the deactivation of the catalysts, the optimal amount had a stoichiometric correlation with the amount of tin and the acidity measured by  $\text{NH}_3$ -TPD. The interaction with different metals and the preparation of Sn-M-Beta zeolites were also investigated in the same chapter. However, the studied systems showed catalytic behaviors comparable to the use of alkali salts.



# Appendix A- Case Study on Homogeneous Catalysis

## Conversion of Glucose in Aqueous Solutions Catalyzed by $\text{CrCl}_3$

In this appendix, the case study for the analysis of the conversion of glucose catalyzed by  $\text{CrCl}_3$  in aqueous solutions is summarized. The study employed *in situ* NMR methods developed herein to the discovery of new reaction pathways and byproducts in a widely studied model reaction. Among the different processes for the conversion of carbohydrates, the conversion of glucose catalyzed by Lewis acid salts in aqueous solution is relevant to study.<sup>225</sup> Glucose is the most abundant carbohydrate occurring in nature and the use of Lewis acids as catalysts promotes the first isomerization to fructose and the rapid conversion into different types of products. The process can be used for the production of 5-hydroxymethylfurfural (HMF), which can be used for the preparation of monomers for polymeric materials.<sup>226</sup> Despite the importance of the process for industrial applications, the reaction pathway is unclear and several products are still unknown.<sup>132</sup> Advanced NMR techniques were applied to the identification of products and intermediates formed in the reaction mixture and a general overview of the catalytic process is presented in this appendix.<sup>8</sup>

### Conversion of Glucose in Aqueous Solutions Catalyzed by $\text{CrCl}_3$

Among the different chemicals obtainable from the conversion of biomasses, 5-hydroxymethylfurfural (HMF) is one of the most relevant because of the wide range of applications. Biomasses can be converted into HMF using different heterogeneous and homogeneous systems.<sup>225</sup> In particular, the conversion of glucose into HMF has received much attention because of the large availability of this starting substrate. The process is generally catalyzed by Lewis acid salts, such as  $\text{CrCl}_3$ , using water as the solvent.<sup>227</sup> Despite the general interest for the process, the production of HMF from glucose catalyzed by Lewis acid can still be improved. In fact, the catalytic mechanism is still not completely understood and several unknown byproducts are formed.<sup>132</sup> The identification of the different byproducts can simplify the understanding of the mechanism and bring advantages for the optimization of the production. Moreover, a clear overview of the identity of all the products present in the final mixture is highly desired for industrial applications and for the design of downstream purification.<sup>132</sup> The reaction for the conversion of glucose catalyzed by the Lewis acid  $\text{CrCl}_3$  in water was studied by a serie of NMR

---

<sup>8</sup> The appendix was adapted from the article “Uncharted Pathways for  $\text{CrCl}_3$  Catalyzed Glucose Conversion in Aqueous Solution” published in Topics in Catalysis.<sup>228</sup> The project was carried out with the help and under the supervision of Senior Researcher Sebastian Meier (DTU).

experiments at high magnetic field (800 MHz) for the identification of unknown compounds. Two-dimensional NMR techniques were applied in order to increase the signal and resolution and to ensure a correct interpretation of the molecular structures of the different products.

### A.1 Identification of formed acetals in the conversion of glucose catalyzed by $\text{CrCl}_3$

The conversion of glucose was performed in aqueous solution of 17 mM  $\text{CrCl}_3 \cdot 6\text{H}_2\text{O}$  and 10% (w/v) glucose at 140 °C for one hour. First, the products 1,6-anhydroglucofuranose (AGF) and 1,6-anhydroglucopyranose (AGP) (Figure A.1) were identified in the reaction mixtures by comparison with the data in the literature and the spectra of the commercial levoglucosan standard.

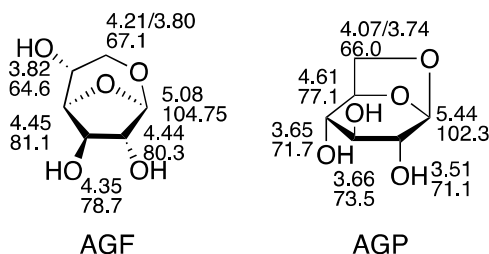


Figure A.1. Spin systems of 1,6-anhydroglucofuranose (AGF) and 1,6-anhydroglucopyranose (AGP). Adapted from Ref 228.

Although the  $\beta$ -pyranose precursor was much more abundant in aqueous solution than the  $\beta$ -furanose form, AGF and AGP were found in very similar amounts. The equal concentrations gave indication of the kinetic preference for the formation of the furanoside. The process was also studied using DMSO as the solvent, since the formation of these products has been reported in literature<sup>229</sup> as more relevant under these conditions. The concentration of both AGF and AGP increased greatly using DMSO as solvent. The reaction was then followed *in situ* by 1D  $^{13}\text{C}$  NMR spectroscopy at 110 °C. The formation of AGF was faster than formation of AGP, confirming the kinetic preference for the former product. Moreover, upon addition of 17% (v/v) of water to the final DMSO mixture, AGF was slowly hydrolyzed. In contrast, AGP was stable and the concentration was constant in the presence of water.

The formation of AGF and AGP was due to the intramolecular reaction of glucose. On the other hand, intermolecular reactions also occurred, resulting in the presence of different disaccharides in the reaction media. All the different combinations of glucose in disaccharides were detected and identified by comparison with the  $^1\text{H}$ - $^{13}\text{C}$  HSQC spectra of the standards. The disaccharides formed *via* 1-6 glycosidic bond, such as isomaltose and gentiobiose were observed in higher amounts than the other disaccharides. In general, byproducts were formed in higher concentrations in the reaction in DMSO compared to the use of water as solvent. Other disaccharides were also visible in traces: cellobiose, maltose, trehalose, kojibiose, sophorose, nigerose and laminaribiose (Figure A.2).

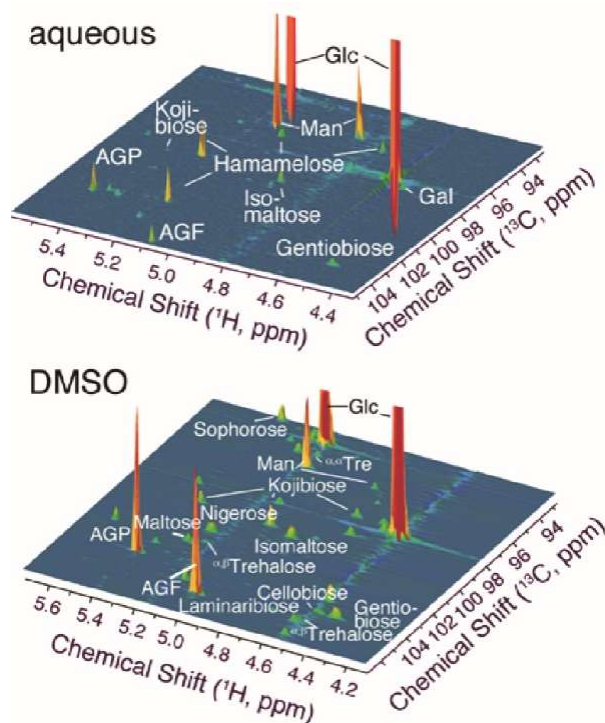


Figure A.2. Identification of the different disaccharides in the  $^1\text{H}$ - $^{13}\text{C}$  HSQC NMR spectra. Adapted from Ref 228.

## A.2 Formation of branched hexose during the conversion of glucose catalyzed by $\text{CrCl}_3$

The formation of branched carbohydrates during the conversion of glucose catalyzed by homogeneous Lewis acid has been hypothesized in previous studies.<sup>132</sup> Although the previously unknown signals were identified in this work as 1,6-anhydroglucofuranose (AGF), the presence of branched hexoses was also confirmed. Hamamelose (2-C-(hydroxymethyl)-D-ribose) and 2-C-(hydroxymethyl)-L-lyxose (Figure A.3) were detected in the final reaction mixtures. The former compound was visible in all the  $\alpha$ - and  $\beta$ -, furano- and pyrano- forms. In contrast, 2-C-(hydroxymethyl)-L-lyxose was observed prevalently in the pyranose form.

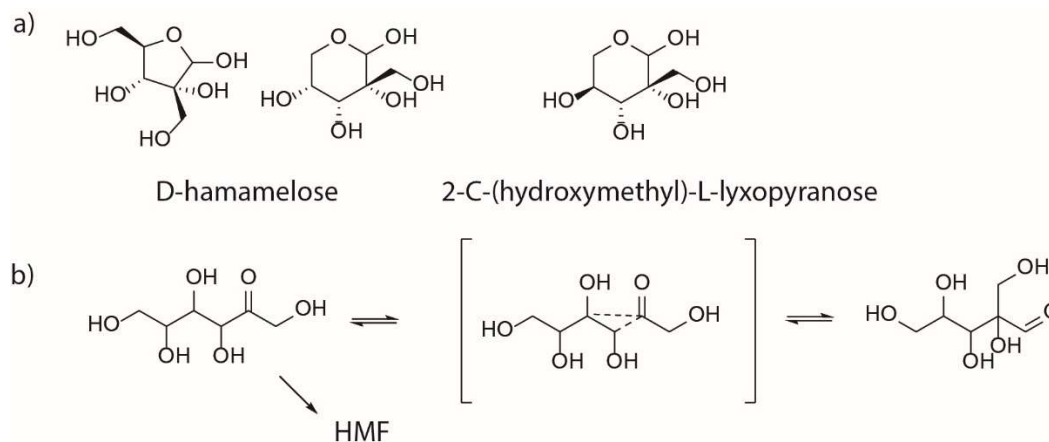


Figure A.3. a) Structures of Hamamelose and 2-C-(hydroxymethyl)-L-lyxose, b) proposed mechanism for the formation of branched carbohydrates in the reaction mixture. Adapted from Ref 228.

Experiments using D-[1- $^{13}\text{C}$ ]glucose as starting substrate were carried out in order to confirm the plausible mechanism for the formation of branched hexoses during the conversion of glucose. The formation of branched sugars could be due to a Bilik-type carbon shift and, as confirmation, the label  $^{13}\text{C}$  was found in the 2-hydroxymethyl group of hamamelose. In addition, branched hexoses could derive from the aldol condensation of small linear sugars. This latter hypothesis is less probable than the Bilik reaction since the dehydration of sugars is irreversible and hexoses hardly fragmentize under these conditions. Branched sugars were probably ketose-derived intermediates in a pathway leading to HMF.

### A.3 Identification of different hexoses

The Lewis acid  $\text{CrCl}_3$  can catalyze the interconversion between hexoses and different types of shifts, such as the 1,2-hydride shift and the Bilik reaction. Moreover, Lewis acid salts can also promote retro-aldol cleavage reactions followed by further condensations. The latter pathway was confirmed by the identification of C3 sugars, like dihydroxyacetone. In the spectral region of the primary alcohols in the  $^1\text{H}$ - $^{13}\text{C}$  HSQC spectra, different ketoses were visible, such as fructose, sorbose and tagatose. Moreover, beyond glucose, different C6 aldoses were present in the reaction mixtures: galactose, altrose, idose and allose (Figure A.4).

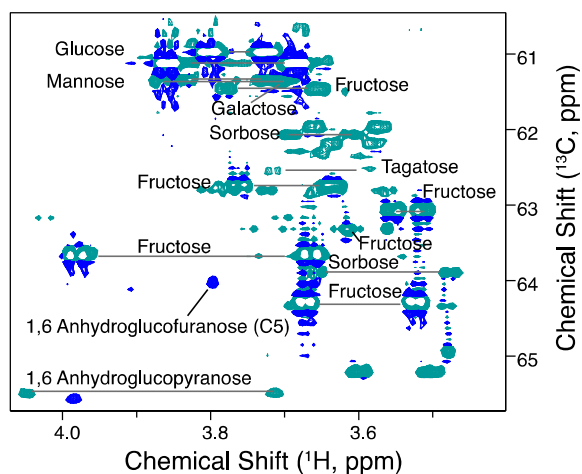


Figure A.4. Identification of different hexoses in the spectral region of the primary alcohols in the  $^1\text{H}$ - $^{13}\text{C}$  HSQC spectra of the crude reaction mixtures. Adapted from Ref 228.

Thus, in the reaction for the conversion of glucose catalyzed by  $\text{CrCl}_3$ , a complex mixture of carbohydrates was formed, including different hexoses, anhydrosugars, disaccharides and branched hexoses.

### A.4 Reactions catalyzed by $\text{CrCl}_3$ starting from glucose

Finally, products different from carbohydrates were studied. As expected, HMF and levulinic acid were formed during the reaction. Moreover, the byproduct (2E)-2,4-pentadienal was identified. The structure was assigned by the study using complementary NMR experiments. In the  $^1\text{H}$ - $^1\text{H}$  TOCSY spectra, correlations of the spin system are shown (Figure A.5).

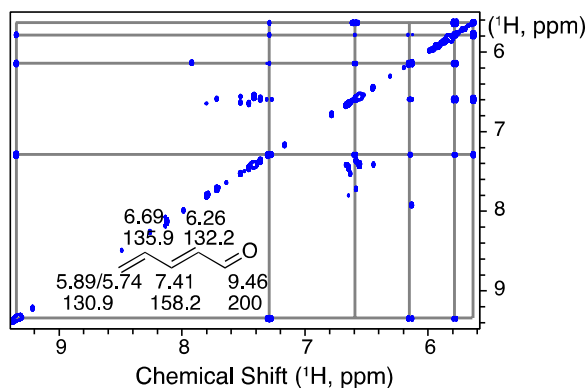
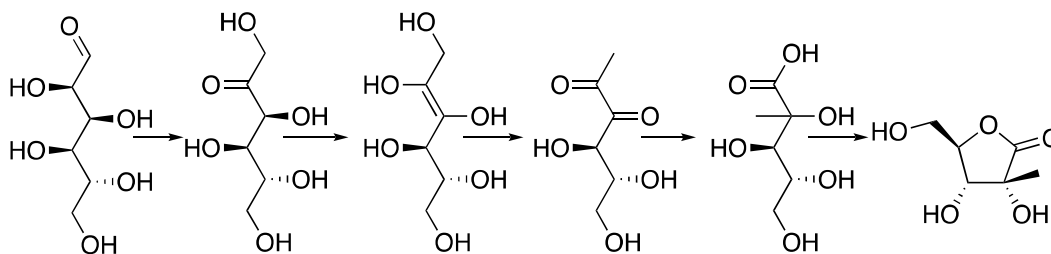


Figure A.5.  $^1\text{H}$ - $^1\text{H}$  TOCSY spectra of the byproduct (2E)-2,4-pentadienal. Adapted from Ref 228.

Lactone byproducts were also present in the reaction mixtures. 2-C-methyl-ribonolactone was identified. The presence of this compounds is due to a cascade process including the isomerization between glucose and fructose followed by dehydration and rearrangement catalyzed by Brønsted bases (Scheme A.1).



Scheme A.1. Mechanism for the formation of 2-C-methyl-ribonolactone. Adapted from Ref 228.

### A.5 Conclusion on the study for the identification of products and intermediates during the conversion of glucose in water catalyzed by $\text{CrCl}_3$

The appendix aimed to give a short overview of the potential applications of NMR techniques on the study of catalytic processes for the conversion of carbohydrates. The identification of products and intermediates is essential for industrial processes and for the design of downstream purifications. In this case, the crude reaction mixture for the conversion of glucose in aqueous solutions catalyzed by the homogeneous Lewis acid salt  $\text{CrCl}_3 \cdot 6\text{H}_2\text{O}$  was studied in detail by NMR spectroscopy. Products, byproducts and intermediates were characterized and pathways leading to their formation were proposed. Different carbohydrates were identified, such as different hexoses, anhydrosugars, disaccharides and branched hexoses. The formation of HMF and levulinic acid occurred, as expected. Moreover, (2E)-2,4-pentadienal and 2-C-methyl-ribonolactone were visible in the mixtures as byproducts.

## Appendix B- Applications

# Application of MVG as Bio-based Reagent for Coatings

The purpose of the thesis was the characterization and optimization of materials catalyzing innovative chemicals for novel polymer applications. This appendix includes considerations about possible applications of methyl vinyl glycolate (MVG) in commercial formulation for coatings.<sup>9</sup> The appendix aims to give a general overview on the possible applications of the studied hydroxy esters. Detailed results and experimental procedures are not included due to confidentiality. The use of MVG in formulations for alkyd resins and UV-cured coatings was investigated. Moreover, the epoxide derived from MVG was also studied in cationic UV-cured coatings.

### B.1 MVG as reactive diluent in alkyd paints

Alkyds are oil-modified polyesters and they find large application as coatings. Traditionally, alkyd paints are diluted with volatile organic solvents and after the application, they dry by evaporation of the solvent. However, formulations without organic solvents are attractive from an environmental point of view. An alternative application is the use of reactive diluents, such as methacrylate. In this case, the diluent agent acts as a solvent, but it reacts and it is converted to a part of the coating during the curing process.<sup>230</sup> Because of the similarity in functionality between MVG and methacrylate, MVG was tested in formulations as the reactive diluent for alkyd paints. However, it did not show optimal behavior for the application because of the high volatility. Thus, MVG evaporated during the drying process and it was not incorporated in the final product.

### B.2 MVG as monomer in UV-cured coatings

The UV-curing is the process of polymerization promoted by ultra-violet light. It was proposed as a method to avoid the use of organic solvents in manufacturing industries. Formulations for coatings derived by photopolymerization contain the reactive monomers or oligomers, e.g. acrylates, in the presence of a photo-initiator. Moreover, the presence of additional linker helps the cross-linking and enhances final physical properties.<sup>231</sup>

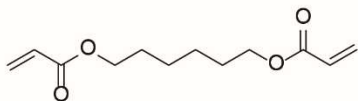
MVG and 1,6-hexanediol (HDO) were tested as reactive components for different formulations in the presence and in the absence of 1,1,1-trimethylolpropane triacrylate (TMPTA) as cross-linker for UV-cured coatings. The blends were compared with reference blends containing 1,6-hexanediol diacrylate (HDDA) (Figure B.1). All the prepared blends were successfully dried; however, the curing process was completed in much longer times compared to the reference blend containing 1,6-hexanediol and acrylic acid. The physical properties of the final film were tested. The coatings containing MVG showed high flexibility and low hardness compared to the

---

<sup>9</sup> The work discussed in this appendix was carried out in collaboration with Ph.D. Samuel G. Elliot (DTU) during an external working visit at Perstorp AB.

reference. The results indicated the incomplete cross-linking of the blend and further optimizations of the formulations were necessary.

Reference blend with HDDA monomer



Tested blend with MVG+HDO monomer

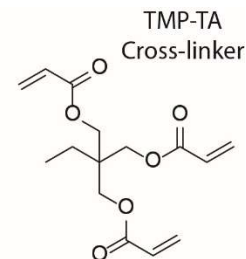
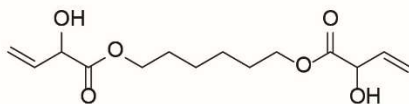


Figure B.1. Structures of the monomers of the blends studied for UV-curing and structure of TMP-TA cross linker.

### B.3 The epoxide of MVG in cationic UV-cured coatings

MVG was epoxidized by meta-chloroperoxybenzoic acid to give methyl 2-hydroxy-2-(oxiran-2-yl)acetate (Figure B.2).<sup>10</sup> First, the reactivity of the compound was studied by Differential Scanning Calorimetry (DSC) and FT-IR spectroscopy. The results confirmed the high reactivity of the epoxide and the possibility to react it both with acids and with itself. Thus, possible applications of the compound in formulations for cationic UV-cured coatings were tested.

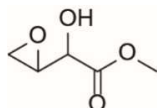


Figure B.2. MVG epoxide, methyl 2-hydroxy-2-(oxiran-2-yl)acetate

Epoxy resins can also be polymerized by UV-curing in the presence of a photo-initiator. In this case, the process of polymerization occurs by the formation of highly reactive epoxy cations, which propagate the reaction forming the polymeric chain.<sup>231</sup> The epoxide of MVG was tested as reactive initiator in different blends for the UV-curing of 3,4-epoxycyclohexylmethyl-3',4'-epoxycyclohexane carboxylate (ECC). All the blends dried quickly and homogeneous films were rapidly obtained. The characterization of the physical properties indicated high hardness and chemical resistance. The results indicated the possibility to apply the MVG epoxide to formulations for cationic UV-cured coatings.

### B.4 Conclusions on the study of the applicability of MVG in coatings

In this appendix, an overview of possible applications of MVG as bio-based monomer in formulations for coatings was presented. The pure MVG as reactive diluent in alkyd resins did not present optimal behavior and MVG was not integrated in the final product. In contrast, the photo-polymerization of MVG with 1,6-hexanediol occurred successfully. However, the characterization of physical properties of the final product suggested the incomplete cross-linking of the blend and further studies are needed for the optimization of the application. Finally, the epoxide derived from MVG was studied in formulations for the cationic UV-curing of epoxy resins. The films obtained in the presence of MVG epoxide were polymerized quickly and the resulting coatings showed high hardness and resistance. The results indicated the possibility of applications in formulations for coatings for MVG and MVG-derived molecules.

<sup>10</sup> Synthesis and purification of the epoxide were carried out by Ph.D. Bo Jessen (DTU).

# References

1. Solid Acids and Bases as Catalysts. *Green Chemistry and Catalysis* (2007). doi:doi:10.1002/9783527611003.ch2
2. Martínez, C. & Corma, A. 5.05 - Zeolites. in (eds. Reedijk, J. & Poeppelmeier, K. B. T.-C. I. C. I. I. (Second E.) 103–131 (Elsevier, 2013). doi:https://doi.org/10.1016/B978-0-08-097774-4.00506-4
3. Luo, H. Y., Lewis, J. D. & Román-Leshkov, Y. Lewis Acid Zeolites for Biomass Conversion: Perspectives and Challenges on Reactivity, Synthesis, and Stability. *Annu. Rev. Chem. Biomol. Eng.* **7**, 663–692 (2016).
4. Gürbüz, E., Bond, J. Q., Dumesic, J. A. & Román-Leshkov, Y. Chapter 8 - Role of Acid Catalysis in the Conversion of Lignocellulosic Biomass to Fuels and Chemicals. in (eds. Triantafyllidis, K. S., Lappas, A. A. & Stöcker, M. B. T.-T. R. of C. for the S. P. of B. and B.) 261–288 (Elsevier, 2013). doi:https://doi.org/10.1016/B978-0-444-56330-9.00008-5
5. Ferrini, P. *et al.* Lewis acid catalysis on single site Sn centers incorporated into silica hosts. *Coord. Chem. Rev.* **343**, 220–255 (2017).
6. Auerbach, S. M., Carrado, K. A. & Dutta, P. K. *Handbook of Zeolite Science and Technology*. (CRO, 2003).
7. The International Zeolite Association. Available at: <http://www.iza-structure.org/>.
8. Csicsery, S. M. Shape-selective catalysis in zeolites. *Zeolites* **4**, 202–213 (1984).
9. Plank, C. J., Rosinski, E. J. & Hawthorne, W. P. Acidic Crystalline Aluminosilicates. New Superactive, Superselective Cracking Catalysts. *IEC Prod. Res. Dev.* **3**, 165–169 (1964).
10. Hammond, C., Padovan, D. & Tarantino, G. Porous metallosilicates for heterogeneous, liquid-phase catalysis: perspectives and pertaining challenges. *R. Soc. Open Sci.* **5**, 171315 (2019).
11. Yu, J. Chapter 3 - Synthesis of Zeolites. in *Introduction to Zeolite Science and Practice* (eds. Čejka, J., van Bekkum, H., Corma, A. & Schüth, F. B. T.-S. in S. S. and C.) **168**, 39–103 (Elsevier, 2007).
12. Milton, R. M. Molecular Sieve Science and Technology. in *Zeolite Synthesis* **398**, 1 (American Chemical Society, 1989).
13. Cooper, E. R. *et al.* Ionic liquids and eutectic mixtures as solvent and template in synthesis of zeolite analogues. *Nature* **430**, 1012–1016 (2004).
14. Chen, C.-Y. & Zones, S. I. Post-Synthetic Treatment and Modification of Zeolites. *Zeolites and Catalysis* (2010). doi:doi:10.1002/9783527630295.ch6
15. Silaghi, M.-C., Chizallet, C. & Raybaud, P. Challenges on molecular aspects of dealumination and desilication of zeolites. *Microporous Mesoporous Mater.* **191**, 82–96 (2014).
16. Khan, W., Jia, X., Wu, Z., Choi, J. & Yip, C. A. Incorporating Hierarchy into Conventional Zeolites for Catalytic Biomass Conversions: A Review. *Catalysts* **9**, (2019).
17. Feliczak-Guzik, A. Hierarchical zeolites: Synthesis and catalytic properties. *Microporous Mesoporous Mater.* **259**, 33–45 (2018).
18. Hartmann, M., Machoke, A. G. & Schwieger, W. Catalytic test reactions for the evaluation of hierarchical zeolites. *Chem. Soc. Rev.* **45**, 3313–3330 (2016).



19. Serrano, D. P., Escola, J. M. & Pizarro, P. Synthesis strategies in the search for hierarchical zeolites. *Chem. Soc. Rev.* **42**, 4004–4035 (2013).
20. van Donk, S., Janssen, A. H., Bitter, J. H. & de Jong, K. P. Generation, Characterization, and Impact of Mesopores in Zeolite Catalysts. *Catal. Rev.* **45**, 297–319 (2003).
21. Verboekend, D. & Pérez-Ramírez, J. Design of hierarchical zeolite catalysts by desilication. *Catal. Sci. Technol.* **1**, 879–890 (2011).
22. Sachse, A. & García-Martínez, J. Surfactant-Templating of Zeolites: From Design to Application. *Chem. Mater.* **29**, 3827–3853 (2017).
23. Ivanova, I. I. & Knyazeva, E. E. Micro–mesoporous materials obtained by zeolite recrystallization: synthesis, characterization and catalytic applications. *Chem. Soc. Rev.* **42**, 3671–3688 (2013).
24. Li, K., Valla, J. & Garcia-Martinez, J. Realizing the Commercial Potential of Hierarchical Zeolites: New Opportunities in Catalytic Cracking. *ChemCatChem* **6**, 46–66 (2014).
25. Dapsens, P. Y., Mondelli, C. & Pérez-Ramírez, J. Design of Lewis-acid centres in zeolitic matrices for the conversion of renewables. *Chem. Soc. Rev.* **44**, 7025–7043 (2015).
26. Goodarzi, F. *et al.* Methanation of Carbon Dioxide over Zeolite-Encapsulated Nickel Nanoparticles. *ChemCatChem* **10**, 1566–1570 (2018).
27. Mielby, J. *et al.* Oxidation of Bioethanol using Zeolite-Encapsulated Gold Nanoparticles. *Angew. Chemie Int. Ed.* **53**, 12513–12516 (2014).
28. Bellussi, G. & Rigutto, M. S. Metal Ions Associated to the Molecular Sieve Framework: Possible Catalytic Oxidation Sites. in *Advanced Zeolite Science and Applications* (eds. Jansen, J. C., Stöcker, M., Karge, H. G. & Weitkamp, J. B. T.-S. in S. S. and C.) **85**, 177–213 (Elsevier, 1994).
29. Taramasso, M., Perego, G. & Notari, B. Preparation of Porous Crystalline Synthetic Material Comprised of Silicon and Titanium Oxides. (1979).
30. Notari, B. Titanium Silicalite: A New Selective Oxidation Catalyst. in *Chemistry of Microporous Crystals* (eds. Inui, T., Namba, S. & Tatsumi, T. B. T.-S. in S. S. and C.) **60**, 343–352 (Elsevier, 1991).
31. Cambor, M. A., Corma, A. & Pérez-Pariente, J. Synthesis of titanoaluminosilicates isomorphous to zeolite Beta, active as oxidation catalysts. *Zeolites* **13**, 82–87 (1993).
32. Corma, A., Cambor, M. A., Esteve, P., Martinez, A. & Perezpariente, J. Activity of Ti-Beta Catalyst for the Selective Oxidation of Alkenes and Alkanes. *J. Catal.* **145**, 151–158 (1994).
33. Orazov, M. & Davis, M. E. Catalysis by framework zinc in silica-based molecular sieves. *Chem. Sci.* **7**, 2264–2274 (2016).
34. Sushkevich, V. L., Ivanova, I. I., Tolborg, S. & Taarning, E. Meerwein–Ponndorf–Verley–Oppenauer reaction of crotonaldehyde with ethanol over Zr-containing catalysts. *J. Catal.* **316**, 121–129 (2014).
35. Mal, N. K., Bhaumik, A., Ramaswamy, V., Belhekar, A. A. & Ramaswamy, A. V. Synthesis of Al-free Sn-containing molecular sieves of MFI, MEL and MTWtypes and their catalytic activity in oxidation reactions. in *Catalysis by Microporous Materials* (eds. Beyer, H. K., Karge, H. G., Kiricsi, I. & Nagy, J. B. B. T.-S. in S. S. and C.) **94**, 317–324 (Elsevier, 1995).
36. Corma, A., Nemeth, L. T., Renz, M. & Valencia, S. Sn-zeolite beta as a heterogeneous chemoselective catalyst for Baeyer–Villiger oxidations. *Nature* **412**, 423 (2001).
37. Nemeth, L. & Bare, S. R. Science and Technology of Framework Metal-Containing Zeotype Catalysts.

- Adv. Catal.* **57**, 1–97 (2014).
38. Corma, A., Domine, M. E., Nemeth, L. & Valencia, S. Al-Free Sn-Beta Zeolite as a Catalyst for the Selective Reduction of Carbonyl Compounds (Meerwein–Ponndorf–Verley Reaction). *J. Am. Chem. Soc.* **124**, 3194–3195 (2002).
39. Boronat, M., Corma, A. & Renz, M. Mechanism of the Meerwein–Ponndorf–Verley–Oppenauer (MPVO) Redox Equilibrium on Sn- and Zr-Beta Zeolite Catalysts. *J. Phys. Chem. B* **110**, 21168–21174 (2006).
40. Boronat, M., Corma, A., Renz, M. & Viruela, P. M. Predicting the Activity of Single Isolated Lewis Acid Sites in Solid Catalysts. *Chem. – A Eur. J.* **12**, 7067–7077 (2006).
41. Corma, A., Domine, M. E. & Valencia, S. Water-resistant solid Lewis acid catalysts: Meerwein–Ponndorf–Verley and Oppenauer reactions catalyzed by tin-beta zeolite. *J. Catal.* **215**, 294–304 (2003).
42. Nikolla, E., Román-Leshkov, Y., Moliner, M. & Davis, M. E. “One-Pot” Synthesis of 5-(Hydroxymethyl)furfural from Carbohydrates using Tin-Beta Zeolite. *ACS Catal.* **1**, 408–410 (2011).
43. Moliner, M., Román-Leshkov, Y. & Davis, M. E. Tin-containing zeolites are highly active catalysts for the isomerization of glucose in water. *Proc. Natl. Acad. Sci.* **107**, 6164 LP – 6168 (2010).
44. Taarning, E. *et al.* Zeolite-Catalyzed Isomerization of Triose Sugars. *ChemSusChem* **2**, 625–627 (2009).
45. Mal, N. K., Ramaswamy, V., Rajamohanam, P. R. & Ramaswamy, A. V. Sn-MFI molecular sieves: synthesis methods, <sup>29</sup>Si liquid and solid MAS-NMR, <sup>119</sup>Sn static and MAS NMR studies. *Microporous Mater.* **12**, 331–340 (1997).
46. Li, L. *et al.* Selective conversion of trioses to lactates over Lewis acid heterogeneous catalysts. *Green Chem.* **13**, 1175–1181 (2011).
47. Tolborg, S. *et al.* Tin-containing Silicates: Alkali Salts Improve Methyl Lactate Yield from Sugars. *ChemSusChem* **8**, 613–617 (2015).
48. Shetti, V. N., Srinivas, D. & Ratnasamy, P. Enhancement of chemoselectivity in epoxidation reactions over TS-1 catalysts by alkali and alkaline metal ions. *J. Mol. Catal. A Chem.* **210**, 171–178 (2004).
49. Khouw, C. B. & Davis, M. E. Catalytic Activity of Titanium Silicates Synthesized in the Presence of Alkali-Metal and Alkaline-Earth Ions. *J. Catal.* **151**, 77–86 (1995).
50. Corma, A., Llabrés i Xamena, F. X., Prestipino, C., Renz, M. & Valencia, S. Water Resistant, Catalytically Active Nb and Ta Isolated Lewis Acid Sites, Homogeneously Distributed by Direct Synthesis in a Beta Zeolite. *J. Phys. Chem. C* **113**, 11306–11315 (2009).
51. Yakimov, A. V., Kolyagin, Y. G., Tolborg, S., Vennestrom, P. N. R. & Ivanova, I. I. Accelerated synthesis of Sn-BEA in fluoride media: effect of H<sub>2</sub>O content in the gel. *New J. Chem.* **40**, 4367–4374 (2016).
52. Tolborg, S. *et al.* Incorporation of tin affects crystallization, morphology, and crystal composition of Sn-Beta. *J. Mater. Chem. A* **2**, 20252–20262 (2014).
53. Chang, C.-C., Wang, Z., Dornath, P., Je Cho, H. & Fan, W. Rapid synthesis of Sn-Beta for the isomerization of cellulosic sugars. *RSC Adv.* **2**, 10475–10477 (2012).
54. Kang, Z. *et al.* Factors affecting the formation of Sn-Beta zeolites by steam-assisted conversion method. *Mater. Chem. Phys.* **141**, 519–529 (2013).
55. Hammond, C., Conrad, S. & Hermans, I. Simple and Scalable Preparation of Highly Active Lewis Acidic Sn-β. *Angew. Chemie Int. Ed.* **51**, 11736–11739 (2012).

56. Dijkmans, J. *et al.* Cooperative Catalysis for Multistep Biomass Conversion with Sn/Al Beta Zeolite. *ACS Catal.* **5**, 928–940 (2015).
57. Wolf, P., Hammond, C., Conrad, S. & Hermans, I. Post-synthetic preparation of Sn-, Ti- and Zr-beta: a facile route to water tolerant, highly active Lewis acidic zeolites. *Dalt. Trans.* **43**, 4514–4519 (2014).
58. Dijkmans, J. *et al.* Productive sugar isomerization with highly active Sn in dealuminated  $\beta$  zeolites. *Green Chem.* **15**, 2777–2785 (2013).
59. Li, P. *et al.* Postsynthesis and Selective Oxidation Properties of Nanosized Sn-Beta Zeolite. *J. Phys. Chem. C* **115**, 3663–3670 (2011).
60. van der Graaff, W. N. P., Li, G., Mezari, B., Pidko, E. A. & Hensen, E. J. M. Synthesis of Sn-Beta with Exclusive and High Framework Sn Content. *ChemCatChem* **7**, 1152–1160 (2015).
61. Dijkmans, J. *et al.* Post-synthesis Sn $\beta$ : An exploration of synthesis parameters and catalysis. *J. Catal.* **330**, 545–557 (2015).
62. Botti, L. *et al.* Influence of Composition and Preparation Method on the Continuous Performance of Sn-Beta for Glucose-Fructose Isomerisation. *Top. Catal.* (2018). doi:10.1007/s11244-018-1078-z
63. Kolyagin, Y. G., Yakimov, A. V., Tolborg, S., Vennestrom, P. N. R. & Ivanova, I. I. Direct Observation of Tin in Different T-Sites of Sn-BEA by One- and Two-Dimensional  $^{119}\text{Sn}$  MAS NMR Spectroscopy. *J. Phys. Chem. Lett.* **9**, 3738–3743 (2018).
64. Gounder, R. & Davis, M. E. Monosaccharide and disaccharide isomerization over Lewis acid sites in hydrophobic and hydrophilic molecular sieves. *J. Catal.* **308**, 176–188 (2013).
65. Gunther, W. R., Michaelis, V. K., Caporini, M. A., Griffin, R. G. & Román-Leshkov, Y. Dynamic Nuclear Polarization NMR Enables the Analysis of Sn-Beta Zeolite Prepared with Natural Abundance  $^{119}\text{Sn}$  Precursors. *J. Am. Chem. Soc.* **136**, 6219–6222 (2014).
66. Kolyagin, Y. G., Yakimov, A. V., Tolborg, S., Vennestrom, P. N. R. & Ivanova, I. I. Application of  $^{119}\text{Sn}$  CPMG MAS NMR for Fast Characterization of Sn Sites in Zeolites with Natural  $^{119}\text{Sn}$  Isotope Abundance. *J. Phys. Chem. Lett.* **7**, 1249–1253 (2016).
67. Wolf, P. *et al.* Identifying Sn Site Heterogeneities Prevalent Among Sn-Beta Zeolites. *Helv. Chim. Acta* **99**, 916–927 (2016).
68. M., O. C., Spangsberg, H. M., Søren, D. & Esben, T. Tin-containing silicates: structure–activity relations. *Proc. R. Soc. A Math. Phys. Eng. Sci.* **468**, 2000–2016 (2012).
69. Wolf, P. *et al.* Correlating Synthetic Methods, Morphology, Atomic-Level Structure, and Catalytic Activity of Sn- $\beta$  Catalysts. *ACS Catal.* **6**, 4047–4063 (2016).
70. Boronat, M., Concepción, P., Corma, A., Renz, M. & Valencia, S. Determination of the catalytically active oxidation Lewis acid sites in Sn-beta zeolites, and their optimisation by the combination of theoretical and experimental studies. *J. Catal.* **234**, 111–118 (2005).
71. Bermejo-Deval, R. *et al.* Metalloenzyme-like catalyzed isomerizations of sugars by Lewis acid zeolites. *Proc. Natl. Acad. Sci.* **109**, 9727 LP – 9732 (2012).
72. Li, Y.-P., Head-Gordon, M. & Bell, A. T. Analysis of the Reaction Mechanism and Catalytic Activity of Metal-Substituted Beta Zeolite for the Isomerization of Glucose to Fructose. *ACS Catal.* **4**, 1537–1545 (2014).
73. Bellussi, G., Carati, A., Clerici, M. G., Maddinelli, G. & Millini, R. Reactions of titanium silicalite with protic molecules and hydrogen peroxide. *J. Catal.* **133**, 220–230 (1992).

- 
74. Wolf, P. *et al.* NMR Signatures of the Active Sites in Sn- $\beta$  Zeolite. *Angew. Chemie Int. Ed.* **53**, 10179–10183 (2014).
75. Hwang, S.-J. *et al.* Solid State NMR Characterization of Sn-Beta Zeolites that Catalyze Glucose Isomerization and Epimerization. *Top. Catal.* **58**, 435–440 (2015).
76. Yakimov, A. V, Kolyagin, Y. G., Tolborg, S., Vennestrom, P. N. R. & Ivanova, I. I.  $^{119}\text{Sn}$  MAS NMR Study of the Interaction of Probe Molecules with Sn-BEA: The Origin of Penta- and Hexacoordinated Tin Formation. *J. Phys. Chem. C* **120**, 28083–28092 (2016).
77. Josephson, T. R., Jenness, G. R., Vlachos, D. G. & Caratzoulas, S. Distribution of open sites in Sn-Beta zeolite. *Microporous Mesoporous Mater.* **245**, 45–50 (2017).
78. Yang, G., Pidko, E. A. & Hensen, E. J. M. The Mechanism of Glucose Isomerization to Fructose over Sn-BEA Zeolite: A Periodic Density Functional Theory Study. *ChemSusChem* **6**, 1688–1696 (2013).
79. Li, G., Pidko, E. A. & Hensen, E. J. M. Synergy between Lewis acid sites and hydroxyl groups for the isomerization of glucose to fructose over Sn-containing zeolites: a theoretical perspective. *Catal. Sci. Technol.* **4**, 2241–2250 (2014).
80. Courtney, T. D. *et al.* Effect of water treatment on Sn-BEA zeolite: Origin of 960  $\text{cm}^{-1}$  FTIR peak. *Microporous Mesoporous Mater.* **210**, 69–76 (2015).
81. Rai, N., Caratzoulas, S. & Vlachos, D. G. Role of Silanol Group in Sn-Beta Zeolite for Glucose Isomerization and Epimerization Reactions. *ACS Catal.* **3**, 2294–2298 (2013).
82. Bermejo-Deval, R., Orazov, M., Gounder, R., Hwang, S.-J. & Davis, M. E. Active Sites in Sn-Beta for Glucose Isomerization to Fructose and Epimerization to Mannose. *ACS Catal.* **4**, 2288–2297 (2014).
83. Gunther, W. R. *et al.* Sn-Beta zeolites with borate salts catalyse the epimerization of carbohydrates via an intramolecular carbon shift. *Nat. Commun.* **3**, 1109 (2012).
84. Brand, S. K., Labinger, J. A. & Davis, M. E. Tin Silsesquioxanes as Models for the “Open” Site in Tin-Containing Zeolite Beta. *ChemCatChem* **8**, 121–124 (2016).
85. Josephson, T. R., Brand, S. K., Caratzoulas, S. & Vlachos, D. G. 1,2-H- versus 1,2-C-Shift on Sn-Silsesquioxanes. *ACS Catal.* **7**, 25–33 (2017).
86. Brand, S. K. *et al.* Methyl-ligated tin silsesquioxane catalyzed reactions of glucose. *J. Catal.* **341**, 62–71 (2016).
87. Otomo, R., Kosugi, R., Kamiya, Y., Tatsumi, T. & Yokoi, T. Modification of Sn-Beta zeolite: characterization of acidic/basic properties and catalytic performance in Baeyer–Villiger oxidation. *Catal. Sci. Technol.* **6**, 2787–2795 (2016).
88. Li, S., Josephson, T., Vlachos, D. G. & Caratzoulas, S. The origin of selectivity in the conversion of glucose to fructose and mannose in Sn-BEA and Na-exchanged Sn-BEA zeolites. *J. Catal.* **355**, 11–16 (2017).
89. Hammond, C. *et al.* Identification of Active and Spectator Sn Sites in Sn- $\beta$  Following Solid-State Stannation, and Consequences for Lewis Acid Catalysis. *ChemCatChem* **7**, 3322–3331 (2015).
90. Hammond, C. *et al.* Elucidation and Evolution of the Active Component within Cu/Fe/ZSM-5 for Catalytic Methane Oxidation: From Synthesis to Catalysis. *ACS Catal.* **3**, 689–699 (2013).
91. Bare, S. R. *et al.* Uniform Catalytic Site in Sn- $\beta$ -Zeolite Determined Using X-ray Absorption Fine Structure. *J. Am. Chem. Soc.* **127**, 12924–12932 (2005).
-

92. Farneth, W. E. & Gorte, R. J. Methods for Characterizing Zeolite Acidity. *Chem. Rev.* **95**, 615–635 (1995).
93. Harris, J. W. *et al.* Titration and quantification of open and closed Lewis acid sites in Sn-Beta zeolites that catalyze glucose isomerization. *J. Catal.* **335**, 141–154 (2016).
94. Parrillo, D. J., Adamo, A. T., Kokotailo, G. T. & Gorte, R. J. Amine adsorption in H-ZSM-5. *Appl. Catal.* **67**, 107–118 (1990).
95. Pelmenschikov, A. G., van Santen, R. A., Janchen, J. & Meijer, E. Acetonitrile-d<sub>3</sub> as a probe of Lewis and Brønsted acidity of zeolites. *J. Phys. Chem.* **97**, 11071–11074 (1993).
96. Roy, S., Bakhmutsky, K., Mahmoud, E., Lobo, R. F. & Gorte, R. J. Probing Lewis Acid Sites in Sn-Beta Zeolite. *ACS Catal.* **3**, 573–580 (2013).
97. Sushkevich, V. L., Ivanova, I. I. & Yakimov, A. V. Revisiting Acidity of SnBEA Catalysts by Combined Application of FTIR Spectroscopy of Different Probe Molecules. *J. Phys. Chem. C* **121**, 11437–11447 (2017).
98. Gunther, W. R., Michaelis, V. K., Griffin, R. G. & Román-Leshkov, Y. Interrogating the Lewis Acidity of Metal Sites in Beta Zeolites with <sup>15</sup>N Pyridine Adsorption Coupled with MAS NMR Spectroscopy. *J. Phys. Chem. C* **120**, 28533–28544 (2016).
99. Lewis, J. D. *et al.* Distinguishing Active Site Identity in Sn-Beta Zeolites Using <sup>31</sup>P MAS NMR of Adsorbed Trimethylphosphine Oxide. *ACS Catal.* **8**, 3076–3086 (2018).
100. Sádaba, I., López Granados, M., Riisager, A. & Taarning, E. Deactivation of solid catalysts in liquid media: the case of leaching of active sites in biomass conversion reactions. *Green Chem.* **17**, 4133–4145 (2015).
101. Hammond, C. Intensification studies of heterogeneous catalysts: probing and overcoming catalyst deactivation during liquid phase operation. *Green Chem.* **19**, 2711–2728 (2017).
102. Yakabi, K., Milne, K., Buchard, A. & Hammond, C. Selectivity and Lifetime Effects in Zeolite-Catalysed Baeyer–Villiger Oxidation Investigated in Batch and Continuous Flow. *ChemCatChem* **8**, 3490–3498 (2016).
103. Yakabi, K. *et al.* Continuous Production of Biorenewable, Polymer-Grade Lactone Monomers through Sn-β-Catalyzed Baeyer–Villiger Oxidation with H<sub>2</sub>O<sub>2</sub>. *ChemSusChem* **10**, 3652–3659 (2017).
104. Al-Nayili, A., Yakabi, K. & Hammond, C. Hierarchically porous BEA stannosilicates as unique catalysts for bulky ketone conversion and continuous operation. *J. Mater. Chem. A* **4**, 1373–1382 (2016).
105. Lari, G. M. *et al.* Deactivation mechanisms of tin-zeolites in biomass conversions. *Green Chem.* **18**, 1249–1260 (2016).
106. van der Graaff, W. N. P. *et al.* Deactivation of Sn-Beta during carbohydrate conversion. *Appl. Catal. A Gen.* **564**, 113–122 (2018).
107. Padovan, D., Parsons, C., Simplicio Grasina, M. & Hammond, C. Intensification and deactivation of Sn-beta investigated in the continuous regime. *Green Chem.* **18**, 5041–5049 (2016).
108. Cordon, M. J. *et al.* Deactivation of Sn-Beta zeolites caused by structural transformation of hydrophobic to hydrophilic micropores during aqueous-phase glucose isomerization. *Catal. Sci. Technol.* (2019). doi:10.1039/C8CY02589D
109. Padovan, D., Botti, L. & Hammond, C. Active Site Hydration Governs the Stability of Sn-Beta during Continuous Glucose Conversion. *ACS Catal.* **8**, 7131–7140 (2018).

- 
110. Padovan, D. *et al.* Overcoming catalyst deactivation during the continuous conversion of sugars to chemicals: maximising the performance of Sn-Beta with a little drop of water. *React. Chem. Eng.* **3**, 155–163 (2018).
111. Holm, M. S., Saravanamurugan, S. & Taarning, E. Conversion of Sugars to Lactic Acid Derivatives Using Heterogeneous Zeotype Catalysts. *Science (80-. )*. **328**, 602–605 (2010).
112. Tolborg, S. *et al.* Tin-containing silicates: identification of a glycolytic pathway via 3-deoxyglucosone. *Green Chem.* **18**, 3360–3369 (2016).
113. BP plc. Available at: <https://www.bp.com/>.
114. U.S. Energy Information Administration. Available at: <https://www.eia.gov/>.
115. Joint science academies' statement: Global response to climate change. (2005).
116. Taarning, E. *et al.* Zeolite-catalyzed biomass conversion to fuels and chemicals. *Energy Environ. Sci.* **4**, 793–804 (2011).
117. Vennestrom, P. N. R., Osmundsen, C. M., Christensen, C. H. & Taarning, E. Beyond Petrochemicals: The Renewable Chemicals Industry. *Angew. Chemie Int. Ed.* **50**, 10502–10509 (2011).
118. Osmundsen, C. M., Egeblad, K. & Taarning, E. Chapter 4 - Trends and Challenges in Catalytic Biomass Conversion. in (ed. Suib, S. L. B. T.-N. and F. D. in C.) 73–89 (Elsevier, 2013). doi:<https://doi.org/10.1016/B978-0-444-53878-9.00004-7>
119. Bonechi, C. *et al.* 1 - Biomass: An overview. in (eds. Dalena, F., Basile, A. & Rossi, C. B. T.-B. S. for the F.) 3–42 (Woodhead Publishing, 2017). doi:<https://doi.org/10.1016/B978-0-08-101031-0.00001-6>
120. Vision for Bioenergy and Biobased Products in the United States. Available at: [https://www1.eere.energy.gov/bioenergy/pdfs/final\\_2006\\_vision.pdf](https://www1.eere.energy.gov/bioenergy/pdfs/final_2006_vision.pdf).
121. Rouilly, A. & Vaca-Garcia, C. Bio-Based Materials. *Introduction to Chemicals from Biomass* (2015). doi:doi:10.1002/9781118714478.ch6
122. Deneyer, A., Ennaert, T. & Sels, B. F. Straightforward sustainability assessment of sugar-derived molecules from first-generation biomass. *Curr. Opin. Green Sustain. Chem.* **10**, 11–20 (2018).
123. Carus, M. & Dammer, L. Food or Non-Food: Which Agricultural Feedstocks Are Best for Industrial Uses? *Ind. Biotechnol.* **9**, 171–176 (2013).
124. Abdelaziz, O. Y. & Hultberg, C. P. Physicochemical Characterisation of Technical Lignins for Their Potential Valorisation. *Waste and Biomass Valorization* **8**, 859–869 (2017).
125. Li, H., Yang, S., Saravanamurugan, S. & Riisager, A. Glucose Isomerization by Enzymes and Chemo-catalysts: Status and Current Advances. *ACS Catal.* **7**, 3010–3029 (2017).
126. Vuilleumier, S. Worldwide production of high-fructose syrup and crystalline fructose. *Am. J. Clin. Nutr.* **58**, 733S–736S (1993).
127. Zhang, Z. & Deng, K. Recent Advances in the Catalytic Synthesis of 2,5-Furandicarboxylic Acid and Its Derivatives. *ACS Catal.* **5**, 6529–6544 (2015).
128. Allen, K. N. *et al.* Isotopic Exchange plus Substrate and Inhibition Kinetics of D-Xylose Isomerase Do Not Support a Proton-Transfer Mechanism. *Biochemistry* **33**, 1481–1487 (1994).
129. de Bruyn, C. A. L. & van Ekenstein, W. A. Action des alcalis sur les sucres, II. Transformation réciproque des uns dans les autres des sucres glucose, fructose et mannose. *Recl. des Trav. Chim. des Pays-Bas* **14**, 203–216 (1895).
-

130. Chheda, J. N., Román-Leshkov, Y. & Dumesic, J. A. Production of 5-hydroxymethylfurfural and furfural by dehydration of biomass-derived mono- and poly-saccharides. *Green Chem.* **9**, 342–350 (2007).
131. Enslow, K. R. & Bell, A. T. SnCl<sub>4</sub>-catalyzed isomerization/dehydration of xylose and glucose to furanics in water. *Catal. Sci. Technol.* **5**, 2839–2847 (2015).
132. Nguyen, H., Nikolakis, V. & Vlachos, D. G. Mechanistic Insights into Lewis Acid Metal Salt-Catalyzed Glucose Chemistry in Aqueous Solution. *ACS Catal.* **6**, 1497–1504 (2016).
133. Sowden, J. C. & Schaffer, R. The Isomerization of D-Glucose by Alkali in D<sub>2</sub>O at 25°1. *J. Am. Chem. Soc.* **74**, 505–507 (1952).
134. Lima, S. *et al.* Isomerization of d-glucose to d-fructose over metallosilicate solid bases. *Appl. Catal. A Gen.* **339**, 21–27 (2008).
135. Lecomte, J., Finiels, A. & Moreau, C. Kinetic Study of the Isomerization of Glucose into Fructose in the Presence of Anion-modified Hydrotalcites. *Starch - Stärke* **54**, 75–79 (2002).
136. Holm, M. S. *et al.* Sn-Beta catalysed conversion of hemicellulosic sugars. *Green Chem.* **14**, 702–706 (2012).
137. Román-Leshkov, Y., Moliner, M., Labinger, J. A. & Davis, M. E. Mechanism of Glucose Isomerization Using a Solid Lewis Acid Catalyst in Water. *Angew. Chemie Int. Ed.* **49**, 8954–8957 (2010).
138. Choudhary, V., Pinar, A. B., Sandler, S. I., Vlachos, D. G. & Lobo, R. F. Xylose Isomerization to Xylulose and its Dehydration to Furfural in Aqueous Media. *ACS Catal.* **1**, 1724–1728 (2011).
139. Gounder, R. & Davis, M. E. Titanium-Beta Zeolites Catalyze the Stereospecific Isomerization of d-Glucose to l-Sorbose via Intramolecular C5–C1 Hydride Shift. *ACS Catal.* **3**, 1469–1476 (2013).
140. Zebiri, I., Balieu, S., Guilleret, A., Reynaud, R. & Haudrechy, A. The Chemistry of L-Sorbose. *European J. Org. Chem.* **2011**, 2905–2910 (2011).
141. Lew, C. M., Rajabbeigi, N. & Tsapatsis, M. Tin-containing zeolite for the isomerization of cellulosic sugars. *Microporous Mesoporous Mater.* **153**, 55–58 (2012).
142. Bermejo-Deval, R., Gounder, R. & Davis, M. E. Framework and Extraframework Tin Sites in Zeolite Beta React Glucose Differently. *ACS Catal.* **2**, 2705–2713 (2012).
143. Christianson, J. R., Caratzoulas, S. & Vlachos, D. G. Computational Insight into the Effect of Sn-Beta Na Exchange and Solvent on Glucose Isomerization and Epimerization. *ACS Catal.* **5**, 5256–5263 (2015).
144. Chethana, B. K. & Mushrif, S. H. Brønsted and Lewis acid sites of Sn-beta zeolite, in combination with the borate salt, catalyze the epimerization of glucose: A density functional theory study. *J. Catal.* **323**, 158–164 (2015).
145. Moliner, M. State of the art of Lewis acid-containing zeolites: lessons from fine chemistry to new biomass transformation processes. *Dalt. Trans.* **43**, 4197–4208 (2014).
146. Choudhary, V., Pinar, A. B., Lobo, R. F., Vlachos, D. G. & Sandler, S. I. Comparison of Homogeneous and Heterogeneous Catalysts for Glucose-to-Fructose Isomerization in Aqueous Media. *ChemSusChem* **6**, 2369–2376 (2013).
147. Rajabbeigi, N. *et al.* On the kinetics of the isomerization of glucose to fructose using Sn-Beta. *Chem. Eng. Sci.* **116**, 235–242 (2014).
148. Ren, L. *et al.* Self-Pillared, Single-Unit-Cell Sn-MFI Zeolite Nanosheets and Their Use for Glucose and Lactose Isomerization. *Angew. Chemie Int. Ed.* **54**, 10848–10851 (2015).

- 
149. Saravanamurugan, S., Paniagua, M., Melero, J. A. & Riisager, A. Efficient Isomerization of Glucose to Fructose over Zeolites in Consecutive Reactions in Alcohol and Aqueous Media. *J. Am. Chem. Soc.* **135**, 5246–5249 (2013).
150. Paniagua, M., Saravanamurugan, S., Melian-Rodriguez, M., Melero, J. A. & Riisager, A. Xylose Isomerization with Zeolites in a Two-Step Alcohol–Water Process. *ChemSusChem* **8**, 1088–1094 (2015).
151. Saravanamurugan, S. & Riisager, A. Zeolite-catalyzed isomerization of tetroses in aqueous medium. *Catal. Sci. Technol.* **4**, 3186–3190 (2014).
152. Saravanamurugan, S., Riisager, A., Taarning, E. & Meier, S. Combined Function of Brønsted and Lewis Acidity in the Zeolite-Catalyzed Isomerization of Glucose to Fructose in Alcohols. *ChemCatChem* **8**, 3107–3111 (2016).
153. Saravanamurugan, S., Riisager, A., Taarning, E. & Meier, S. Mechanism and stereoselectivity of zeolite-catalysed sugar isomerisation in alcohols. *Chem. Commun.* **52**, 12773–12776 (2016).
154. Saravanamurugan, S. & Riisager, A. Zeolite Catalyzed Transformation of Carbohydrates to Alkyl Levulinates. *ChemCatChem* **5**, 1754–1757 (2013).
155. Saravanamurugan, S. & Riisager, A. Solid acid catalysed formation of ethyl levulinate and ethyl glucopyranoside from mono- and disaccharides. *Catal. Commun.* **17**, 71–75 (2012).
156. Li, H., Saravanamurugan, S., Yang, S. & Riisager, A. Direct transformation of carbohydrates to the biofuel 5-ethoxymethylfurfural by solid acid catalysts. *Green Chem.* **18**, 726–734 (2016).
157. Komesu, A., Oliveira, J. A. R. de, Martins, L. H. da S., Wolf Maciel, M. R. & Maciel Filho, R. Lactic Acid Production to Purification: A Review. *Bioresour. Vol 12, No 2* (2017).
158. Dusselier, M., Van Wouwe, P., Dewaele, A., Makshina, E. & Sels, B. F. Lactic acid as a platform chemical in the biobased economy: the role of chemocatalysis. *Energy Environ. Sci.* **6**, 1415–1442 (2013).
159. Hayashi, Y. & Sasaki, Y. Tin-catalyzed conversion of trioses to alkyl lactates in alcohol solution. *Chem. Commun.* 2716–2718 (2005). doi:10.1039/B501964H
160. De Clercq, R., Dusselier, M. & Sels, B. F. Heterogeneous catalysis for bio-based polyester monomers from cellulosic biomass: advances, challenges and prospects. *Green Chem.* **19**, 5012–5040 (2017).
161. Rasrendra, C. B., Fachri, B. A., Makertihartha, I. G. B. N., Adisasmito, S. & Heeres, H. J. Catalytic Conversion of Dihydroxyacetone to Lactic Acid Using Metal Salts in Water. *ChemSusChem* **4**, 768–777 (2011).
162. Janssen, K. P. F., Paul, J. S., Sels, B. F. & Jacobs, P. A. Glyoxylase biomimics: zeolite catalyzed conversion of trioses. in *From Zeolites to Porous MOF Materials - The 40th Anniversary of International Zeolite Conference* (eds. Xu, R., Gao, Z., Chen, J. & Yan, W. B. T.-S. in S. S. and C.) **170**, 1222–1227 (Elsevier, 2007).
163. Pescarmona, P. P. *et al.* Zeolite-catalysed conversion of C3 sugars to alkyl lactates. *Green Chem.* **12**, 1083–1089 (2010).
164. West, R. M. *et al.* Zeolite H-USY for the production of lactic acid and methyl lactate from C3-sugars. *J. Catal.* **269**, 122–130 (2010).
165. de Clippel, F. *et al.* Fast and Selective Sugar Conversion to Alkyl Lactate and Lactic Acid with Bifunctional Carbon–Silica Catalysts. *J. Am. Chem. Soc.* **134**, 10089–10101 (2012).
166. Pighin, E. A., Di Cosimo, J. I. & Díez, V. K. Kinetic and mechanistic study of triose sugar conversion on Lewis and Brønsted acid solids. *Mol. Catal.* **458**, 189–197 (2018).
-



167. Yang, L. *et al.* Mechanistic insights into the production of methyl lactate by catalytic conversion of carbohydrates on mesoporous Zr-SBA-15. *J. Catal.* **333**, 207–216 (2016).
168. Elliot, S. G., Tolborg, S., Madsen, R., Taarning, E. & Meier, S. Effects of Alkali-Metal Ions and Counter Ions in Sn-Beta-Catalyzed Carbohydrate Conversion. *ChemSusChem* **11**, 1198–1203 (2018).
169. Dusselier, M. *et al.* Mechanistic Insight into the Conversion of Tetrose Sugars to Novel  $\alpha$ -Hydroxy Acid Platform Molecules. *ChemCatChem* **5**, 569–575 (2013).
170. Chen, H.-S. *et al.* Production of Hydroxyl-rich Acids from Xylose and Glucose Using Sn-BEA Zeolite. *ChemistrySelect* **1**, 4167–4172 (2016).
171. Elliot, S. G., Tolborg, S., Sádaba, I., Taarning, E. & Meier, S. Quantitative NMR Approach to Optimize the Formation of Chemical Building Blocks from Abundant Carbohydrates. *ChemSusChem* **10**, 2990–2996 (2017).
172. Elliot, S. G., Taarning, E., Madsen, R. & Meier, S. NMR Spectroscopic Isotope Tracking Reveals Cascade Steps in Carbohydrate Conversion by Tin-Beta. *ChemCatChem* **10**, 1414–1419 (2018).
173. Romano, A. H. & Conway, T. Evolution of carbohydrate metabolic pathways. *Res. Microbiol.* **147**, 448–455 (1996).
174. Elliot, S. G. *et al.* Synthesis of a novel polyester building block from pentoses by tin-containing silicates. *RSC Adv.* **7**, 985–996 (2017).
175. Richards, G. N. Glycolaldehyde from pyrolysis of cellulose. *J. Anal. Appl. Pyrolysis* **10**, 251–255 (1987).
176. Zhou, X., Li, W., Mabon, R. & Broadbelt, L. J. A mechanistic model of fast pyrolysis of hemicellulose. *Energy Environ. Sci.* **11**, 1240–1260 (2018).
177. Vinu, R. & Broadbelt, L. J. A mechanistic model of fast pyrolysis of glucose-based carbohydrates to predict bio-oil composition. *Energy Environ. Sci.* **5**, 9808–9826 (2012).
178. Vitasari, C. R., Meindersma, G. W. & de Haan, A. B. Laboratory scale conceptual process development for the isolation of renewable glycolaldehyde from pyrolysis oil to produce fermentation feedstock. *Green Chem.* **14**, 321–325 (2012).
179. Li, X., Kersten, S. R. A. & Schuur, B. Extraction of acetic acid, glycolaldehyde and acetol from aqueous solutions mimicking pyrolysis oil cuts using ionic liquids. *Sep. Purif. Technol.* **175**, 498–505 (2017).
180. Sasaki, M., Goto, K., Tajima, K., Adschiri, T. & Arai, K. Rapid and selective retro-aldol condensation of glucose to glycolaldehyde in supercritical water. *Green Chem.* **4**, 285–287 (2002).
181. Wang, T. & Bowie, J. H. Radical routes to interstellar glycolaldehyde. The possibility of stereoselectivity in gas-phase polymerization reactions involving CH<sub>2</sub>O and  $\dot{\text{C}}\text{H}_2\text{OH}$ . *Org. Biomol. Chem.* **8**, 4757–4766 (2010).
182. Kim, H.-J. *et al.* Synthesis of Carbohydrates in Mineral-Guided Prebiotic Cycles. *J. Am. Chem. Soc.* **133**, 9457–9468 (2011).
183. Dusselier, M. *et al.* Toward Functional Polyester Building Blocks from Renewable Glycolaldehyde with Sn Cascade Catalysis. *ACS Catal.* **3**, 1786–1800 (2013).
184. De Clercq, R. *et al.* Confinement Effects in Lewis Acid-Catalyzed Sugar Conversion: Steering Toward Functional Polyester Building Blocks. *ACS Catal.* **5**, 5803–5811 (2015).
185. Tolborg, S. *et al.* Shape-selective Valorization of Biomass-derived Glycolaldehyde using Tin-containing Zeolites. *ChemSusChem* **9**, 3054–3061 (2016).

- 
186. Kishida, H., Jin, F., Yan, X., Moriya, T. & Enomoto, H. Formation of lactic acid from glycolaldehyde by alkaline hydrothermal reaction. *Carbohydr. Res.* **341**, 2619–2623 (2006).
187. Yamaguchi, S. & Baba, T. A Novel Strategy for Biomass Upgrade: Cascade Approach to the Synthesis of Useful Compounds via C-C Bond Formation Using Biomass-Derived Sugars as Carbon Nucleophiles. *Molecules* **21**, (2016).
188. Yamaguchi, S. *et al.* Mechanistic Studies on the Cascade Conversion of 1,3-Dihydroxyacetone and Formaldehyde into  $\alpha$ -Hydroxy- $\gamma$ -butyrolactone. *ChemSusChem* **8**, 853–860 (2015).
189. Van de Vyver, S., Odermatt, C., Romero, K., Prasomsri, T. & Román-Leshkov, Y. Solid Lewis Acids Catalyze the Carbon–Carbon Coupling between Carbohydrates and Formaldehyde. *ACS Catal.* **5**, 972–977 (2015).
190. Dewaele, A. *et al.* Synthesis of Novel Renewable Polyesters and Polyamides with Olefin Metathesis. *ACS Sustain. Chem. Eng.* **4**, 5943–5952 (2016).
191. Sølvhøj, A., Taarning, E. & Madsen, R. Methyl vinyl glycolate as a diverse platform molecule. *Green Chem.* **18**, 5448–5455 (2016).
192. He, Z., Wu, J., Gao, B. & He, H. Hydrothermal Synthesis and Characterization of Aluminum-Free Mn- $\beta$  Zeolite: A Catalyst for Phenol Hydroxylation. *ACS Appl. Mater. Interfaces* **7**, 2424–2432 (2015).
193. García-Martínez, J., Johnson, M., Valla, J., Li, K. & Ying, J. Y. Mesoporous zeolite Y—high hydrothermal stability and superior FCC catalytic performance. *Catal. Sci. Technol.* **2**, 987–994 (2012).
194. Goto, Y. *et al.* Mesoporous Material from Zeolite. *J. Porous Mater.* **9**, 43–48 (2002).
195. Wang, L., Zhang, Z., Yin, C., Shan, Z. & Xiao, F.-S. Hierarchical mesoporous zeolites with controllable mesoporosity templated from cationic polymers. *Microporous Mesoporous Mater.* **131**, 58–67 (2010).
196. Tosi, I., Riisager, A., Taarning, E., Jensen, P. R. & Meier, S. Kinetic analysis of hexose conversion to methyl lactate by Sn-Beta: effects of substrate masking and of water. *Catal. Sci. Technol.* **8**, 2137–2145 (2018).
197. Elliot, S. G., Tosi, I., Riisager, A., Taarning, E. & Meier, S. Response Factors Enable Rapid Quantitative 2D NMR Analysis in Catalytic Biomass Conversion to Renewable Chemicals. *Top. Catal.* (2019). doi:10.1007/s11244-019-01131-y
198. Moreau, C. *et al.* Hydrolysis of sucrose in the presence of H-form zeolites. *Ind. Crops Prod.* **11**, 237–242 (2000).
199. Agrawal, P. K. NMR Spectroscopy in the structural elucidation of oligosaccharides and glycosides. *Phytochemistry* **31**, 3307–3330 (1992).
200. Saravanamurugan, S. *et al.* Facile and benign conversion of sucrose to fructose using zeolites with balanced Brønsted and Lewis acidity. *Catal. Sci. Technol.* **7**, 2782–2788 (2017).
201. Levin, G. V. Tagatose, the New GRAS Sweetener and Health Product. *J. Med. Food* **5**, 23–36 (2002).
202. Torres, A. I., Daoutidis, P. & Tsapatsis, M. Continuous production of 5-hydroxymethylfurfural from fructose: a design case study. *Energy Environ. Sci.* **3**, 1560–1572 (2010).
203. Chernyshev, V. M., Kravchenko, O. A. & Ananikov, V. P. Conversion of plant biomass to furan derivatives and sustainable access to the new generation of polymers, functional materials and fuels. *Russ. Chem. Rev.* **86**, 357–387 (2017).
204. STINSON, S. Use of microwave heating to speed organic reactions continues to grow. *Chem. Eng. News*
-

- Arch.* **74**, 45–46 (1996).
205. van Putten, R.-J., van der Waal, J. C., de Jong, E. & Heeres, H. J. Reactivity studies in water on the acid-catalysed dehydration of psicose compared to other ketohexoses into 5-hydroxymethylfurfural. *Carbohydr. Res.* **446–447**, 1–6 (2017).
206. De, S. K. & Gibbs, R. A. Ruthenium(III) chloride-catalyzed chemoselective synthesis of acetals from aldehydes. *Tetrahedron Lett.* **45**, 8141–8144 (2004).
207. Granström, T. B., Takata, G., Tokuda, M. & Izumori, K. Izumoring: A novel and complete strategy for bioproduction of rare sugars. *J. Biosci. Bioeng.* **97**, 89–94 (2004).
208. Herrmann, C., Haas, J. & Fetting, F. Effect of the crystal size on the activity of ZSM-5 catalysts in various reactions. *Appl. Catal.* **35**, 299–310 (1987).
209. Serrano, D. P., Melero, J. A., Morales, G., Iglesias, J. & Pizarro, P. Progress in the design of zeolite catalysts for biomass conversion into biofuels and bio-based chemicals. *Catal. Rev.* **60**, 1–70 (2018).
210. Derouane, E. G. Shape selectivity in catalysis by zeolites: The nest effect. *J. Catal.* **100**, 541–544 (1986).
211. Barclay, T., Ginic-Markovic, M., Johnston, M. R., Cooper, P. D. & Petrovsky, N. Analysis of the hydrolysis of inulin using real time <sup>1</sup>H NMR spectroscopy. *Carbohydr. Res.* **352**, 117–125 (2012).
212. Tosi, I., Sacchetti, A., Martinez-Espin, J. S., Meier, S. & Riisager, A. Exploring the Synthesis of Mesoporous Stannosilicates as Catalysts for the Conversion of Mono- and Oligosaccharides into Methyl Lactate. *Top. Catal.* (2019). doi:10.1007/s11244-019-01135-8
213. Bordiga, S., Lamberti, C., Bonino, F., Travert, A. & Thibault-Starzyk, F. Probing zeolites by vibrational spectroscopies. *Chem. Soc. Rev.* **44**, 7262–7341 (2015).
214. Conrad, S. *et al.* Silica-Grafted SnIV Catalysts in Hydrogen-Transfer Reactions. *ChemCatChem* **7**, 3270–3278 (2015).
215. Bordiga, S. *et al.* Hydroxyls nests in defective silicalites and strained structures derived upon dehydroxylation: vibrational properties and theoretical modelling. *Top. Catal.* **15**, 43–52 (2001).
216. Yin, F., Blumenfeld, A. L., Gruver, V. & Fripiat, J. J. NH<sub>3</sub> as a Probe Molecule for NMR and IR Study of Zeolite Catalyst Acidity. *J. Phys. Chem. B* **101**, 1824–1830 (1997).
217. Bodoardo, S., Chiappetta, R., Onida, B., Figueras, F. & Garrone, E. Ammonia interaction and reaction with Al-pillared montmorillonite: an IR study. *Microporous Mesoporous Mater.* **20**, 187–196 (1998).
218. Wilmshurst, J. K. SENSITIVE FREQUENCIES. V. THE SENSITIVE AMMINE FREQUENCIES AND ELECTRONEGATIVITIES OF COMPLEX TRANSITION METAL ION RADICALS. *Can. J. Chem.* **38**, 467–472 (1960).
219. Wang, J., Yao, G. & Jin, F. One-pot catalytic conversion of carbohydrates into alkyl lactates with Lewis acids in alcohols. *Mol. Catal.* **435**, 82–90 (2017).
220. Fierke, C. A., Huang, C. & McCall, K. A. Function and Mechanism of Zinc Metalloenzymes. *J. Nutr.* **130**, 1437S–1446S (2000).
221. Xia, M. *et al.* Synergetic effects of bimetals in modified beta zeolite for lactic acid synthesis from biomass-derived carbohydrates. *RSC Adv.* **8**, 8965–8975 (2018).
222. Dong, W. *et al.* Selective Chemical Conversion of Sugars in Aqueous Solutions without Alkali to Lactic Acid Over a Zn-Sn-Beta Lewis Acid-Base Catalyst. *Sci. Rep.* **6**, 26713 (2016).
223. Liang, J. *et al.* Synthesis of acid–base bifunctional CaO/ITQ-2 zeolite catalyst for phosphorylation of

- dodecanol. *Catal. Commun.* **69**, 174–178 (2015).
224. Graça, I., Bacariza, M. C., Fernandes, A. & Chadwick, D. Desilicated NaY zeolites impregnated with magnesium as catalysts for glucose isomerisation into fructose. *Appl. Catal. B Environ.* **224**, 660–670 (2018).
225. Yu, I. K. M. & Tsang, D. C. W. Conversion of biomass to hydroxymethylfurfural: A review of catalytic systems and underlying mechanisms. *Bioresour. Technol.* **238**, 716–732 (2017).
226. Gandini, A. Furan Monomers and their Polymers: Synthesis, Properties and Applications. *Biopolymers – New Materials for Sustainable Films and Coatings* (2011). doi:doi:10.1002/9781119994312.ch9
227. Choudhary, V. *et al.* Insights into the Interplay of Lewis and Brønsted Acid Catalysts in Glucose and Fructose Conversion to 5-(Hydroxymethyl)furfural and Levulinic Acid in Aqueous Media. *J. Am. Chem. Soc.* **135**, 3997–4006 (2013).
228. Tosi, I. *et al.* Uncharted Pathways for CrCl<sub>3</sub> Catalyzed Glucose Conversion in Aqueous Solution. *Top. Catal.* (2019). doi:10.1007/s11244-019-01144-7
229. Choudhary, V., Burnett, R. I., Vlachos, D. G. & Sandler, S. I. Dehydration of Glucose to 5-(Hydroxymethyl)furfural and Anhydroglucose: Thermodynamic Insights. *J. Phys. Chem. C* **116**, 5116–5120 (2012).
230. B. Larson, D. & D. Emmons, W. *CHEMISTRY OF HIGH SOLIDS ALKYD/REACTIVE DILUENT COATINGS*. *Journal of Coatings Technology* **55**, (1983).
231. Decker, C. Chapter 5 - UV-Radiation Curing of Adhesives. in *Adhesives and Sealants* (ed. Cognard, P. B. T.-H. of A. and S.) **2**, 303–353 (Elsevier Science Ltd, 2006).

# Supplementary Information

In this section, additional information to the results discussed in Chapter 3-6 are enclosed.

## SI.1 Catalysts characterization

Table SI.1.1. Physical properties of the catalysts containing different amount of tin used for the conversion of glucose to ML, MVG/THM and methyl glycosides discussed in Chapter 5.1.3.

Entry	Catalyst	Elemental Analysis	X-ray diffraction	N <sub>2</sub> -adsorption S <sub>BET</sub> (m <sup>2</sup> /g)	NH <sub>3</sub> -TPD	
		Si / Metal	Primary Phase		T <sub>max</sub> °C	Absorption μmol/g
1	Sn-Beta (PT, 12.5)	20	*BEA	778	191	316.7
2	Sn-Beta (PT, 50)	45	*BEA	771	202	265.3
3	Sn-Beta (PT, 100)	98	*BEA	758	191	141.9
4	Sn-Beta (PT, 150)	152	*BEA	773	248	47.1
5	Sn-Beta (PT, 200)	165	*BEA	792	252	39.3

Table SI.1.2. Physical properties of the catalysts containing different amount of Sn used for the conversion of glycolaldehyde to MVG discussed in Chapter 5.1.3.

Entry	Catalyst	Elemental Analysis	X-ray diffraction	N <sub>2</sub> -adsorption				NH <sub>3</sub> -TPD		
		Si / Sn		S <sub>BET</sub>	S <sub>micropore</sub>	V <sub>total</sub>	V <sub>micropore</sub>	T <sub>max</sub>	Absorption	
				m <sup>2</sup> /g		mL/g		°C	μmol/g	mol/mol Sn
1	Sn-Beta (PT, 25)	23	*BEA	617	415	1.01	0.166	257	184	0.28
2	Sn-Beta (PT, 50)	50	*BEA	638	433	1.01	0.174	263	133	0.41
3	Sn-Beta (PT, 100)	98	*BEA	645	439	1.07	0.177	255	71.9	0.43
4	Sn-Beta (PT, 150)	145	*BEA	657	454	1.10	0.183	248	47.1	0.42
5	Sn-Beta (PT, 200)	198	*BEA	657	444	1.06	0.179	252	38.6	0.47
6	Sn-Beta (PT, 400)	411	*BEA	661	425	1.12	0.163	258	27.2	0.68

Table SI.1.3. Correlation between tin content and Si/Sn nominal ratio in the studied stannosilicates.

<b>Si/Sn</b>	100	150	200	400
<b>Tin (wt%)</b>	2.0	1.3	1.0	0.5

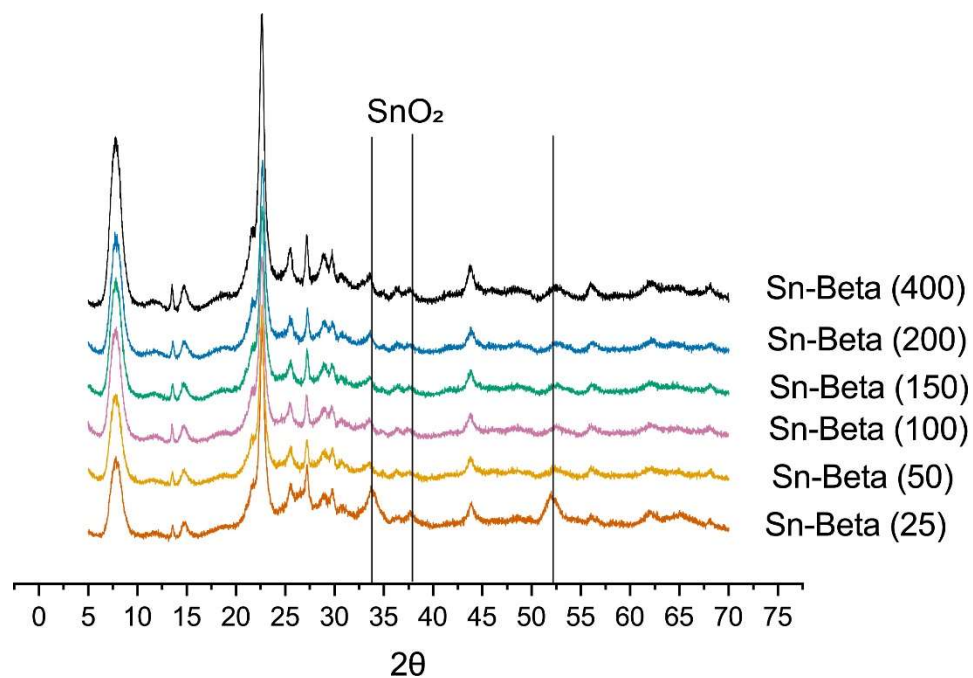


Figure SI.1.1. XRD patterns of post-treated Sn-Beta zeolites containing different amounts of tin.

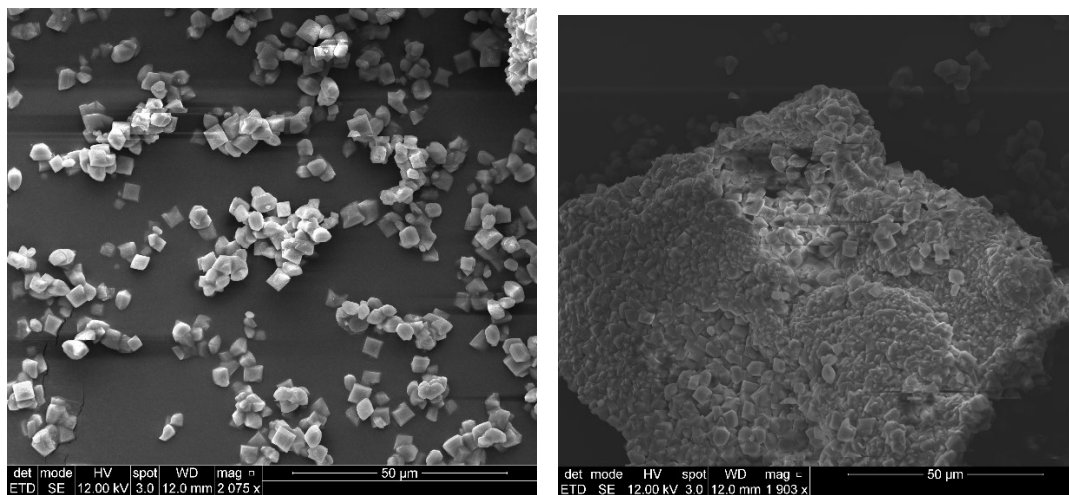


Figure SI.1.2. SEM images of hydrothermal Sn-Beta (150) zeolite discussed in Chapter 3-6.

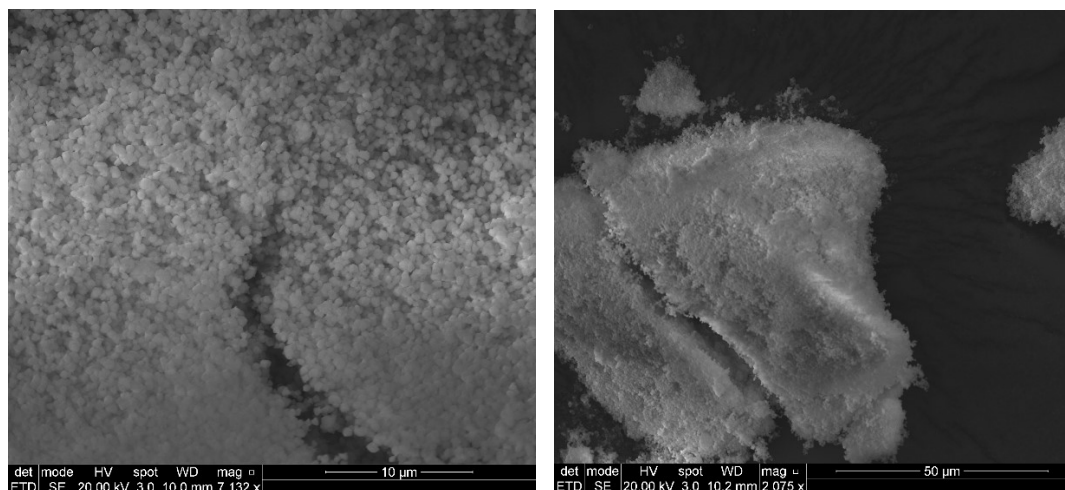


Figure SI.1.3. SEM images of post-treated Sn-Beta (150) zeolite discussed in Chapter 3-6.

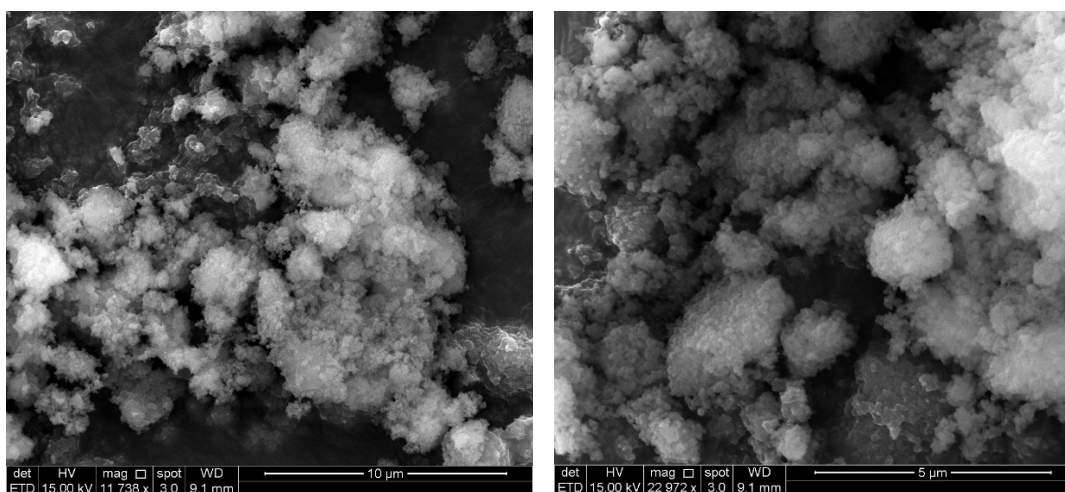


Figure SI.1.4. SEM images of post-treated Sn-Beta (25) zeolite discussed in Chapter 5-6.

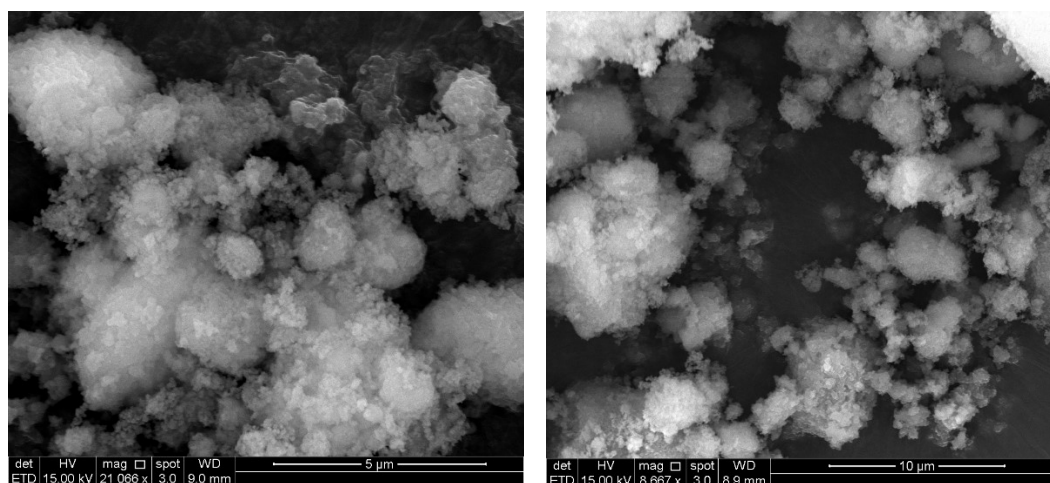


Figure SI.1.5. SEM images of Beta zeolite dealuminated by acidic treatment discussed in Chapter 3-6.

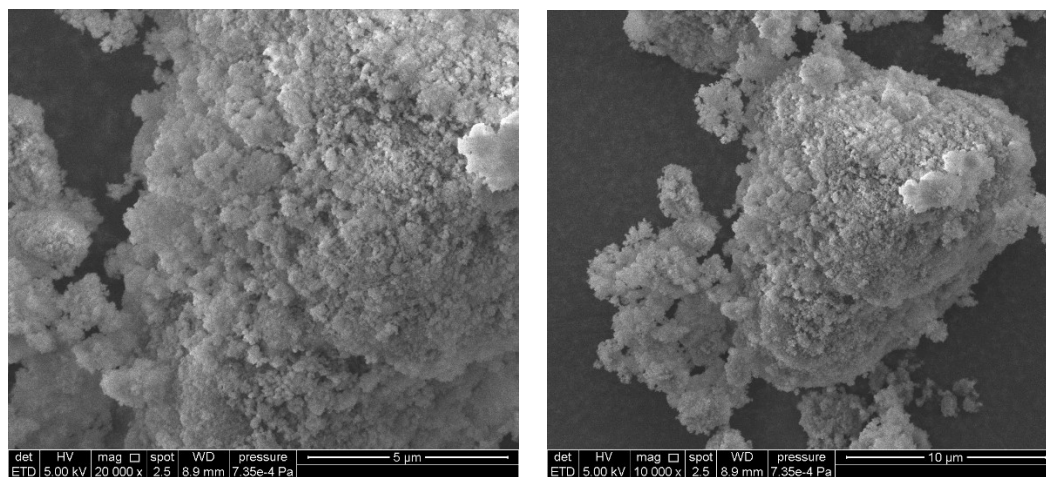


Figure SI.1.6. SEM images of Beta zeolite dealuminated by thermal treatment discussed in Chapter 3

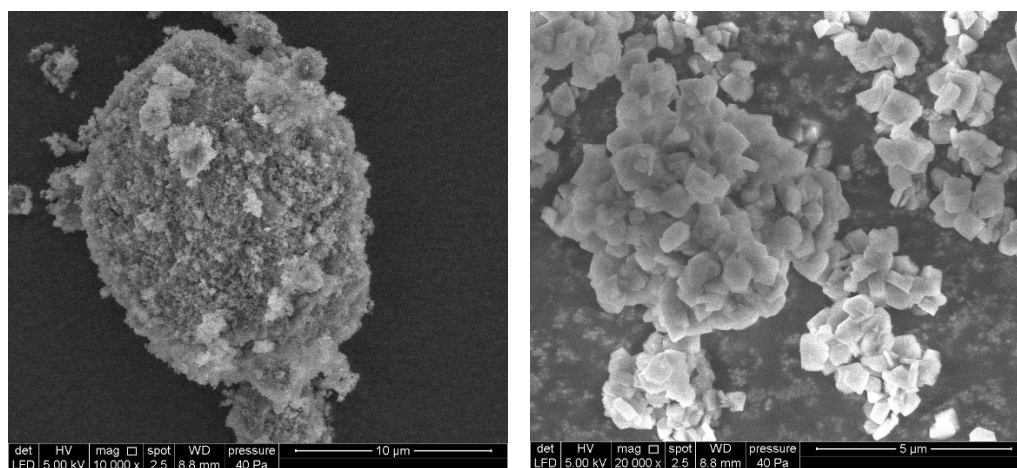


Figure SI.1.7. SEM images of the parental Beta zeolite (left) discussed in Chapter 3-6 and the parental USY zeolite (right) discussed in Chapter 5.



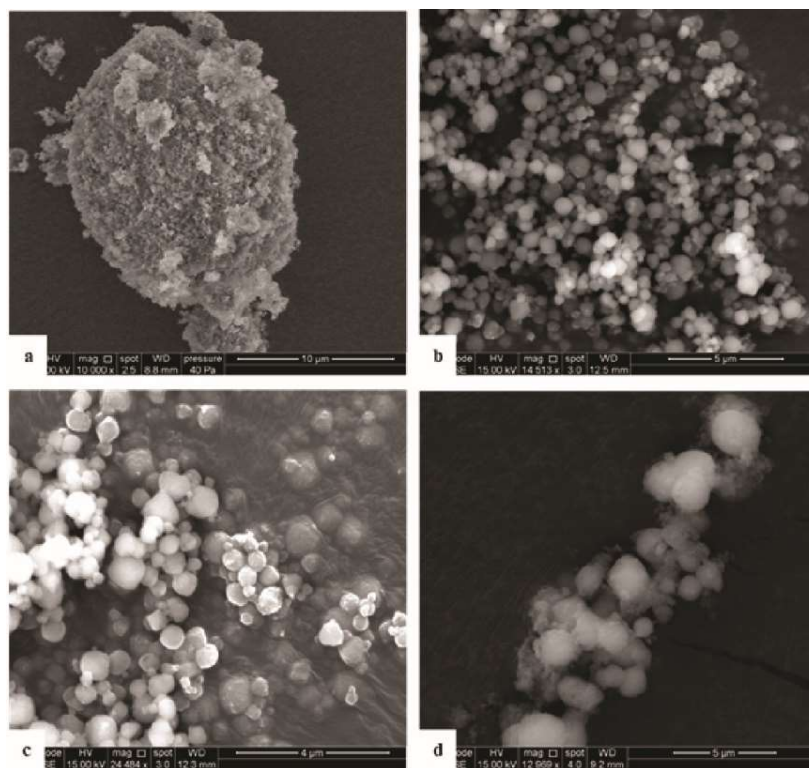


Figure SI.1.8. SEM images of the mesoporous Sn-Beta zeolites discussed in Chapter 5: a) parent H-Beta zeolite, b) microporous Sn-Beta (100), c) [deSi] Sn-Beta (100), d) hydrothermal mesoporous [HT] Sn-Beta (100). Adapted from Ref. 212.

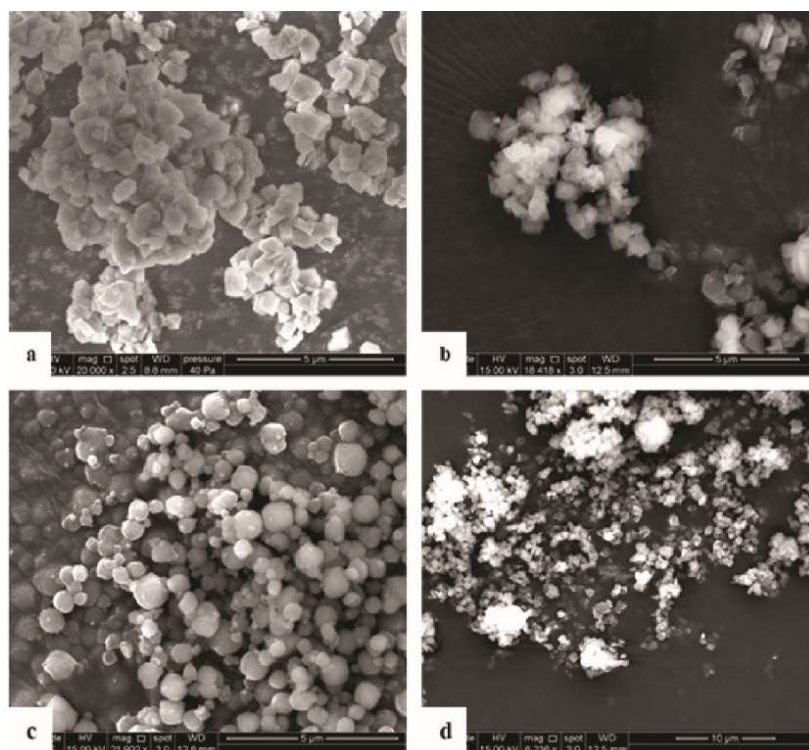


Figure SI.1.9. SEM images of the mesoporous Sn-USY zeolites discussed in Chapter 5: a) parent H-USY, b) microporous Sn-USY, c) [ST] Sn-USY (25), d) [DR] Sn-USY (25). Adapted from Ref. 212.

## SI.2 Structures

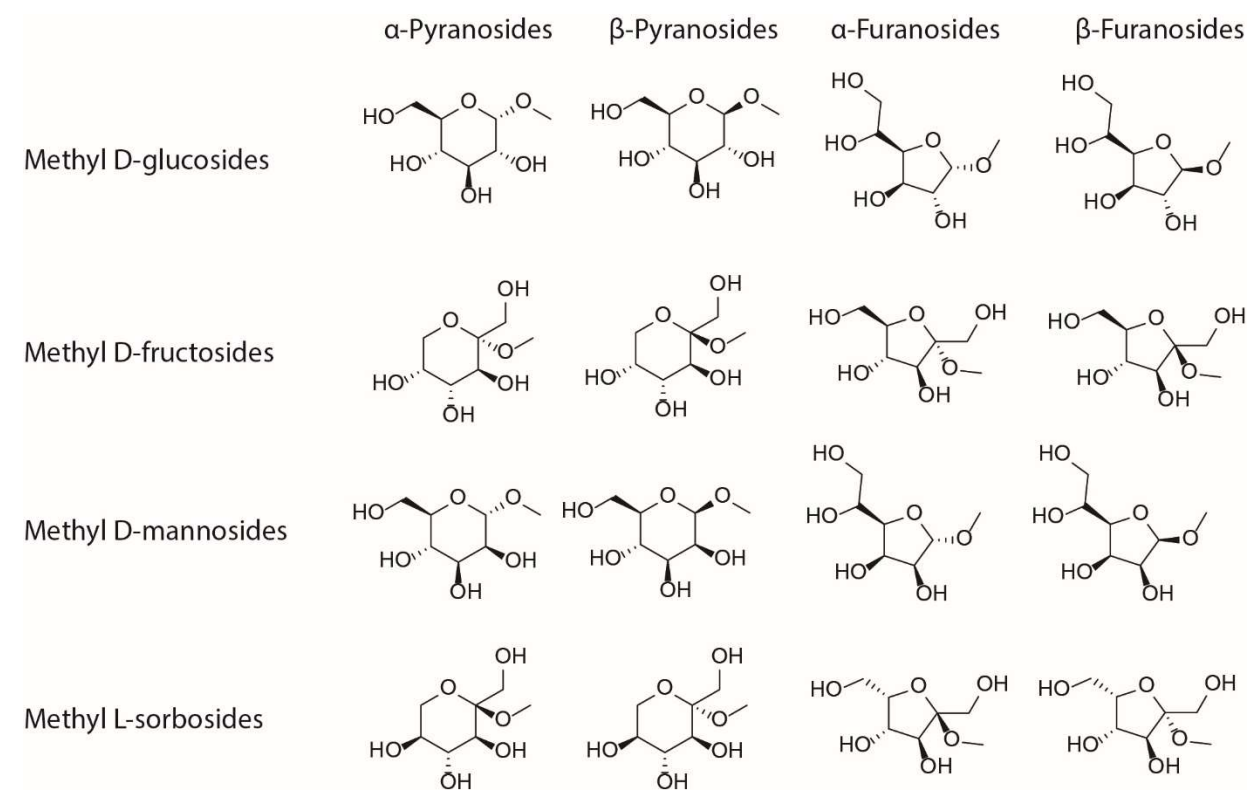
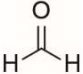
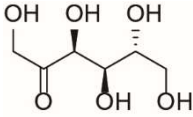
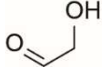
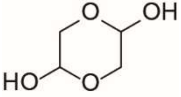
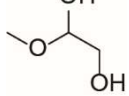
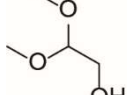
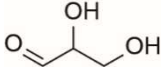
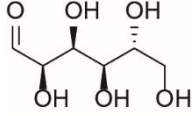
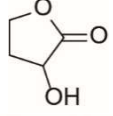
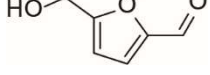
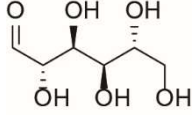
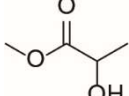
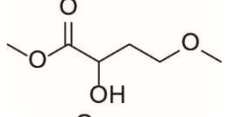
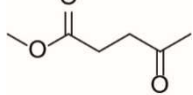
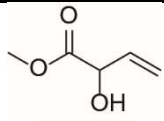
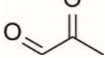
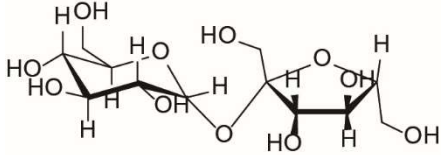
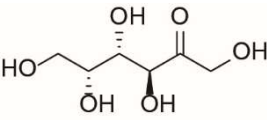
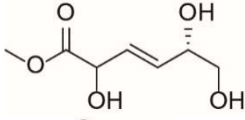
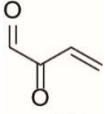
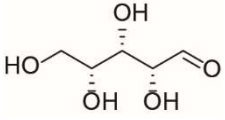
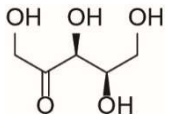


Figure SI.2.1. Structures of methyl glycosides of the hexoses discussed in Chapter 3

Table SI.2.1. Structures and names of compounds considered in this thesis

Abbreviation	Name	Structure
3DG	3-Deoxyglucosone	
DHA	Dihydroxyacetone	
DPM	Methyl 2,5-dihydroxy-3-pentenoate	
ERO	Erythrose	
ERU	Erythrulose	
Fur	Furfural	

FA	Formaldehyde	
Fru	Fructose	
GA	Glycolaldehyde	
GA dimer	Glycolaldehyde dimer	
GA-HA	Glycolaldehyde hemiacetal	
GA-DMA	Glycolaldehyde dimethyl acetal	
GLA	Glyceraldehyde	
Glu	Glucose	
HBL	3-Deoxy-γ-butyrolactone	
HMF	5-Hydroxymethylfurfural	
Man	Mannose	
ML	Methyl lactate	
MMHB	methyl 2,4-dihydroxybutanoate	
Me-Lev	Methyl levulinate	

MVG	Methyl vinyl glycolate	
PAL	Pyruvaldehyde	
Sucr	Sucrose	
Tag	Tagatose	
THM	2,5,6-Trihydroxy-3-hexanoate	
VG	Vinylglyoxal	
Xyl	Xylose	
Xylu	Xylulose	

# List of Publications

Tosi, I., Sacchetti, A., Martinez-Espin, J. S., Meier, S., Riisager, A., Exploring the Synthesis of Mesoporous Stannosilicates as Catalysts for the Conversion of Mono- and Oligosaccharides into Methyl Lactate, *Top. Catal.*, *in press*, (2019)<sup>212</sup>

Tosi, I., Elliot, S. G., Jessen, B., Riisager, A., Taarning, E., Meier, S., Uncharted Pathways for CrCl<sub>3</sub> Catalyzed Glucose Conversion in Aqueous Solution, *Top. Catal.*, *in press*, (2019)<sup>228</sup>

Elliot, S. G., Tosi, I., Riisager, A., Taarning, E., Meier, S., Response Factors Enable Rapid Quantitative 2D NMR Analysis in Catalytic Biomass Conversion to Renewable Chemicals, *Top. Catal.*, *in press*, (2019)<sup>197</sup>

Tosi, I., Riisager, A., Taarning, E., Jensen, P. R., Meier, S., Kinetic Analysis of Hexose Conversion to Methyl Lactate by Sn-Beta: Effects of Substrate Masking and of Water, *Catal. Sci. Technol.*, **8**, 2137-2145, (2018)<sup>196</sup>

Shunmugavel, S., Tosi, I., Rasmussen, K. H., Jensen, R. E., Taarning, E., Meier, S., Riisager, A., Facile and Benign Conversion of Sucrose to Fructose Using Zeolites with Balanced Brønsted and Lewis Acidity, *Catal. Sci. Technol.*, **7**, 2782-2788, (2017)<sup>200</sup>



# Exploring the Synthesis of Mesoporous Stannosilicates as Catalysts for the Conversion of Mono- and Oligosaccharides into Methyl Lactate

Irene Tosi<sup>1</sup> · Annalisa Sacchetti<sup>2</sup> · Juan S. Martinez-Espin<sup>3</sup> · Sebastian Meier<sup>1</sup> · Anders Riisager<sup>1</sup>

© Springer Science+Business Media, LLC, part of Springer Nature 2019

## Abstract

Sn-beta zeolites are among the most promising catalysts for the conversion of biomasses due to their high Lewis acidity, which allows coordination to functionalized molecules and promotes cleavage and rearrangement reactions. For applications in biorefining zeolite porosity would ideally be optimized to avoid diffusional limitations, which otherwise may decrease reaction rates and restrict the conversion of bulky substrates. The synthesis of mesoporous zeolites can help alleviating limitations and is a central topic in heterogeneous catalysis, with many synthetic procedures for mesoporous zeolites proposed over the last decades. Here, we explore different syntheses routes to prepare Lewis acidic Sn-containing zeolites, and the main features of the prepared mesoporous materials are characterized. We investigate the correlation between different types of porosity and the activity for the conversion of sugars into methyl lactate. The monomer glucose, the dimer sucrose and the oligomer inulin are applied as model substrates for the reaction in order to probe the accessibility of molecules with different sizes to active sites in zeolites with different pore systems.

**Keywords** Biomass conversion · Inulin · Mesoporous zeolites · Methyl lactate · Sn-beta

## 1 Introduction

Sustainable production of fuels and chemicals requires the replacement of fossil feedstocks with renewable resources. Among those, abundant low cost biomass feedstock composed of highly functionalized molecules promises a favorable carbon footprint and the ability for transformation into many relevant chemicals along several chemo-catalytic routes [1].

In the last two decades, Lewis acidic zeotype materials have received much attention for biomass conversion due to

their high Lewis acidity, which allows the coordination to functionalized molecules and promotes cleavage and rearrangement reactions [2, 3]. Among the Lewis acidic zeotype materials, Sn-beta zeolite is perhaps the most studied catalyst due to its versatile catalytic activity in the conversion of simple sugars, promoting transformations such as isomerization [4, 5] and epimerization [6] of glucose, retro-aldol reactions [3], hydride-shifts and rearrangements into different products [7]. The production of methyl lactate starting from either glucose, fructose or sucrose has arguably remained the most important process catalyzed by Sn-beta, as this process permits the sustainable production of the monomer for polylactic acid (PLA) formation [8]. PLAs represent about 10% of the raw material globally produced for bioplastics, and their production capacity is expected to grow by 50% by 2022 as a consequence of the biobased origin and biodegradability of the compounds [9]. Additional  $\alpha$ -hydroxy esters, such as methyl vinyl glycolate (MVG) and methyl trans-2,5,6-trihydroxy-3-hexenoate (THM) are formed in the sugar conversion reaction, making the process a possible source for the production of diverse polyester monomers that contain additional groups for functionalization [7, 10–12] (Fig. 1).

**Electronic supplementary material** The online version of this article (<https://doi.org/10.1007/s11244-019-01135-8>) contains supplementary material, which is available to authorized users.

✉ Anders Riisager  
 ar@kemi.dtu.dk

<sup>1</sup> Department of Chemistry, Technical University of Denmark, Kemitorvet, 2800 Kgs. Lyngby, Denmark

<sup>2</sup> Dipartimento di Chimica Industriale “Toso Montanari”, Alma Mater Studiorum-University of Bologna, Viale del Risorgimento 4, 40136 Bologna, Italy

<sup>3</sup> Haldor Topsøe A/S, Haldor Topsøes Alle 1, 2800 Kgs. Lyngby, Denmark





# Uncharted Pathways for $\text{CrCl}_3$ Catalyzed Glucose Conversion in Aqueous Solution

Irene Tosi<sup>1</sup> · Samuel G. Elliot<sup>1</sup> · Bo M. Jessen<sup>1</sup> · Anders Riisager<sup>1</sup> · Esben Taarning<sup>2</sup> · Sebastian Meier<sup>1</sup>

© Springer Science+Business Media, LLC, part of Springer Nature 2019

## Abstract

Innovative processes for converting carbohydrates to materials and fuels form the basis for profitable bio-based economies of the future. For such innovation, approaches that provide detailed structural information would be desirable to detect uncharted chemistries of carbohydrate conversion. Among the most important value-added products accessible through conversion of biomass is 5-hydroxymethylfurfural (HMF), whose market values strongly depend on the quality of the product. Here, we use high-field in situ NMR spectroscopy to shed light on obscure competing reactions of  $\text{CrCl}_3$ -catalyzed carbohydrate conversion to HMF in water. High-field NMR spectroscopy has enormous prowess in distinguishing isomeric and dehydrated products formed from glucose. Previously unidentified compounds were identified with this approach and include anhydrosugars and a variety of branched and linear mono- and disaccharides. Other identified compounds leverage the understanding of the active catalyst species. In addition to providing mechanistic insight, the approaches and findings described herein help to measure and manage carbon balances and product quality in HMF production.

**Keywords** 2D NMR · Cascade reactions · Catalysis · Chromium trichloride · HMF · Sugars

## 1 Introduction

A change towards sustainable production of materials and fuels is increasingly imminent. Sustainable production using rapidly renewable resources involves both challenges and opportunities for developing novel catalytic approaches towards the use of resources such as carbohydrates and lignin [1, 2]. The high oxygen content in these substrates as compared to fossil compounds is accompanied by high functionality present in biomass [3]. Such abundant functionality in biomass raises the question, how novel processes can selectively transform the substrate to a product with selected functionality [3].

The most important value-added products accessible from carbohydrates include 5-hydroxymethylfurfural (HMF) [4, 5]. HMF is being investigated by several academic and industrial groups as a promising precursor of polymers, resins, pharmaceuticals, fuel additives and solvents [2]. Depending on its quality, market values in the range of (2–300 USD/kg) have been described [6, 7]. Hence, a production of highly pure compound is desirable for profitability. Processes of production have included transformations of carbohydrates using Lewis acidic salts and water as an obvious green solvent [6]. In addition, water is a more promising option for HMF purification than high-boiling organic solvents or ionic liquids [8–10].

While glucose is the cheaper and hence economically more attractive substrate than fructose, HMF yields from glucose in water have left room for improvement. Such improvement should be based on reliable carbon balances, but reported carbon yields often imply a significant amount of unidentified compounds in the reaction mixtures. The quantity of these compounds would help close the carbon balance of the processes, while their identity would be indicative of reaction mechanisms that are accessible under the given reaction conditions. The nature of byproducts in the

**Electronic supplementary material** The online version of this article (<https://doi.org/10.1007/s11244-019-01144-7>) contains supplementary material, which is available to authorized users.

✉ Sebastian Meier  
semei@kemi.dtu.dk

<sup>1</sup> Department of Chemistry, Technical University of Denmark, Kemitorvet, 2800-Kgs Lyngby, Denmark

<sup>2</sup> Haldor Topsøe A/S, Haldor Topsøes Alle 1, 2800-Kgs Lyngby, Denmark



# Response Factors Enable Rapid Quantitative 2D NMR Analysis in Catalytic Biomass Conversion to Renewable Chemicals

Samuel G. Elliot<sup>1</sup> · Irene Tosi<sup>1</sup> · Anders Riisager<sup>1</sup> · Esben Taarning<sup>2</sup> · Sebastian Meier<sup>1</sup>

© Springer Science+Business Media, LLC, part of Springer Nature 2019

## Abstract

Carbohydrate conversion offers access to a variety of chemicals with diverse functionalities. An accurate analysis of the multiple products in post-reaction material is indispensable for enabling good atom economy in biorefining. A certain need for reconsidering current analytical approaches to chemocatalytic biomass conversion is witnessed by the often poor carbon balances that are reported for carbohydrate conversion processes. Carbohydrate conversion usually includes isomerization and/or dehydration, therefore analytical approaches that are suitable for the distinction and concurrent quantification of isomers are desirable for developing sustainable processes towards known and new chemicals. Quantitative 1D NMR spectroscopy can be used to determine absolute concentrations in the absence of purified reference compounds and can thereafter be used to obtain response factors in other analytical methods resolving the compounds of interest. Here, we show that this approach is applicable for obtaining response factors relative to an internal standard for rapid, highly resolved 2D NMR spectra at natural isotopic abundance. Following calibration, this approach provides a limit of quantification in the order of 0.8 mM within an experiment time of a few minutes. The approach is particularly beneficial for the quantification of compounds at low concentrations, for instance in initial rate experiments, and for the quantification of low populated reaction intermediates.

**Keywords** Biomass · Catalysis · qNMR · Quantitative analysis · Reference standard · Response factor

## 1 Introduction

The current trajectories of global population growth and of natural resource consumption are unsustainable, as many natural resources are poised to deplete within the next few generations. Hence, sustainable means of producing known and new chemicals to sustain our materials- and energy-demanding lifestyles are needed. In this shift to alternative industries that rely more on renewables and less on

petroleum refining, biomass is a promising feedstock [1, 2]. Biomass conversion offers access to a variety of chemicals with diverse functionalities, for instance through the use of solid acid catalysts such as zeolites [3, 4].

Accurate qualitative and quantitative analysis of the multiple products in post-reaction material is indispensable for the development of biorefinery technology. The conversion of biomass often includes the isomerization or dehydration of carbohydrates [3, 5–10]. Therefore, analytical approaches that are suitable for the distinction and concurrent quantification of isomers (such as monosaccharides and their respective dehydration products) are poised to be particularly valuable for the analysis of biomass conversion products, and thus for aiding sustainable processes towards known and new chemicals. A certain need for reconsidering analytical approaches to chemocatalytic biomass conversion is witnessed by the often poor yields and low carbon balances that are reported for carbohydrate conversion processes, with little effort to identify and quantify the byproduct “dark matter” in the mixture [11].

NMR spectroscopy has been used in qualitative and quantitative analysis for more than five decades [12].

**Electronic supplementary material** The online version of this article (<https://doi.org/10.1007/s11244-019-01131-y>) contains supplementary material, which is available to authorized users.

✉ Samuel G. Elliot  
sgiel@kemi.dtu.dk

✉ Sebastian Meier  
semei@kemi.dtu.dk

<sup>1</sup> Department of Chemistry, Technical University of Denmark, Kemitorvet, 2800 Kgs. Lyngby, Denmark

<sup>2</sup> Haldor Topsøe A/S, Haldor Topsøes Alle 1, 2800 Kgs. Lyngby, Denmark



## PAPER

[View Article Online](#)  
[View Journal](#) | [View Issue](#)

 Cite this: *Catal. Sci. Technol.*, 2018, 8, 2137

# Kinetic analysis of hexose conversion to methyl lactate by Sn-Beta: effects of substrate masking and of water†

 Irene Tosi, <sup>a</sup> Anders Riisager, <sup>\*a</sup> Esben Taarning,<sup>b</sup> Pernille Rose Jensen <sup>c</sup> and Sebastian Meier <sup>\*a</sup>

Simple sugars show promise as substrates for the formation of fuels and chemicals using heterogeneous catalysts in alcoholic solvents. Sn-Beta is a particularly well-suited catalyst for the cleavage, isomerization and dehydration of sugars into more valuable chemicals. In order to understand these processes and save resources and time by optimising them, kinetic and mechanistic analyses are helpful. Herein, we study substrate entry into the Sn-Beta-catalysed methyl lactate process using abundant hexose substrates. NMR spectroscopy is applied to show that the formation of methyl lactate occurs in two kinetic regimes for fructose, glucose and sucrose. The majority of methyl lactate is not formed from the substrate directly, but from methyl fructosides in a slow regime. At 160 °C, more than 40% of substrate carbon are masked (*i.e.* reversibly protected *in situ*) as methyl fructosides within a few minutes when using hydrothermally synthesised Sn-Beta, while more than 60% methyl fructosides can be produced within a few minutes using post-synthetically treated Sn-Beta. A significant fraction of the substrate is thus masked by rapid methyl fructoside formation prior to subsequent slow release of fructose. This release is the rate-limiting step in the Sn-Beta-catalysed methyl lactate process, but it can be accelerated by the addition of small amounts of water at the expense of the maximum methyl lactate yield.

 Received 14th February 2018,  
 Accepted 12th March 2018

DOI: 10.1039/c8cy00335a

rsc.li/catalysis

## Introduction

Simple sugars can be converted into fuels and chemicals, including levulinic acid,<sup>1–6</sup> 5-hydroxymethylfurfural (HMF),<sup>5,7–9</sup> lactic acid<sup>10,11</sup> and others,<sup>9,12–19</sup> using zeolite-based materials as heterogeneous catalysts. Sn-Beta in particular is able to promote the cleavage, isomerization and dehydration of carbohydrates into more valuable chemicals. Such reactions include valorisations of abundant simple sugars by converting them into rare sugars<sup>9,11,17–25</sup> at moderate temperatures near 100 °C, or the formation of different hydroxyl esters as prospective building blocks for the production of biomass-derived polymers at temperatures near 160 °C.<sup>13,14,16,26</sup> Since the stability of the catalysts for the production of Sn-Beta is increased in alcoholic solvents compared to water,<sup>6</sup> a high temperature process is normally carried out in short-chain alcohols. The use of alcoholic solvents leads to the formation of activated and pH-neutral methyl esters and glycoside by-prod-

ucts.<sup>12,17,19</sup> The transformation of simple sugars into methyl lactate<sup>10,11</sup> or other  $\alpha$ -hydroxy esters<sup>12–14,16,26</sup> is a possible route for the sustainable production of polymers in bio-based processes. PLA (polylactic acid) has attracted great interest because of its mechanical and physical properties, and the possibility to combine lactic acid with other monomers and thus obtain a large variety of copolymer materials for diverse applications.<sup>27</sup> In addition, lactic acid is a platform for other chemicals and alkyl lactates are promising green solvents.<sup>17</sup>

Knowledge-based approaches to improving biomass conversion processes could benefit from a detailed kinetic and mechanistic understanding of the processes. Relatively little attention has been devoted to the systematic study of reaction kinetics in the Sn-Beta-catalysed methyl lactate process. Herein, we therefore employ a quantitative NMR methodology to derive a kinetic model of carbohydrate influx into the pathway that ultimately converts a fructose intermediate to methyl lactate. Glucose and fructose had previously been shown to yield similar product mixtures in the Sn-Beta-catalysed methyl lactate process, while the non-reducing disaccharide sucrose resulted in higher methyl lactate yields, possibly due to a slower release of reducing sugars. We hypothesised that a slow release of reducing sugars may play a generally neglected role in Sn-Beta catalysed conversions of glucose, fructose and sucrose at temperatures near 160 °C,

<sup>a</sup> Department of Chemistry, Technical University of Denmark, Kemitorvet, 2800 Kgs. Lyngby, Denmark. E-mail: ar@kemi.dtu.dk, semei@kemi.dtu.dk

<sup>b</sup> Haldor Topsøe A/S, Haldor Topsøes Alle 1, 2800 Kgs. Lyngby, Denmark

<sup>c</sup> Department of Electrical Engineering, Technical University of Denmark, 2800 Kgs. Lyngby, Denmark

† Electronic supplementary information (ESI) available. See DOI: 10.1039/c8cy00335a



Cite this: *Catal. Sci. Technol.*, 2017, 7, 2782

## Facile and benign conversion of sucrose to fructose using zeolites with balanced Brønsted and Lewis acidity†

Shunmugavel Saravanamurugan,<sup>a,b</sup> Irene Tosi,<sup>a</sup> Kristoffer H. Rasmussen,<sup>‡a</sup> Rasmus E. Jensen,<sup>‡a</sup> Esben Taarning,<sup>c</sup> Sebastian Meier<sup>\*,a</sup> and Anders Riisager<sup>\*a</sup>

Sucrose is by far the industrially most abundant simple carbohydrate with a production volume of more than 160 million metric tons from sugar cane and sugar beet per year. Many promising pathways towards bio-based organic compounds use, however, fructose as the pathway substrate. Hence, a chemocatalytic approach to convert sucrose into fructose would provide a means to channel sucrose into pathways for sugar valorization. Here, we show that a variety of heterogeneous zeolite catalysts with balanced Brønsted and Lewis acidity enable a simple route for the conversion of sucrose to more than 80% fructosides or fructose at 100 °C. The catalysts can encompass aluminium or tin Lewis acidic sites in various zeolite frameworks. The reaction proceeds in volatile alcohol solvents and broadly enables the channelling of sucrose into processes that use fructose as the pathway substrate.

Received 20th March 2017,  
Accepted 14th May 2017

DOI: 10.1039/c7cy00540g

rsc.li/catalysis

## Introduction

Carbohydrates constitute the predominant fraction of annually renewable biomass, mostly in the form of structural polysaccharides, storage polysaccharides or simple carbohydrates.<sup>1</sup> Among the simple carbohydrates, the disaccharide sucrose ( $\alpha$ -D-glucopyranosyl-(1 $\rightarrow$ 2)- $\beta$ -D-fructofuranoside) refined from sugar beet or sugar cane has particular relevance, reaching global production volumes of more than 160 million metric tons per year, orders of magnitude higher than worldwide glucose and fructose production.<sup>1,2</sup>

While its use as a chemical feedstock has remained limited, sucrose as the most abundant simple carbohydrate is poised to play a role as a substrate for the production of organic compounds from renewable biomass.<sup>3,4</sup> So far, fructose has played a central role as the entry point for molecular pathways leading to bio-based chemicals and fuels due to the higher reactivity of fructose relative to glucose.<sup>5</sup> These pathways often involve dehydration of the furanose form or dehydration and retro-aldol reactions of the open-chain form to products such as 5-hydroxymethylfurfural (HMF), levulinic acid, lactic acid or unsaturated  $\alpha$ -hydroxy esters.<sup>4–7</sup> Both fura-

nose and acyclic forms are orders of magnitude more highly populated in fructose solutions than in glucose solutions. Accordingly, chemocatalytic glucose-to-fructose isomerization procedures have been devised using Lewis acidic zeolite catalysts that also exhibit activity in carbohydrate dehydration and cleavage.<sup>4,8,9</sup> These Lewis acidic zeolite catalysts exhibit strongly improved stability in short-chain alcohols such as methanol, if compared to water.<sup>9</sup> In addition, the use of alcohols in glucose-to-fructose isomerization has been proven beneficial due to the fast sequestration of the formed fructose as fructosides.<sup>10,11</sup> Hence, the use of methanol in glucose-to-fructose isomerization permits the formation of fructosides in amounts near 60% from glucose, higher than the equilibrium distribution of 42% fructose (50% glucose, 8% other sugars, especially mannose) attainable in water.<sup>11,12</sup> Glucose-to-fructose isomerization has been shown to proceed by a stereoselective 1,2-hydride shift in the acyclic form in methanol when aluminium- and tin-containing zeolite catalysts were used.<sup>10</sup> This reaction mechanistically resembles the enzymatic glucose-to-fructose isomerization by xylose isomerase.

Sucrose is a non-reducing carbohydrate that does not lend itself directly to biomass conversion reactions occurring in the open-chain form. Accordingly, sucrose has been considered stable in isomerization reactions using Lewis acidic zeolites under mild reaction conditions (near 100 °C) in water.<sup>13</sup> Sucrose is, however, easily hydrolysed by Brønsted acids, but the instability of fructose under usual process conditions employing homogeneous Brønsted acids for biomass hydrolysis poses a potential problem for fructose production by such

<sup>a</sup> Department of Chemistry, Technical University of Denmark, Kemitorvet, 2800-Kgs. Lyngby, Denmark. E-mail: semei@kemi.dtu.dk, ar@kemi.dtu.dk

<sup>b</sup> Center of Innovative and Applied Bioprocessing (CIAB), Mohali 140 306, Punjab, India

<sup>c</sup> Haldor Topsøe A/S, Haldor Topsøes Allé 1, 2800-Kgs. Lyngby, Denmark

† Electronic supplementary information (ESI) available. See DOI: 10.1039/c7cy00540g

‡ These authors contributed equally.

# Conferences Proceedings

Nov. 2018	Poster presentation at the Lundenser meeting 2018 titled <i>Zeolite Catalysts for the Selective Conversion of Sugars into Polymers Monomers</i> , Copenhagen, Denmark, 15 <sup>th</sup> of November 2018.
Aug. 2018	Oral presentation at the Nordic Symposium on Catalysis titled <i>Kinetic Insight into the Production of Methyl Lactate from Sugars with Sn-Beta Catalyst</i> , Copenhagen, Denmark, 26-28 <sup>th</sup> of August 2018
Dec. 2017	Oral presentation at the DTU Sustain titled <i>Off-Pathway Intermediates in the Conversion of Sugars to Plastic</i> , Kgs. Lyngby, Denmark, 6 <sup>th</sup> of December 2017
Sep. 2017	Poster and flash presentation at the GEZ School on Zeolites titled <i>Conversion of Sucrose to Fructose Using Zeolites</i> , University Rey Juan Carlos, Madrid, Spain, 27-29 <sup>th</sup> of September 2017
Aug. 2017	Poster presentation at Europacat 2017 titled <i>Conversion of Sucrose to Fructose Using Zeolites with Balanced Brønsted and Lewis Acidity</i> , Florence, Italy, 27 <sup>th</sup> -31 <sup>st</sup> of August 2017
May 2017	Poster presentation at the International Symposium of Green Chemistry 2017 (ISGC) titled <i>Zeolite-catalyzed Conversion of Sucrose to Fructose</i> , La Rochelle, France, 16-19 <sup>th</sup> of May 2017
2016-2019	Oral and poster presentations at the Annual Ph.D. Symposium organized by the department of Chemistry of the Technical University of Denmark
2016-2019	Oral presentations internally at the Technical University of Denmark and at Haldor Topsøe A/S.